UAB

Universitat Autònoma de Barcelona

Alternative components of the cellular immunity to SARS-CoV-2 and HIV infection: beyond the classical CTL

Luis Romero Martín

Departament de Biologia Cel·lular, Fisiologia i d'Immunologia

Facultat de Medicina

Universitat Autònoma de Barcelona

Alternative components of the cellular immunity to SARS-CoV-2 and HIV infection: beyond the classical CTL

Luis Romero Martín

Institut de Recera de la Sida (IrsiCaixa), Hospital Germans Trias i Pujol i Institut d'Investigació en Ciències de la Salut Germans Trias i Pujol (IGTP)

Directores de tesis:

Dr. Alex Olvera y Dr. Christian Brander

UAB
Universitat Autònoma
de Barcelona

IrsiCaixa
Institut de Recerca de la Sida

IGTP
Germans Trias i Pujol Research Institute

Germans Trias i Pujol
Hospital

El Dr. Christian Brander (Director y tutor) y el Dr. Alex Olvera (Director), investigadores del Institut de Recerca de la Sida (IrsiCaixa) del Hospital Germans Trias i Pujol,

Hacen constar:

Que el trabajo experimental y la redacción de la memoria de la Tesis Doctoral titulada "Alternative components of the celular immunity to SARS-CoV-2 and HIV infection: beyond the classical CTL" ha sido realizada por Luis Romero Martín bajo su tutoría y dirección y consideran que es apta para ser presentada para optar al grado de Doctor en Inmunología por la Universidad Autónoma de Barcelona.

Y para que quede constancia, firman el presente documento:

Badalona, a 3 de Agosto de 2022

Dr. Christian Brander   Dr. Alex Olvera

RESULTS

ABREVIATIONS

3CL	3C-like
ACE2	Angiotensin converting enzyme 2
ADCC	Antibody dependent cytotoxicity
AIDS	Acquired immunodeficiency syndrome
AMP	Antimicrobial peptide
APC	Antigen presenting cell
ARDS	Acute respiratory distress syndrome
ARS	Acute retroviral syndrome
ART	Antiretroviral therapy
bnAb	Broadly neutralizing antibody
CA	Capsid protein p24 (HIV)
CCR5	C-C chemokine receptor type 5
CCR7	C-C chemokine receptor type 7
CLP	Common lymphoid precursors
CL-SF	C-type lectin-like receptor superfamilly
CNS	Central nervous system
COVID-19	Coronavirus disease - 19
CRF	Circulating recombinant forms
CRTH2	Chemoattractant receptor-homologous 2
CXCR4	C-X-C chemokine receptor type 4
DAD	Diffuse alveolar damage
DAMP	Damage-associated molecular pattern
DAP12	DNAX activation protein 12
DC	Dendritic cells
dsDNA	Double-stranded deoxyribonucleic acid
E	Envelope protein (SARS-CoV-2)
ELISA	Enzyme-linked immunosorbent assay
Env	Envelope protein (HIV)
ERGIC	Endoplasmic reticulum – Golgi apparatus intermediate compartment
Foxp3	Forkhead box protein 3
FP	Fusion peptide (HIV)
Gag	Group specific antigen
GALT	Gut-associated lymphoid tissue
GC	Germinal center
G-CSF	Granulocyte colony-stimulating factor
HEV	High endothelial venules
HIV	Human immunodeficiency virus
HLA	Human leukocyte antigen
HP	Heptad repeat (HIV)
HSC	Hematopoietic stem cell
IFN-I	Interferon type I
IFN-γ	Interferon γ
Ig-SF	Immunoglobulin-like receptor superfamily
IL-10	Interleukin 10
IL-13	Interleukin 13
IL-17	Interleukin 17

IL-2	Interleukin 2
IL-21	Interleukin 21
IL-22	Interleukin 22
IL-4	Interleukin 4
IL-5	Interleukin 5
IL-6	Interleukin 6
IN	Integrase (HIV)
iNK	Immature NK cell
IP-10	Interferon γ - induced protein 10
IRF3/7	Interferon-regulatory factor 3/7
ITAM	Tyrosine-based activating motifs
ITIM	Tyrosine-based inhibitory motifs
KIR	Killer Ig-Like Receptors
LILR	Leukocyte immunoglobulin-like receptor
LRA	Latency reversing agents
M	Membrane protein (SARS-CoV-2)
MA	Matrix protein p17 (HIV)
mAb	Monoclonal antibody
MAVS	Mitochondrial antiviral signaling
MCP-1	Monocyte chemoattractant protein 1
MDA5	Melanoma differentiation-associated protein 5
mDC	Myeloid dendritic cell
MERS	Middle East respiratory syndrome
MIP-1α	Macrophage inflammatory protein 1α
mNK	Mature NK cell
MPER	Membrane proximal external region
N	Nucleocapsid protein (SARS-CoV-2)
NC	Nucleocapsid p7 protein (HIV)
NCR	Natural cytotoxic receptors
Nef	Negative effector
NF-κβ	Nuclear factor – κβ
NHP	Non-human primates
NK	Natural killer
NKP	Natural killer precursors
NKT	Natural Killer T-cells
NPC	Nuclear pore complex
nsp	Non-structural protein
ORF	Open-reading frame
PAMP	Pathogen-associated molecular pattern
PASC	Post-acute sequelae of COVID-19
PD-1	Programmed death 1
PIC	Pre-integration complex
PL	Papain-like
Pol	Polymerase (HIV)
PR	Protease (HIV)
preNKPs	preNK precursors
PRR	Pattern recognition receptor
PVR	Poliovirus receptor

RAAS	Renin-angiotensin-aldosterone system
RANTES	Regulated upon activation, normal T cell expressed and presumably secreted
RBD	Receptor binding domain
RdRP	RNA-dependent RNA-polymerase activity
Rev	Regulator of viral expression
RIG-I	Retinoic acid-inducible gene I
RLR	RIG-I-like receptor
RNA	Ribonucleic acid
RNP	Ribonucleoprotein
RORγt	Retinoic orphan receptor γt
RT	Reverse transcriptase protein (HIV)
RTC	Replication and transcription complex
S	Spike protein (SARS-CoV-2)
SARS-Cov	Severe acute respiratory syndrome coronavirus
SARS-CoV-2	Severe acute respiratory syndrome coronavirus 2
SU	Surface protein (SARS-CoV-2)
Tat	Transcriptional activator (HIV)
T_{CM}	Central memory T-cell
T_{EM}	Effector memory T-cell
TGF-β	Transforming growth factor beta
TIGIT	T cell immunoreceptor with Ig and ITIM domains
TLR	Toll-like receptor
TM	Transmembrane
TMPRSS2	Transmembrane serine 1 protease 2
$T_{naïve}$	Naïve T-cell
TNFR1	TNF receptor 1
TNF-α	Tumor necrosis factor α
UNAIDS	United Nations Program on HIV/AIDS
UTR	Untranslated regions
Vif	Viral infectivity factor (HIV)
Vpr	Viral protein R (HIV)
Vpu	Viral protein U (HIV)
WHO	World Health Organization

Abstract

Two viral agents, human immunodeficiency virus (HIV) and severe acute respiratory syndrome coronavirus 2 (SARS-CoV-2), are responsible for two biggest pandemics that have hit the human population over the last few years, causing more than 36 HIV- and 6 million SARS-CoV2-associated deaths, respectively. Although AIDS and COVID-19 associated mortality has been dramatically reduced by combined antiretroviral therapy for HIV and vaccination against SARS-CoV-2, both have significant limitations. For HIV, antiretroviral therapy requires lifelong adherence and is linked to long-term side effects. For SARS-CoV-2, emerging variants have compromised herd immunity achieved by vaccination. In addition, global social and economic differences result in unequal access to those treatments. Understanding the underlying mechanisms of viral control will be essential in order to limit the further spread of these infections and develop novel preventive and therapeutic strategies.

Research on the immune response to infectious diseases has been focused on two important components of viral immunity, the elicitation of neutralizing antibodies and cytotoxic T cells (CTL). Other components of the cellular immune response have been less well investigated, including i) NK cells with innate antiviral properties and ii) alternatively polarized T-cells with effector functions beyond those of classical CTL.

In the present thesis, we aimed to provide a better understanding of cellular mechanisms that support HIV and SARS-CoV-2 viral control by comparing individuals with natural control of the infection and individuals with progressive disease. Chapters I and II are focused on the regulation of NK cell activity through the HLA-E/NKG2X axis. We observed common patterns between both infections, including elevated HLA-E expression, reduction of the circulating CD56^{bright} NK cells population and impaired NK cell effector function in individuals with uncontrolled infections, suggesting a common mechanism of ineffective NK cell immunosurveillance linked to worse disease course in both infections. In Chapters III and IV, a novel flow cytometry approach allowed us to identify alternative CD4$^+$ and CD8$^+$ effector functions that might be missed otherwise. In particular, in Chapter III we identified Th1, Th17 and Treg CD4$^+$ responses to SARS-CoV-2 N protein that distinguished individuals with mild or severe course of COVID-19. On the other hand, in Chapter IV we showed increased CD8$^+$ Tfc-like responses in HIV controllers that were linked to humoral responses and to viral control.

Together, this work provides supports an important role of NK cell and alternative T-cell effector function in the natural control of HIV and SARS-CoV-2 infections. This could benefit future research towards new cellular-based immunotherapies in these and other viral infections, including the rescue of exhausted NK cells and the elicitation of specific T-cell profiles that could lead to better disease prognosis.

Resumen

Dos infecciones virales, causadas por el virus de la inmunodeficiencia humana (VIH) y el coronavirus 2 causante del síndrome agudo respiratorio severo (SARS-CoV-2), son responsables de las dos mayores pandemias que la humanidad ha vivido en los últimos 50 años, causando más de 36 asociadas al VIH y 6 millones de muertes asociadas al SARS-CoV-2, respectivamente. Aunque la mortalidad del SIDA de y de la COVID-19 se ha reducido dramáticamente gracias a la terapia antirretroviral combinada para el VIH y la vacunación contra el SARS-CoV-2, ambos tratamientos tienen limitaciones. La terapia antirretroviral contra el VIH requiere una adhesión al tratamiento de por vida y existen efectos secundarios del tratamiento. Por otro lado, nuevas variantes de SARS-CoV-2 han puesto en riesgo en peligro la inmunidad de grupo conseguida mediante la vacunación. Además, las diferencias socioeconómicas entre distintas regiones del mundo provocan un acceso desigual a dichos tratamientos. Por estos motivos, entender los mecanismos que sostienen el control natural de la infección puede ser esencial para limitar la propagación de estas infecciones y desarrollas nuevas estrategias terapéuticas.

La investigación en la respuesta inmune a las enfermedades infecciosas tradicionalmente se ha centrado en dos grandes componentes de la inmunidad viral, como el desarrollo de anticuerpos neutralizantes y la generación de linfocitos T citotóxicos (CTL). Mientras tanto, otros componentes de la inmunidad celular han sido menos explorados, incluyendo i) las células NK con capacidades antivirales innatas y ii) los linfocitos T que adquieren respuestas efectoras más allá de los CTL.

En esta tesis, nuestro objetivo es conseguir una mejor comprensión de los mecanismos celulares asociados a un control natural de las infecciones por VIH y SARS-CoV-2 mediante la comparación de individuos con un control natural de la infección e individuos cuya enfermedad progresa. Los capítulos I y II están centrados en la regulación de las células NK a través del eje HLA-E/NKG2X. Hemos hallado patrones comunes a través de esta señalización en las infecciones por VIH y SARS-CoV-2, como una expresión más alta de HLA-E, una pérdida de la población de CD56^{bright} circulante y una respuestas efectora de las células NK deficiente en los pacientes con infecciones no controladas, lo que sugiere que existe un mecanismo común de inmunovigilancia ineficaz asociado a una peor evolución de la enfermedad en ambas infecciones. En los capítulos III y IV hemos empleado una nueva aproximación por citometría de flujo que nos ha permitido identificar respuestas efectoras alternativas en linfocitos T CD4^{+} y CD8^{+}. En más detalle, en el

Capítulo III hemos identificado respuestas Th1, Th17 y Treg en linfocitos T CD4+ contra la proteína N de SARS-CoV-2 que discriminan entre pacientes con una enfermedad leve o grave. Por otra parte, en el capítulo IV encontramos respuestas más altas de linfocitos CD8+ Tfc-like en controladores de VIH que están relacionadas con las respuestas humorales y el control viral.

En conclusión, este trabajo proporciona evidencias sobre un papel importante de las células NKs y las funciones efectoras alternativas de los linfocitos T en el control natural de las infecciones de por VIH y SARS-CoV-2. Esto podría beneficiar futuras investigaciones hacia nuevas inmunoterapias celulares en estas y otras infecciones virales, incluyendo el rescate de células exhaustas y la generación de respuestas de células T específicas que pueden llevar a un mejor pronóstico.

Resum

Dues infeccions virals, causades pel virus de la immunodeficiència humana (VIH) i el coronavirus 2 causant de la síndrome respiratòria aguda greu (SARS-CoV-2), són responsables de les dues pandèmies més grans que la humanitat ha viscut en els últims 50 anys, provocant més de 36 milions de morts associades al VIH i 6 milions associades al SARS-CoV-2. Tot i que la mortalitat del SIDA i de la COVID-19 s'ha reduït dràsticament gràcies a la teràpia antirretroviral combinada per al VIH i la vacunació contra el SARS-CoV-2, ambdós tractaments presenten limitacions. La teràpia antirretroviral contra el VIH requereix una adhesió al tractament de per vida i existeixen efectes secundaris del tractament. Per altre banda, noves variants de SARS-CoV-2 han posat en risc la immunitat de grup aconseguida mitjançant la vacunació. Addicionalment, les diferències socioeconòmiques entre diferents regions del món provoquen un accés desigual als tractaments. Per aquests motius, entendre els mecanismes que permeten el control natural de la infecció pot ser essencial per limitar la propagació d'aquestes infeccions i desenvolupar noves estratègies terapèutiques.

La investigació en la resposta immune a les malalties infeccioses tradicionalment s'ha centrat en dos grans components de la immunitat viral, com el desenvolupament d'anticossos neutralitzants i la generació de limfòcits T citotòxics (CTL). Mentrestant, altres components de la immunitat cel·lular han estat menys explorats, incloent-hi i) les cèl·lules NK amb capacitats antivirals innates i ii) els limfòcits T que adquireixen respostes efectores més enllà dels CTL.

En aquesta tesi, el nostre objectiu és aconseguir una millor comprensió dels mecanismes cel·lulars associats a un control natural de les infeccions per VIH i SARS-CoV-2 mitjançant la comparació d'individus amb un control natural de la infecció i individus en els quals la malaltia progresa. Els capítols I i II es centren en la regulació de les cèl·lules NK a través de l'eix HLA-E/NKG2X. Hem trobat patrons comuns a través d'aquesta senyalització en les infeccions per VIH i SARS-CoV-2, així com una expressió més alta de HLA-E, una pèrdua de la població de CD56bright circulant i una resposta efectora de les cèl·lules NK deficient en els pacients amb infeccions no controlades, que suggereix l'existència d'un mecanisme comú d'immunovigilància ineficaç associada a una pitjor evolució de la malaltia en ambdues infeccions. En els capítols III i IV hem utilitzat una nova aproximació per citometría de flux que ens ha permès identificar respostes efectores alternatives en limfòcits T CD4+ i CD8+. Més detalladament, en el Capítol III hem identificat respostes Th1, Th17 i Treg en limfòcits T CD4+ contra la proteïna N de Sars-CoV-2 que

discrimina entre pacients amb una malaltia lleu o greu. Per altre banda, en el capítol IV trobem respostes més altes de limfòcits CD8+ Tfc-like en controladors de VIH que estan relacionades amb les respostes humorals i el control viral.

En conclusió, aquest treball proporciona evidències sobre un paper important de les cèl·lules NKs i les funcions efectores alternatives dels limfòcits T en el control natural de les infeccions de VIH i SARS-CoV-2, Això podria beneficiar futures investigacions cap a noves immunoteràpies cel·lulars en aquestes i altres infeccions virals, incloent la recuperació de cèl·lules exhaustes i la generació de respostes de cèl·lules T específiques que poden portar a un millor pronòstic.
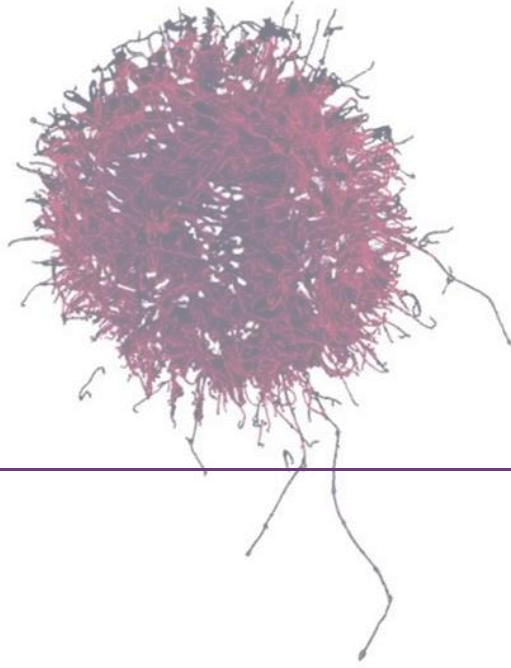
INTRODUCTION

1. Severe acute respiratory syndrome coronavirus 2 (SARS-Cov2)

1.1. History of the SARS-CoV-2 pandemic

Over the last 20 years, seven out of the nine described coronaviruses have broken the species barrier and spilled over into humans. The last of these events occurred in December 2019, when first SARS-CoV-2 infections were described in Wuhan, China[1].

Two years after the SARS-CoV-2 outbreak, the World Health Organization (WHO) has registered more than 560 million cases of infection worldwide and more than 6 million associated deaths[2].

Severe acute respiratory syndrome coronavirus 2 (SARS-CoV-2) is an enveloped positive-stranded single ribonucleic acid (RNA) virus that belongs to the *Coronaviridae* family[3,4].

Genetic evolution has led to the emergence of different SARS-CoV-2 variants, five of them of concern: alpha (B.1.1.7), beta (B.1.351), Gamma (P.1), Delta (B.1.617.2) and Omicron (B.1.1.529), but only the last two are currently circulating. The Delta variant is a 225% more transmissible than the original Wuhan strain[5] while Omicron, the current leading variant (up to 85% of worldwide cases), multiplies in lung cells up to 70% faster than Delta. Despite a less fatal disease caused by Omicron, its rapid spread and the unequal access to vaccination opens the door for new variants to emerge[6].

1.2. SARS-CoV-2 genome and structure

The 30kb SARS-CoV-2 genome consists of 11 open-reading frames (ORFs) that encode two large polyproteins (ORF1a and ORF1b that are cleaved to form 16 nonstructural proteins -nsps-), four structural proteins: spike (S), further cleaved by the host furin protein into S1 and S2[7], envelope (E), membrane (M) and nucleocapsid (N) and six accessory proteins (ORF3a, ORF6, ORF7a, ORF7b, ORF8, ORF10)[8] (Figure 1). ORF1ab contains, among others, the machinery responsible for polyprotein cleaving (3C-like -3CL- protease and papain-like -PL- protease), RNA replication (helicase, exonuclease, RNA polymerase) and immune system evasion[9], by exerting an endoRNAse activity, which prevents sensing of pathogen RNA[10]. The S, E, M and N proteins are necessary for virion assembly and release[11]. ORF3a and ORF8 play a role in the dismantling of host cell antiviral activity and survival. ORF6 appears to be involved in RNA polymerization, whereas ORF7a and ORF7b are localized in the cell membrane and the Golgi compartment, respectively[11]. ORF10 transcription is not essential in humans cells and its function remains unknown[12].
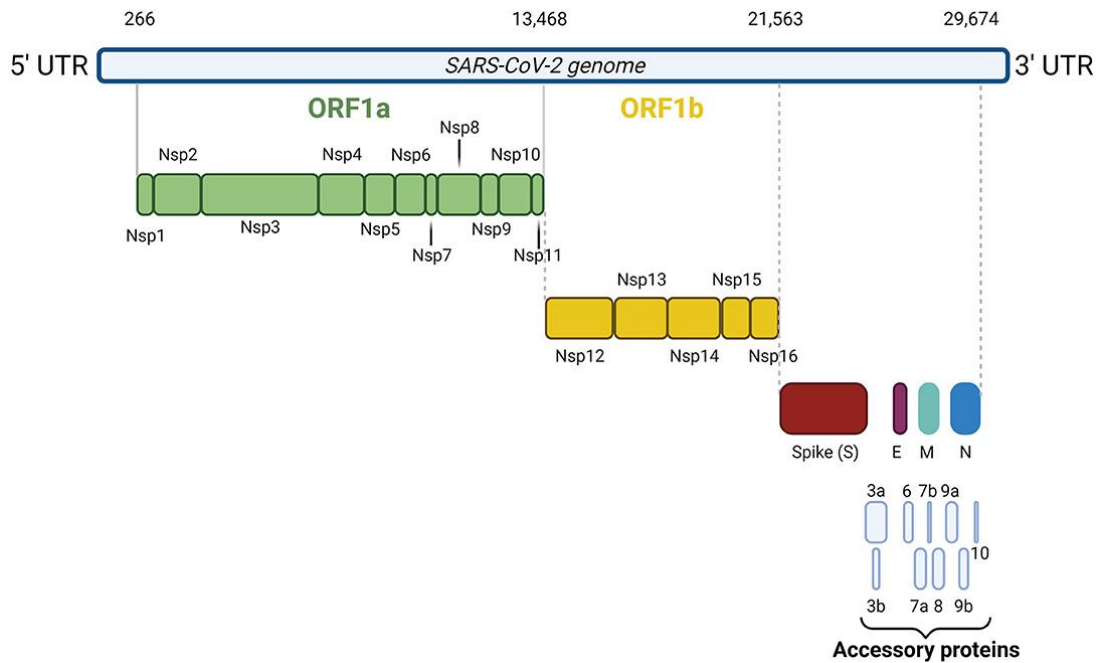
Figure 1. SARS-CoV-2 genome organization[13]**.** Different colors represent different viral ORF.

SARS-CoV-2 virion is spherical with a diameter of about 90nm (Figure 2). On the lipid bilayer, an average of 26 S protein trimers protrude from each viral particle. SARS-CoV-2 M and E proteins are major membrane components[14]. On the inside, the N protein is responsible for binding genomic RNA and packaging it into the ribonucleoprotein (RNP) complex[15].
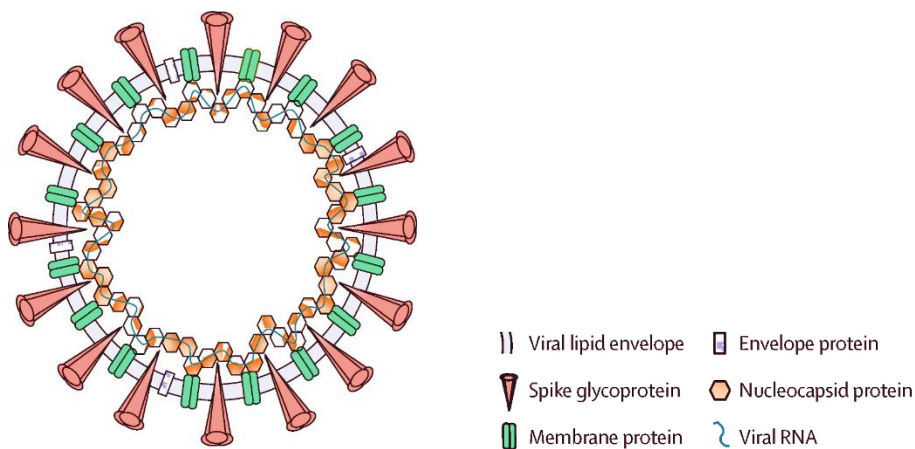
Figure 2. Structure of SARS-CoV-2 virions[16]. SARS-CoV-2 is a spherical enveloped virus with three structural proteins in the lipid bilayer (S, M, E) and RNP complex (N and RNA) on the inside.

1.3. SARS-CoV-2 life cycle

Coronaviruses S protein is fundamental for viral entry and can be divided into two functional parts (S1 and S2). The receptor binding domain (RBD) is contained within the S1, while the fusion peptide and heptad repeats in S2 promote viral entry[17]. SARS-CoV-2 infects human cells by binding to cell surface angiotensin-converting enzyme 2 (ACE2) through RBD. Additionally, the cellular transmembrane serine 1 protease 2 (TMPRSS2) is required for priming S before viral entry[18], an event that is assisted by the host furin protein or cathepsins if viral entry occurs via endosomes[17,19] (Figure 3).

After membrane fusion, the RNA genome is released in the cytoplasm. ORF1a and ORF1ab contain 15-16 nsp that constitute the replication and transcription complex (RTC)[20]. Then a full-length negative-sense genomic RNA copy is synthesized as a template for new positive-sense genomic RNA that can either be packed into new virions or used for translation of more nsps[8,21].

New virions assembly requires M, E, S and N proteins and it is thought to take place in the intracellular membranes of the endoplasmic reticulum – Golgi apparatus intermediate compartment (ERGIC). SARS-Cov2, as other betacoronaviruses, exploits the lysosomal exocytic pathway to be released from the cell[22].
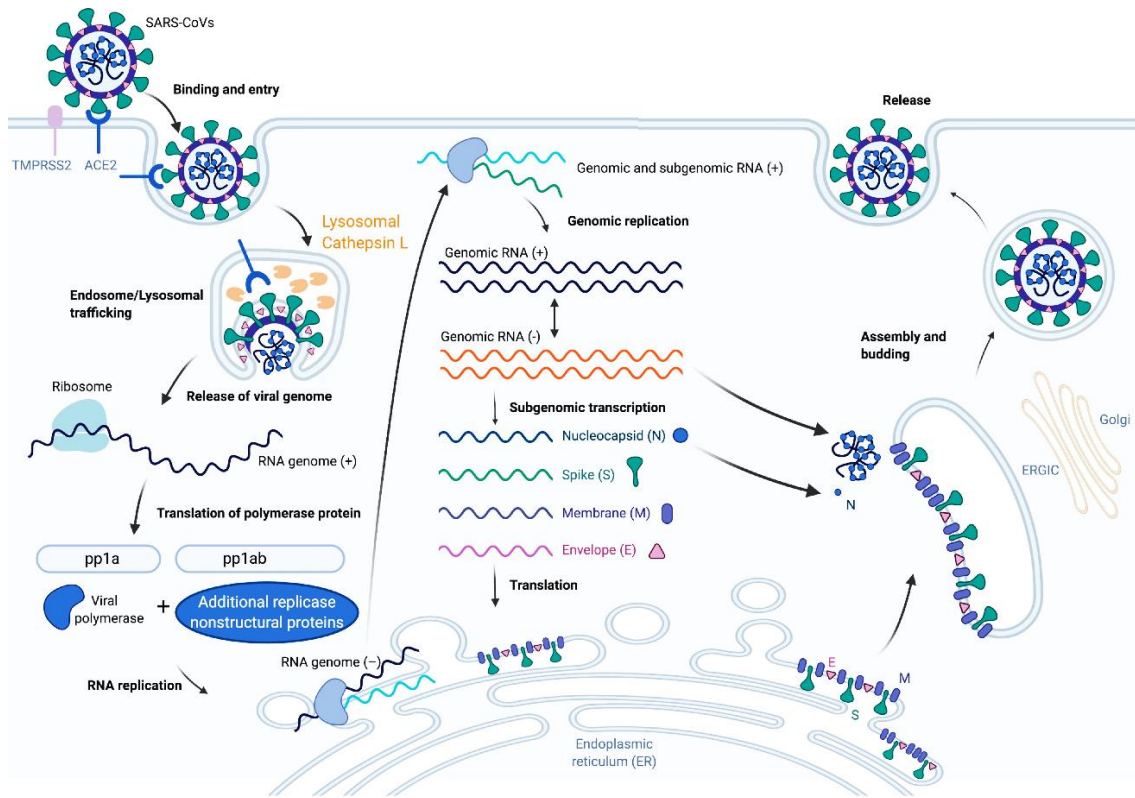
Figure 3. SARS-CoV-2 life cycle[23]. SARS-CoV-2 life cycle starts with S and ACE2 interaction. TMPRSS2 or endolysosomal cathepsins can cleave S and expose the fusion peptide. After releasing the genomic RNA, translation of ORF1a and ORF1ab occurrs. The autocleavage of those polyproteins allows the RdRP to replicate the viral genome and the start the translation of structural and accessory proteins. Virus budding takes place within ERGIC through N-M interactions and new virions are released through the lysosomal exocytosis pathway.

1.4. SARS-CoV-2 pathogenesis: Coronavirus disease 19 (COVID-19)

In humans, ACE2 expression has been tracked to more than 72 tissues, including the epithelia of the respiratory system, cardiovascular system, gastrointestinal track, urogenital system, liver, gallbladder and nervous system[24] (Figure 4). This fact may render many of the body organs susceptible to SARS-CoV-2 infection. Consequently, although Coronavirus disease-19 (COVID-19) is best known for being a respiratory pathology, several extrapulmonary manifestations can occur. Four major potential pathological mechanisms have been described so far: 1) cytopathic death of ACE2-expressing, virally infected cells; 2) dysregulation of the renin-angiotensin-aldosterone system (RAAS); 3) endothelial cell injury and thrombo-inflammation and 4) tissue damage.
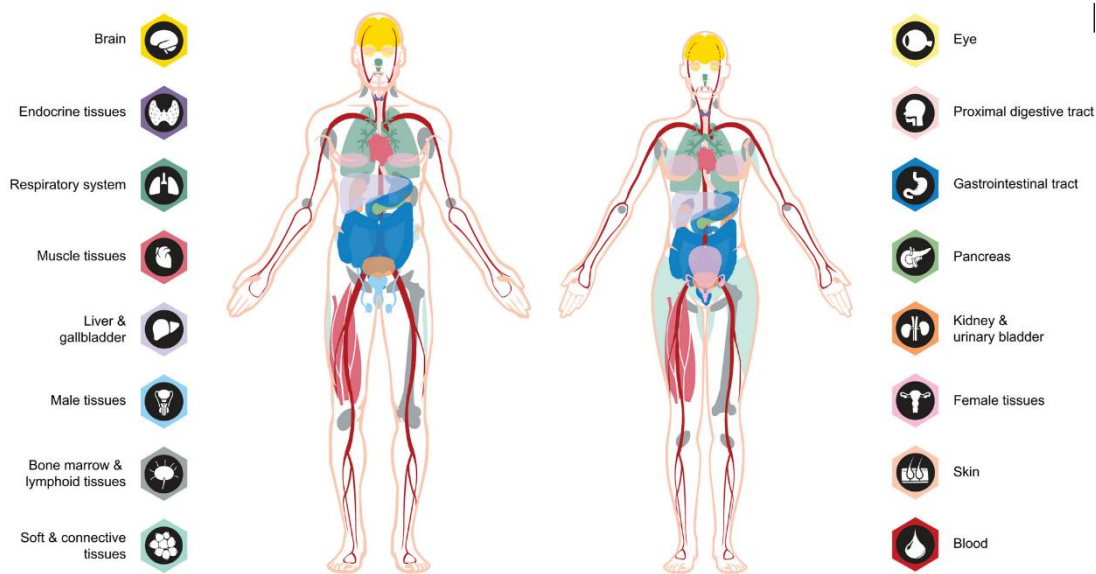
Figure 4. ACE-2 expressing tissues among human body systems[25]**.**

WHO classified COVID-19 into five severity groups[26]:

- **Asymptomatic**
- **Mild**: upper respiratory infection and nonspecific symptoms (fever, sore throat, cough,..)
- **Moderate**: pneumonia with fever, cough, dyspnea
- **Severe**: severe pneumonia, breathing rate >30/min, saturation oxygen <94%
- **Critical**: acute respiratory distress syndrome (ARDS), sepsis, septic shock

1.4.1. Immunological features of COVID-19

Patients with COVID-19 usually present an aberrant immune landscape characterized by hyper-active innate immune responses and delayed or inefficient adaptive immune responses. These are common features in patients with more severe forms of the disease[27].

- **Lymphopenia:** a significant reduction on peripheral B and T-cells as well as NK cells is commonly observed in patients with Severe COVID-19[28]. $CD4^+$ and $CD8^+$ T-cell were markedly different between mild and severe COVID-19 and immune-monitoring of T-cell responses have been suggested to improve intervention efficacy[29,30]. Several mechanisms

have been proposed to lead to lymphopenia: i) cellular exhaustion, observed as an increase of programmed death-1 (PD-1) expression in both T-cells and NK cells[31,32]; ii) interleukin-6 (IL-6) -driven reduced cytotoxicity[33] or iii) direct viral interaction with T-cell function since *MAP2K7* and *SOS1*, involved in T-cell activation and proliferation, are reduced in severe COVID-19[34].

▪ **Neutrophilia:** COVID-19 is associated with an augmentation of circulating neutrophils and the neutrophil-to-lymphocyte ratio[35]. Excessive neutrophilic activity appears to be caused by immune-metabolic reprogramming and triggers cell damage that might disrupt connective tissues[27].

▪ **Impaired IFN-I response:** although the exact mechanisms remain unclear, several SARS-CoV-2 proteins (nsp6, nps13 and ORF6, for instance) interfere with different steps of the interferon type I (IFN-I) signaling/production[36].

▪ **Antibody-dependent enhancement (ADE) of infection:** pre-existing antibodies to coronaviruses could increase virus entry through interactions with Fc-receptors on cell surface. This mechanism has been previously reported in other viral infections, including severe acute respiratory syndrome coronavirus (SARS-CoV) and middle-east respiratory syndrome virus (MERS)[27].

▪ **Monocyte and macrophage dysregulation:** severe COVID-19 is associated with an expansion of classical monocytes (CD14$^+$CD16$^-$), which acquire a more pro-inflammatory phenotype in tissues and the loss of non-classical monocyte populations (CD14$^-$CD16$^-$), generally seen as anti-inflammatory cells with functions related to tissue repair and vascular homeostasis[37]. The recognition of damage-associated molecular patterns (DAMPs) or pathogen-associated molecular patterns (PAMPs) by pattern recognition receptors (PRRs) of macrophages elicits a massive secretion of pro-inflammatory cytokines[38]. In severe COVID-19, macrophage showed a diminution of human leukocyte antigen – DR (HLA-DR) expression[39], indicating an impaired antigen presentation that has been associated with T-cell suppression in prolonged inflammation states[40].

▪ **Cytokine storm:** detection of SARS-CoV-2 RNA by PRRs in infected cells activates the signaling cascade of nuclear factor – κβ (NF-κβ) and interferon-regulatory factor 3/7 (IRF3/7)[41–43]. This event results in the massive secretion of pro-inflammatory molecules

,including tumor necrosis factor α (TNF- α), IL-6, interferon γ-induced protein (IP)-10, monocyte chemoattractant protein (MCP)-1, macrophage inflammatory protein (MIP)-1α and Regulated upon Activation, Normal T Cell Expressed and Presumably Secreted (RANTES)[44,45]. These pro-inflammatory molecules attract several immune cells to the tissue as T-cells, NK cells, DCs, macrophages or natural killer T-cells (NKT) that elicit a second wave of cytokines within seven days after the infection[46] accompanied by lymphopenia, suggesting an innate cell origin of the cytokine storm[27].

1.4.2.   Respiratory manifestations

The lung is possibly the most impacted organ by SARS-CoV-2 infection and severe pneumonia is the most common COVID-19 feature[47]. SARS-CoV-2 may infect the mucosa of the upper respiratory track or the bronchial and alveolar epithelial cells in the lower respiratory track, given the fact that ACE2 is widely express in different cell types within the respiratory system[48].

Alveolar damage pattern observed in severe COVID-19 is related to an acute respiratory distress syndrome (ARDS) that occurs in two phases[49]:

- **Exudative phase:** where the host immune system recruits proinflammatory cells to the tissue that produce low levels of antiviral cytokines (IFN) but high levels of pro-inflammatory molecules (IL-1B, IL-6, TNF) and chemokines[50]. Monocytes increase capillary permeability, neutrophils migration and the consequent damage to pneumocytes and endothelium, named diffuse alveolar damage (DAD)[49].

- **Proliferative phase:** leads to parenchymal remodeling and tissue fibrosis[51]. Both phases can take place simultaneously in different histopathological regions. Deep venous thrombosis and pulmonary embolism rapidly worsen lung damage and trigger respiratory failure[51].

1.4.3.   Extrapulmonary manifestations:

Non-pulmonary cell types also express ACE2 and are susceptible to be infected by SARS-CoV-2, causing clinical manifestations outside the lung:

- **Cardiovascular system:** the pathophysiology underlying cardiovascular damage in severe COVID-19 is probably multifactorial and may include direct infection of myocytes, endothelial damage and systemic-inflammatory response syndrome (cytokine storm)[52] that

can cause: acute coronary syndromes, cardiomyopathy, cardiogenic shock and especially myocardial injury (20-30% of hospitalized patients), among others[53].

- **Liver:** liver dysfunction was observed in more than 50% of severe COVID-19 patients and hepatic steatosis (aberrant accumulation of fat lipids) is frequently found in those patients. Direct damage to biliary ducts by infection of ACE2-expressing cholangiocytes, lymphocyte infiltration, Kupffer cell proliferation and cytokine storm have been cited as some putative contributors to liver damage[54,55].

- **Kidney**: acute kidney injury (AKI) can be observed in critically ill patients while proteinuria and haematuria have been observed in 43% and 26% of severe patients, respectively. Histopathological studies revealed the presence of SARS-CoV-2 infected cells within the renal system, endothelial damage, lymphocytic infiltration and erythrocyte aggregation. Cytokine storm and deposition of immune complexes have also been suggested as mechanisms leading to renal damage[56].

- **Nervous system:** over a third of COVID-19 patients developed neurological symptoms affecting both the central nervous system (CNS) and peripheral nervous system (PND) as well as skeletal muscles[57]. Headache, dizziness, myalgia and fatigue, anorexia, anosmia and ageusia are some of the most common symptoms. SARS-CoV-2 infection, even in milder forms, has been associated with microglial reactivation and myelinating impairment[58]. In addition, direct viral invasion of neural parenchyma and neuroinflammation derived from the systemic cytokine storm can affect the brain vasculature and blood-brain barrier and have both been proposed as potential causes of nervous system damage[52].

- **Coagulation:** Life-threatening thrombotic complications are common among COVID-19 hospitalized patients[59] and elevated levels of D-dimer and fibrinogen have been linked to worse mortality rates[60]. A vicious cycle of increased ACE2 expression in endothelial infected cells and the consequent endothelialitis could be the cause of such blood hypercoagulability[52].

1.4.4. Long COVID or Post-acute sequelae of COVID-19 (PASC)

By current definition, PASC patients suffer from COVID-19 related pathologies including myopathy, neuropathy, cardio-respiratory impairments, cognitive impairments or a

combination of them for more than 12 weeks[61]. Symptoms include fatigue, dyspnea, headache, cognitive impairments, cough, joint and chest pains, mood alterations, palpitations, excessive bruising, problems with coagulation, alterations within the gastrointestinal system, smell and taste dysfunction and myalgia, among others[62]. More than 70% of COVID-19 patients requiring hospitalization experienced at least one symptom for longer than six months after the infection[63]. However, PASC can occur also to people with milder or asymptomatic forms of acute COVID-19 and women show generally a higher predisposition[64].

At least four different mechanisms have been postulated to explain PASC etiology:

- **Viral reservoirs and non-infectious viral fragments:** SARS-CoV-2 virions or viral fragments could be seeded in immune-privileged sites expressing ACE2 (eye, testis, placenta, central nervous system) leading to prolonged immune activation[65].

- **Prolonged COVID-19-associated cell exhaustion:** T and NK cell exhaustion observed during the acute phase of infection, along with broad tissue injury might lead to the accumulation of senescent cells and inflammation across the body, causing immune dysfunction[65].

- **Viral-induced autoimmunity:** anti-SARS-CoV-2 antibodies can cross-react with host proteins and induce auto-reactive responses. Anti-neuronal, anti-phospholipids and anti-IFN-I reactive auto-antibodies have been described in patients with COVID-19 and may explain part of the spectrum of PASCs symptoms[66].

- **Metabolic reprogramming:** chronic fatigue described in PASC patients could be related to mitochondrial dysfunction caused by several SARS-CoV-2 proteins (nsp4, nsp8, ORF9) predicted to interact with mitochondria metabolism and mitochondrial antiviral signaling proteins (MAVS)[67,68].

1.5. Fighting the SARS-CoV-2 infection

1.5.1. Immune response to SARS-CoV-2

Several PRRs contribute to SARS-CoV-2 sensing, including Toll-like receptor 2 (TLR2), which detects the viral E protein, and RIG-I-like receptors (RLRs) such as retinoic acid inducible gene I (RIG-I) and melanoma differentiation-associate protein 5 (MDA5), which can sense SARS-CoV-2 ssRNA[69]. Nevertheless, SARS-CoV-2 nsps dampen the innate immune response by reducing IFN

type I and type III levels, disrupting the orchestration of the immune response against the infection[70]. APCs present SARS-CoV-2 -derived peptides to both CD8^{+} and CD4^{+} T-cells[71], being essential for the development of both cytotoxic CD8^{+} T-cells, CD4^{+} T helper cells and antibody-producing B-cells. Activated HLA-DR^{+} CD8^{+} T-cells have been demonstrated to be increased in patients with severe COVID-19, while HLA-DR^{+} CD4^{+} T-cells are equally observed in asymptomatic, mild and severe patients[72]. Over 80% of the patients had detectable levels of IgM and IgG between 8 and 10 days post-onset of symptoms[73]. However, the peak of the anti-SARS-CoV-2 neutralizing activity is reached earlier in more severe patients than in non-hospitalized individuals[74]. Interestingly, 2-17% of COVID-19 convalescent individuals are non-seroconvertors (NSC). Since NSCs can control SARS-CoV-2 infection in the absence of antibodies, it has been suggested that CD8^{+} T-cells might play a prominent role in the adaptive immunity against SARS-CoV-2[75,76].

1.5.2. Preventive vaccines

Although different control strategies such as full lockdown resulted effective to reduce SARS-CoV-2 spread, the impact of such measures on global economy and social wellbeing highlighted the need to control the pandemic by vaccination[77]. The discovery of neutralizing antibodies from convalescent patients mostly binding the S protein, promptly indicated that S was a promising antigen to develop a preventive SARS-CoV-2 vaccine[78].

By March 2022, 35 different SARS-CoV-2 vaccines have been approved in at least one country using six different platforms[79]:

- **Inactivated virus:** inactivated and live-attenuated vaccines have been developed by using formaldehyde, formalin, β-propiolactone, UV or a combination of such inactivating agents[80].

- **Non-replicating viral vector:** Replication deficient adenoviruses expressing the SARS-CoV-2 S protein have been widely used to develop SARS-CoV-2 vaccines, because of their relatively simple gene edition and their capacity to elicit strong humoral and cellular responses[81].

- **Recombinant proteins:** genes encoding the antigenic components of SARS-CoV-2 (Spike or Spike subunits such as RBD, RBD-Fc or N-terminal domain) have been engineered to resist protein degradation and to be produce in protein expression cell lines. The purified recombinant immunogens are combined with potent adjuvants to trigger proper humoral and cellular responses[82,83].

- **Virus-like particles (VLPs):** VLP based vaccine are generated by transient transfection of the S gene of SARS-CoV-2 in *N. benthamiana* plants using *A. tumifaciens* transfection. VLP-based vaccines usually trigger broader and more potent immune responses than protein or protein subunit-based vaccines[84]**.**

- **RNA:** mRNA encoding antigenic proteins/immunogens are synthesized *in vitro* using phage RNA polymerase and optimized by containing 5' and 3' untranslated regions (UTRs), 5' cap and 3' poly(A) tail[85]. Moreover, the two approved mRNA-based vaccines Spikevax (Moderna) and Comirnaty (Pfizer/Biontech) contain nucleoside modifications in order to avoid excessive activation of the innate immune system through PRRs recognition[86]. After injection, RNA vaccines reach host antigen presenting cells and express the desired immunogen.

- **DNA:** DNA plasmids are used as vectors to introduce antigens into host cells, expecting them to be expressed in antigen presenting cells (APCs)[87].

As of March 2022, more than 10 billion vaccine doses have been administered[2]. WHO set a goal for all countries to vaccinate at least 10% of the population by September 2021. However, 56 countries -most of them African- were not able to achieve this milestone. Hence, it is likely many of them will not reach the new target of 70% of vaccinated population by mid 2022[88].

2. The human immunodeficiency virus (HIV)

2.1. History of the AIDS pandemic

HIV is a member of the *Retroviridae* family, *Orthoretroviridae* subfamily and *Lentivirus* genus, which consists of enveloped virions that contain two copies of single-stranded positive RNA which is retrotranscribed into double-stranded DNA and integrated into the host genome[89].

First cases of HIV infection were reported as rare opportunistic infections observed in immunocompromised patients in 1981 in Los Angeles[90]. Two years later, the retrovirus causing those acquired immunodeficiencies was isolated by two independent studies, led by Françoise Barré-Sinoussi along with Luc Montaigner and Robert Gallo[91,92]. The discovery of a HIV-related virus with T cell tropism in non-human primates (NHP) suggested a zoonotic transmission as the origin of the acquired immunodeficiency syndrome (AIDS) pandemic[93,94]. HIV can be subdivided in HIV-1 and HIV-2, two subtypes that share similarities including basic gene arrangement, mode of transmission, tropism and clinical outcome: both cause AIDS[95]. However, given its higher infectivity rate, more severe disease progression and worldwide distribution, HIV-1 is the major cause of the AIDS pandemic[95,96]. As a consequence of its spread and evolution in the human population, HIV-1 strains have been classified in M-P groups, where M contains subtypes A-K (except E an I, which are circulating recombinant forms [CRF])[97].

The Joint United Nations Program on HIV/AIDS (UNAIDS) estimates that 79.3 million people have been infected with HIV since the beginning of the pandemic, of which 36.3 million people have deceased of AIDS-related causes. Although the UNAIDS 2020 90-90-90 objectives (90% of people living with HIV (PLWH) diagnosed, 90% of PLWH on antiretroviral treatment (ART), 90% of PLWH with suppressed viral load) have not been reached yet, the number of new diagnoses in 2020 (1.5 million) represent a drop of a half to those registered in 1997 (3 million). Similarly, AIDS-related deaths in 2020 (680000) were reduced to a third when compared to 2004 (1.9 million). Notwithstanding these new promising data, HIV is still one of the biggest global health challenge[98].

2.2. HIV genome and structure

The 9.6kb HIV genome contains ORFs that encode sixteen viral proteins[99–102], some of them with overlapping sequences on different reading frames[103] (Fig. 5). Three of those, group-specific

antigen (Gag), envelope (Env) and polymerase (Pol), are structural polyproteins which are consequently proteolyzed into individual proteins. The core virion and outer membrane envelope are constituted by the matrix protein p17 (MA), the capsid protein p24 (CA), the nucleocapsid p7 (NC), the late assembly protein (p6), encoded in gag, and the precursor glycoprotein Gp160, encoded in the env gene. Gp160 is subsequently split into surface (SU, gp120) and transmembrane (TM, gp41). The three Pol proteins provide essential enzymatic functions: protease (PR), reverse transcriptase (RT) and integrase (IN). Additionally, six accessory proteins are encoded in the HIV genome: transcriptional activator (Tat), regulator of viral gene expression (Rev), viral protein U (Vpu), viral protein R (Vpr), viral infectivity factor (Vif) and negative effector (Nef). Tat is required for viral transcripts elongation, while Rev promotes the export of unspliced viral RNAs from the nucleus. Vpu, Vpr, Vif and Nef can assist in viral replication and mediate evasion of host immune response against HIIV-1 infection[104].
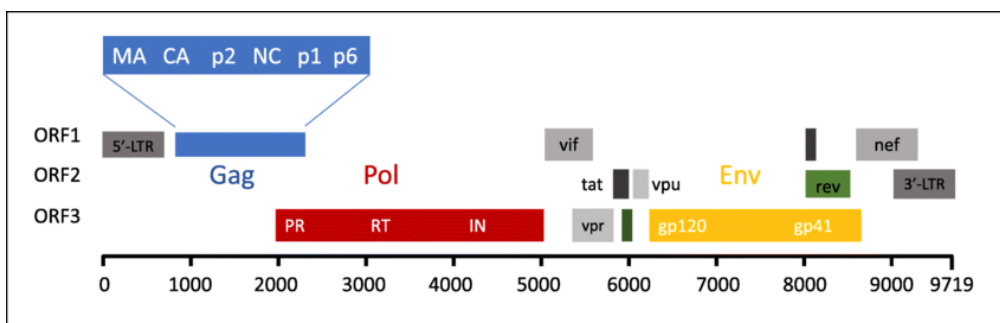
Figure 5. HIV genome organization[105]**.** Long-terminal repeats (LTRs) at the extremes allow viral insertion into host genome. Different colors represent different viral ORF.

HIV is a 120nm spherical virion containing two copies of single-stranded positive RNA[89]. HIV envelope derive from the host plasma membrane from where approximately 14 trimer Env spikes protrude per viron[106,107]. Below the lipid bilayer, an outer p17 protein matrix is surrounding the nucleocapsid, a cone-shaped core composed of CA that encapsulates the RNP complex (viral RNA, NC and viral enzymes such as RT and IN)[100]. Immature virions contain a spherical layer of unprocessed Gag that is cleaved by PR during the maturation of the virion[108] (Fig. 6).

Immature HIV-1 virion   **Mature HIV-1 virion**
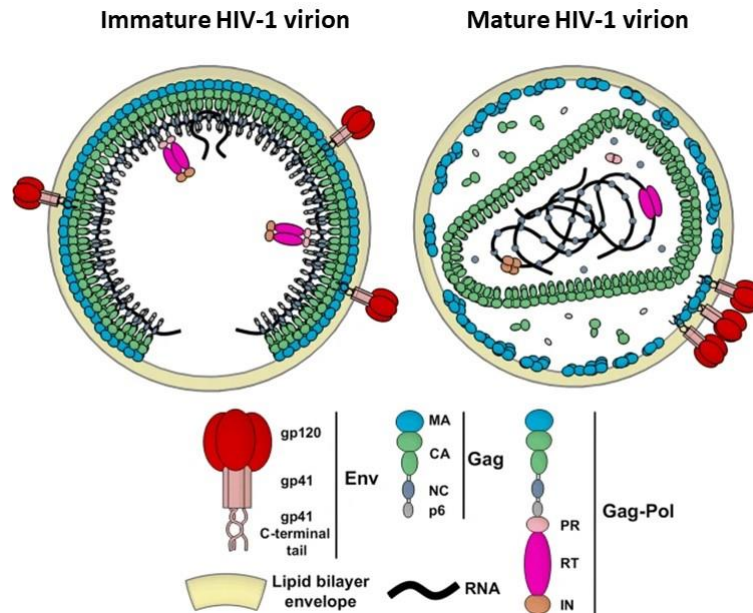
Figure 6. Structure of immature and mature HIV virion[107]**.** Schematic representation of the reorganization during maturation of HIV virions.

2.3. HIV life cycle

The interaction between HIV and host cells requires the interplay of three major components (Fig. 7): i) the trimeric gp160 mature HIV spikes, composed of non-covalently associated gp120 and gp41 trimers; ii) CD4, expressed by T-cells, macrophages or monocytes[37] and iii) C-C chemokine receptor 5 (CCR5)[109] or C-X-C chemokine receptor 4 (CXCR4)[110], which acts as HIV co-receptor. Viral tropism is then defined as the specificity to one or the other co-receptor, although dual-tropic HIV strains have also been reported[111].

Once the viral content is released into the host cell cytoplasm, two models are currently under debate to explain the uncoating and reverse transcription. In a first model, p24-capsid is disassembled and the reverse transcription complex (RTC) is formed. In a second model, the capsid remains intact until reaching the nuclear pore and until reverse transcription has occurred, preventing the dilution of the RT and consequent inefficient reverse transcription[112].

Although some cellular factors contribute to the reverse transcription, HIV carries the RT and RNase H needed to transform its RNA genome into double-stranded deoxyribonucleic acid (dsDNA)[113]. RT is a low fidelity DNA polymerase prone to introducing base mismatches since it lacks the proofreading enzymatic activity. Consequently, the HIV mutational rate is the highest

reported in any biological entity, which is further increased by host cytidine deaminases[114]. This results in an enormous amount of sequence variants within one single individual[115] and allows for a quick evolution of the virus when facing immune system or drug selective pressure[116].

The pre-integration complex (PIC), formed by HIV dsDNA and IN, passes through the nuclear pore complex (NPC) helped by Vpr[117] and IN integrates HIV dsDNA into host's genome preferentially in hotspots of active gene expression[118]. In consequence, HIV forms a latent reservoir in non-dividing cells, where HIV provirus remains silent but maintain the potential the be reactivated upon cell activation or, in the clinical setting, upon specific treatment with latency-reversing agents (LRAs)[119].

When transcription occurs, Tat allows the transcription of full-length HIV mRNA[120] that will migrate to the cytoplasm in a Rev-dependent manner[121]. Gag and Gag-Pol are then translated in the cytosol[122], where they start to oligomerize and bud into new virions while recruiting two chains of viral ssRNA[123]. During virion budding, PR cleaves the Gag-Pol into the functional single proteins (MA, CA, NC, RT and IN)[124]. In the meantime, Env is synthesized in the endoplasmic reticulum and uses the Golgi apparatus vesicle system to migrate to the cell membrane[125] while the host furin protease cleaves Env into gp120 and gp41[126]. Finally, Env is attached at low density on the surface of the virion together with host cell surface proteins[127,128].

In activated cells, the inserted HIV can be efficiently transcribed leading to the generation of ±4000 virions that eventually cause cell death[129]. Infected cells have a lifespan of only 2.2 days, but up to 10×10^9 new virions are generated per day[130].
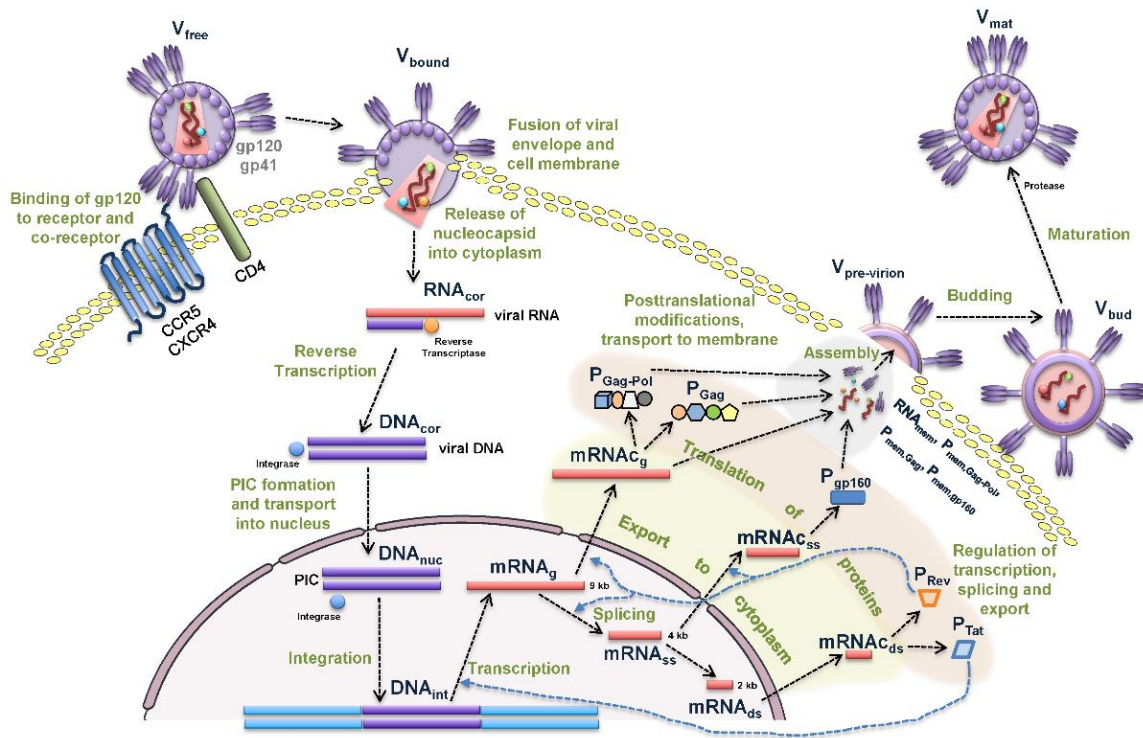
Figure 7. Schematic representation of the HIV life cycle[131]**.** HIV entry is dependent on the binding of Env spikes to CD4 and a coreceptor (CCR5 or CXCR4) on host cell surface. The release of viral content into the cytoplasm is followed by the reverse transcription process. HIV dsDNA is imported in the nucleus and integrates into the host genome. When the viral genome is expressed, RNA migrates to the cytoplasm and is translated into new viral proteins. Two copies of HIV ssRNA, along with viral proteins are assembled in a new virion that buds from the host cell membrane.

2.4. HIV pathogenesis

Sexual transmission is the most common route of HIV infection worldwide, even though other routes such as injection drug use, exposure to contaminated blood via transfusions and mother-fetus exposure exist[132]. The HIV disease course can be divided in three phases: i) acute ii) chronic and iii) AIDS (Figure 8).
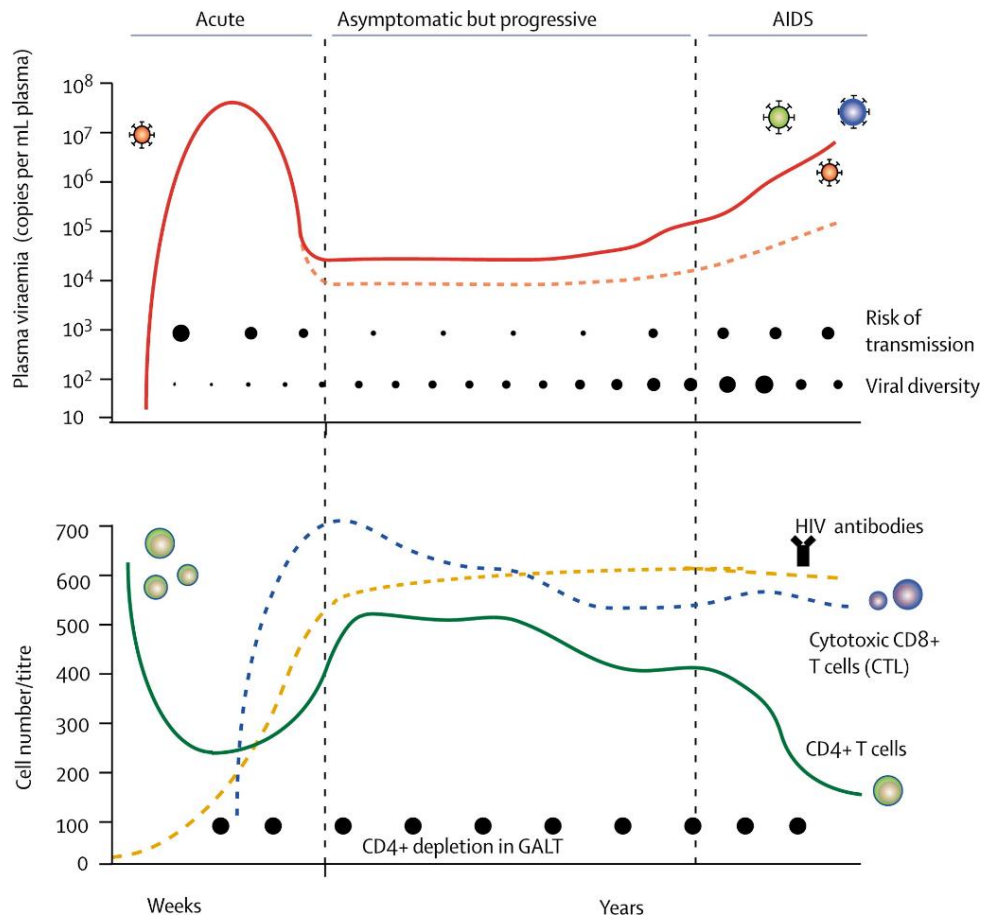
Figure 8. Natural course of HIV infection[133]**.** In the upper graph, evolution of plasma viremia (up) and immune system (bottom) are overlap. In the upper graph, red and orange lines represent different viral set points and risk of transmission and viral diversity are represented with different sized dots. In the bottom graph, CD4+ T-cells (green line), anti-HIV antibodies (yellow line) and cytotoxic CD8+ T-cells (blue line) are shown. Different sized dots represent the depletion of CD4+ T-cell populations within the gut.

2.4.1. Acute HIV infection

HIV needs to breach the mucosal barrier in order to infect susceptible cells, usually achieved due to some degree of epithelial damage during sexual intercourse[134]. Epithelial cells are mostly CD4^{neg}, but tissue-residents Langerhans cells (LC) and CD4+ T-cells are susceptible to be infected by the virus[54]. A modest initial replication takes places in the proximal draining lymph node, from where the virus migrates to gut-associated lymphoid tissue (GALT), the spleen and bone marrow. Consequently, a massive viral replication results in a peak of viremia (10^6 to 10^7 RNA copies/mL, Fig. 8)[133]. Usually, the founder virus (the genetic variant that sets up the infection) presents a CCR5-tropism that allows the infection of macrophages and memory CD4+ T-cells, which are depleted to a large extent[136]. Viral expansion is accompanied by genetic evolution

towards a CXCR4 tropism, which is expressed in distinct T-cell subsets[137]. CCR5-tropic HIV strains infect preferentially effector memory CD4^{+} T-cells (T$_{EM}$), which can partially be restored from central memory CD4^{+} T-cells (T$_{CM}$). Later stages of chronic HIV infection lead to a homeostatic failure where naïve T-cells (T$_{Naïve}$) and T$_{CM}$ cannot replace T$_{EM}$ and effector cell deficiency manifests itself[138]. Even though circulating CD4^{+} T-cells count might recover partially after the acute phase, GALT-associated populations suffer a delay to restore even in the presence of ART[139,140]. The establishment of latent HIV reservoir occurs early during the acute phase of the infection, possibly before viral RNA can be detected in plasma.

Up to 93% of the patients suffer a mononucleosis-like illness during the acute phase of infection named acute retroviral syndrome (ARS). ARS is characterized by retro-orbital pain, muscle aches, sore throat, fever, swollen lymph nodes and non-pruritic macular erythematous rash that last an average of 2 to 3 weeks[141].

2.4.2.   Chronic HIV infection

The transition from acute HIV infection to early-chronic stage can be monitored using Fiebig stages (I-VI)), based on the sequential positivity to clinical diagnostic assays: RNA in plasma by PCR, p24 antigen measured by enzyme-linked immunosorbent assay (ELISA), HIV specific antibodies detected by ELISA and HIV specific antibodies measured by western blot[142].

During early chronic HIV infection, the elicitation of HIV specific humoral and cellular responses (mediated by both CD4^{+} and CD8^{+} T-cells) reduces the acute peak of viremia that diminishes to a steady state (viral set point) some 21-119 days after the primoinfection[143]. Peripheral CD4^{+} counts often recover partially to pre-infection levels but then decrease progressively until the onset of AIDS due to continuous HIV replication on target cells and failure of the CD4^{+} memory T-cells homeostasis[144,145].

Chronic HIV infection usually lasts years (10 years on average) and is characterized by the continuous systemic inflammation and immune activation that leads to a progressive exhaustion of the immune response. This immune burnout is reflected by the increased expression of exhaustion markers (such as PD-1, LAG-3 or Tim-3) on both CD4^{+} and CD8^{+} T-cells[146]. The depletion and dysfunction of CD4^{+} T-cells over years, which play a crucial role in the orchestration of the immune response, result in the onset of AIDS[147].

2.4.3.   AIDS

AIDS is defined as a CD4^{+} cell count of <200 cells/µL and/or the apparition of malignancies and opportunistic infections by other viruses, bacteria, fungi and parasites that are generally not life-threatening in non-immunocompromised individuals[148]. After AIDS diagnose, the survival rate of patients who do not receive ART is below 50% after 2 years and below 20% after 6 years[149].

2.5. Fighting the HIV infection

2.5.1.   Immune response to HIV: natural control

A small percentage of the individuals (5-8%), named long-term non-progressors (LTNP), does not develop AIDS over the years and are capable of maintaining CD4 counts[150]. Of those, controllers (C) are defined as individuals with stable levels of viremia below 2000 HIV RNA copies/mL. Further categories split C into elite controllers (EC) and viremic controllers (VC), with <50 HIV RNA copies/mL or 50-2000 HIV RNA copies/mL, respectively[151].
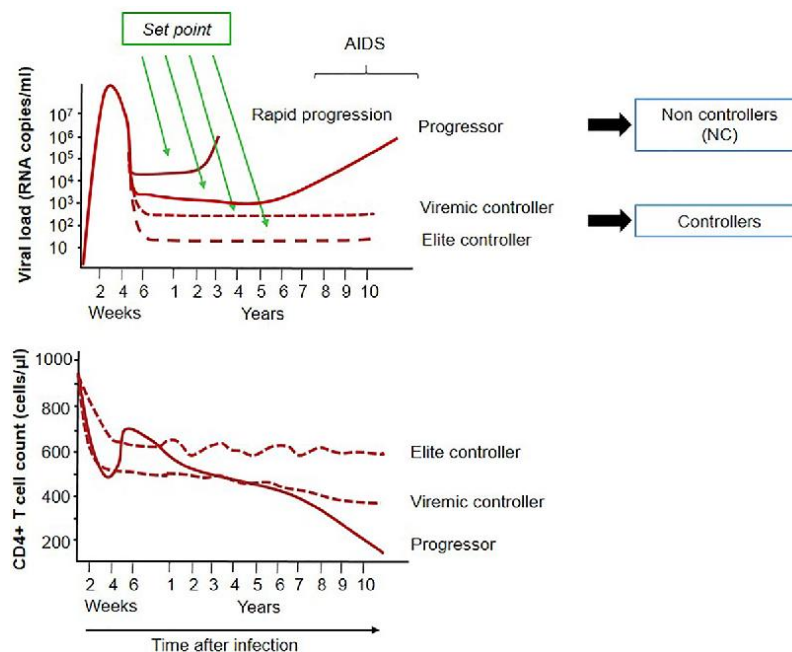
Figure 6. HIV disease progression in different groups of patients[152]. HIV viremia (up) and CD4^{+} T-cell count (bottom) in progressors (red lines) and controllers (elite controllers and viremic controllers, dotted lines).

The characterization of this natural immune-mediated control may allow to identify effective immune responses[153] and has become one of the main areas of HIV research. Unfortunately, no study has reported a unique, and functionally relevant immune correlate of viral control. HIV infection suppression might depend on several factors, including immunological and non-immunological features[154]:

Natural host suppression of HIV infection has been associated with some immunological features:

- **Innate immunity:**
  - Natural killer (NK) cell function: the combination of specific NK cell Killer Ig-Like Receptors (KIRs) and HLA CLASS I alleles have been associated with slower progression to AIDS. This has been shown for KIRDL1 and KIR3DS1, in combination with *Bw4* HLA-B alleles (encoding isoleucine at position 80)[155–157]. The relevance of NK mediated responses in LTNP will be further detailed below.
  - Antigen presenting cells (APC): when comparing EC with HIV progressors and uninfected individuals, circulating myeloid dendritic cells (mDC) maintain better antigen-presentation properties promoting increased proliferation of autologous T-cells and secreting lower levels of pro-inflammatory cytokines but augmented levels of interferon γ (IFN-γ)[158,159].
- **Adaptive immunity:**
  - CD4+ T-cells: EC have been reported to better preserve the central memory compartment of CD4+ T-cells expressing C-C chemokine receptor type 7 (CCR7) capable of migrating to lymphoid organs and with higher activation level than progressors[160]. The role of polarized CD4+ T-cells mediated responses in natural control of HIV will also be detailed further in the following section.
  - CD8+ T-cells: Specific HLA class I genotypes have been associated with HIV disease control by inducing efficient cytotoxic CD8+ T-cell responses (CTL or Tc)[161], but they only account for 10-15% variability of the infection course in untreated hosts[162]. Moreover, the relative contribution of different CTL specificities to overall virus control remains controversial due to its high variability among HIV controllers[163,164]. The contribution of polarized CD8+ T-cells mediated responses in natural control of HIV is only emerging and is a central part of this thesis (see below).
  - Humoral responses: passive immunization with broadly neutralizing antibodies (bnAb) has shown compelling clinical efficacy[165], especially when using structurally

engineered antibodies. These studies have shown that both neutralizing, and non-neutralizing HIV-specific antibodies can trigger additional antiviral effector functions, including Fc-mediated mechanisms such as antibody-dependent cellular cytotoxicity (ADCC)[166]. However, naturally-induced neutralizing antibodies seem to have a limited capacity to control established viral replication, and broadly neutralizing antibodies are only elicited in a minority of infected individuals. Furthermore, their presence is generally associated with increased HIV replication and diversity and lags the emergence of viral escape variants[167,168]. Mechanisms that lead to induction and maintenance of humoral responses with effector functions is less well understood.

Moreover, the physiological relevance of the innate and adaptive immune response in HIV infection control is further confused because it may also rely on non-immunological factors[154] (Fig. 10):

- **Viral factors of attenuated virus:**
  - Deletions on key regulatory genes: mutations in regulatory proteins, such as Vif or Nef, are more frequent in LTNP[169]. Indeed, the loss of Nef's capacity to downregulate human leukocyte antigen (HLA) class I would increase the susceptibility of infected cells to be targeted by cytotoxic CD8^{+} T-cells[170].
  - Decreased replicative capacity: HIV variants with Gag, Pol and Env proteins are more frequent in EC. Additionally, cellular responses can also reduce viral replication capacity by selecting mutations with a replicative fitness cost[171].
- **Susceptibility of target cells:**
  - Genetic polymorphisms that affect viral entry: the 32-base-pair deletion in CCR5 receptor (CCR5-Δ32) homozygosity confer resistance to CCR5-tropic HIV[171], while CCR5/ CCR5-Δ32 heterozygosity is associated with lower levels of CCR5 expression and slower HIV disease progression[172]. Other mutations in promoter regions of genes encoding chemokines (RANTES, MIP-1α, MIP-1β, MIP1αP and DC-SIGN, for instance) partially protect cells from being infected[173].
  - Host restriction factors that inhibit viral replication: cells express intracellular proteins that counteract viral replication, including HIV. Of those, APOBEC3G, tetherin and SAMHD1 have been linked to LTNP phenotype[150,174]. However, the specific mechanism of HIV replication restriction in target cells from LTNP is still missing[175].

- ▪ Inactivation of apoptosis pathways: previous studies reported T-cells from EC to have a differently regulated FOXO3a pathway with increased capacity to persist continuous activation compared to progressors, revealing an inherent resistance to apoptosis[176].
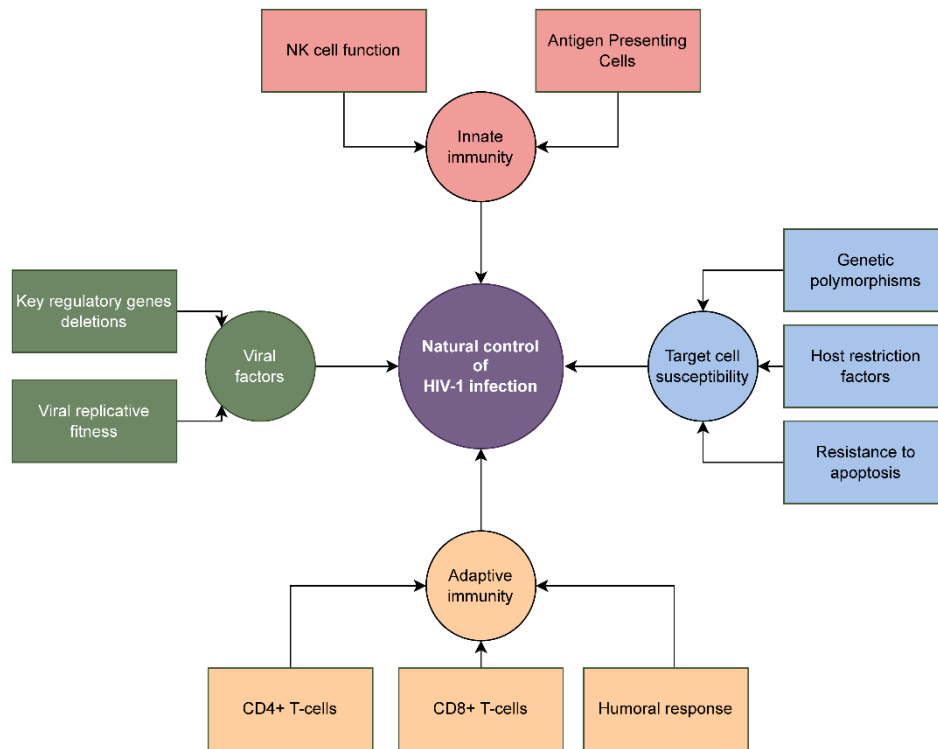

Figure 10. Natural control of HIV: a multifactorial event. Adapted from[154].

3. The innate cellular response: Natural killer (NK) cells

Natural killer cells are the most dominant innate lymphoid cell (ILC) subset and represent 5-10% of peripheral PBMCs. NK cells play pivotal roles in immunosurveillance against infected cells and malignancies. NK cell activity rests on the balance of both germ-line encoded activating and inhibitory receptors that spare "self" from "non-self" signals: the so-called missing-self paradigm[177].

3.1. Development and maturation

NK cells are originated from hematopoietic stem cells (HSCs) and follow a stepwise maturation process into common lymphoid precursors (CLPs), preNK precursors (preNKPs), NK precursors (NKPs), immature NK cells (iNKs), mature NK cells (mNKs) and memory or adaptive NK cells. This process is driven by the interaction with stromal cells, growth factors, cytokines and other soluble molecules[178]. Stage-specific surface proteins are summarized in Fig. 11.

NK cell maturation is defined by the expression of CD56 and can be divided into two different subsets based on the level of CD56 expression (CD56^{bright} and CD56^{dim})[179]. Two functional features, regulatory versus cytotoxic capacity, as well as its compartmentalization further differentiate CD56^{bright} from CD56^{dim} NK cells. Depending on the condition of the stimulation, CD56^{bright} are capable of producing type 1 (IFN-γ and/or TNF-α) or type 2 (IL-10 and/or IL-13) cytokines[180] and hence have been usually considered as cells with a regulatory function[181,182]. CD56^{dim} NK show high expression level of CD16 (which is a FcRIII receptor) and increased contents of granzymes, perforin and lytic granules. This cytolytic repertoire allows CD56^{dim} to perform antibody-dependent cellular cytotoxicity (ADCC) very efficiently, whereas CD56^{bright} have been usually considered to have a restricted killing capacity[183,184]. Nevertheless, CD56^{bright} showed a comparable cytotoxic activity against autologous activated CD4$^+$ T-cells that was regulated by the HLA-E/NKG2X axis[185] and expressed high amounts of perforin and granzyme K when cocultured with activated autologous T cells[186]. Moreover, the CD56^{brght} and CD56^{dim} dichotomy is also observed in tissue distribution as they express a divergent variety of chemokine receptor repertoire and adhesion molecules, resulting into different migration routes[180]. CD56^{bright} only represents 8-15% of peripheral blood total NK in healthy conditions[187], but they are enriched in most human tissues, including secondary lymphoid organs such as lymph nodes and tonsils, where they represent the majority of the NK cell population[188,189]. Furthermore, a relatively new memory-like CD56^{dim}CD16$^+$CD57$^+$ NK cell subset has been characterized, which has a senescent-like profile. These "adaptive" NK cells have been reported

to expand after HCMV infection and have an imprint in the *IFNG* gene locus that triggers a strong IFN-γ secretion when stimulation occurs through NKG2C/CD94 heterodimer[190,191]. Finally, a fourth group of unconventional CD56^{neg} NK cells has been identified during chronic viral infections such as EBV, CMV or HIV, presenting an unresponsive profile[192,193].

preNKPs	NKPs		Immature NK cells	Mature NK cells			Adaptive NK cells
CD34 (+)	CD34 (+)	CD34 (+)	CD34 (-)	CD34 (-)	CD34 (-)	CD34 (-)	CD34 (-)
CD38 (-)	CD38 (+)	CD7 (+)	CD7 (+)	CD7 (+)	CD7 (+)	CD7 (+)	CD7 (+)
CD133 (+)	CD7 (+)	CD45RA (+)	CD45RA (+)	CD244 (+)	CD244 (+)	CD244 (+)	CD117 (-)
CD45RA (+)	CD10 (+)	CD244 (+)	CD244 (+)	CD117 (+/lo)	CD117 (lo/-)	CD117 (lo/-)	CD127 (-)
CD244 (+)	CD133 (+)	CD117 (+)	CD117 (+)	CD127 (-)	CD127 (-)	CD127 (-)	CD122 (+)
CD117 (-)	CD45RA (+)	CD127 (+)	CD127 (-)	CD122 (+)	CD122 (+)	CD122 (+)	CD244 (+)
IL1R1 (-)	CD244 (+)	CD122 (+)	CD122 (+)	IL1R1 (+/lo)	IL1R1 (lo/-)	IL1R1 (lo/-)	IL1R1 (lo/-)
	CD127 (+)	IL1R1 (+)	IL1R1 (+)	NKG2D (+)	NKG2D (+)	NKG2D (+)	NKG2D (+)
	CD122 (-)	NKG2D (-)	NKG2D (-/+)	CD335 (+)	CD335 (+)	CD335 (+)	CD335 (+)
	CD117 (+)	CD335 (-)	CD335 (-/+)	CD337 (+)	CD337 (+)	CD337 (+)	CD337 (+)
	IL1R1 (-)	CD337 (-)	CD337 (-/+)	NKG2A (+)	NKG2A (+)	NKG2A (+/-)	NKG2A (+/-)
		NKG2A (-)	NKG2A (-)	NKG2C (-/+)	NKG2C (-/+)	NKG2C (-/+)	NKG2C (+)
		NKP80 (-)	NKP80 (-)	NKP80 (-)	NKP80 (+)	NKP80 (+)	NKP80 (+)
		CD161 (-)	CD161 (-/+)	CD161 (+)	CD161 (+)	CD161 (+)	CD161 (+)
		CD16 (-)	CD16 (-)	CD16 (-)	CD16 (-)	CD16 (+)	CD16 (+)
		CD57 (-)	CD57 (-)	KIR (-)	KIR (-)	KIR (-/+)	KIR (+)
		CD56 (-)	CD56 (-)	CD57 (-)	CD57 (-)	CD57 (-)	CD57 (+)
				CD56 (bright)	CD56 (bright)	CD56 (dim)	CD56 (dim)

Figure11. Common schema of human NK cells development and maturation (adapted from[177]). Six distinct developmental stages have been defined. CD244 is expressed only in preNKPs. Two stages corresponding to NKPs express CD7 and CD127 but with different levels of CD122. the expressions of NKG2D, CD335 (NKp46), CD337 (NKp30), and CD161 (NK1.1) is observed in iNKs. CD56 peak determine the entry into mNKs, first CD56^{bright} and then CD56^{dim}CD16^{+} NK subsets. Adaptive NK cells are defined by high levels of CD57 and NKG2C.

3.2. NK cell receptors

NK-cell stimulation is the result of a balance between the activating and inhibitory signals they are exposed to, signals that can vary depending on the nature of the binding cell[194]. NK cells express diverse receptors, which usually use classical or non-classical HLA-class I molecules as ligands (Fig. 12). According to their function, they can be divided in inhibitory and activating receptors:

- **Inhibitory receptors:** are responsible of the tolerance to self and the avoidance of NK mediated killing of healthy cells, but elicit NK activation if they cannot detect MHC molecules presenting canonical self-derived peptides on the surface of target cells (what is called "the missing self")[195]. Inhibitory receptors contain tyrosine-based inhibitory motifs (ITIM) that dephosphorylate downstream signaling substrates and result in an inhibition of the signaling cascade[196].

- **Activating receptors:** trigger NK cells function upon recognition of MHC molecules presenting non-self-peptides[197]. However, except for CD16, responsible for antibody dependent cytotoxicity (ADCC), activating receptors need to associate with the immunoreceptor tyrosine-based activating motif (ITAM) on the DNAX activation protein (DAP12), which phosphorylates downstream signaling substrates and transduces an activatory signal to the N[195,198].

3.2.1.   Immunoglobulin-like receptor super family

- **Killer cell immunoglobulin receptors (KIRs):** are type I transmembrane glycoproteins. They can have two or three extracellular domains (named as 2D or 3D) and can act as inhibitory receptors when having a long tail (L) with ITIM, or activating if they have a short tail (S) that associates with DAP12[199]. KIRs bind to classical HLA CLASS I (-A, -B, -C) molecules and are highly polymorphic.

- **Leukocyte immunoglobulin-like receptors (LILRs):** can be categorized into class A (LILRA), with activating functions via ITAM domains, and class B (LILRB), with inhibitory functions through ITIM[200]. Despite the initial reports, LILRs can bind a broad spectrum of ligands, including classical and non-classical HLA CLASS I, but also angiopoietin-like (ANGPTL) protein family, β-amyloid or myelin[201].

- **Natural cytotoxic receptors (NCRs):** NKp30 and NKp46 are expressed by all NK cells, while NKp44 expression is limited to activated NK cells[202]. The extensive and heterogeneous list of NCRs ligands includes surface glycoproteins and proteoglycans and nuclear proteins that can be exposed in stressed cells[37,203–205].

3.2.2.   C-type lectin-like receptor superfamily

The C-type lectin-like receptor superfamily (NKG2) are NK receptors and most of its members (NKG2A, B, C, E and H) bind non-classical HLA class Ib molecules (including HLA-E) after forming heterodimers with CD94. CD94/NKG2A or B heterodimers have an inhibitory effect in NK function, while heterodimers with NKG2C, E or H have an activating effect. Of note, NKG2C expression is increased at later stages of NK cells maturation and binds HLA-E with lower affinity than NKG2A[206]. The biology of NKG2B, E and H is less well understood. NKG2H, for instance, have been reported to be expressed preferentially on the surface of a small population of T-cells rather than NK cells[207]. On the other hand, NKG2E lacks the transmembrane domain and is found in a cytoplasmatic form, its role in NK activity still needs to be explored[208]. NKG2D is the only member of the NKG2 family whose ligand is not a non-classical HLA class Ib, but HLA CLASS I chain-related molecules (MICA and MICB), and does not form an heterodimer with CD94[209].
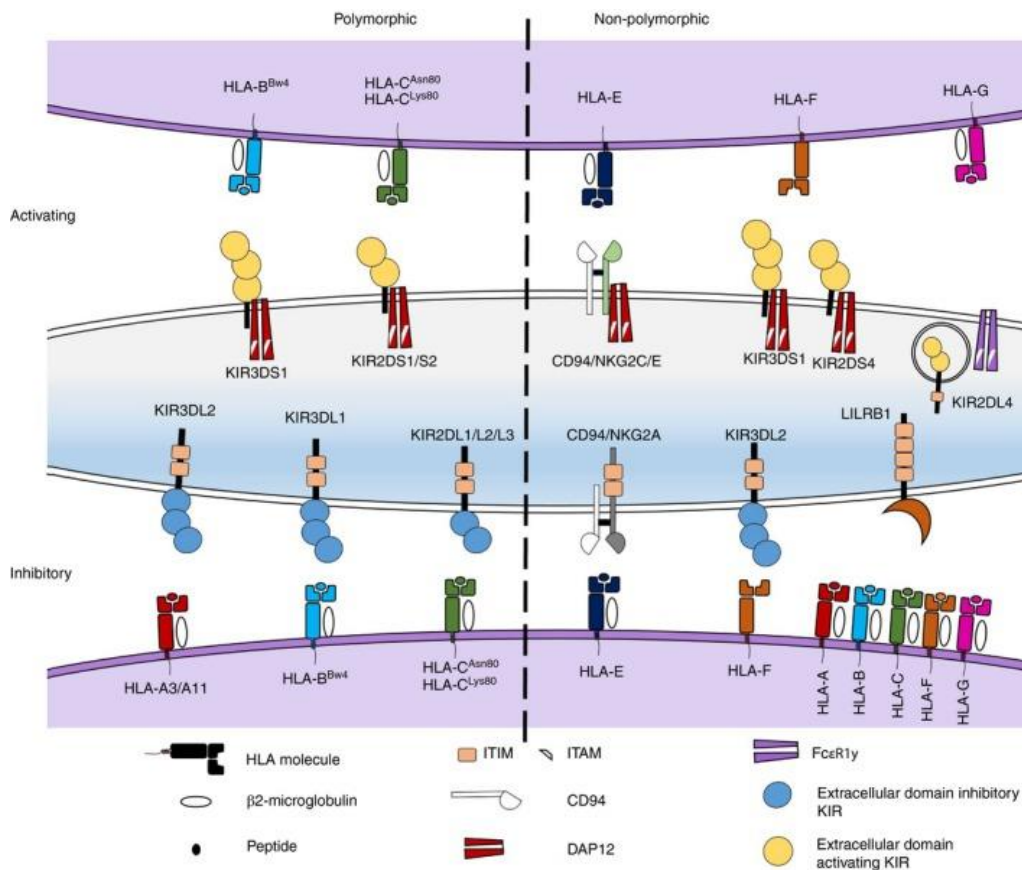

Figure 12. Repertoire of activating and inhibitory NK cell receptors binding classical and non-classical HLA CLASS I molecules[199]**.**

3.3. Educating NK cells: the licensing

The interaction between HLA class I-expressing cells presenting self-ligands and inhibitory receptors in NK cells is a process referred to as "licensing". Licensed-NK cells are more responsive to activation and eliminate more efficiently HLA class I deficient target cells[210]. Indeed, the specific association between HLA CLASS I and KIRs alleles affect the NK cell mediated response to viral infections. Bw4 and Bw6, two HLA-B motives, seem to be particularly relevant in NK licensing since Bw4 homozygosity, for instance, is associated with increased NK cell potency compared to Bw4/Bw6 heterozygosity or Bw6 homozygosis[211]. Of note, NK cell education throughout KIR and HLA class I have been postulated to be related to distinct HIV disease course in children[212].

3.4. The HLA-E/NKG2X axis

HLA-E is a non-classical class Ib histocompatibility molecule with very limited polymorphism. Only two alleles (HLA-E*01:01 and HLA-E*01:03) have been demonstrated to be properly expressed on the cell surface and together cover >99% of the global allelic diversity of HLA-E[213]. Structural differences between these two dominant HLA-E alleles are very limited since only one change, in position 107 within the α2 domain, differentiates HLA-E*01:01 (arginine) from HLA-E*01:03 (glycine)[214]. The presence of a positive amino acid at this position in HLA-E*01:01 has been proposed as an explanation for the lower surface stability of HLA-E*01:01 compared to HLA-E*01:03[215]. In addition, this change may also cause a subtle structural shift in the binding-cleft α2 helix resulting in an altered repertoire of presented epitopes. HLA-E was first described as part of the innate immune system and was reported to inhibit NK mediated lysis of healthy cells by presenting peptides derived from the leader sequences of HLA class I molecules to the CD94/NKG2A heterodimer[216]. Growing evidence now supports a role of HLA-E in the adaptive immune response through the presentation of pathogen-derived epitopes to specific CD8+ T-cells[217,218]. Given its limited allelic diversity, targeting HLA-E epitope presentation has been considered for developing universal immunotherapies and vaccines[219].

3.5. NK cell mediated response to infection

NK cells unquestionably play a major role in the defense against viral infections, as evidenced by NK cell depletion or dysfunction, which results in a dramatic increase in the susceptibility to viral infections[220]. Furthermore, the importance of the NK response in the control of viral infections has been demonstrated for multiple pathogens, including Epstein-Barr virus (EBV)[221], human cytomegalovirus (HCMV), dengue virus[222] and human hepatitis virus C (HCV)[223].

In normal conditions, a prominent stimulation through inhibitory receptors of potential target cells induces NK cells unresponsiveness. However, if the balance between inhibitory and activating signals is shifted in favor of the activating signals, the NK response is activated[224]. NK effector function is mediated by at least three different mechanisms: 1) release of cytokines, 2) release of cytolytic granules and 3) induction of cell-death mediated by surface receptors[225–227]. Nonetheless, novel mechanisms to control viral replication have been reported, such as the release of microvesicles with cytotoxic activity[228] and the secretion of soluble molecules that effectively block viral entry[229]. Although NK cells were first described as a part of the innate immune system, they are capable of performing additional functions beyond the killing of infected cells, acting as link between the innate and the adaptive immune response[230]. In fact, NK cells, especially CD56^bright NK cells, can either prime or kill hyperactivated macrophages, maturing dendritic cells, activated B-cells as well as CD4+ and CD8+ T-cells, shaping thereby an important portion of the immune response[231–233].

Several viruses have developed mechanisms to evade NK killing of infected cells, such as the expression of peptides mimicking human canonical self-repertoire to effectively bind inhibitory NK receptors[234] or the modulation of surface molecules like HLA to hamper NK recognition via the missing self-axis[235]. For instance, HCMV-derived UL40 peptide presented through HLA-E induces an inhibitory signal through CD94/NKG2A recognition[236] and HIV p24 epitopes presented in HLA-C molecules are recognized by inhibitory KIRs[237].

3.5.1. Role of NK cells in SARS-CoV-2 infection

NK cell depletion and exhaustion has been related to COVID-19 severity[28,238]. Immunophenotyping of NK cells in COVID-19 patients revealed decreased numbers of CD56^dim and CD56^bright NK cells in patients with severe disease course and with increased basal level of cytokine secretion within the CD56^bright subset[239]. Dramatically increased plasma levels of pro-

inflammatory cytokines, including IL-6 during the cytokine storm in COVID-19 patients[32] have been associated with attenuation of perforin and granzyme B production in NK cells, limiting their cytolytic capacity and preventing the elimination of infected and hyperactivated immune cells[240]. Of note, anti-IL-6 monoclonal antibody (mAb) tocilizumab have been shown to restore NK cell functionality *ex vivo*[33].

The HLA-E*01:01 allele has also been reported as a risk factor for severe COVID-19, as has the deletion of the KLRC2 gene which encodes NKG2C receptor [241]. These findings indicate that the regulation of the HLA-E/NKG2X axis could be relevant in the NK-mediated response to SARS-CoV-2 infection. In addition, SARS-CoV-2 Spike-1 has been reported to diminish NK cell degranulation and IFN-γ production, also via HLA-E/NKG2A axis. However, the specific HLA-E restricted Spike-1 derived epitopes involved in this process have not been described[242]. Adaptive CD57+NKG2C+ NK were also increased in severe COVID-19 patients, highlighting the role of HLA-E/NKG2X mediated NK cell responses in COVID-19[239]. Hence, COVID-19 severity might be associated with a change in the NK cell subset landscape, reflected by a shift towards a more exhausted profile. In that scenario, increased HLA-E expression levels in severe COVID-19 patients as well as a reversion of the NKG2A/NKG2C axis could lead to a reduced capacity to properly eliminate infected cells.

Vaccines delivered with viral vectors have also demonstrated to benefit NK cell function[243] by inducing a prolonged effector profile[244]. Vaccine booster injections triggered stronger cytolytic activity with diverse homing and adhesion surface molecules expression, pointing out a imprinting on NK cell repertoire after vaccine prime[245]. Although some authors suggested a bystander effect that depended on antigen-specific CD4+ T-cell response[246], specific vaccine formulations and adjuvants contribute to promote NK cell response[247]. Yet, the effects of mRNA-based genetic vaccines Comirnaty (Pfizer/Biontech) and Spikevax (Moderna) on the innate response remains largely unknown. However, those vaccines also included chemical modification of mRNA nucleotides to avoid pathogen recognition receptor (PRR) sense of ssRNA and consequent excessive immune reaction[86]. Nevertheless, unspecific stimulation of NK cells can happen through the proinflammatory effect of the lipid nanoparticle vehicle that stabilize and deliver such mRNA vaccines[248].

3.5.2. Role of NK cells in HIV infection

The role of NK mediated antiviral response against HIV infection reaches from direct killing of infected cells to the modulation of the overall antiviral response by secreting diverse cytokines and chemokines to shape DC, T and B-cells responses[249] (Fig. 13).

- **Natural cytotoxicity:** significantly higher NK cell mediated cytotoxicity against HLA-null target cells was observed in a cohort of highly HIV-exposed, yet persistently seronegative (HESN) individuals, suggesting a potential role of NK cell function in preventing HIV acquisition[250]. ADCC activity was linked to natural control of the infection in a cohort of EC[251] as well as to the modest protective efficacy of the RV144 HIV preventive vaccine trial[252]. In addition, there is evidence that HIV has developed several mechanisms to avoid NK-mediated lysis of infected cells. First, poliovirus receptor (PVR), who regulates ADCC interacting with the T cell immunoreceptor with Ig and ITIM domains (TIGIT) on the surface of NK cells, is increased in circulating CD4$^+$ T-cells from PLWH[253]. Secondly, macrophages, a possibly important part of the HIV reservoir, are more resistant to NK killing than CD4$^+$ T-cells, probably due to antibody internalization and the expression of NK surface ligands[254].

- **Chemokine and cytokine secretion:** CCL production has been associated with natural resistance to HIV in HESN[250] and reduced mother-to-child transmission[255]. Interestingly, large amounts of chemokines are produced by NK, specially CCR5 ligands (CCL3, CCL4 and CCL5), representing an additional antiviral mechanism by blocking HIV entry[229]. Furthermore, a link between NK cell cytokine secretion and viral control has been suggested by a negative correlation between IFN-γ secretion and viremia in LTNP, but no in primary-infected individuals or typical HIV progressors[256]. Remarkably, increased CD56^{bright} IFN-γ secretion was also reported in HESN compared to healthy controls[257].

- **Shaping the adaptive immune response:** NK cell and DC crosstalk is essential during the development of adaptive responses: primed DCs promote NK cell proliferation, cytotoxicity and IFN-I secretion. In turn, activated NK promote DC maturation by eliminating immature DCs while maintaining mature DCs (DC editing)[258,259]. This immune crosstalk may be impacted by HIV infection as Nef-pulsed DCs have been shown to promote CD56^{bright} activation while reducing the cytolytic capacity of CD56^{dim} [260]. NK cell interaction with B and T cells can potentially induce or suppress the generation of adaptive immune responses by different mechanisms. For instance, certain NK cell cytokines (i.e. IFN-γ) can promote T cell responses, although others (i.e. IL-10) can hamper T-cell function. In addition, NK cells can

compete with T cells for survival cytokines (i.e. IL-2) or directly kill hyperactivated T-cells[261]. On the opposite, B cells elicit NK cell to secrete IFN-γ and, in return, NK cells are thought to favor antibody isotype switching to IgG in a T-cell independent manner through CD40-CD40L attachment[262].

HIV infection also has an impact on NK cell function and phenotype. For instance, the loss of CCR7^{+} CD56^{bright} NK cells was correlated with HIV viral load [263]. In addition, the CD56^{dim} compartment has also reported to be diminished in HIV infected individuals, while an aberrant CD56^{neg}CD16^{dim} NK population with poor cytotoxic capacity increases[263]. Interestingly, those shifts on NK cell landscape appear to be sequential and start early during acute HIV infection[263].
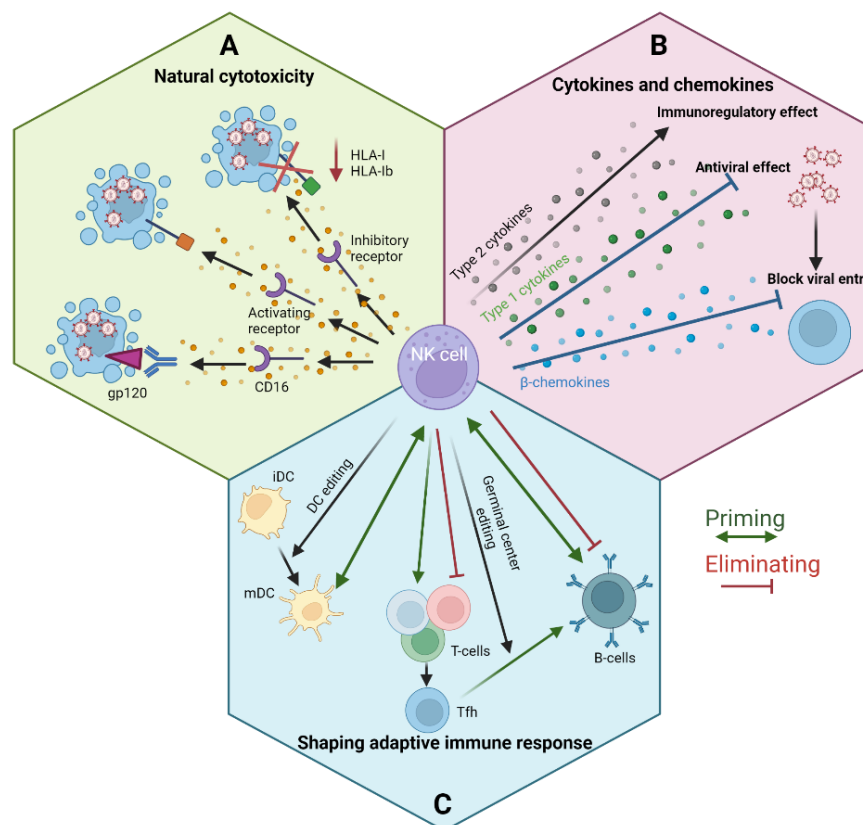
Figure 13. NK cell role during HIV infection[249]. (A) NK cell cytolytic activity can occur after CD16 binding HIV-derived proteins expressed on cell surface (ADCC), recognition of surface ligands by activating receptors or the lack of inhibitory signals. (B) β-chemokines (CCL) secreted by NK cells can block HIV entry. Type 1 cytokines (i.e. IFN-γ) are related to better prognosis, while type 2 cytokines (i.e. IL-10) are related to uncontrolled HIV infection. (C) NK cells edit adaptive immune responses by interacting with dendritic cells, B cells or T cells. NK cells have been demonstrated to eliminate infected CD4^{+} Tfh.

A number of past studies support an important role of HLA-E and NK cells activity also in the context of HIV infection. First, the HIV Nef protein downregulates surface expression of HLA-E,

impairing the recognition of infected cells by either the T cell receptors or NKG2X/CD94, thereby avoiding lysis of the infected cell[264]. Second, five HIV derived epitopes have been reported to be presented by HLA-E: RMYSPVSIL (RL9), PEIVIYDYM (PM9), TALSEGATP (TP9), RIRTWKSLV (RV9)[265] and AISPRTLNA (AA9)[266], while some others have been reported as HLA-E candidates based on elution studies as they only show slight increases of HLA-E stabilization: EKIKALVEI (EI9), MYSPVSILD (MD9), NEEAAEWDR (NR9), QMAVFIHNF (QF9) and YFSVPLDEG (YG9)[265]. However, among them, only AA9 has been shown to have a functional impact on the NK response by increasing the activation of NKG2A^{+} NK cells. This observation suggests that HIV might alter the presented HLA-E peptide repertoire and trigger NK cells degranulation by blocking the inhibitory signal of the NKG2A receptor[266].

3.6. NK cell exhaustion, anergy and senescence

In the context of anti-tumoral immunity, inhibitory ligands such as PD-L1, appear to be the leading cause of NK cell impairment. However, aside from reduced NK cell cytotoxicity and cytokine secretion, there is no established NK cell "exhausted" phenotype[267]. Still, several studies in the cancer field have attempted to classify NK cell dysfunction in three different stages: exhaustion, anergy and senescence, mirroring those of T-cells.

- **Exhaustion:** NK cells from cancer patients showed diminished cytotoxic and cytokine production capacity[268–271]. PD-1, LAG-3, Tim-3 and TIGIT have been suggested as potential surface markers of exhausted NK cell and blocking therapies against PD-1[268,272], TIGIT[269] and Tim-3[273] *ex vivo* rescued NK cell function. However, different studies reported contradictory findings and phenotyping of NK cell exhaustion remains controversial[274].

- **Anergy:** NK cell anergy could take place after insufficient stimulation, which could occur on different levels: NK cell and target cell contact, CD137 activation and IL-2, IL-15 and IL-21 signaling[275].

- **Senescence:** although a proper characterization of NK cell senescence has not been established, it is assumed that they would show a pro-inflammatory senescence-associated secretory phenotype (SASP) with reduced proliferation capacity[267]. In this regard, CD57^{+} CD56^{dim} NK cells (also referred to as adaptive or memory NK cells) showed a decreased proliferative capacity compared to CD57^{-}CD56^{dim} NK cells, but stronger cytolytic activity and IFN-γ secretion when stimulated via CD16, suggesting a terminally-differentiated state[276].

4. The adaptive cellular response: T-cell polarization

4.1. T-cell development and maturation

Long-term protection against infection is mediated by antigen-specific memory populations of B and T- cells[277]. The generation of this memory T-cell subsets is highly dependent on tissue migration and regulated by both epigenetic and metabolic reprogramming[278]. Each memory T-cells subset show a variety of functional properties and tissue distribution that can help distinguish between them[279] (Fig.14).
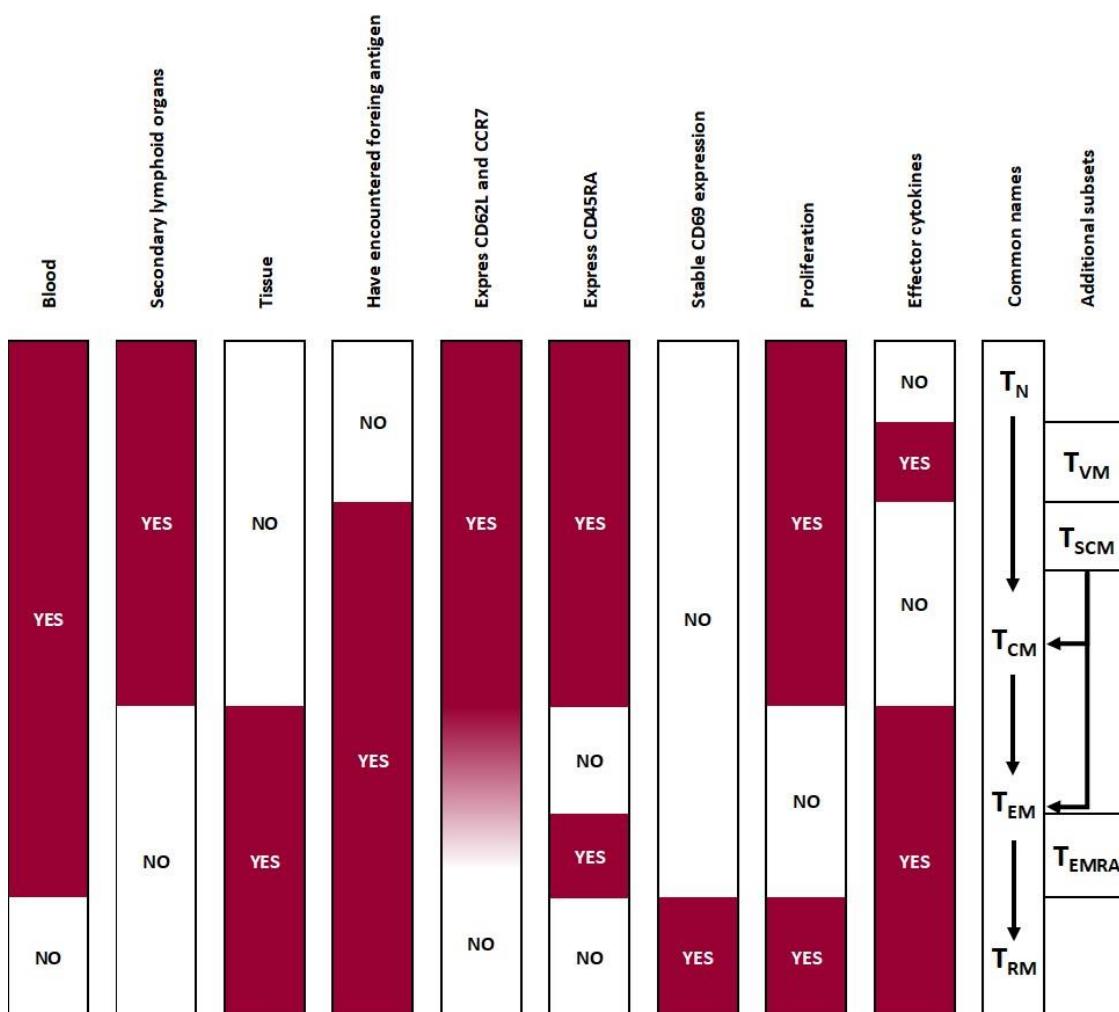
Figure 14. Adapted chart with traits of different memory T cell populations[279]**.** The bars indicated different features that can distinguish specific T cell memory subsets. The three first bars indicated migration capacity, the next three ones indicate phenotypic characteristics focused on molecules associated with trafficking, tissue retention and memory markers, while the last two indicate T-cell effector functions. Naïve T-cells, T_N; Virtual memory T-cells, T_{VM}; Stem cell memory T-cells, T_{SCM}; central memory T-cells, T_{CM}; effector memory T-cells, T_{EM}; CD45RA+ effector memory T-cells, T_{EMRA}; resident memory T-cells, T_{RM}.

After T-cell receptor (TCR)-mediated positive and negative selection in the thymus, immunocompetent and self-tolerant naïve T-cells are generated[280]. These $T_{Naïve}$ cells travel to secondary lymphoid organs in search for antigen presented by DCs and, if they encounter their cognate epitope, they undergo a remarkable expansion, with an up to a 10^5 fold increase in their numbers[281].

T-cell migration mainly relies on two key receptors required for the entry into lymph nodes through high endothelial venules (HEVs), CD62L and CCR7, which show different expression patterns in naïve and memory T-cells. $T_{Naïve}$ are uniform in expressing high levels of both molecules, but memory T-cells lose the expression of CD62L and/or CCR7. This shift allows $T_{Naïve}$ to extravasate from HEV and memory T-cells and enter into peripheral tissues[282]. Circulating memory T-cells were initially classified into two groups: $CCR7^+CD62L^{high}CD45RA^-$ central memory (T_{CM}) and $CCR7^-CD45RA^-$ effector memory (T_{EM}), which expresses CD62L in an heterogenous manner[283]. T_{CM} migrate to secondary lymphoid organs, show an elevated proliferative capacity and produce higher amounts of IL-2, while T_{EM} are directed to peripheral inflamed tissues and produce higher amounts of effector cytokines (including IFN-γ, IL-4 and IL-5) and perforin[284]. Remarkably, *in vitro* experiments reported a decreased expression of CCR7 on T_{CM} surface after antigenic stimulation and suggested that T_{CM} are a source to generate T_{EM}[285].

However, classification of memory T-cells based on a rigid use of the respective markers could be misleading, and several intermediate states have been described. Virtual memory T-cells (TVM) proliferate and elicit cytokine secretion as well as exert cytotoxicity following a similar kinetic as conventional memory T-cells[286]. Stem cell memory T-cells (T_{SCM}) share surface expression pattern with naïve T-cells and have been postulated to keep the multipotency to derive all memory T cell subsets[287]. However, they have many functional characteristics of memory T-cells like high survival rate, self-renewal capacity and potent antitumor responses. $CD8^+$ T_{EM} expressing CD45RA (defined as T_{EMRA}) exhibit reduced proliferation, but higher cytotoxicity than conventional T_{EM}[288]. Non-lymphoid tissue resident memory T-cells (T_{RM}) are terminally differentiated T-cells that do not recirculate into bloodstream or lymph tissues. These T_{RM} ensure accelerated protection from reinfection in barriers sites (mucosae, skin and solid organs) and proliferate efficiently upon infection[289].

Finally, circulating $CD4^+$ and $CD8^+$ T-cells display disparities in terms of memory populations: $CD4^+$ are maintained as $T_{Naïve}$, T_{CM} and T_{EM}, while $CD8^+$ persists as naïve, T_{EMRA} and T_{EM} with few T_{CM} set in lymphoid tissues[290].

4.2. T-cell polarization

T-cells play a central role in the orchestration of the appropriate adaptive immune response against specific pathogen by supporting B-cells and cytotoxic T-cells through cytokine release. After being activated in the interfollicular areas of secondary lymphoid organs by antigen presenting cells (APCs), T-cells differentiate into diverse effector profiles[291]. Of note, different pathogen-specific T-cell clones might lead to different polarized-responses[292]. However, while much is known about CD4 T-cells and their differentiation into different Th subsets (such as Th1, Th2 or Th17)[293], such classification is less evolved for CD8^{+} T-cells. Interestingly, CD8^{+} T-cells have been recently reported to also differentiate into distinctly polarized subsets, characterized by effector functions other than their classical cytotoxic capacity (CTL)[294].

Based on the broad spectrum of effector functions, mostly defined by cytokine production signatures, T-cells are thought to acquire three major polarization profiles: type 1 (CD4^{+} Th1 and CD8^{+} Tc1) characterized by the secretion of IFN-γ, IL-2 and TNF-α and the expression of the transcription factor T-bet, type 2 (CD4^{+} Th2 and CD8^{+} Tc2) which mainly produce IL-4, IL-5, IL-10 and IL-13 and express GATA-3, and type 3 (CD4^{+} Th17 and CD8^{+} Tc17) with IL-17 and IL-22 as signature cytokines and retinoic orphan receptor γt (RORγt) as transcription factor[295]. T-cell subset diversity is completed by regulatory T-cells (Treg, either CD4^{+} or CD8^{+}), which produce IL-10 and TGF-β[296], as well as several less well characterized, rarer subsets (Th9, Th22 and others). Importantly, follicular T-cells (Tfh and Tfc), with IL-4 and IL-21 as signature cytokines and expressing the transcription factor B-cell lymphoma 6 (Bcl-6) have also been shown to play an important role in the development of humoral immunity.

Of note, there is evidence that polarized T-cells, at least CD4+, maintain a certain degree of plasticity. *In vitro* experiments revealed that fully differentiated Th1 and Th2 clonotypes were capable of switching their gene expression signature under specific culture conditions within a few days[297]. This flexibility appears to be especially relevant in the case of Th17 and allows them to acquire Th1, Th2 or mixed effector phenotypes when facing the appropiate conditions[298]. Within the follicle, CXCR5^{+} expressing T-cells with Th1, Th2 or Th17 characteristics have also been reported[299]. However, terminal differentiation stages of T-cell development have been associated with reduced plasticity. T_{EM} with Th2 phenotype, for instance, cannot upregulate T-bet and consequently secrete IFN-γ, revealing an inverse relation between polarization capacity and memory generation[298].

4.2.1. Type 1 responses: Th1 and Tc1

Type 1 T-cells responses seem to be induced by monocytes, macrophages and DCs in response to viral and intracellular bacterial infections through IL-12 and IFN-γ signaling[300]. The transcriptional signature of CD4$^+$ (Th1) and CD8$^+$ (Tc1) T-cells includes the expression of T-bet transcription factor and CXCR3 and CCR5 chemokine receptors[291].

The gold standard cytokine mediating type 1 responses is IFN-γ, which is particularly important for APCs and promotes antigen presentation by increasing HLA class I and II gene expression and slowing lysosomal degradation of pathogen derived antigens[301]. APCs can be further activated by other type 1 pro-inflammatory cytokines, such as TNF-α[302].

Type 1 immunity also comprises cytolytic activity mainly mediated by CD4+ or CD8+ Tc1 cells producing granzyme B and perforin and the consequent elimination of target cells upon interaction of the TCR with the HLA class I or II epitope complex[303].

4.2.2. Type 2 responses: Th2 and Tc2

Type 2 responses promote protection against helminths, venom and ensure tissue repair[291]. Although still controversial, it is believed that Th2/Tc2 priming relies on specialized DCs and, to some extent, basophils[304]. IL-4 is essential for type 2 T-cell polarization as its signal transduction increases the expression of the canonical Th2/Tc2 transcription factor GATA-3[305]. To date, the chemoattractant receptor-homologous 2 (CRTH2), a receptor of prostaglandin D2, is the most selective marker for human Th2[300].

The most typical type 2 cytokines are IL-4 and IL-13, which drive B cell proliferation and immunoglobulin class-switching to IgE[306]; IL-5, which is essential for eosinophils differentiation, activation and survival[307]; and IL-10.

4.2.3. Type 3 response: Th17 and Tc17

Type 3 immune responses are committed to barrier protection against extracellular bacterial and fungal infections[300]. Th17/Tc17 polarization requires a specific combination of cytokines: IL-6, TGF-β and IL-21 trigger RORγt expression in naïve T-cells, an event that is enhanced by IL-1β. IL-23 is required to promote the expansion of polarized Th17/Tc17 cells[308,309]. The chemokine

receptor CCR6 is used by Th17/Tc17 cells to migrate to the intestine and associated lymphoid tissues[310,311] and has been used to track Th17 cells[291].

The most characteristic type 3 cytokine is IL-17, which represents a strong regulator in the cellular and humoral response in tissues. Under normal conditions, IL-17A and IL-17F induce the recruitment and activation of neutrophils as well as the synthesis of antimicrobial peptides (AMPs)[312,313], while protecting from gut inflammation[314]. Another landmark type 3 cytokine is IL-22, which elicits the secretion of AMPs and induces a pro-inflammatory state by boosting the secretion of inflammatory mediators, including IL-6, IL-1β and granulocyte colony-stimulating factor (G-CSF). Moreover, IL-22 helps in the maintenance of epithelial barrier by promoting epithelial proliferation[315].

4.2.4.   Follicular T-cells: Tfh and Tfc

Follicular T-helper cells (Tfh) have been shown to play an important role in the development of humoral immunity. Located at the edge of the T-cell zone in secondary lymphoid organs, activated naïve CD4$^+$ pre-Tfh cells are primed by DCs-secreted IL-6 and start expressing Bcl6, CXCR5, PD-1 and ICOS[316] while migrating to the germinal center of the follicles.

Once in the follicle they interact with B-cells, supporting their proliferation, isotype class switching and antibody affinity maturation through cyclic somatic hypermutations[317]. Tfh functionality is related to IL-4 and IL-21 secretion, which is necessary for the establishment of antigen-specific, long-lived plasma cells and circulating memory B-cells[318]. Although it was initially thought that follicle-organizing properties are reserved to CD4$^+$ T-cells, there is growing evidence that CXCR5-expressing CD8$^+$ T-cells also localize in, or proximal to, B-cell follicles. These CD8$^+$ T follicular cytotoxic cells (Tfc) have been reported to have a self-renewal and less-exhausted profile and to keep their cytotoxic functionality, allowing them to eliminate infected cells while also contributing to the regulation of the antibody response[319].

4.2.5.   Regulatory T-cells: CD4$^+$ and CD8$^+$T$_{reg}$

Generally, CD4$^+$ Treg cells are classified as tTreg, originated in the thymus, and iTreg (*induced* Tregs), whose polarization occurs later in the periphery. While tTreg differentiation occurs after strong TCR signals in order to avoid self-reactive immune response, iTreg seems to prevent

responses against allergens, food and commensal microbiota and requires IL-10 and TGF-β priming[320]. The transcription factor forkhead box protein 3 (Foxp3) expression is significantly higher in CD4^{+} and Foxp3^{+} CD28^{+} CD8^{+} T-cells also have demonstrated to perform regulatory functions[321].

Both CD4^{+} and CD8^{+} Tregs secrete various inhibitory cytokines, including IL-10 and TGF-β, which work as a key immunomodulator during infection and ameliorates excessive responses by inhibiting chemokine and cytokine production by APCs and lymphocytes while reducing the expression of HLA class II and costimulatory molecules on APCs[322]. TGF-β inhibits innate immune response (NK cells, neutrophils and macrophages) as well as the adaptive immune response (effector T-cells and antigen presentation by DCs)[323].

4.3. T-cell polarized responses against infectious diseases

4.3.1.   Role of polarized effector functions in SARS-CoV-2 infection

The relevance of the adequate T-cell polarization in COVID-19 is reflected by the association between Th1/Th2 balance and disease outcome. Some studies reported a beneficial role of Th1 cells in the clearance of SARS-CoV-2 infection, while exacerbated Th2 response was more commonly observed in patients who died from COVID-19[324,325]. Mirroring the detrimental impact of the Th2 over Th1 balance in COVID-19 patients, augmented proportion of Tc2 and Tc17 circulating cells, alongside with reduced Tc1 responses were observed in severe patients[326]. Increased levels of IL-6 in severe patients might lead to expansion of Th17 cells, which participate in lung injury and consequent ARDS by facilitating neutrophil recruitment[327]. Increased levels of IL-22 alone were found in patients with milder pneumonia, while elevated Tc17 among PBMCs were linked to more severe symptoms[328]. These findings seem to indicate that the specific polarization of SARS-CoV-2 specific CD4^{+} and CD8^{+} T-cells might be relevant in the disease outcome.

Less is known about other alternative CD8^{+} T-cell effector functions, such as CD8^{+} Tregs and Tfc, and their contribution to the course of SARS-CoV-2 infection course. Similarly, the role of CD4^{+} Tregs in COVID-19 severity is still controversial, since some studies reported decreased levels of circulating Tregs in patients with severe forms of the disease, while others observed an aberrant

Treg signature in severe patients[329], characterized by high levels of suppressive but also pro-inflammatory cytokines[330]. Also, CCR6+CXCR3+CXCR5+ Tfh cells have been shown to be involved in the generation of neutralizing antibodies and were observed more frequently in patients with severe COVID-19[331]. By contrast, an early increase in cytotoxic Tfh cells in hospitalized COVID-19 patients was correlated with lower levels of anti-spike IgG, probably due to direct killing of B-cells within the GC[332]. Of note, Bcl-6+ B-cells and Tfh are diminished in acute COVID-19, which may explain the early absence of germinal center formation. These observations reveal a profound alteration of the adaptive immunity during acute infection, reflected by the accumulation of aberrant Th1 within the lymph nodes and SARS-CoV-2 specific activated B-cells in the peripheral blood[333].

4.3.2. Role of polarized effector functions in HIV infection

The association between type 1 responses and reduced HIV viremia has been demonstrated for CD8+[334] and CD4+[335] T-cells. Although postulated years ago[336], the importance of other T-cell subsets exerting alternative effector functions (not mediated by IFN-γ) in HIV pathogenesis remains less well studied. This gap might be partly explained by factors including the small size of some T-cell subsets in the peripheral blood, their heterogeneity and plasticity, or the severe CD4+ T-cell depletion suffered during acute HIV infection[337]. In the early 1990's, the CD4+ Th1/Th2 balance was considered a hallmark of HIV disease progression, although that view was not uniformly shared[338,339]. Nowadays, while HIV-specific type 2 and type 3 responses remain poorly understood, the relevance of CD4+ Th2 and Th17 in disease control and vaccine response begins to emerge[336,340–344]. Conversely, HIV-specific CD8+ Tc2 responses are associated with reduced cytotoxic activity[345], while the preservation of tissue-resident Tc17 during HIV infection is important to regulate immune activation[346]. Regulatory CD4+ T-cells have been associated with weaker HIV-specific cellular immune responses and have been shown to suppress HIV-induced immune hyperactivation and thus, limit infection of conventional CD4+ T-cells[340,341]. CD4+ Tfh cells have been reported to have different HIV antigen specificities compared to conventional CD4+ Th1 cells and to provide help to differentiate and mature HIV-specific B-cells, while supporting CTL responses[347–349]. Such Tfh cells seem to be very permissive to HIV entry and contain a significant proportion of the latent viral reservoir[350,351] and expansion of this cell subset is associated with disease progression[352,353]. Less is known about CD8+ Tfc cells in HIV infection, but some studies results attribute them a higher *ex vivo* cytotoxic activity compared to non-CD8+ Tfc[354]. These findings are in line with the possibility that CD8+ T-cells having Tfc and Tc2-

like phenotypes mediate lower viral loads in animal models of chronic infection, including LCMV-infected mice[355] and SIV-infected macaques[356]. These observations support the hypothesis that CD8^{+} Tfc T-cells, with increased cytotoxic capacity and localized to lymph node follicles, could be critical in limiting the viral reservoir established in CD4^{+} Tfh T-cells and , at the same time, provide additional help for maturation of the humoral immunity in the B-cell follicles[357].
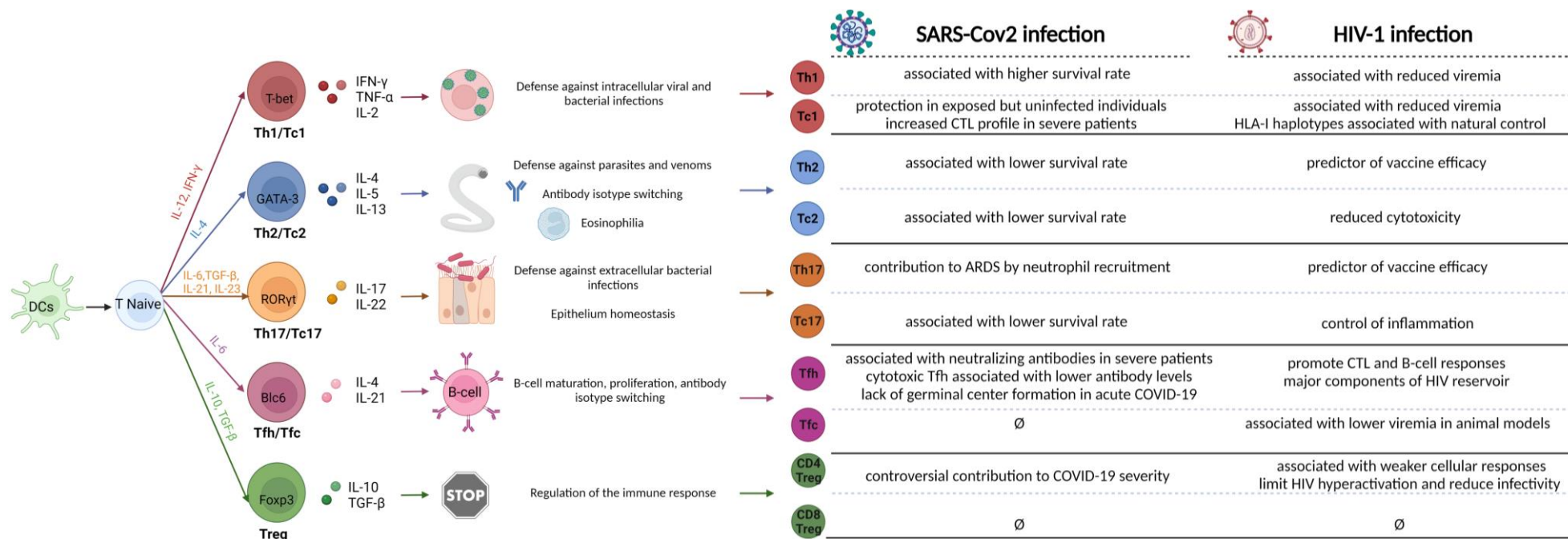
Figure 15. T-cell effector functions and their role in the immune response against SARS-CoV-2 and HIV infections.
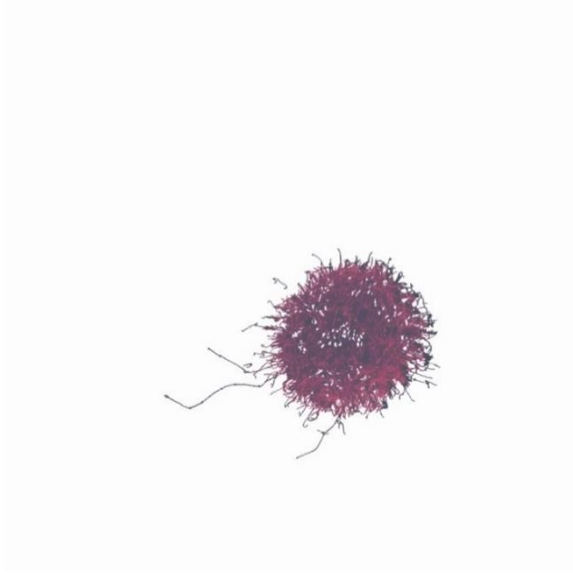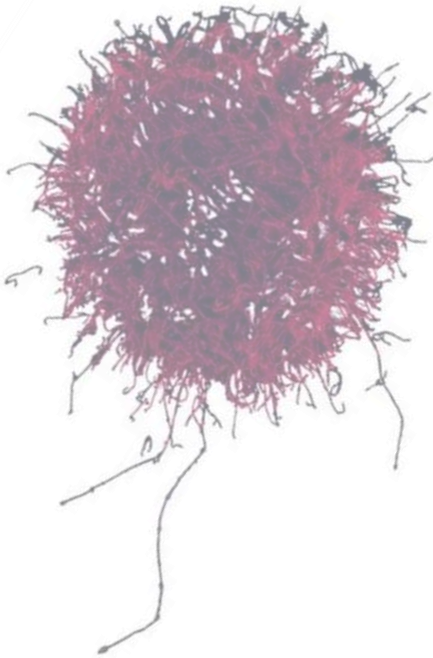
5. Hypothesis

Although it is widely accepted that effective control of viral infections is achieved thanks to complex and interconnected mechanisms of the innate and adaptive cellular response, research has been mainly focused on neutralizing antibodies and cytotoxic T-cells for years. The contribution of other innate and adaptative lymphoid cells to the immune response has been poorly studied and the characteristics of most appropriate NK cell phenotypes and T-cell polarization profiles to support viral control remain elusive.

We hypothesized that cytotoxic immune responses against virus-infected cells, mediated by innate lymphoid cells, together with alternative adaptive cellular responses have an important role in effective control of viral infections. We also posited that these mechanisms are relevant for viral infections with different disease progression. For these reasons, we selected SARS-CoV-2 and HIV-1 as infections with transient versus chronic nature, respectively, to study:

i) **The role of NK cell activation through the HLA-E/NKG2X axis**. Here we postulated that increased HLA-E surface expression in uncontrolled infections leads to a chronic NK stimulation through NKG2C, disrupting the balance between NKG2A and NKG2C expression, and inducing NK exhaustion.

ii) **Specific polarized-responses of T-cells.** Our main hypothesis was that alternative (non-type 1, IFN-γ-mediated) polarized T cell subtypes were associated with control of chronic viral infection, especially through the support of follicular T-cells to the regulation of B-cell responses.

Understanding these immunological mechanisms would help to define mechanisms of natural control of SARS-CoV-2 and HIV infections and might be crucial for the development of targeted immunotherapeutic interventions.

6. Objectives

The principal aim of the present thesis was to i) understand the regulation of the NK immune responses through the HLA-E/NKG2X axis and ii) define alternative adaptive T-cell responses involved in the control of acute and chronic viral infections. In consequence we developed the following specific objectives:

Natural killer responses to viral infections: the role of HLA-E/NKG2X axis

- To evaluate the relationship between HLA-E expression levels, host HLA-E genotype and disease course of acute SARS-CoV-2 and chronic HIV-1 infection.
- To identify links between the distribution of NK cell subpopulations, surface receptor repertoire and disease progression.
- To assess NK cell functionality in terms of degranulation, cytokine secretion and cytotoxicity through HLA-E/NKG2X stimulation in the context of viral infections.
- To determine NK cell activation and exhaustion levels in patients with severe or mild COVID-19 and uninfected individuals.
- To measure the impact of SARS-CoV-2 vaccination on NK cell function.
- To examine the ability of the HIV-1 derived HLA-E restricted immunopeptidome to alter NK cell function.
- To create a structural model of the interaction between HLA-E and NKG2X to understand allelic differences in the HLA-E restricted immunopeptidome.

Alternative T-cell responses to viral infections: the role of T-cell polarization

- To measure global and antigen-specific $CD4^+$ and $CD8^+$ T-cell polarization profiles in response to SARS-CoV-2 and HIV-1 antigens and define their contribution to natural control of either infection.
- To assess the relationship between humoral responses and viral control in terms of antibody levels, neutralization and ADCC capacity.
- To link T-follicular-like responses with the development of humoral responses.

7. MATERIAL AND METHODS
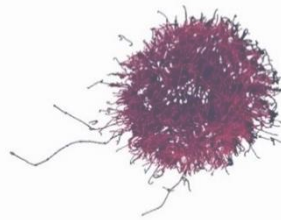
7.1. Study cohorts

Samples from forty-two participants from the KING cohort extension (n=42), recruited at the Hospital Germans Trias i Pujol (Badalona, Spain) between March 2020 to CCC and showing different degree of COVID-19 severity, were selected. These included individuals with severe COVID-19 (Severe, n=12), mild COVID-19 (Mild, n=12), uninfected, non-vaccinated for SARS-CoV-2, individuals (Uninfected, n=12) and individuals receiving the complete dose of mRNA-vaccines against SARS-CoV-2 (Spikevax-Moderna, n = 3; Comirnaty – Pfizer/Biontech, n =3). Severe status was differentiated from mild infection as hospitalization and oxygen saturation below 94%. Epidemiological data of the patients are shown in Table 2.

Group	Severe	Mild	Uninfected	Vaccinated
Age	54 ± 8	50 ± 14	53 ± 8	49 ± 3
% of female	42%	65%	42%	50%
n	12	12	12	6
Days post Infection/vaccination	18 ± 7	15± 5	-	31.5

Table 2. Epidemiological data of the patients in this study.

For SARS-CoV-2 infected individuals, blood samples were collected a median of 18 ± 7 (Severe COVID-19) or 15 ± 5 (Mild COVID-19) days from first symptoms and during the acute phase of infection. Blood from vaccinated individuals was collected a median of 31.5 days after receiving the last dose. We performed a serology test against S2+RBD-protein in uninfected individuals to verify the absence of anti-S2+RBD antibodies and confirm their SARS-CoV-2-naïve status. The study was approved by the Ethics board of the Hospital Germans Trias i Pujol (CEIC PI-20-77), and all participants provided written informed consent.

Study cohort for Chapter II. Innate cellular responses to chronic viral infections.

HIV-infected subjects (n=51) recruited at the Hospital Germans Trias i Pujol (Badalona, Spain) and the IMPACTA clinics in Lima (Peru) were included in this study. This included individuals that were not receiving antiretroviral treatment and had plasma viral loads of <10,000 HIV RNA copies/mL (range: 25 to 9,999; median: 1877 HIV RNA copies/mL) and CD4 counts that ranged from 434 to 1343 cells/mm3 (median: 762 cells/mm3) (HIV-low, n=31) or plasma viral loads of >50,000 HIV RNA copies/mL (range: 50,295 to 1,200,000; median: 239,511 HIV RNA copies/mL) and CD4 counts that ranged from 11 to 726 cells/mm3 (median: 284 cells/mm3) (HIV-high, n=20) (Table 3). Fresh blood from HIV seronegative donors was obtained from the Catalonia Blood and Tissue Bank (Banc de Sang I Teixit, BST) (n=18).

Group	HIV-low	HIV-high	Seronegative
n	31	20	18
CD4 count (cells/mm3)	672 (434-1343)	284 (11-726)	-
Plasma viral load (HIV RNA copies/mL)	1877 (25-9999)	239511 (50295 - 1200000)	-
Proviral (HIV DNA copies/10^6 PBMCs)	31.30 (0-1662.4)	1160.55 (80.1-2346.6)	-
HLA-E qPCR	n=31	n=20	n=18
Genotyping	n=31	n=20	n=18
NK phenotyping	n=8	n=8	n=18
NK degranulation	n=8	n=8	n=8
NK cytotoxicity	n=8	n=8	n=8
NK-VIA	-	-	n=12
HIV peptides effect	-	-	n=6

Table 3. Clinical data of the sample used and number of samples included in each experiment. CD4 count, plasma viral load medians and ranges (between brackets are provided)

Additional unrelated cohorts were included as comparison groups (n=54, Table 3): i) highly exposed seronegative individuals six months prior to infection (n=6, pre-HIV), ii) acute/recent HIV infected, sampled within a median of 6 months from HIV acquisition (n=8, acute), iii) low risk HIV seronegative individuals (n=24, seronegative), iv) chronically HIV infected individuals not receiving cART for at least one year (n=11, chronics), v) chronically infected individuals cART after receiving cART for at least one year (n=6, treated) and an additional validation HIV-low viremia cohort (n=23, controllers).

Group	Acute	Chronics	Treated	LTNP
n	8	11	6	23
CD4 count (cells/mm3)	574 (317-891)	529 (328-914)	608.5 (426-1053)	594 (76-1840)
Plasma viral load	57860.5 (400-904569)	13284 (4900-50000)	45 (25-50)	55 (25-1978)
Proviral	570 (414-3070)	252 (9-596)	116 (43-388)	24 (0-1600)
HLA-E qPCR	n=8	n=11	n=6	n=23

Table 4. Clinical data of the samples used and number of samples included in each experiment. CD4 count, plasma viral load medians and ranges (between brackets are provided) are provided.

The study was approved by the Ethics board of the Hospital Germans Trias i Pujol (CEIC EO-12-042), and all participants provided written informed consent.

Study cohort for Chapter III. Alternative adaptive cellular responses to acute viral infections.

Samples from twenty-nine participants from the KING cohort extension study (n=29), recruited at the Hospital Germans Trias i Pujol (Badalona, Spain) between March 2020 to November 2020 and showing different degree of COVID-19 severity, were selected. These included individuals with severe COVID-19 (Severe, n=10), mild COVID-19 (Mild, n=10) and individuals that did not elicit IgM or IgG antibodies against SARS-CoV-2 Spike (non-seroconvertors, NSC, n=9). Severe status was differentiated from mild infection as requiring hospitalization and oxygen saturation below 94%. Epidemiological data of the patients is shown in Table 5. Additionally, we included 5 pre-COVID-19 outbreak (March 2020) samples of healthy donors (SN).

Group	Severe	Mild	Non-Seroconvertors
Age	60± 19	44.5 ± 12	44 ± 8
% of female	40%	80%	78%
n	10	10	9

Table 5. Epidemiological data of the patients in this study.

The study was approved by the Ethics board of the Hospital Germans Trias i Pujol (CEIC PI-20-77), and all participants provided written informed consent.

Study cohort for Chapter IV. Alternative adaptive cellular responses to chronic viral infections.

Forty-four HIV infected, treatment-naïve individuals (HIV[+]) and 8 HIV seronegative were included in this study (Table 6). Twenty-four participants had plasma viral loads (pVL) <2000 copies/mL and were considered *HIV controllers*. An additional 20 participants presenting pVL>5000 copies/mL were considered *non-controllers*. Plasma samples from all the individuals were tested for anti-Env IgM, IgA and IgG titers, plasma avidity as well as the plasma neutralization titters and ADCC activity. Due to limited sample availability, boosted flow analysis for cellular responses included 29 individuals (15 HIV controllers and 14 HIV non-controllers) and phenotypic characterization

based on Th2/Tc2 markers (CRTH2) and Tfh/Tfc markers (CXCR5+ PD-1+ ICOS+) was performed in 22 of the samples used in the boosted flow analysis (8 HIV controllers and 14 HIV non-controllers). Clinical parameters and number of samples included in each experiment are represented in table 6. *Ex-vivo* experiments were performed without blinding or randomization. The study was carried out in accordance with the recommendations of the Ethics board of the Hospital Universitari Germans Trias i Pujol in Badalona, Spain (PI-18-011). All subjects gave written informed consent in accordance with the Declaration of Helsinki.

Group	HIV Controllers	HIV Non-controllers
Fiebig stage	VI	VI
CD4 count (cells/mm³)	786 (364-1638)	406 (6-986)
Plasma viral load (HIV RNA copies/mL)	210 (25-1900)	52435 (5576 - 640803)
Boosted flow	n=15	n=14
ELISpot	n=8	n=14
Polarization markers	n=8	n=14
IgM/IgA/IgG titers	n=24	n=20
Neutralization assay	n=24	n=20
ADCC	n=24	n=20

Table 6. Clinical data (CD4 count, plasma viral load) and number of samples included in each experiment.

7.2. Cell lines

K562

NK cell response to "missing-self" was measured by using HLA-null K562 cells (ATCC) as target cells. NK cell activity was determined by measuring cytokine secretion, degranulation and cytotoxic activity. This cell line was cultured at a density of $3x10^5$ cells per mL in RPMI supplemented with 10% fetal bovine serum (FBS).

HLA-E*(01:03) transfected K562 cell line (HLA-E/VL9-K562), co-expressing the HLA-B*0702 signal sequence derived VL9 peptide (VMAPRTVLL)[358], were kindly provided by Dr. Joosten (University of Leiden, The Netherlands) and originally produced by Dr. E. Weiss (Ludwig-Maximilians-Universitat, Munich, Germany)[359]. This cell line was cultured at a density of $3x10^5$ cells per mL in IMDM supplemented with 10% fetal bovine serum (FBS) and 200ug/mL of G418 (I10 medium).

TZM-bl

TZM-bl luciferase-reporter target cells were used for HIV neutralization assays. Cells were cultured in DMEM supplemented with 10% of fetal bovine serum (FBS).

CEM.NKR-CCR5

HIV_{NL4-3} infected CEM.NKR-CCR5 cells expressing the firefly luciferase downstream from the SIV long terminal repeat (LTR) were used as target cells for antibody-dependent cellular cytotoxicity. This cell line was cultured at a density of $3x10^5$ cells per ml in RPMI supplemented with 10% fetal bovine serum (FBS) and fed every two days with uninfected CEM.NKR-CCR5 cells in infected:uninfected ratio of 1:5.

CD16+ KHYG-1

The human CD16+ KHYG-1 NK cell line was used as effector cells for antibody-dependent cellular cytotoxicity assay (ADCC). The NK cell lines were maintained at a density of 3×10^5 cells per ml

in R10 cell culture medium consisting of RPMI medium supplemented with 10% fetal bovine serum (FBS), 25 mM HEPES (Invitrogen), 1 µg/ml cyclosporine (CsA) (Sigma), and 10U/mL of interleukin-2 (IL-2) (Roche).

7.3. NK cell immunity

NK cell enrichment

Peripheral blood mononuclear cells (PBMCs) were isolated from whole blood using Lymphoprep™ (Stemcell) density gradient. NK cells were negatively isolated by magnetic bead separation (MACS Miltenyi Biotec) from PBMC, following the manufacturer's instructions.

Surface characterization

To discriminate different NK cells subpopulations, isolated NK cells were stained with Amcyan anti-CD3 (BD), BV-785 anti-CD56, BV-605 anti-CD16, PerCP-Cy5 anti-CD57 (Biolegend). Exhaustion and activation were evaluated on the above-mentioned NK cell subsets by staining with APC-Cy7 anti-PD-1 and BV-650 anti-LAG-3 (BioLegend), while HLA-E/NKG2X was measured by PE anti-NKG2A and APC anti-NKG2C (R&D Systems) staining. Samples were run on a LSRII BD Cytometer (approximately 30.000 events were acquired) and analyzed using FlowJo v10 software. Additionally, data sets from CD3-negative cells were downsampled to obtain 3,000 events/fcs file. An unsupervised tSNE dimensional reduction was performed on FlowJo 10.5.2 using the default settings of a nearest neighbours of 15 and a minimum Euclidean distance of 0.5. Number of clusters was determined by X-Shift (Number nearest neighbors: 132, Euclidean distance metric) and FlowSOM and was applied to determine the level of expression of CD56, CD16, CD57, NKG2A, NKG2C, PD-1 and LAG-3 in a total of 10 clusters in the CD3-negative population. Already established NK cell subpopulations were also studied, the gating strategy used is summarized in Fig. S1. NK cells subpopulations were classified as (i) CD56neg (CD3-CD56-CD16-CD57-), (ii) CD56dim (CD3-CD56dimCD16+CD57-), (iii) adaptive NK cells (CD3-CD56dimCD16+CD57+) and (iv) CD56bright (CD3-CD56brightCD16-CD57-).

NK degranulation and cytokine secretion assay

The "missing self" cytotoxic response mediated by the HLA-E/NKG2X axis was measured using HLA-E null K562 cell line. NK cells were co-cultured with K562 cells in an effector:target ratio of 5:1 for 4 hours in the presence of Golgi Stop, Golgi Plug as well as APC anti-human CD107 (Biolegend) and stained for surface markers (CD16, CD56, CD57, PD-1, LAG-3, NKG2A and NKG2C). Subsequently, cells were fixed, permeabilized (Fix&Perm Cell Permeabilization Kit, Thermofisher) and stained with FITC anti-human TNF-α and PE-Cy7 anti-human IFN-γ (BD). Approximately 30.000 events per samples were acquired on a Canto II BD Cytometer and analyzed using FlowJo v10 software.

NK cytotoxicity assay

NK-mediated cytotoxicity was measured at 10:1, 5:1, 2,5:1, and 1:1 NK effector to target cell ratio (HLA-E*0103/VL9-K562 targets). Target cells were labeled using calcein-AM to perform a retention assay as previously described[360]. Briefly, 12.500 peptide-pulsed HLA-E*0103/VL9-K562 cells were stained for 30 minutes at 37ºC 5% CO2 with calcein-AM at 10nM and then cultured in R10 medium (RPMI supplemented with 10% FBS, penicillin 100U/mL and streptavidin 100 ug/mL), together with the different ratios of NK cells isolated from the HIV seronegative individuals, for 4 hours at 37ºC 5% CO2. Cultures were then run on a Canto II BD Cytometer and the percentage of killing of labelled target cells calculated as 100-%calcein-AM^{+} K562 cells. In each condition, an exponential regression curve was determined by the percentage of killing resulted from the different effector to target ratios in the co-culture. Results were expressed in lytic units[361] calculated as the number of NK cells contained in 10^6 PBMCs able to lyse 20% of 100.000 target cells.

Granzyme ELISPOT

Mabtech ELISPOT kits were used to count Granzyme-B (capture clone MT28, biotinylated clone MT8610) producing cells following manufacturer's instructions. A total of $2,5x10^5$ NK cells/well were stimulated for 16h at 37ºC with $5x10^4$ HLA-E null K562 cells. Spot forming cells (SFC) were counted using an automated Cellular Technology Limited (C.T.L.) ELISPOT Reader Unit. The threshold for positive responses was set as the highest of: a) 50 SFC/10^6 PBMCs b) negative

control mean plus 3 times standard deviations of the negative control SFC/10^6 PBMCs or c) 3 times the mean of negative control SFC/10^6 PBMCs.

NK-mediated viral inhibition assay (NK-VIA)

CD4+ T cell enriched fraction were obtained using specific NK cells and CD8+ T-cell specific magnetic beads depletion (MACS Miltenyi Biotec NK Isolation kit, CD8+ T-cell isolation kit) and stimulated with PHA (5ug/mL) in R10. HLA-E surface expression was measured on the CD3+ CD4+ population by flow cytometry after three days of stimulation. This fraction cell culture was then infected by spinoculation (720g for 2h at 25ºC) with HIVBaL and HIVNL4-3 laboratory-adapted strains at a multiplicity of infection (MOI) of 0.01. The day before the co-culture, one vial of frozen PBMCs from the same subject was thawed and cultured overnight with 20 U/mL of IL-2, prior to positive NK cells sorting by magnetic bead separation (MACS Miltenyi Biotec, NK isolation kit). The assay was performed in triplicates by culturing 50000 HIV-infected or uninfected autologous CD4+ T-cells alone or in the presence of different ratios (2:1, 1:1, 1:2 and 1:10 NK effector to CD4 target ratio) of unstimulated autologous NK cells. NK cells were rested for 2 hours at 37ºC 5%CO$_2$ after magnetic sorting in R10 medium, supplemented with 50 U/mL of IL-2 and 1 ng/mL of IL-15, After one week, half of the medium was collected and replaced with 50uL of R10 supplemented with 100U/mL of IL-2 and 2 ng/mL of IL-15. At day 14, the culture supernatant was harvested and NK cells from the long-term culture characterized by flow cytometry (n=6). HIV p24 Gag concentration in the supernatant was measured at day 7 and day 14 by the commercially available HIV p24 ELISA kit (Innogenetics) in accordance with the manufacturer's instructions. Samples were read on a Perkin Elmer Ensight Plate reader. NK-mediated inhibition of viral replication was calculated as %inhibition = [(HIV p24 Gag concentration in CD4+ T-cells cultured alone)-(HIV p24 Gag concentration in CD4+ T-cells cultured with NK cells)]/(HIV p24 Gag concentration in CD4+ T-cells cultured alone)x100.

7.4. T cell immunity

Boosted flow screening T-cell responses

5×10^5 PBMC/well were cultured in R10 (RPMI medium (Gibco) supplemented with 2 mM L-glutamine (Gibco), 100U/ml penicillin (Gibco), 100 μg/mL streptomycin (Gibco) and 10% heat-inactivated inactivated fetal bovine serum (FBS – Invitrogen), for 16h at 37°C. For measuring HIV specific responses, PBMCs were stimulated with a set of 425 18mer overlapping peptides (OLPs) divided in 17 peptide pools (range 21-27 OLPs/pool, final concentration for each peptide 10 μg/mL) covering all the HIV proteome, in the presence of anti-CD49d and anti-CD28 (BD) and GolgiStop (BD) (Table 7). To determine SARS-CoV-2 specific responses, PBMCs were stimulated in parallel for 12h and 5 days with a final recall for 25h with two recombinant proteins (S and N) at a concentration of 5 μg/mL and a pool of conserved peptides among human coronavirus (16 OLPs) at a concentration of 10 μg/mL (Hu-CoV pool) (Table 8)[362]. Anti-CD3/anti-CD28 magnetic beads (Gibco) were used as positive control. As negative controls, culture medium was used instead of peptide pools. Cells were stained first with BD Horizon™ Fixable Viability Stain 575V, followed by extracellular staining for T-cell lineage markers (anti-CD3 APC-Cy7, anti-CD4 BV786, anti CD8-PerCP, anti-CCR7 BV711 – Biolegend; anti-CD45RA FITC – BD), B-cell lineage marker (anti-CD19 PE-Dazzle594 – Biolegend) and myeloid lineage marker (anti-CD14 A700 – Biolegend). Following the fixation and permeabilization step (Fix and Perm kit - Invitrogen) intracellular staining (ICS) was performed, following the boosting strategy established by Ruiz-Riol et al.[363], for Type 1, Type 2, Type 3, Treg and T follicular defining cytokines. Antibodies against Type 1 related cytokines were conjugated with BV605 (anti-IFN-γ, anti-IL-2, anti-TNF-α – Biolegend), antibodies against Type 2 related cytokines with BV421 (anti-IL-4, anti-IL-10, anti-IL-13 – Biolegend), antibodies against Type 3 related cytokines with PE-Cy7 (anti-IL-17-A, anti-IL-22 – Biolegend), antibodies against Treg related cytokines with PE (anti-IL-10, anti-LAP – Biolegend) and antibodies against T follicular related cytokines with APC (anti-IL-4, anti-IL-21 – Biolegend). Different clones were used for the detection of IL-4 in type 2 and follicular responses. Approximately 10^5 cells were acquired on a LSR Fortessa BD Instrument and analysis was performed using FlowJo 10.5.2. The gating strategy is summarized on supplementary Figure S2. Cells were classified as T_{CM} (CD45RA- CCR7+), T_{EM} (CD45RA- CCR7-), T_{EMRA} (CD45RA+ CCR7-) and T_{Naive} (CD45RA+ CCR7+). The percentage of cytokine producing cells (magnitude) detected in unstimulated controls was subtracted from the magnitude of the antigen-stimulated cells for each individual. The value of the most negative magnitude value after control subtraction across

all individuals determined the threshold for positive responses, as described by Roederer et al[364]. Polyfunctional cytokine profiling was done applying Boolean gates in FlowJo 10.5.2, following the same strategy for unstimulated cell signal subtraction and represented using SPICE v6 (provided by the National Institute of Health, Mario Roederer, ImmunoTecnhnology Section, Vaccine Research Center, NIAID, NIH, Bethesda).

Human coronavirus sequence	OLP	ID	C position
VGVLTLDNQDLNG	VGVLTLDNQDLNGNW	CoV-2_Pol-1300	C1303
TQMNLKYAISAKNRARTVAGVSI	TQMNLKYAISAKNRA	CoV-2_Pol-1395	C1402
	LKYAISAKNRARTVA	CoV-2_Pol-1396	C1403
	ISAKNRARTVAGVSI	CoV-2_Pol-1397	C1404
LMGWDYPLCDRAMPN	MGWDYPKCDRAMPNM	CoV-2_Pol-1416	C1423
KHFSMMILSDDAVVCFN	YLRKHFSMMILSDDA	CoV-2_Pol-1453	C1460
	HFSMMILSDDAVVCF	CoV-2_Pol-1454	C1461
	MILSDDAVVCFNSTY	CoV-2_Pol-1455	C1462
GPHEFCSQHT	TKGPHEFCSQHTMLV	CoV-2_Pol-1471	C1478
ERFVSLAIDAYPL	IERFVSLAIDAYPL	CoV-2_Pol-1485	C1492
AVFISPYNSQN	AWRKAVFISPYNSQNA	CoV-2_Hel-1651	C1662
NRFNVAITRA	SCNVNRFNVAITRAK	CoV-2_Hel-1665	C1680
RSFIEDLLF	PSKRSFIEDLLFNKV	CoV-2_S2-2247	C2266
QIDRLITGRL	VEAEVQIDRLITGRL	CoV-2_S2-2299	C2318
KWPWYIWL	EQYIKWPWYIWLGFI	CoV-2_S2-2364	C2383
PRWYFYYLGTGP	DLSPRWYFYYLGTGPEA	CoV-2_NC-2640	C2667
Total	16 peptides		

Table 8. Set of 16 OLPS corresponding to conserved sequences among human coronavirus.

Phenotypic characterization of CD4^{+} Th2- and Tfh cells and CD8^{+} Tc2- and Tfc- cells

Surface markers for Th2/Tc2 (CRTH2) and Tfh/Tfc T cell polarization (CXCR5, ICOS and PD-1) were characterized in cryopreserved PBMC from patients previously yielding CD8+ Tfc responses in the boosted flow whole proteome analysis. Cells were thawed and plated at 5×10^5 PBMCs/well in R10 for 16h at 37ºC. PBMCs were stimulated with peptide pools that showed activation of CD8^{+} Tfc in the initial screening or control stimulations as above. Cells were stained first with BD Horizon™ Fixable Viability Stain 575V, followed by extracellular staining for T-cell lineage markers (anti-CD3 APC-Cy7, anti-CD4 BV786, anti-CD8-PerCP, anti-CCR7 BV711 – Biolegend; anti-CD45RA FITC – BD), Th2/Tc2 marker (anti-CRTH2 BV605 – Biolegend) and Tfh/Tfc markers (anti-CXCR5 PE, anti-ICOS PE-Dazzle594, anti-PD-1 PE-Cy7 – Biolegend). Following the fixation and permeabilization step (Fix and Perm kit - Invitrogen) intracellular staining was performed using anti-IL-4 BV421 and anti-IL-21 APC (Biolegend).

Approximately 10^5 cells were acquired on a LSR Fortessa BD Instrument and analysis was performed using FlowJo 10.5.2 software. The gating strategy is summarized in supplementary

figure S3. Additionally, data sets from CD3+ cells of the negative control phenotypic characterization were downsampled to obtain 3000 events/fcs file. An unsupervised UMAP dimensional reduction was performed on FlowJo 10.5.2 using the default settings of a nearest neighbours of 15 and a minimum Euclidean distance of 0,5. The number of clusters was determined by X-Shift (Number nearest neighbors: 132, Euclidean distance metric) and FlowSOM and was applied to determine the level of expression of our proteins of interest in a total of 45 clusters in the CD3+ population. The abundance of each cluster was determined in HIV^{+} controllers and non-controllers and results were represented for each cluster as $\log_2$(%CD3^{+} cells in C/%CD3^{+} cells in NC). UMAP plot and clustering are summarized in figure S4.

IL-4, IL-21 and IFN-γ ELISpot

Mabtech ELISpot kits were used to count IFN-γ (capture clone 1-D1K, biotinylated clone 7-B6-1), IL-4 (capture clone IL-4I, biotinylated clone IL-4II) and IL-21 (capture clone MT216G, biotinylated clone MT21.3m) producing cells following manufacturer's instructions. An additional assay, analogous to the *boosted Flow* technology was performed to enhance the sensitivity of detection by ELISpot. To that end, plates were coated with multiple capturing antibodies to allow for the detection of IL-4 and IL-21 producing cells. A total of $2x10^5$ PBMCs/well were stimulated for 48h at 37°C with peptide pools to which the individuals responded in the initial screening with CD8^{+} Tfc-like-reactive cells, using R10 as negative control in triplicates and PHA (25µg/mL) as positive control. Spot forming cells (SFC) were counted using an automated Cellular Technology Limited (C.T.L.) ELISpot Reader Unit. The threshold for positivity was set as the highest of: a) 50 SFC/10^6 PBMCs b) mean SFC/10^6 PBMCs in the negative controls plus 3 times standard deviations of the negative control wells or c) 3 times the mean of negative control well SFC/10^6 PBMCs.

7.5. B cell immunity

Determination of anti-Env IgM, IgA and IgG humoral response

HIV$_{NL4-3}$ and HIV$_{BaL}$ infected MOLT cells[365] were pre-incubated at room temperature for 30 minutes with plasma samples diluted 1/300 in PBS 1% BSA (Miltenyi Biotec). After three washes with PBS, the secondary antibodies: PE-F(ab)2 Goat anti-human IgG (Fc-specific); DyLight 649 Goat anti-human IgA and DyLight 488-F(ab)2 Goat anti-human IgM (Fcm5-specific) (Jackson Immunoresearch) were added separately and incubated for 15 minutes at room temperature. Stained cells were washed with PBS twice and fixed in 1% formaldehyde (Sigma-Aldrich). Samples were acquired in a BD LSR II flow cytometer (BD Biosciences) and the analysis was performed using FlowJo 10.5.2 software. HIV$_{NL4-3}$ and HIV$_{BaL}$ Envelope protein-specific IgM, IgA and IgG titers were correlated positively between them (Figure S5) suggesting that the difference in the signals is due to differences in surface stability of the strain-specific Env.

IgG Avidity ELISA

To assess the avidity of gp120-specific IgG plasma antibodies of HIV controllers and non-controllers, we coated ELISA plates with gp120 at 1 µg/ml in PBS overnight at 4ºC. The following day, plates were blocked with PBS containing 10% bovine serum albumin (BSA) for two hours at room temperature. Plasma samples were diluted and added to all wells for two additional hours at room temperature. Each sample was added to four wells. Plates were then washed and incubated with either 2M guanidine HCl (two wells/sample) or PBS (two wells/sample) for 15 minutes at room temperature to allow disassociation. All wells were incubated for 30 minutes at room temperature with HRP-conjugated goat anti-human IgG (Jackson ImmunoResearch) at 1: 20,000. O-phenylenediamine dihydrochloride (OPD) was added to the plates. The enzymatic reaction was stopped with 2M of H_2SO_4. The signal was determined as the optical density at 492 nm, with noise correction at 620 nm. Avidity index of each sample was defined as the ratio between the mean signal obtained with and without guanidine treatment.

Neutralization assays (SARS-CoV-2)

SARS-CoV-2.SctΔ19 WH1 was generated (Geneart) from the full protein sequence of the original SARS-CoV-2 isolate Wuhan-Hu-1 (WH1)) spike sequence, with the deletion of the last 19 amino

acids at the C-terminal end[366], human-codon optimized and inserted into pcDNA3.1(+). HIV reporter pseudoviruses expressing SARS-CoV-2 S protein and Luciferase were generated using the defective HIV plasmid pNL4-3.Luc.R-.E- obtained from the NIH AIDS Reagent Program[367]. Expi293F cells were transfected using ExpiFectamine293 Reagent (Thermo Fisher Scientific) with pNL4-3.Luc.R-.E- and SARS-CoV-2.SctΔ19 WH1, at an 8:1 ratio, respectively. Control pseudoviruses were obtained by replacing the S protein expression plasmid with a VSV-G protein expression plasmid as reported[368]. Supernatants were harvested 48 h after transfection, filtered at 0.45 μm, frozen and titrated on HEK293T cells overexpressing WT human ACE-2 (Integral Molecular). Neutralization assays were performed in duplicate. Briefly, in Nunc 96-well cell culture plates (Thermo Fisher Scientific), 200 TCID50 of pseudovirus were preincubated with three-fold serial dilutions (1/60–1/14,580) of heat-inactivated plasma samples for 1 h at 37 ∘C. Then, 2×10^4 HEK293T/hACE2 cells treated with DEAE-Dextran (Sigma-Aldrich) were added. Results were read after 48 h using the EnSight Multimode Plate Reader and BriteLite Plus Luciferase reagent (Perkin Elmer, Waltham, MA, USA). The values were normalized, and the ID50 (the reciprocal dilution inhibiting 50% of the infection) was calculated by plotting and fitting the log of plasma dilution vs. response to a 4-parameter equation in Prism 8.4.3 (GraphPad Software). This neutralization assay had been previously validated in a large subset of samples[74,369]. The lower limit of detection was 60 and the upper limit was 14,580 (reciprocal dilution).

Neutralization assays (HIV)

The neutralizing capacity of plasma against HIV was determined using a TZM-bl based pseudovirus neutralization assay as described[370] using a panel of 5 pseudovirus, including HIV strains classified as tier 1A (NL4-3), 1B (BaL.01), 2B (398F1) and 2A (TRO11 and AC10). Briefly, serial dilutions of heat inactivated (56ºC 30 min) plasma samples were incubated with pseudoviruses in D10, DMEM supplemented with 100U/ml penicillin (Gibco), 100 μg/mL streptomycin (Gibco) and 10% heat-inactivated FBS (Invitrogen). Afterwards, they were added to TZM-bl cells treated with DEAE-Dextran (Sigma), plated at 10^4 cells/well and cultured at 37°C for 48h. Then, 100μL of the supernatant was replaced with 100 μL of Britelite Luciferase Assay Substrate (Promega) and incubated for 1.5 minutes at room temperature. The cell-associated luciferase signal for each well was determined on an EnSight Multimode Plate Reader (Perkin Elmer). Neutralizing activity for each serum dilution was calculated as the percent of inhibition of viral entry compared to positive and negative controls, untreated infected cells and uninfected cells, respectively. Neutralization curves (percent viral entry inhibition versus plasma

dilution) was generated using GraphPad Prism version 7 by fitting $\log_{10}$-transformed data with sigmoidal dose-response curve and IC_{50} was determined. Results were expressed as % of neutralizers in each group, neutralizing breadth (number of HIV strains neutralized/number of HIV strains tested * 100) and logIC50 (reciprocal plasma dilution) when data fitted a sigmoidal curve (HIV_{NL4-3} and HIV_{BaL}).

Antibody-dependent cellular cytotoxicity (ADCC)

The ability of plasma to induce ADCC was determined by flow cytometry using a modified calcein-AM retention assay previously described[360]. HIV_{NL4-3}-infected target cells (CEM.NKR-CCR5[371]) were washed and resuspended in 10nM calcein-AM (BioLegend) diluted in R10 at a cell concentration of 10^6 cells/mL for 30 min with intermittent shakes. Target cells were washed twice with R10 and 10^4 target cells were cocultured in R10 supplemented with 10U/mL rh-IL-2 (Roche) in duplicates for 4 h with the NK effector cell line (human CD16+ KHYG-1[371]) at an E:T ratio of 5:1 in the presence or absence of serial dilutions (1:1000 to 1:256.000) of HIV+ individuals' plasma. After incubation, cells were washed with PBS plus 1% heat-inactivated FBS (Invitrogen) and $3x10^4$ cells were acquired on a LSRII BD instrument and analyzed on FlowJo 10.5.2 software. Results were normalized with a control condition in the absence of human plasma and lysis was calculated as the average of 100%-%calcein-AM+ cells in each duplicated condition.

7.6. Molecular assays

DNA/RNA extraction and real-time PCR

DNA and RNA were simultaneously extracted using the AllPrep DNA/RNA Mini kit (QIAGEN) from cryopreservedcell pellets. Retrotranscription (SuperScript II first-strand synthesis Supermix) was performed on those samples and the resulting cDNA was used for reverse transcription-PCR using TaqMan gene expression assay for detection of HLA-E (Hs03045171_m1) and TATA binding protein (TBP) (Hs99999910_m1) all from Applied Biosystems in an Applied Biosystems™ 7500 Real-Time PCR Systems. Relative expression was calculated as $2^{-\Delta Ct}$ (where Ct is the median threshold cycle from 3 replicates).

HLA-E genotyping

An in-house developed strategy based on Next Generation Sequencing (NGS) was used for HLA-E genotyping at the Laboratori d'Histocompatibilitat i Immunogenètica in Barcelona (BST). This strategy consists of a long-range PCR to amplify the HLA-E gene from 5' UTR to 3' UTR. Library preparation (enzymatic fragmentation, adapter ligation, and barcoding) was performed using the NGSgo-LibrX and NGSgo-IndX kits (GenDx, Utrecht, The Netherlands) according to the manufacturer's instructions. The final denatured library was sequenced using a MiSeq system with a 300-cycle MiSeq Reagent Kit (Illumina, San Diego, CA, USA). HLA-E genotype determination was performed with NGSengine software (GenDX, version 2.21.0.20156) using the IPD-IMGT/HLA database as a reference (version 3.38.0).

Soluble HLA-E ELISA

Soluble HLA-E in plasma was measured by the commercially available HLA Class I Histocompatibility Antigen, alpha Chain E (HLA-E) ELISA Kit (Antibodies online GmbH) in accordance with the manufacturer's instructions. Samples were read on a Perkin Elmer Ensight Plate reader.

Total HIV DNA quantification

Total HIV DNA was quantified in PBMC lysates by droplet digital PCR (ddPCR) in duplicate as described previously.[372] Briefly, two different primer/probe sets annealing to the 5' long terminal repeat and Gag regions, respectively, were used to circumvent sequence mismatch in the patients' proviruses, and the RPP30 housekeeping gene was quantified in parallel to normalize sample input. Raw ddPCR data were analyzed using the QX100 droplet reader and QuantaSoft v.1.6 software (Bio-Rad).

7.7. Selection of HIV-derived HLA-E candidates

A total of 14 HLA-E binding epitopes were evaluated, including 2 described canonical HLA-E epitopes (VL9-Cw1and VL9-CMV[359]) and 12 non-canonical peptides derived from EBV (SL9)[373]

and HIV (AA9, KG9, MD9, PM9, QE9, RL9, RV9, SN9, TP9, VI9, YG9). HIV-derived peptides were selected based on described HLA-E surface stabilization assays (MD9,PM9, RV9, TP9, YG9)[265], alteration of NK degranulation activity (AA9)[266] and HIV homologies to described SIV epitopes shown to be the targeted by SIV-specific T-cell responses in rhesus macaques (KG9, QE9, RL9, SN9, VI9)[374].

ID	Sequence	Organism	Protein	
VL9-B7	VMAPRTVLL	Human	HLA-B7	Leader sequence
VL9-Cw1	VMAPRTLIL	Human	HLA-Cw1	Leader sequence
VL9-CMV	VMAPRTLIL	CMV	UL40	
E SL9	SQAPLPCVL	EBV	BZLF1	
HIV AA9	AISPRTLNA	HIV	Gag	p24
HIV KG9	KRIKCFNCG	HIV	Gag	p24
HIV MD9	MYSPVSILD	HIV	Gag	p24
HIV PM9	PEIVIYQYM	HIV	Pol	Retrotranscriptase
HIV QE9	QMLKETINE	HIV	Gag	p24
HIV RL9	RMYSPTSIL	HIV	Gag	p24
HIV RV9	RIRTWKSLV	HIV	Vif	
HIV SL9	SEELRSLYN	HIV	Gag	p24
HIV TP9	TALSEGATP	HIV	Gag	p17
HIV VI9	VGEIYKRWI	HIV	Gag	p24
HIV YG9	YFSVPLDEG	HIV	Pol	Protease

Table 9. HLA-E binding epitopes tested in this study.

7.8. Structural analysis of HLA-E and TCR/NKG2 receptors interaction

A molecular model was constructed for HLA-E*01:01 and HLA-E*01:03 bound to PM9 and RL9 peptides based on the 6GL1 X-ray crystal structure. The initial molecular model of HLA-E-peptides interacting with NKG2A/2C-CD94 and TCR was constructed based on available X-ray crystal structure in the Protein Data Bank (3CDG and 5W1V). The initial models were Energy Minimized using Gromacs 5.0.

7.9. Statistical analysis

GraphPad Prism version 8 for Mac OS X (La Jolla, CA) was used for statistical analysis. For comparisons between group medians, non-parametric Mann-Whitney (MW) test was performed for unpaired data and Wilcoxon test (W) for paired data. χ^2 analysis was used to detect differences in frequencies. Multiple comparisons were performed by two-way ANOVA for unpaired data and Friedman's test (F) for paired data with post-hoc false discovery rate correction (FDR). HLA-E mRNA expression levels measured by RT-PCR were corrected for CD4+ T cell counts when possible. Correlations were plotted using R.4.1.2 (R Core Team, 2018) and circlize package (Gu, 2014). Statistical significance criteria were set at $p < 0.05$ and q-value <0.1.
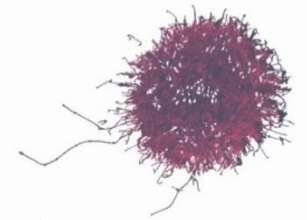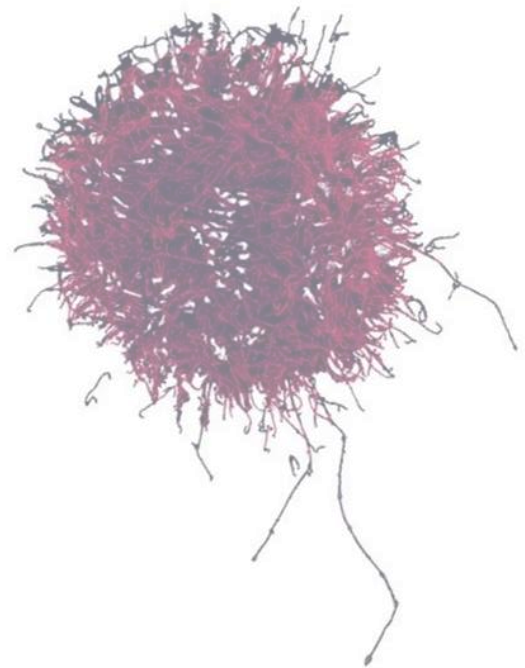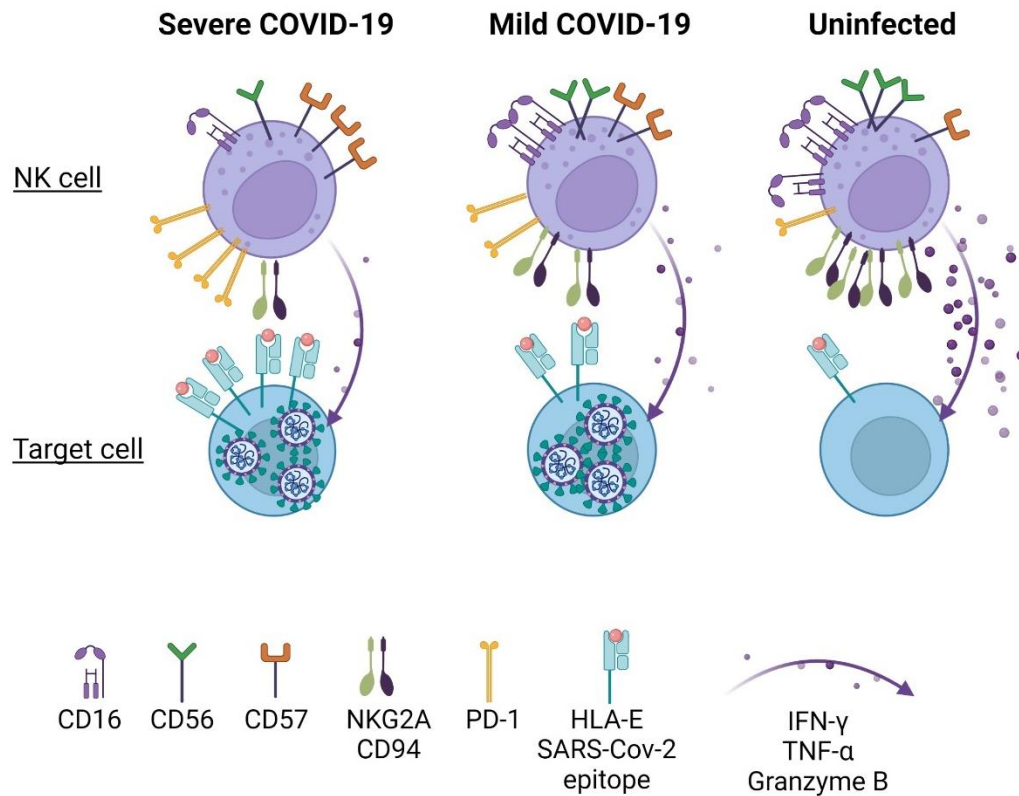
RESULTS

NK cell response to acute viral infection

COVID-19 severity is related to the presence of exhausted NK

cells unresponsive to HLA-E mediated signaling

Abstract

We studied the relationship between HLA-E expression, NK cell phenotype, effector functions and COVID-19 course. Our results showed that increased HLA-E levels in severe COVID-19 patients were associated with NK cell exhaustion, reversion of the NKG2A/NKG2C ratio and reduced NK cell response when stimulated through HLA-E/NKG2X axis. SARS-CoV-2 infection was linked to a loss of the highly active CD56^{bright} and CD56^{dim} subsets, while CD56^{neg} and adaptive NK cells were augmented, especially in people with more severe forms of the disease. We then tested NK cell phenotype and response in people with complete dose of mRNA-based anti-SARS-CoV-2 vaccines. Vaccination led to a dramatic drop of the PD-1 expression within the total NK cell fraction and increased IFN-γ production in the CD56^{bright} population, revealing a bystander effect of the vaccines in the innate immune response. Of note, NKG2A expression was also significantly reduced in these participants, suggesting that the loss of NKG2A$^+$ NK cells might be related to the exposure to Spike-1 epitopes.

1. COVID-19 severity is related to high expression of HLA-E and presence of soluble HLA-E in plasma

To test whether or not HLA-E expression and genotype (HLA-E*01:01 and *01:03) had an impact on the course of COVID-19, we measured HLA-E mRNA levels in total PBMCs from HLA-E genotyped individuals with severe or mild COVID-19, as well as a group of SARS-CoV-2 uninfected and non-vaccinated individuals.

No differences in allele frequencies were observed among the different groups, suggesting that HLA-E genotype did not severely impact COVID-19 outcome (Fig. 16A). HLA-E allelic polymorphism did not influence HLA-E expression levels neither (data not shown). However, a highly significant increase in total HLA-E transcripts in total PBMC was observed when we compared the Severe with the Uninfected (MW, p = 0.0001) and the Mild (MW, p = 0.0173) groups (Fig. 16B). To validate these observations, we analyzed the presence of soluble HLA-E (sHLA-E) in plasma. Although the comparison did not reach statistical significance, we observed a trend to detect sHLA-E in plasma in patients suffering severe COVID-19 (50% of the samples sHLA-E+, 6/12) when compared to mild patients (25% of the samples sHLA-E+, 3/12) and uninfected individuals (17% of the samples sHLA-E+, 2/12) (χ^2, p = 0.0833, Fig. 16C).

These data indicate that NK cells from severe COVID-19 patients may be exposed to higher levels of cell-bound and sHLA-E, compared to people suffering milder forms of the disease or uninfected individuals, and may thus be more continuously and more vigorously stimulated.
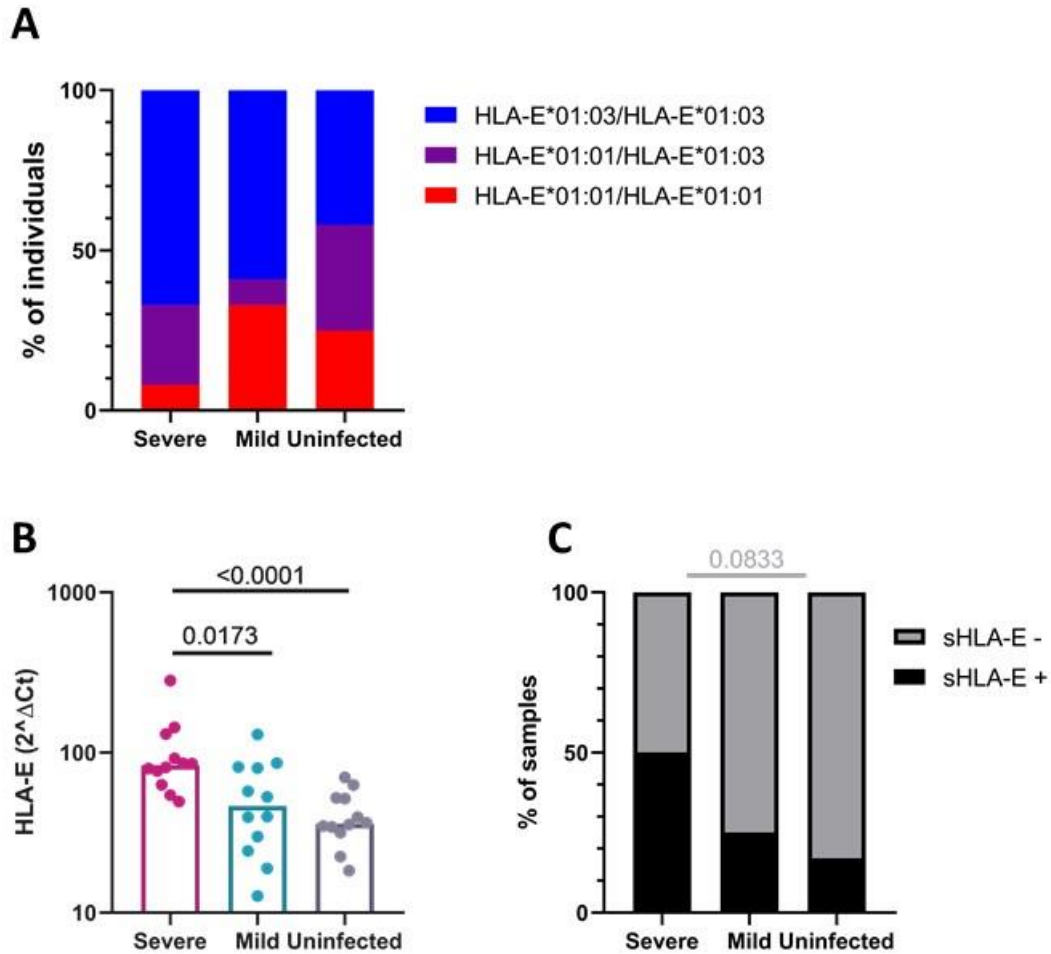
Figure 16. Molecular study of HLA-E expression in the context of COVID-19. (A) Frequency of HLA-E haplotypes within each of the groups (HLA-E*01:03 homozygosity in blue; heterozygosity in purple; HLA-E*01:01 homozygosity in red). **(B)** HLA-E mRNA expression in PBMC, measured by qPCR in individuals suffering from Severe COVID-19 (n=12, magenta), Mild COVID-19 (n=12, blue) and SARS-Cov2 naïve (n=12, grey). **(C)** Percentage of samples showing detectable levels of soluble HLA-E measured by ELISA. Chi-square was performed to determine the significance of HLA-E allele among COVID-19 severity (A) and the presence of soluble HLA-E (C), while Mann-Whitney test was performed to compare differences between groups (B). Results were considered statistically significant when $p < 0.05$ while trends ($p<0.1$) are indicated in grey.

2. Severe COVID-19 infection is associated with a profoundly changed NK cell landscape with a significant loss of CD56^{bright}

To build on the finding of enhanced HLA-E expression and increased plasma levels of sHLA-E, we examined the potential associations between COVID-19 severity and changes in NK cell phenotypes and subpopulations. Using flow cytometry, the expression of CD16, CD56, CD57, PD-1, LAG-3, NKG2A and NKG2C was determined in unstimulated NK cells, negatively isolated from total PBMCs of individuals suffering severe or mild COVID-19, in comparison with uninfected individuals.

Dimensional reduction was performed by tSNE and X-Shift (Fig. 17). A total of 13 clusters within the CD3-negative fraction were determined (Fig. 18A). Figure 18B differentiates between immature CD16$^-$CD56$^-$ (clusters 2,3,5), senescent CD56^{dim}CD16$^-$ (clusters 1,4,6,7,9), CD56^{bright}CD16$^-$CD57$^-$ (cluster 8), CD56$^-$CD16$^+$ (cluster 10) and adaptive CD56$^-$CD16$^+$CD57$^+$ (clusters 11, 12, 13) NK cells. Remarkably, the senescence-associated marker CD57 was also expressed in two clusters within the CD56^{neg} subset and in all the CD56^{dim}CD16$^-$. PD-1, which is usually used as an exhaustion marker, was expressed in one of the CD56^{neg} cluster and three CD56^{dim}CD16$^-$ clusters, suggesting that some effector NK cells might be exhausted. On the other hand, LAG-3 was slightly expressed in all CD56^{dim}CD16$^-$ and highly expressed on CD56^{dim}CD16$^+$ and adaptive NK cells. NKG2A was expressed in at least one cluster of each subset, indicating that it might also be maintained at later stages of NK cell maturation. On the other hand, NKG2C was limited to one CD56^{dim}CD16$^-$ cluster and to the adaptive NK cells, illustrating its appearance only in the final steps of NK cell development.

The contribution of each cluster to the whole NK cell population was then used to evaluate differences between patient groups. Seven of the 13 clusters were significantly altered in COVID-19 patients (severe and mild) compared to uninfected individuals (Fig.18B), including the increase in two of the CD56^{neg} and three of the CD56^{dim}CD16$^-$ clusters, while CD56^{bright}CD16$^-$ and one cluster of the CD56^{dim}CD16$^+$ were reduced. Remarkably, only the CD56^{bright} cluster 8 significantly differentiated between mild and severe forms of COVID-19 (MW, Severe vs Mild, p = 0.0019) (Fig. 18C). Interestingly, four of the five clusters that were more abundant in severely affected COVID-19 patients, expressed PD-1, suggesting a relationship between NK exhaustion and COVID-19 severity.
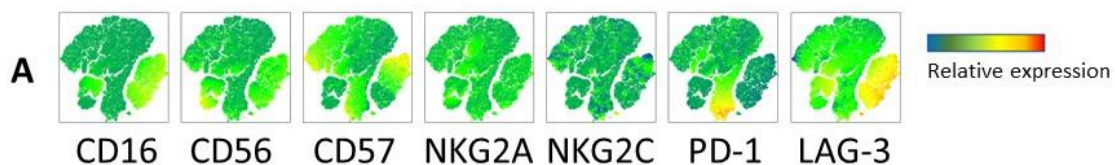
Figure 17. tSNE visualization. Dimensional reduction was applied based on the expression of NK cell lineage (CD56, CD16, CD57), HLA-E receptors (NKG2A, NKG2C) and exhaustion/activation markers (PD-1, LAG-3).
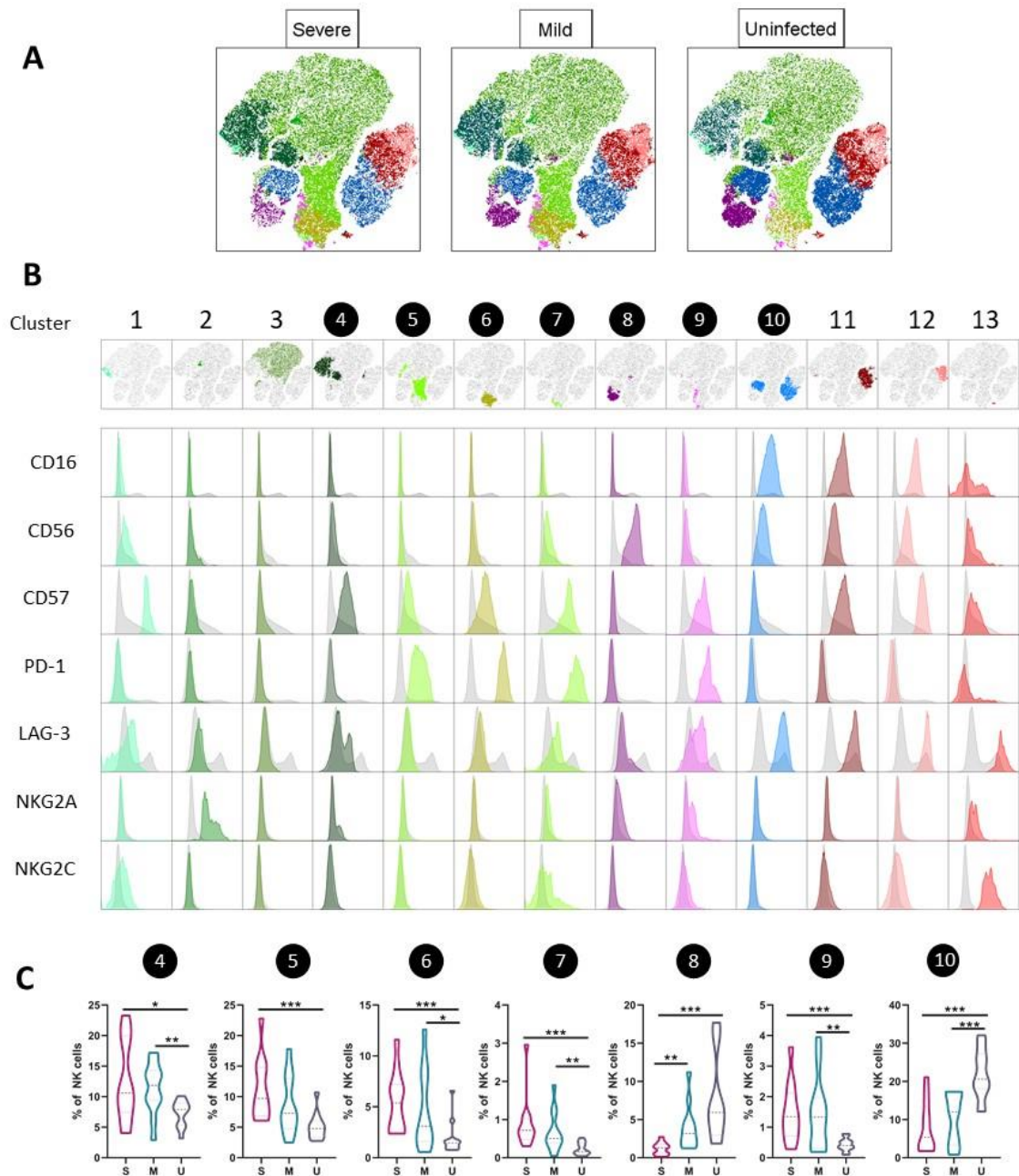
Figure 18. Visualization of unsupervised clustering of tSNE dimensional reduction on NK cell populations. (A) Dimensional reduction was applied by tSNE on 96000 events from sorted NK cells from Severe COVID-19 (n=12, left) Mild COVID-19 (n=12, middle) and SARS-Cov2 naïve (n=12, right) and 13 clusters were determined by FlowSOM. **(B)** Relative expression of surface markers measured by flow cytometry of each cluster compared to the bulk expression on the total NK cell fraction. **(C)** Representation of each cluster in the total NK cell fraction in Severe COVID-19 (n=12, magenta) Mild COVID-19 (n=12, blue) and uninfected (n=12, grey). Mann-Whitney test was performed to compared differences between groups and results were considered significant when p-value<0.05(*), <0.01(**) or <0.001(***).

To further explore changes in NK subpopulation upon SARS-CoV-2 infection, the proportions of CD56^{neg} (CD56$^-$CD16$^-$), CD56^{bright} (CD56$^{brigth+}$CD16$^-$), CD56^{dim} (CD56^{dim}CD16$^+$) and adaptive NK (CD56^{dim}CD16$^+$CD57$^+$) populations were determined by manual gating (Fig. 19A). When comparing subpopulations, severe COVID-19 was related to an increase of the two opposite poles of the NK cell maturation spectrum: CD56^{neg} (MW, Severe vs Mild p = 0.0014; Severe vs Uninfected p < 0.001) (Fig. 19A) and adaptive NK cells (MW, Severe vs Mild p = 0.0284; Severe vs Uninfected p = 0.0009) (Fig. 19D). On the other hand, severity was related to a significant loss of CD56^{bright} (MW, Severe vs Mild p < 0.0001; MW Severe vs Uninfected p < 0.0001) (Fig. 19B). The CD56^{dim} population was decreased when comparing Severe to Uninfected (MW, p = 0.0058) (Fig. 19C).

Together, our results identify a severe impact of SARS-CoV-2 infection on the relative abundance of different NK cell subsets and their exhaustion profiles, especially in patients suffering severe forms of the disease. Hallmarksof these changes are the loss of the highly active CD56^{bright} and CD16^{dim} subsets and a gain of unconventional CD56^{neg}, senescent-like CD56^{dim}CD16$^-$ and adaptive NK cells in severe COVID-19 patients, accompanied by expression of PD-1, suggestive of a profound alteration on the NK-mediated innate immune response in COVID-19 patients.
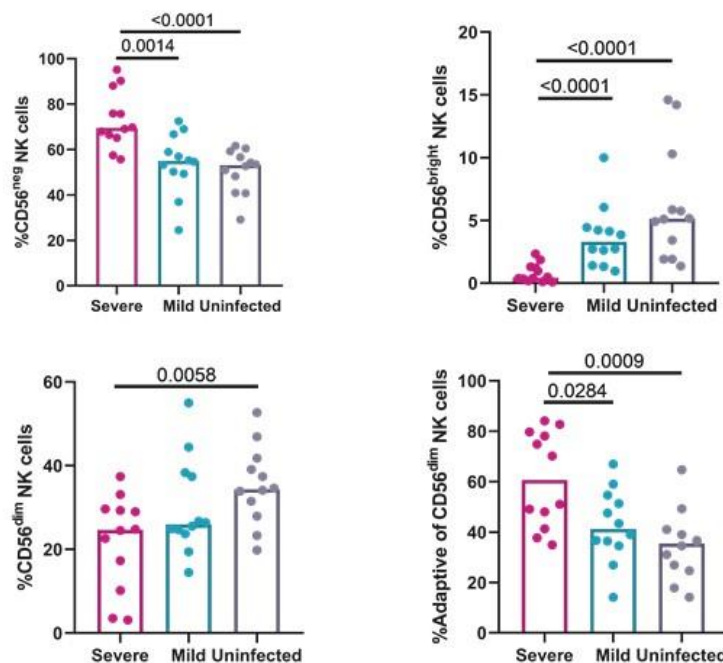
Figure 19. NK cell subsets. (A) Manual gating was applied in sorted NK cells from Severe COVID-19 (n=12, magenta), mild COVID-19 (n=12, blue) and uninfected individuals (n=12, grey). Abundance of CD56^{neg}, CD56^{bright}, CD56^{dim} and

adaptive NK cells was determined. Mann-Whitney test was performed to compared differences between groups and results were considered significant when p-value<0.05.

3. SARS-CoV-2 infection is related to NKG2A/NKG2C ratio switch and more exhausted NK cell profile

Given the differences in NKG2A and C expression in the unsupervised clustering analysis, we explored how the expression of these HLA-E receptors coincided with markers of NK cell exhaustion, including PD-1 and LAG-3, in total NK as well as in well-established NK subpopulations including CD56^{neg}, CD56^{bright}, CD56^{dim} and adaptive NK cells (Fig. 20).

Only a negligible proportion of the NK cells were NKG2A$^+$NKG2C$^+$, indicating its mutually exclusive expression[375]. We asked next whether the expression of both receptors was different in COVID-19 patients from uninfected individuals. When evaluating the NKG2A/NKG2C ratio (defined as the ratio of the % of NK cells positive for either one of the receptors), we observed a significant decrease in the total NK cell fraction ratio in severe COVID-19 patients when compared to uninfected individuals (MW, p = 0.0007) and mild COVID-19 patients (MW, p = 0.0332) (Fig. 20A). Chi-square analysis also showed a difference in the proportion of individuals with preferential expression of NKG2C over NKG2A (NKG2A/NKG2C ratio below 1: Severe 5/12 (41.7%), Mild 1/12 (8.3%) and Uninfected 0/12 (0%), χ^2 p = 0.015) (Fig. 20A). This reduced receptor ratio was also seen in all NK cell subsets individually, except for CD56^{bright}: CD56^{neg} (MW, p = 0.0205), CD56^{dim} (MW, p = 0.0449) (Fig. S6A) and adaptive (MW, p = 0.0036) (Fig. 20B). Furthermore, the ratio of NKG2A/NKG2C in adaptive NK cells was also significantly increased when comparing severe to mild forms of COVID-19 (MW, p = 0.0035) (Fig. S6C). This observation was driven by a significant higher abundance of NKG2C$^+$ adaptive NK cells in this group rather than a reduction of NKG2A$^+$ (Fig. S7).

As CD56^{neg} and CD56^{bright} clusters expressing PD-1 and LAG-3 contributed differently to the NK cell landscape in the tSNE analysis, we explored further the exhaustion and activation level in the total NK cell fraction and in CD56^{neg} and CD56^{bright} NK subpopulations. Total NK cells from severe patients showed a more exhausted profile, measured as PD-1 expression, compared to uninfected individuals (MW, p = 0.0001) and when comparing severe with mild COVID-19 patients (MW, p = 0.0151) (Fig. 20C). NK subset analysis showed this effect to be driven by the CD56^{neg} (MW, p = 0.0009) and CD56^{bright} subsets (MW, p = 0.0449) (Fig. S6B). On the other hand,

uninfected individuals exhibited more LAG-3^{+} cells in total NK cell fraction than SARS-CoV-2 infected individuals (MW, Severe vs uninfected p = 0.0036, Mild vs uninfected p = 0.0387) (Fig. 20C).

These results further validate the findings observed applying unsupervised clustering (Fig. 18) and demonstrate marked changes in the NK cell subpopulations distribution concomitant with exhausted profiles, predominantly affecting patients suffering from severe COVID-19.
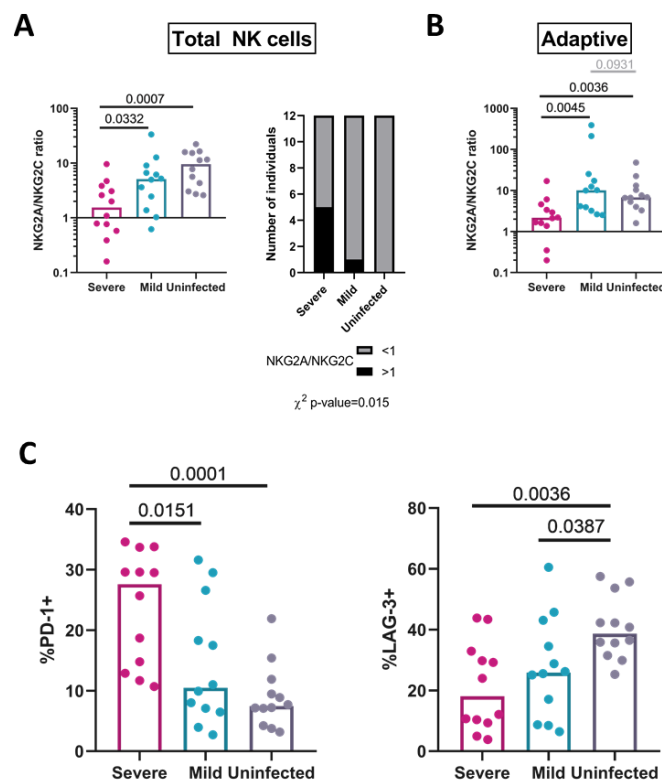
Figure 20. NK cell surface markers of HLA-E recognition (NKG2A, NKG2C), exhaustion and activation (PD-1, LAG-3). Manual gating was applied to sorted NK cells from Severe COVID-19 (n=12, magenta), mild COVID-19 (n=12, blue) and uninfected individuals (n=12, grey). (A) NKG2A/NKG2C ratio and frequency of individuals with NKG2A/NKG2C ratio above or below 1 in total NK cell fraction. (B) NKG2A/NKG2C ratio in adaptive NK cells. (C) PD-1 (left) and LAG-3 (right) expression in the total NK cell fraction. Mann-Whitney test was performed to compared differences between groups and χ2 to compare frequency of individuals with total NK cell NKG2A/NKG2C ratio above or below 1. Results were considered significant when p-value<0.05. Trends are shown in grey.

4. Armed" CD56^{bright} and adaptive NK Cells are functionally impaired in severe COVID-19.

Since previous studies have shown a basal activation of CD56^{bright} NK cells in severe COVID-19 patients[239] and since our data suggest that this could lead to a more exhausted profile (higher PD-1 expression, especially in CD56^{neg} and CD56^{bright}), we evaluated the functionality of NK cells from COVID-19 patients with different disease severity. We assessed the capacity of NK to exert cytotoxicity and produce cytokine in response to an HLA-E null K562 target cells by measuring cell lysis (% of killing), degranulation (% of CD107a^{+} NK cells and granzyme B SFC/106 NK cells) and cytokine secretion (IFN-γ^{+} and TNF-α^{+} NK cells) and determined basal activation levels by measuring INF-γ and TNF-α production in unstimulated NK cells (i.e. without target cell co-culture).

Our data show that CD56^{bright} and adaptive NK cells from severe COVID-19 patients showed a higher level of ongoing production of INF-γ and TNF-α when comparing different patient groups and uninfected individual (Fig. 21A and 21B, respectively), indicating that both subpopulations had higher basal activation.

Curiously, increased basal activation was not reflected by a higher capacity to respond to HLA-E null target cells. In fact, the overall NK cell population from severe patients was less capable to degranulate (measured as %CD107a^{+}) and produce IFN-γ and TNF- α when compared to uninfected individuals (Fig. 21C).

The most affected subset in this comparisons were CD56^{bright} NK cells. We observed that CD56^{bright} from COVID-19 patients showed lower levels of degranulation (measured as %CD107a^{+}), IFN-γ and TNF- α production (Fig. 21D) when compared to SARS-CoV-2 naïve participants, especially in severe COVID-19 patients. Remarkably, IFN-γ and TNF-α production by CD56^{bright} from mild patients was significantly higher than severe patients (MW, p = 0.0203 and p = 0.0141, respectively) (Fig. 21D).

Impaired degranulation and TNF-α production to HLA-E stimulation in severe COVID-19 patients compared to uninfected was also observed in CD56^{neg} (Fig. S8A), but not in CD56^{dim} (Fig. S8B). Still, we observed a reduction in degranulation capacity of adaptive NK cells in severe COVID-19 (Fig. S8C).

This impaired NK functionality in severe and mild COVID19 course was also reflected by a reduced cytolytic activity (Severe vs Mild p = 0.0387, Severe vs Uninfected p = 0.0001 and

Mild vs Uninfected p = 0.0023) and Granzyme B secretion compared to uninfected individuals (Severe vs Mild p = 0.0093, Fig. 21E).

Together, these findings demonstrate that patients suffering more severe forms of COVID-19 indeed harbored CD56^{bright} and adaptive NK cells with higher basal activation, but also at the same time with reduced capacity to respond to missing-self stimulation and effectively eliminate target cells.
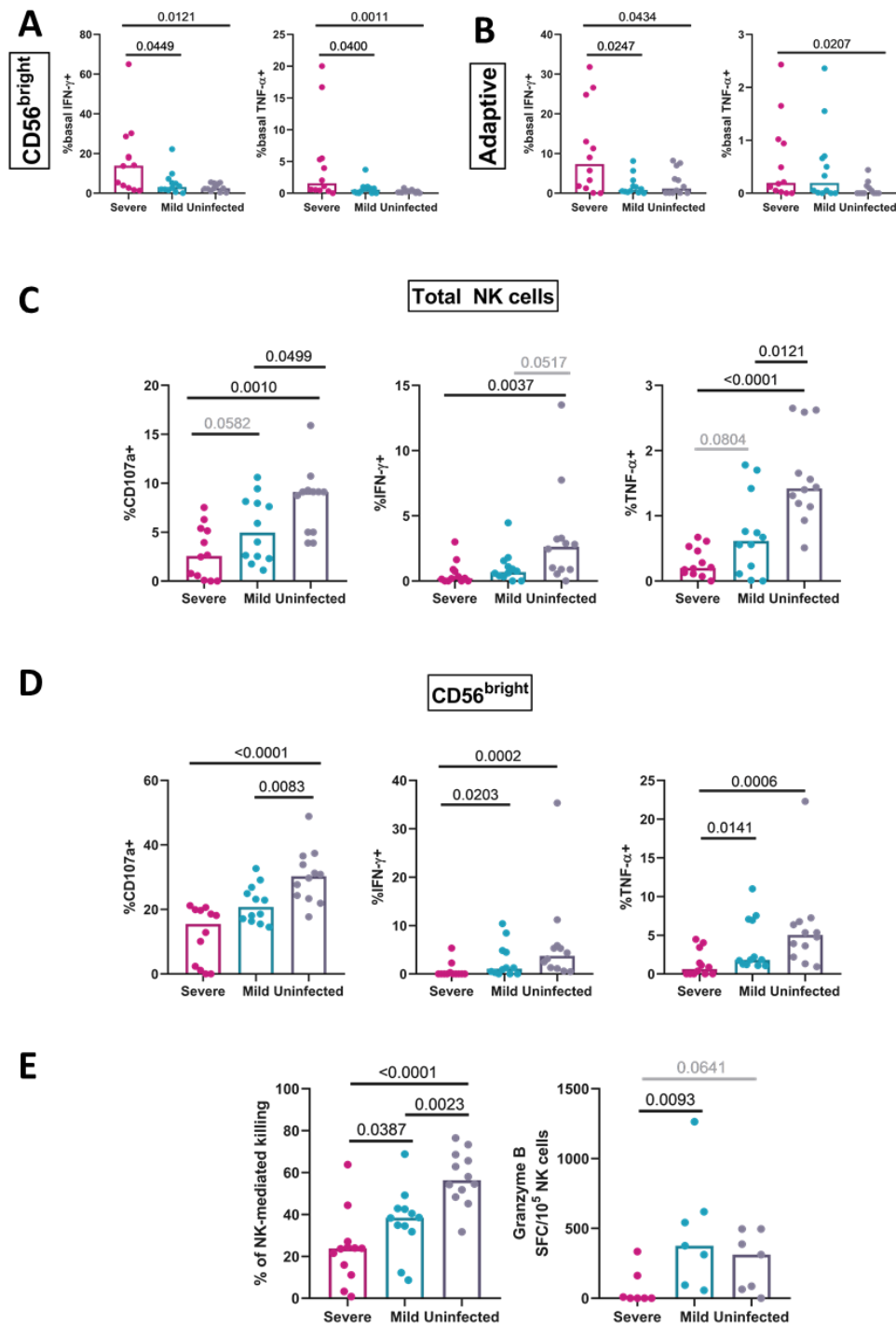
Figure 21. NK cell basal activation and response to HLA-E null K562 cells. Gating of CD107a^{+}, IFN-γ^{+} and TNF-α^{+} NK cells from Severe COVID-19 (n=12, magenta), mild COVID- 19 (n=12, blue) and uninfected individuals (n=12, grey). (A) Basal IFN-γ^{+} and TNF-α^{+} in CD56^{bright} NK cells in the absence of target cells. (B) Basal IFN-γ^{+} and TNF-α^{+} in adaptive NK cells in the absence of target cells. (C) %CD107a^{+}, % IFN-γ^{+} and % TNF- α^{+} of total NK Cells in response to HLA-E null K562 cells. (D) %CD107a^{+}, % IFN-γ^{+} and % TNF- α^{+} of CD56^{bright} NK Cells in response to HLA-E null K562 cells. (E) Total NK cell fraction functional assays: K562 killing (left) measured by calcein-AM retain assay and Granzyme B ELISPOT (right). Mann-Whitney test was performed to compared differences between groups and results were considered significant when p-value<0.05. Trends are marked in grey.

5. Exposure to elevated levels of HLA-E and increased PD-1 expression correlates with impaired NK cell mediated response

In order to elucidate potential correlates that drive impaired NK cell function in COVID-19 patients, we performed a multiple correlation test relating age, HLA-E expression in total PBMCs, NK functional test (Granzyme B and Cytotoxicity), NK cell phenotype including PD-1, LAG-3, NKG2A and NKG2C expression, degranulation (CD107a) and cytokine secretion (IFN-γ and TNF-α) within the total NK cell fraction as well as in CD56^{neg}, CD56^{bright}, CD56^{dim} and adaptive NK cells.

Within the total NK cell population, NKG2C expression was positively correlated with HLA-E expression and PD-1. By contrast, both HLA-E and PD-1 expression showed a negative correlation with cytotoxicity. Additionally, PD-1 showed strong negative correlations with the NK cell degranulation and IFN-γ and TNF-α production. Notwithstanding, LAG-3 could be considered an activation marker given the negative correlation with PD-1 but the positive correlation with NK cell degranulation and cytokine production (Fig. 22A).

Cytotoxicity correlated positively with CD56^{bright} abundance in the total NK cell population and all CD56^{bright} effector parameters (degranulation and cytokine production). These data suggest that CD56^{bright} contribution to total NK cell cytotoxicity might be essential. Of note, CD56^{bright} subset effector functions were negatively impacted by HLA-E and PD-1 expression (Fig. 22B).

The abundance of CD56^{dim} NK cells, which are usually considered the subset with the highest cytotoxic potential, also showed a positive impact on cytotoxicity. However, both CD56^{neg} and adaptive NK cells degranulation marker CD107 also correlated positively with cytotoxicity, but not their respective abundance. This finding suggests that all NK cell subsets

might harbor a cytotoxic potential but the intermediate stages of NK cell development, CD56^bright and CD56^dim, have the higher effector functions (Fig. S9).

Remarkably, although age is a known major risk factor for severe COVID-19, it did not correlate with any of the NK cell parameters. Overall, our results indicate that impaired NK cell responses to HLA-E null target cells was related to i) an increased expression of HLA-E on the PBMCs that were the source of isolated NK cells, and ii) to the PD-1 and NKG2C levels on NK cells. This suggests a more exhausted NK profile in patients with severe COVID-19. The degranulation marker CD107a in all the evaluated subsets indicated that essentially all NK cells might contribute to this function by releasing cytolytic molecules. However, higher proportions of CD56^bright and CD56^dim NK cells, which are highly active, had a beneficial effect on killing activity, in contrast to levels of CD56^neg and adaptive NK cells which were negatively associated with NK killing activity.
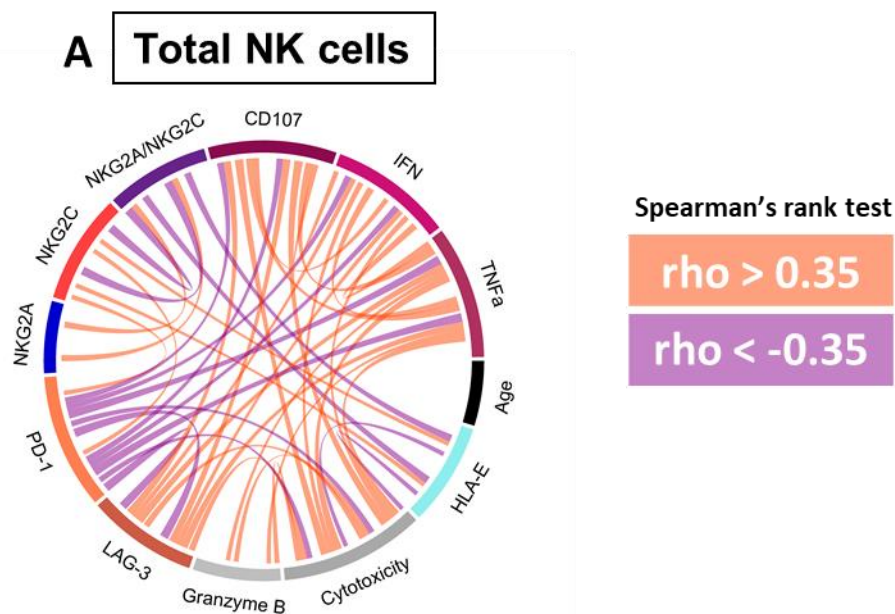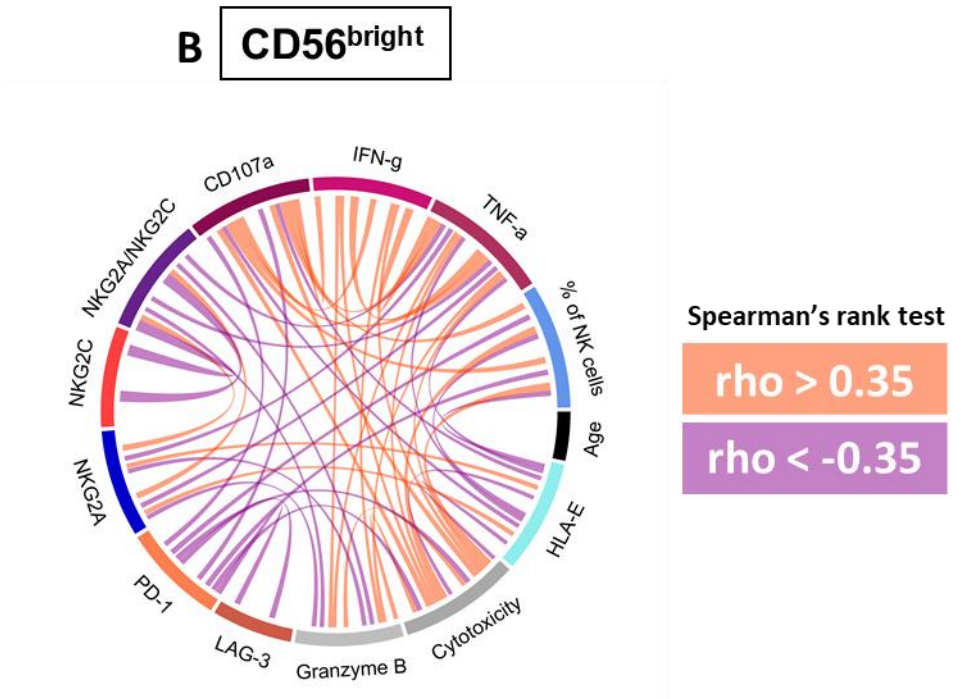
Figure 6. Chord diagrams representing positive and negative correlation between NK cell phenotype, NK cell function and HLA-E expression. Spearman's rank correlation matrix was applied on samples from 36 individuals including Severe COVID-19 (n=12), mild COVID- 19 (n=12) and uninfected individuals (n=12) and significant correlations with p>0.05 and r > 0.35 (orange link) or r < -0.35 (violet link) were plotted using R 4.1.2 and circlize package. This analysis was performed on data based on the (A) total NK Cell fraction and (B) CD56bright NK cells.

6. Reduced NK cell exhaustion and NKG2A expression at week four after SARS-Cov2 Spike-1 mRNA-based vaccination

Immunization with viral-vector delivered vaccines have shown potent increases in IFN-γ responses mediated by NK cells[244]. We thus evaluated the effect of two mRNA-based vaccines against SARS-CoV-2 on the distribution of NK sub-populations and their functional profiles. We performed NK cell surface characterization and functional analysis in 6 SARS-CoV-2 uninfected individuals that received two doses of Comirnaty-Pfizer/Biontech (n=3) or Spikevax-Moderna (n=3) 31.5±2 days after receiving the last injection.

Regardless of the vaccine received, we observed a redistribution of peripheral NK cell subpopulations when comparing their frequencies to those seen severe and mild COVID-19 patients and uninfected and vaccinated individuals. This shift included a loss of the aberrant CD56neg NK cells and the terminally differentiated adaptive NK population in vaccinated individuals. This loss was accompanied by an increase of the CD56bright and CD56dim (Fig. 23A).

Vaccination also had a beneficial effect in terms of cell activation and exhaustion. When comparing the phenotype within the whole NK cell population, vaccinated individuals showed lower levels of PD-1 (MW, p = 0.032) and higher levels of LAG-3 (MW, p = 0.0182) (Fig. 23B), a pattern that was also seen in CD56^{neg} NK cells (MW, PD-1 p = 0.0688, LAG-3 p = 0.0008) (Fig. S10B).

Remarkably, vaccination elicited a dramatic diminution of the NKG2A expression in total NK cells (MW, p = 0.0008) (Fig. 23C). This loss of NKG2A expression was also observed in CD56^{bright} (MW, p = 0.0145) and CD56^{dim} (MW, p = 0.0245) and showed a trend in CD56^{neg} (MW, p = 0.1246) and adaptive NK cells (MW, p = 0.0529) (Fig. S10C).

Vaccination also had an impact on NK cell function. Although there were no differences in degranulation (measured as %CD107a$^+$ cells), vaccinated individuals significantly increased CD56^{bright} IFN-γ secretion towards HLA-E null target cell stimulation (MW, p = 0.0069) (Fig. 7D). Surprisingly, vaccination was also related to lower cytotoxicity when compared to the unvaccinated group (MW, p = 0.0245) (Fig. 23E).

These data identify a beneficial effect of mRNA-based vaccines against SARS-CoV-2 in terms of NK cell phenotype and function with elevated numbers of active NK cells (CD56^{bright} and CD56^{dim}) and a loss of aberrant CD56^{neg} and adaptive subsets, along with a less exhausted profile with decreased NKG2A expression and increased capacity to produce IFN-γ.
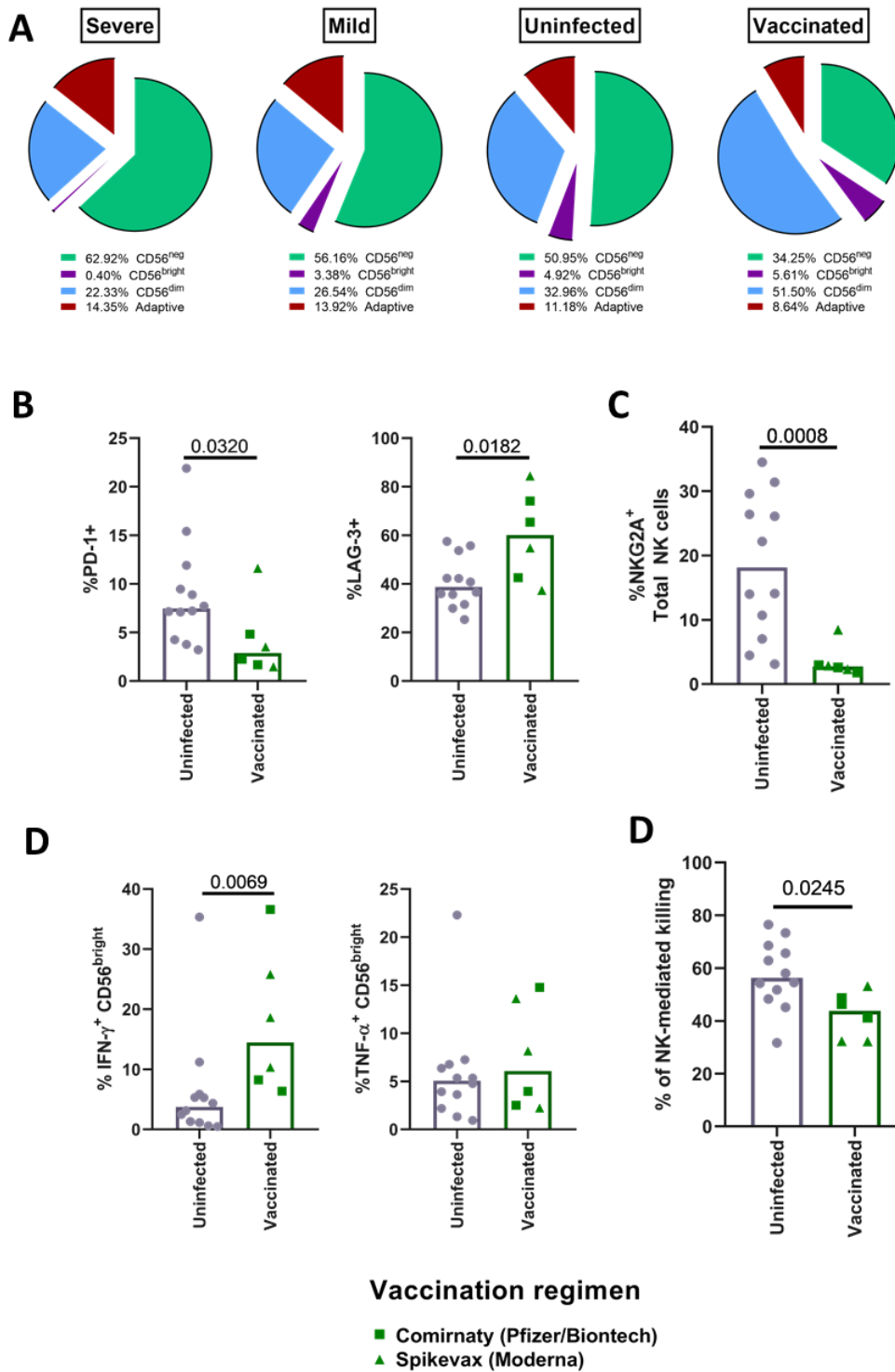
Figure 7. Impact of SARS-Cov2 Spike-1 vaccination on NK cell phenotype. Surface expression of CD56, CD16, CD57, NKG2A, NKG2C, PD-1 and LAG-3 was determined by flow cytometry in sorted NK cells from uninfected individuals who received the complete vaccination regimen against SARS-Cov2 with Spike-1 RNA-based vaccines (2 doses Comirnaty, n=3, 2 doses Spikevax, n=3) and compared to uninfected unvaccinated individuals (n=12). (A) Pie charts comparing NK cell subsets abundance in patients with severe (left) or mild (middle-left) COVID-19, uninfected (middle-right) and vaccinated individuals (right). (B) % of PD-1+ and LAG-3+ cells within the CD56neg NK cell fraction. (C) % of NKG2A+ cells within the total NK cell fraction. (D) %IFN-γ+ and TNF-α+ CD56bright NK cells. (E) Cytotoxicity against HLA-E null target cells. Mann-Whitney test was performed to compared differences between groups and results were considered significant when p-value<0.05.

7. Limitations of the study

Although the HLA-E*01:01 allele has been described as a risk factor for COVID-19 severity[241], we did not observe an association between HLA-E polymorphism and COVID-19 severity in our study cohort. However, the limited number of individuals included in the present study could have underpowered this analysis. Still, our data support the notion that the higher expression of HLA-E in patients suffering severe forms of COVID-19 may influence the HLA-E/NKG2X mediated NK cell regulation and with it, define COVID-19 severity, in line with the previously reported association between a KLRC2 gene mutation encoding a NKG2C variant and COVID-19 severity[241].

Longitudinal studies should be performed in order to clarify whether the NK cell exhaustion and increased HLA-E expression are risk factors for severe COVID-19 or consequence of the infection. The same limitation applies to the study of vaccine effects which, although providing statistically relevant findings could be further strengthened by assessing pre-vaccination, intermediate and long-term time points.

Finally, although patients´ age has been identified as one of the major risk factors for severe COVID-19[376], we did not found any correlation between participants age and NK cell phenotype and functional alteration. However, we selected individuals with a similar age range for this study (from late 40 to early 60) and our sample did not include the most susceptible ages for severe COVID-19 (>65 years). This may have prevented us from drawing further conclusions on the impact of age on NK function during SARS-CoV-2 infection.
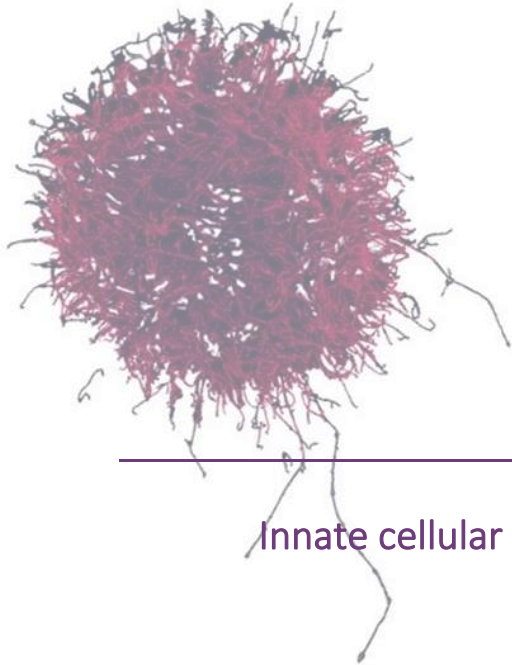
Chapter II

Innate cellular response to chronic viral infection

Disruption of the HLA-E/NKG2X axis is associated with

uncontrolled chronic HIV infections
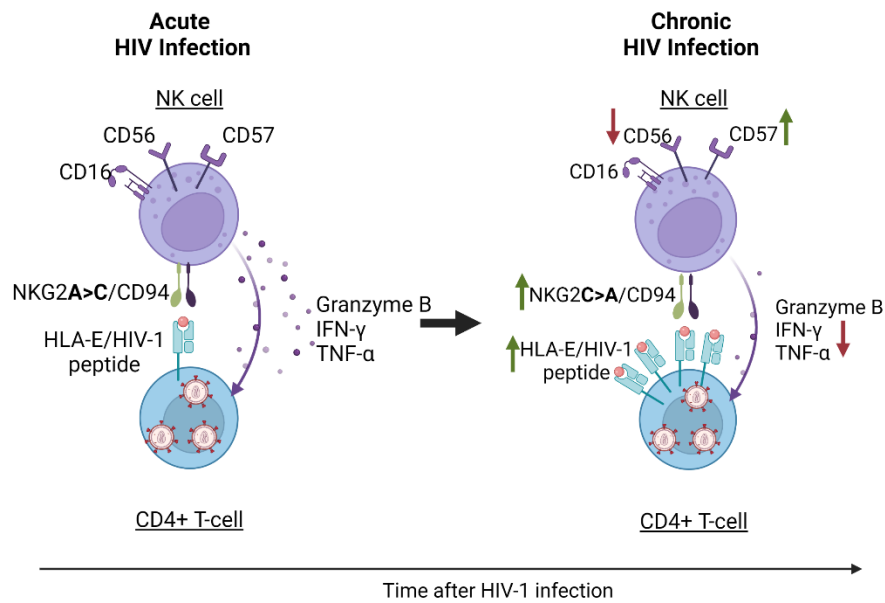
Abstract

The contribution of the HLA-E/NKG2X axis to NK-mediated control of HIV infection remains unclear. We have studied the relationship between HLA-E expression and phenotypical as well as functional characteristics of NK cells, in the context of chronic HIV infection and in an in vitro model of acute infection. High viremia in HIV+ individuals was related to increased HLA-E expression, changes in NK subpopulations, especially a reduction of the CD56^{bright} as well as an increase in adaptive NK subpopulation, a reversion of the NKG2A/NKG2C expression ratio and a loss of positive and negative regulation of NK mediated by HLA-E. This was reflected in a lower cytotoxic, degranulation and cytokine production capacity, especially in CD56^{bright} and adaptive NK. In line with these results, HLA-E expression showed a positive correlation with viral growth inhibition at 7 days in an in vitro model of acute infection, which was lost after 14 days culture. In structural and molecular analysis, we determined that only one out of 11 described HIV-derived HLA-E restricted epitopes increased HLA-E surface stability, although 8 of these were capable of increasing NK cell degranulation and three drove differences in NK-cell mediated cell lysis or cytokine secretion. In conclusion, our results indicate that HLA-E presenting HIV-derived epitopes may sensitize target cells for NK lysis in early infection, whereas prolonged exposure to elevated HLA-E expression levels may lead to NK dysfunction and reduced viral control.

1. Association of HLA-E expression level and allele genotype with HIV disease progression

In order to detect a potential relationship between HLA-E gene expression and the course of HIV infection, we evaluated the HLA-E mRNA levels in total PBMCs from HLA-E genotyped, HIV-seropositive individuals with different levels of viremia and CD4$^+$ T cell counts. Significantly different HLA-E mRNA levels were observed between HIV-high and HIV-low groups, even when correcting for CD4$^+$ T cell counts (Fig. 24A, MW p < 0.0001). This difference was confirmed in unrelated validation cohorts, where a remarkable reduction of HLA-E expression was found in individuals showing control of HIV infection (long-term non-progressors) in comparison to untreated HIV infected individuals with high viral loads (MW p = 0.0006) (Fig. 24A). In addition, when compared to HIV seronegative individuals, the levels of HLA-E expression were significantly higher in PBMC from individuals with chronic HIV infection, receiving cART (MW p = 0.0106) or untreated (MW p < 0.001). In addition, we observed not only a direct positive correlation between HLA-E expression and plasma viral load (r = 0.5681, p < 0.0001) but also between HLA-E expression and proviral HIV copy numbers (r = 0.3828, p = 0.0086, Fig. 24B).

We next clarified whether the single amino acid difference between the HLA-E*01:01 and HLA-E*01:03 alleles resulted in differential associations with virological parameters of HIV infection. HLA-E allele haplotype did not impact HLA-E gene expression and did not show any association with HIV plasma viral load when all samples were compared together (data not shown). However, when we compared the impact of the allele polymorphisms between HLA-E*01:01 and *01:03 on plasma viral load only in individuals with lower HIV viral load (HIV-low, n=31), a significantly higher proportion of individuals with undetectable plasma viral load (<50 HIV RNA copies/mL) were HLA-E heterozygous (χ2, p = 0.0186, Fig. 24C). These data suggest that higher levels of HLA-E expression in PBMCs are related to uncontrolled chronic HIV infection, while reduced expression is associated with natural control of HIV infection. In addition, there was a benefit of HLA-E*01:01/01:03 heterozygosity as individuals with low and undetectable viral loads were enriched for heterozygous genotypes.
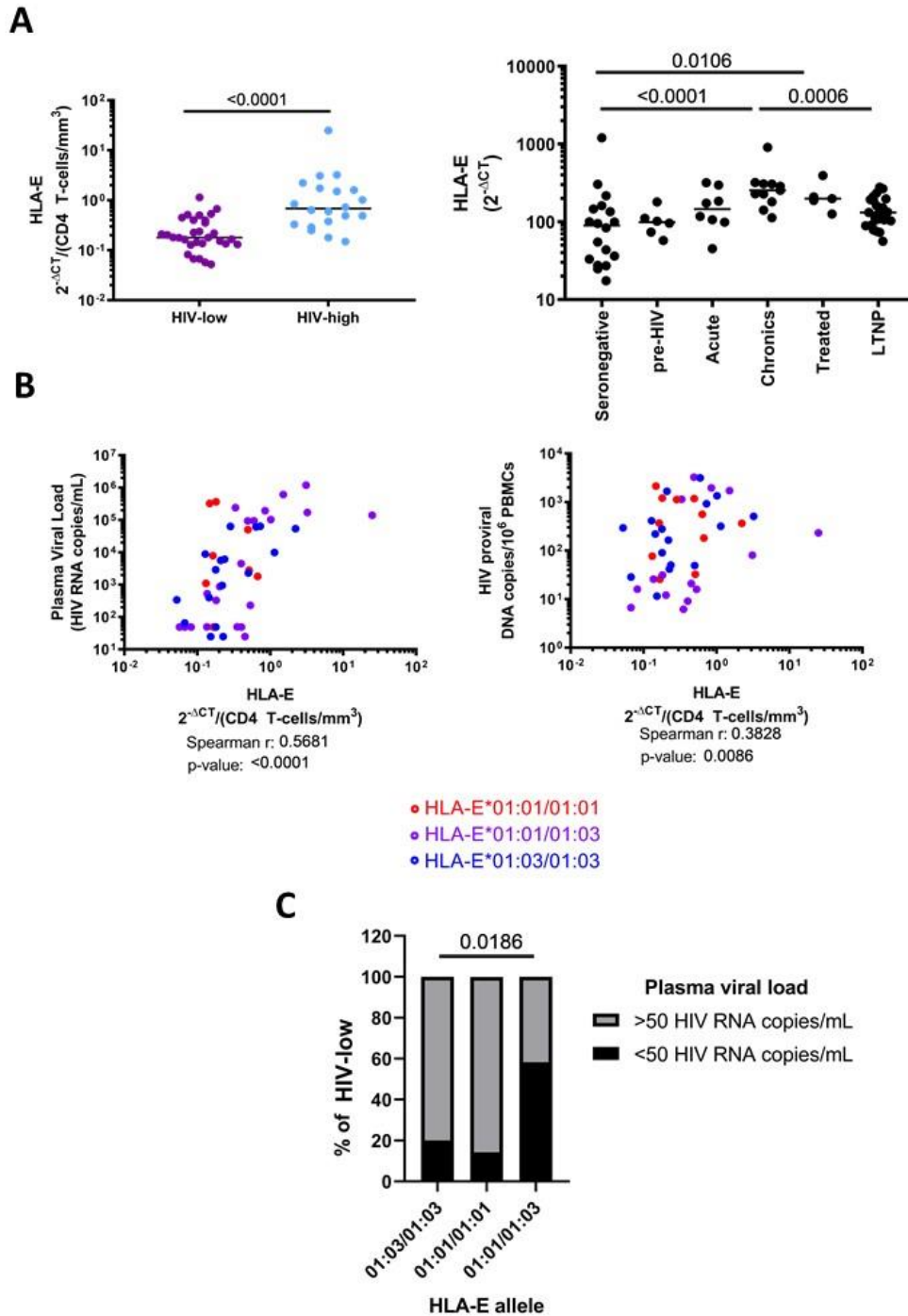
Figure 24. Role of HLA-E allele haplotypes and expression level during HIV infection. (A) HLA-E mRNA expression, measured by qPCR and corrected by CD4 count, is increased in individuals with HIV-high viremia (n=20) compared to HIV-low (n=31) (left). HLA-E expression progressively increases during natural clinical course of the HIV infection (right). **(B)** HLA-E expression levels correlated positively HIV with plasma viral loads and HIV viral reservoir size (determined as copy number of integrated proviral DNA). HLA-E allele genotypes showed no difference in terms of HLA-E expression, plasma viral load and reservoir size. **(C)** Frequency of HLA-E genotypes within the HIV-low group (n=31). Mann-Whitney test was performed to compare differences between groups **(A, C1)**, Spearman's rank correlation coefficient was applied to evaluate correlations **(B)** and Chi-square was performed to determine the significance of HLA-E allele among HIV natural controllers **(C)**. Results were considered statistically significant when p < 0.05 while trends are indicated in grey.

2. Uncontrolled chronic HIV infection is related to an imbalance of the CD56^{bright} NKG2A$^+$ and (CD56^{dim}CD57$^+$) NKG2C$^+$ adaptive NK cell subpopulations

In the context of infectious diseases, HLA-E expression has been linked to activation of NK cells with antiviral capacity. Since our analyses indicated that elevated HLA-E expression was also related with high HIV plasma viral loads, we examined whether this finding could reflect changes in specific NK cell subsets. For this purpose, we compared the prevalence of NK subsets characterized by the surface expression of NK subset markers CD56, CD16, CD57 and NKG2A and NKG2C in seronegative (SN), HIV-low (HL) and HIV-high (HH) individuals.

An exploratory unsupervised clustering analysis yielded a total of 10 clusters within the CD3-negative NK-cell population (Fig. 25A). Fold change (±1.5) in cluster size between SN and HL (SN/HL), SN and HH (SN/HH) and HL and HH (HL/HH), was used to identify differences in the contribution of each NK cell subpopulation to the total NK cell fraction (Fig. 25B). Figure 2C differentiates NK cell subpopulations grouped as immature CD56^{neg}CD16^{neg} (clusters 1 and 2), CD56$^{+/+++}$CD16^{neg} (clusters 3 and 4), CD56^{++}CD16$^{++/+++}$CD57$^-$ (clusters 5 and 6) and adaptive CD56^{++}CD16$^{++/+++}$CD57$^{+/++/+++}$ NK cells (clusters 7, 8, 9 and 10) along with the expression of HLA-E inhibitory (NKG2A) or activating (NKG2C) receptors within each group. Adaptive CD56^{++}CD16^{+++}CD57^{+++}NKG2C^{+++} (cluster 10) NK cells were less abundant in SN compared to both HH and HL, indicating that the expansion of these cells could be related to chronic HIV infection (Fig. 2C). Interestingly, some CD56$^+$ NK cells (clusters 4, 7, 8 and 9) showed a NKG2A/C receptor expression pattern that was comparable between SN and HL but differed markedly from HH (Fig. 25C). Specifically, SN and HL showed an increased percentage of NKG2A$^{+/+++}$cells within the more immature CD56^{bright} NK cells (cluster 4) and the terminally differentiated adaptive CD56^{++}CD16$^{++/+++}$CD57$^{+/++}$ cells (clusters 7 and 8), as well as a reduction in the NKG2C^{++} adaptive CD56^{++}CD16^{++}CD57^{+++} NK subset (cluster 9), when compared to HH. This imbalance in the abundance of CD56^{bright} and adaptive NK cell subsets was also associated with differences in the expression of HLA-E receptors NKG2A and NKG2C, suggesting that HLA-E expression influences this distinct NK differentiation and thus influences their capacity to support control of HIV infection.

A
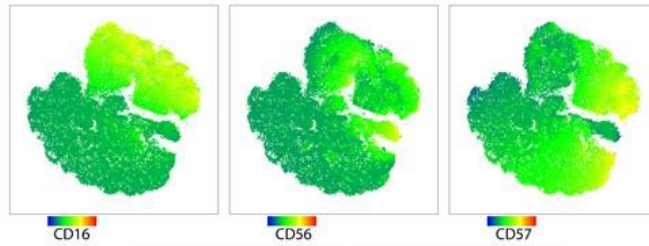
B
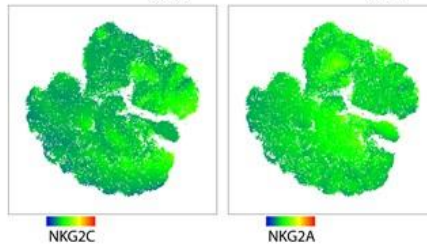
C

	Cluster	CD56	CD16	CD57	NKG2A	NKG2C	SN/HL	SN/HH	HL/HH
CD56neg CD16neg	1	-	-	-	-	-			
	2	-	-	+	-	+			
CD56+ CD16neg	3	+	-	+++	-	+		↓	
	4	+++	-	-	+	-		↑	↑
CD56+ CD16+ CD57neg	5	++	+++	-	-	-			
	6	++	++	-	+	-			
CD56+ CD16+ CD57+	7	++	+++	+	+++	-		↑	↑
	8	++	++	++	+++	+		↑	↑
	9	++	++	+++	-	++		↓	↓
	10	++	++	+++	-	+++	↓	↓	

Fold change	↓	<-1.5
	↑	>1.5

Figure 25. Unsupervised clustering analysis of the NK cell repertoire. (**A**) tSNE dimensional reduction was performed in the CD3 negative fraction of magnetically-sorted NK-cells, based on the expression of CD56, CD16, CD57, NKG2A and NKG2C in a cohort of HIV seronegative individuals (SN, n=18), HIV-low (HL, n=8) and HIV-high (HH, n=8). (**B**) A total of 10 clusters was revealed by X-shift and FLOWSOM was applied to determine their specific markers. (**C**) Characterization of the surface markers of each of the clusters is shown. A fold change was used to compare the representation of each clusters within the NK cell subsets between groups (SN, HL, HH) and considered relevant when > 1.5 or < -1.5.

To further explore this hypothesis, the proportions of CD56^{neg} (CD56$^-$CD16$^-$), CD56^{bright} (CD56$^{brigth+}$CD16$^-$), CD56^{dim} (CD56^{dim}CD16$^+$) and adaptive NK (CD56^{dim}CD16$^+$CD57$^+$) populations, together with their expression of the HLA-E receptors NKG2A and NKG2C in SN, HL and HH were determined. The median % of these subpopulations in HL, HH and SN is represented as a radar chart in Figure 26A. HH showed a significant loss of CD56^{bright} NK cells compared to HL (MW p = 0.0011) and SN (MW p = 0.0004). In addition, in total NK cells, the NKG2A/NKG2C ratio was significantly increased in SN compared to HH (MW p = 0.0008), highlighting the reduced expression of NKG2A in chronic uncontrolled HIV infection. The subpopulation analysis indicated this difference to stem mainly from CD56^{bright} NK cells (MW p = 0.0027) and adaptive NK cells (MW p = 0.0051). The shift towards NKG2C expression was less pronounced in HL compared to SN. Still, a significant reduction was observed in NKG2A/NKG2C ratios in CD56^{bright} compared to SN individuals (MW, p = 0.0111) (Fig. 26B). Overall, these data indicated that CD56^{bright} NK cells were reduced in individuals with higher viremia, while adaptive NK cells were more abundant in those participants. NKG2A/NKG2C ratio was related to uncontrolled infections and observed not only in the whole NK cell population, but also in CD56^{bright} and adaptive NK cells subsets.

We next tested for potential relationships between NK cell subsets size, the relative levels of the NKG2A and NKG2C expression, as well as the NKG2A/NKG2C ratio in each of these subsets and the CD4 count, plasma viral load and HLA-E mRNA levels (Figure 26C). CD4 count correlated positively with NKG2A (r = 0.61, p = 0.002) surface expression in total NK cell fraction, NKG2A expression and NKG2A/NKG2C ratio in adaptive NK cells (r = 0.51, p = 0.048 and r = 0.57, p = 0.024, respectively) and the abundance of CD56^{bright} NK cells (r = 0.67, p = 0.006). Plasma viral load correlated negatively with NKG2A expression in total NK cells (r = -0.527, p = 0.038) as well as with the preservation of CD56^{bright} subpopulation (r = -0.776, p = 0.001). Of note, HLA-E mRNA correlated positively with NKG2C expression in total NK cell fraction (r = 0.367, p = 0.033) and CD56^{bright} (r = 0.508, p = 0.002) NK cells while it correlated negatively with NKG2A expression in adaptive NK cells (r = -0.427, p = 0.012). Consequently, HLA-E expression was correlated with an imbalance in the NKG2A/C ratio in adaptive NK cells (r = -0.344, p = 0.046), indicating a link between the increased expression of NKG2C, its ligand HLA-E in infected cells and uncontrolled HIV infection. Furthermore, these results indicate that NK cell subsets and the expression of NKG2X receptors are severely impacted by chronic HIV infection since HIV infected individuals, and in particular individuals with high viral loads (i.e. HH individuals), showed a loss of CD56^{bright} and an increase of the terminally-differentiated adaptive NK cells (characterized here as CD56^{dim}CD16$^+$CD57$^+$). The HLA-E/NKG2X axis also showed severe alterations depending on CD4

count and plasma viral load, suggesting that the impaired antiviral activity of these NK-subsets could be driven by high levels of HLA-E expression during uncontrolled HIV infection.
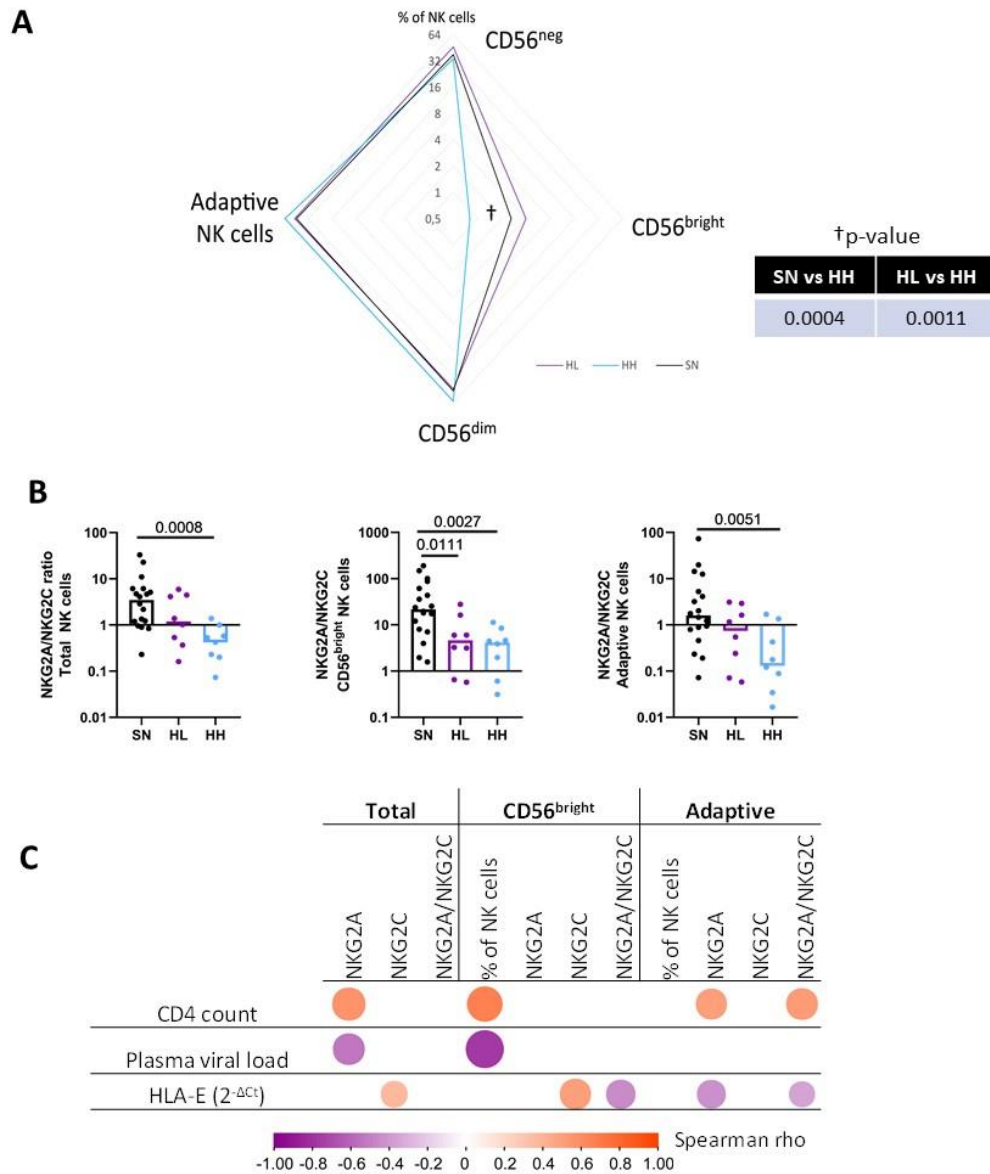
Figure 26. Manual gating analysis of the NK cell fraction. (**A**)) Magnetically-sorted NK cells from HIV seronegative (SN, n=18), HIV-low (HL, n=8) and HIV-high (HH, n=8) were characterized by manual gating. Four different subpopulations were characterized as CD56neg (CD56-CD16-), CD56bright (CD56brigth+CD16-), CD56dim (CD56dimCD16+) and adaptive NK cells (CD56dimCD16+CD57+). Differences between groups (SN, HL, HH) were analyzed by non-parametric Mann-Whitney test and represented in the radar chart. (**B**) NKG2A/NKG2C expression ratio in total NK cell fraction (left), CD56bright (middle) and adaptive NK cells (right) in the different groups (SN-black, HL-purple, HH-blue). (**C**) Correlogram showing Spearman's rank test correlation of NKG2A and NKG2C expression in total NK cells, CD56bright and adaptive NK cells with clinical parameters (CD4 count, plasma viral load) and HLA-E mRNA expression. Only significant correlations are shown. Results were considered statistically significant when p < 0.05.

3. NK cells exposed to high levels of HLA-E show an impaired function

Given the significant changes observed in NK-cell subset distribution, the differences in NKG2X receptor expression and their correlations with HLA-E expression, we next determined the ability of NK cells isolated from the HH, HL and SN groups to respond to signals through HLA-E/NKG2X. To measure NK response to "missing-self", we determined cytotoxicity (measured as % of killed K562), degranulation (% of CD107a$^+$ NK cells) and cytokine production (IFN-γ$^+$ and TNF-α$^+$ NK cells) after coculturing NK cells with HLA-null K562 cells. When testing total NK cells derived from SN, HL and HH, we observed a significant reduction in NK cytotoxic capacity in HIV infected individuals compared with SN, true for both, the HL (MW p = 0.0176), but especially, also HH (MW p = 0.0008, Figure 28A). A direct comparison between HL and HH demonstrated stronger NK cell cytotoxic activity in HL compared to HH, although this did not reach statistical significance (MW, p = 0.077). Impaired NK cell function in HIV-infected individuals was also reflected by reduced IFN-γ production in both HL (MW, p = 0.0007) and HH (MW, p = 0.0007) compared to SN (Fig. 27A). No differences in degranulation levels or TNF-α$^+$ cells were observed between the three groups. We tested then if these impairments were associated with the expression of HLA-E by correlating the different NK effector functions with the basal level of HLA-E mRNA in the PBMC sample used to isolate the NK cells. Indeed, HLA-E expression levels were associated with a detrimental effect on NK cell function since there were negative correlations observed between HLA-E expression and NK cytotoxicity (r = -0.6341, p = 0.0015), degranulation (as %CD107a$^+$) (r = -0.4647, p = 0.0293 and IFN-γ production (r = -0.5744, p = 0.0052, Fig. 27B).

To further test whether HLA-E expression was associated with dysregulated NK function in specific NK subsets, we repeated the effector function analysis focusing on the two NK subsets showing the most significant alterations in chronic HIV infection, namely CD56^{bright} and adaptive NK cells (Fig. 27C). The HIV uninfected group (SN) showed indeed superior capacity of CD56^{bright} cells to degranulate (MW, SN vs HL p = 0.0047, SN vs HH p = 0.0047), secrete IFN-γ (MW, SN vs HL p = 0.0310, SN vs HH p = 0.0093) or produce TNF-α (MW, SN vs HL p = 0.0047, SN vs HH p = 0.0127). No significant differences in CD56^{bright} functional responses were observed between HL and HH, although the CD56^{bright} subset was significantly reduced in HH. Similarly, the adaptive NK subset showed a significantly higher %IFN-γ (MW, SN vs HL p = 0.0003, SN vs HH p = 0.0007) and %TNF-α production (MW, SN vs HL p = 0.0007, SN vs HH p = 0.0023) in uninfected individuals compared to chronically HIV infected individuals. Interestingly, degranulation activity was not

reduced in this adaptive NK subset which was also not reduced in size in HIV infected individuals. In line with the data obtained in the total NK population, HLA-E mRNA expression in the source PBMC was negatively corelated with the degranulation capacity of CD56^{bright} (r = -0.4692, p = 0.0276), IFN-γ and TNF-α production in CD56^{bright} (r = -0.5538, p = 0.0075; r = -0.4363, p = 0.0424, respectively) and adaptive NK cells production of IFN-γ and TNF-α (r = -0.5305, p = 0.0111; r = -0.5598, p = 0.0067, respectively) (Fig. 27D). Overall, these results indicated that higher levels of HLA-E expression in chronic HIV infection are not only associated with shifts in the NKG2A to NKG2C expression ratios, but also related to reductions in cytotoxic effector function, degranulation activity and cytokine production affected NK subsets.
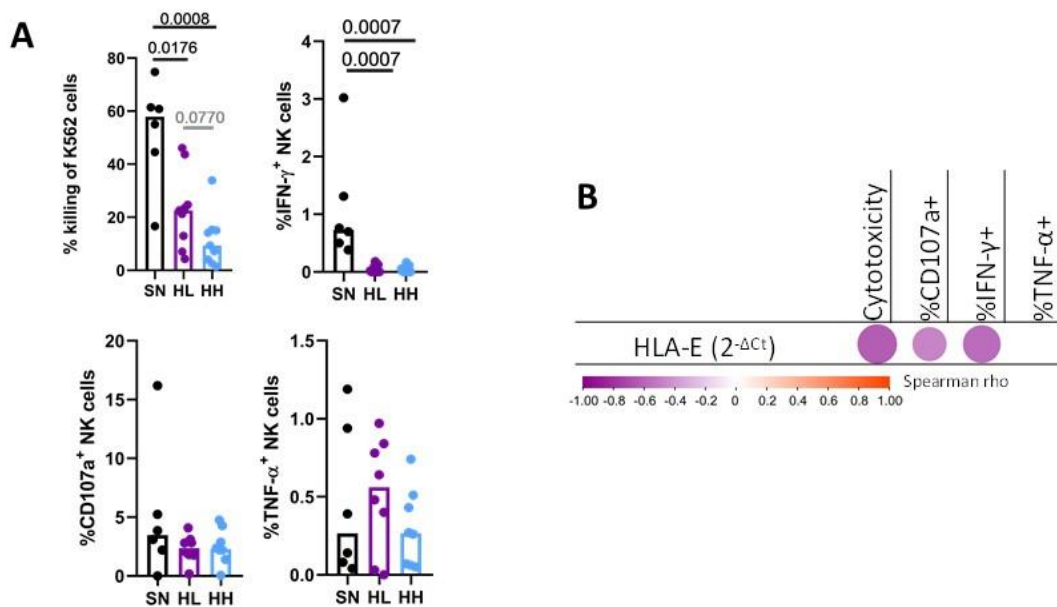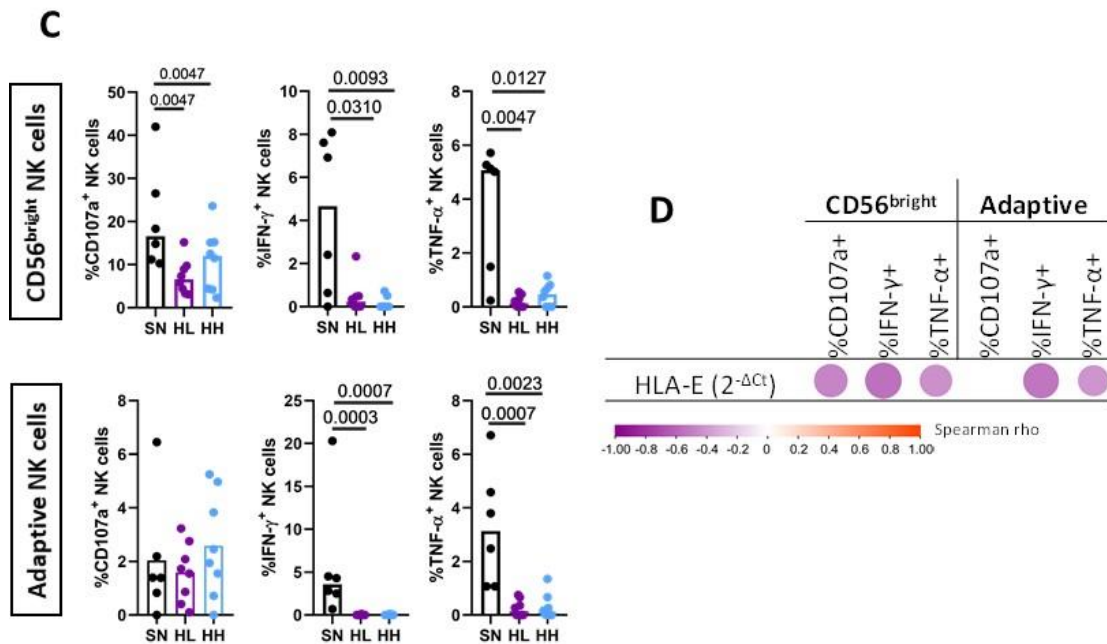
Figure 27. Analysis of NK cell cytotoxic activity, degranulation and cytokine secretion upon HLA-E stimulation. (**A**) Magnetically sorted NK cells from HIV seronegative (SN, black, n=6), HIV-Low (HL, purple, n=8) and HIV-high (HH, blue, n=8) were cocultured with K562 cell lines (lacking the expression of HLA-E) at an effector:target ratio of 5:1. After four hours, NK functional responses were measured by flow cytometry. (**A**) Total NK cell functions: cytotoxicity against K562 (top left), degranulation measured as % of CD107a+ (bottom left), production of IFN-γ (top right) and TNF-α (bottom right). (**B**) Correlogram of HLA-E expression in SN, HL and HH with total NK functionality. **C**) Functional response in the CD56bright (top) and adaptive NK cells (bottom) in terms of degranulation (% of CD107a+) (left), production of IFN-γ (middle) and TNF-α (right). (**D**) Correlogram of HLA-E level of expression withCD56bright and adaptive NK cells functions. Comparisons between groups were evaluated by Mann-Whitney test for non-parametric data while correlations were performed by Spearman's rank correlation test. Results were considered statistically significant when p < 0.05 while trends are shown in grey.

4. Short-term NK-mediated HIV viral growth inhibition is related to HLA-E expression

In order to discern whether the reduced NK cell effector response was the cause or consequence of uncontrolled HIV infection, we modeled acute HIV infection *ex vivo*. Using this model, we assessed antiviral activity of NK cells in an *in vitro* viral replication inhibition assay (NK-VIA) by coculturing sorted NK cells from HIV-negative individuals with *in vitro* HIV infected autologous CD4+ T-cells. For the two HIV strains tested, a strong inhibitory capacity of NK cells was observed at day 7 (Fig 28A), which was however significantly reduced at day 14 for HIV_{NL4-3} (W p = 0.0106) and HIV_{BaL.} (W p = 0.0164). In parallel, the 14-day culture showed marked changes in NK subpopulations, with a loss of CD56dim and a gain of CD56bright and CD56neg subsets (Fig. S11). The

expression of NKG2A was increased in all NK subsets at day 14, while NKG2C was increased in CD56^{neg} and CD56^{dim} (Fig. S12) but reduced in adaptive NK cells (Fig. 29B), all in in line with the observations made in long-term chronically HIV infected individuals. Furthermore, in adaptive NK cells, coculture with HIV$_{BaL}$ infected CD4^{+} T-cells maintained NKG2C expression at higher levels compared to uninfected cultures, which was reflected in a lower NKG2A/NKG2C ratio (Two-way ANOVA, p = 0.0463 (Fig. 28B), suggesting HIV infection might be driving NKG2C expression in NK cells.

Strong correlations were observed at day 7 between NK-mediated inhibition of viral replication and surface HLA-E expression in the HIV infected, CD4^{+} target cells (Fig. 28C) for both, HIV$_{NL4-3}$ (r = 0. 8322; p = 0.0013) and HIV$_{BaL}$ (r = 0.7167; p = 0.0369). The level of inhibition also correlated with the basal HLA-E mRNA expression in the PBMC used to isolate autologous NK and CD4+ T cells (Fig. 28D), in the case of HIV$_{NL4-3}$ (r = 0.6434; p = 0.0278). This was in line with the direct correlation between HLA-E mRNA level in the sample and surface HLA-E expression (Fig.S13, r = 0,6643; p = 0,0219). There was no difference between HLA-E allele genotype and NK-mediate control in our model of acute infection.

Together, these data show that high levels of HLA-E expression mediate, at first, an effective inhibition of virus replication by NK cells. However, our data also suggest that long-term exposure to HIV in untreated chronic infection as well as in extended (day 14) *in vitro* co-cultures with HIV infected CD4 T cells, drives NKG2C expression which, in turn, may cause reduced NK functions due to its diminished affinity for HLA-E presented peptides compared to NKG2A[206].
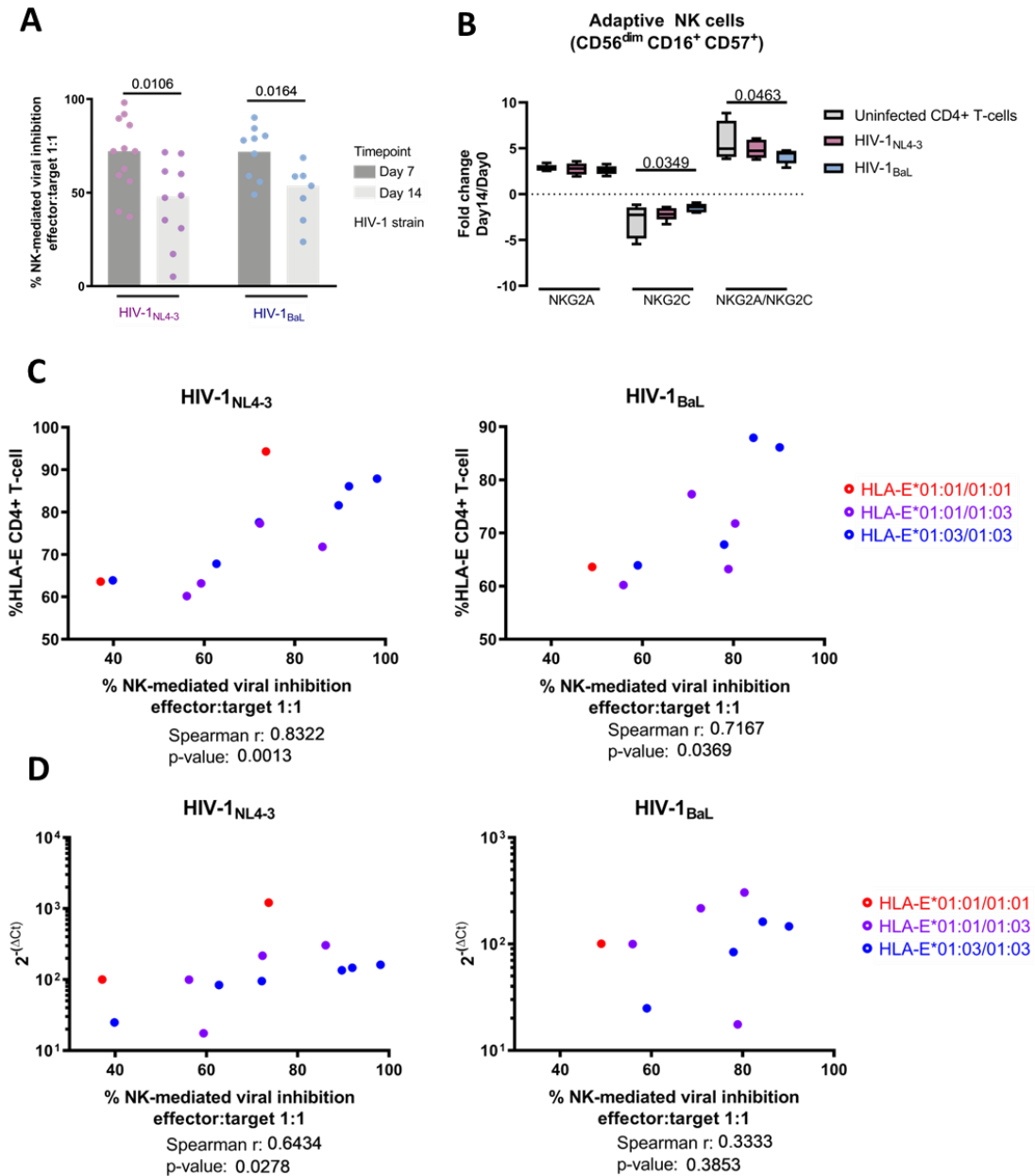
Figure 28. Short term NK-mediated inhibition of viral replication is related to HLA-E expression and diminishes over time. (**A**) Inhibition of viral replication comparing two different laboratory adapted strains (HIV$_{NL4-3}$ in pink and HIV$_{BaL}$ in blue) and two different timepoints (day 7 in dark grey and day 14 in light grey). (**B**) Long-term NK-CD4$^+$ T-cell coculture induced changes on the NK HLA-E receptors favoring the expression of the inhibitor NKG2A. HIV infection resulted in higher levels of NKG2C expression as well as a lower level of NKG2A/NKG2C ratios in adaptive NK cells. (**C**) NK cell-mediated control of viral replication correlated with HLA-E surface expression and basal mRNA levels (**D**). Color code indicate sample genotype. Univariate analysis was performed using Wilcoxon test for paired data (A), while multiple comparisons were performed by one-way ANOVA (B). Correlation was calculated using Spearman 's rank correlation coefficient (C, D). Results were considered statistically significant when p < 0.05.

5. Effect of HIV-derived peptides on HLA-E*01:03 surface stabilization and consequent ability to alter NK cells activation

Since HLA-E was associated with changes in the NKG2A/C ratio as well as the abundance of the different NK subpopulation, we explored the possibility that changes in the HLA-E peptide repertoire could alter signaling through the HLA-E/NKG2X axis and drive these alterations. We thus analyzed the role of HIV-derived, HLA-E-binding epitopes in the activation of NK cells from HIV seronegative individuals (n=6), using HLA-E*01:03 transfected K562 cells, co-expressing the canonical peptide VL9-B7 and pulsed with canonical and non-canonical HLA-E binding peptides. We measured HLA-E surface stability as well as HLA-E restricted NK cytotoxicity, degranulation and cytokine production (IFN-γ and TNF-α). The fold change comparing the effect of each peptide to the canonical, endogenously expressed VL9-B7 epitope was determined.

The external addition of the described canonical HLA-E binding epitopes increased the surface expression when compared with VL9-B7 endogenous expression (F, VL9-Cw1 p-value; 0.0002, CMV p = 0.001). The same was seen for the non-canonical EBV-derived SL9 peptide (F, E SL9, p = 0.0196,). Interestingly, only one of the HIV-derived candidate epitopes (H RL9) increased the surface expression (F, p = 0.0439, Fig. 29A).

Despite the low ability of the HIV derived peptides to increase surface stabilization compared to canonical VL9-B7, we assessed whether these differences would result in more or less effective sensitization of NK cells. Several non-canonical HLA-E binding epitopes mediated increased cytotoxicity. In particular, three HIV-derived peptides increased the cytotoxic activity of NK cells to HLA-E*01:03 K562 target cells significantly above the background levels seen with VL9 B7 (F, KG9 p = 0.0339, MD9 p = 0.0284 and PM9 p = 0.0403, Fig. 29B). These three and plus five additional HIV-derived epitopes triggered significant increases in NK degranulation (F, AA9 p = 0.0310, KG9 p = 0.0002, MD9 p = 0.0011, PM9 p = 0.0011, QE9 p = 0.0027, RV9 p = 0.0019, SN9 p = 0.0033, TP9 p = 0.0162, Fig. 29C). Finally, two of the three HIV-derived peptides that induced cytotoxicity also were able to increase the number of TNF-α+ NK cells (F, KG9 p = 0.0162 and PM9 p = 0.0133, Fig. 29D).

Together, eight of the eleven tested HIV peptides induced increases in at least one of the tested NK- functions when presented by HLA-E*01:03. Remarkably, two of the HIV peptides (KG9 and PM9) presented by HLA-E*01:03 stimulated NK cells and increased three of the four cellular

functions measured (cytotoxicity, degranulation and TNF-α production). These data indicate that the bound epitope repertoire on HLA-E*01:03 might induce structural changes than can be recognized by NKG2X receptors on NK cells.

E	Surface stabilization	Cytotoxicity lytic units	NK cell degranulation %CD107a+	%IFN-γ+	%TNF-α+
VL9 Cw1	0.0002				
VL9 CMV	0.001				
E SL9	0.0196				
HIV AA9			0.031		
HIV KG9		0.0339	0.0002		0.0162
HIV MD9		0.0284	0.0011		
HIV PM9		0.0403	0.0011		0.0133
HIV QE9			0.0027		
HIV RL9	0.0439				
HIV RV9			0.0019		
HIV SN9			0.0033		
HIV TP9			0.0162		
HIV VI9					
HIV YG9					
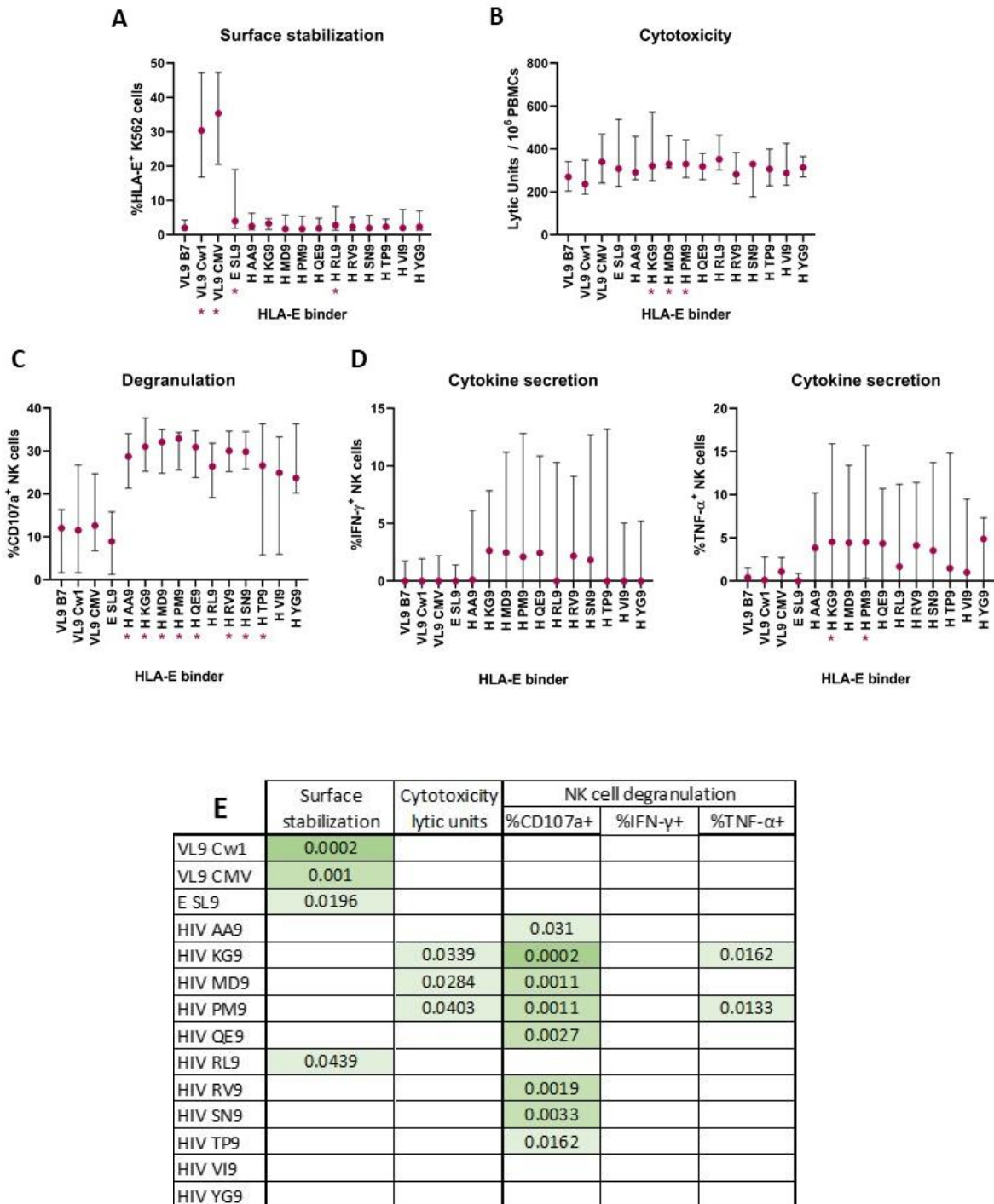
Figure 29. Effect of HIV derived peptides on HLA-E*01:03 surface stabilization and ability to alter NK functionality. HLA-E *01:03 transfected K562 cell lines co-expressing the VL9 epitope were pulsed with canonical and non-canonical HLA-E binding peptides. (**A**) Peptide-pulsed cells induced HLA-E surface stabilization, measured by flow cytometry and recorded as %HLA-E+ K562 cells. Peptide-pulsed cells modified the NK cytotoxic capacity (**B**), degranulation (**C**) and

cytokine secretion (**D**, IFN-γ (left) and TNF-α (right))**.** Multiple comparisons with the control VL9 epitope were performed by Friedman's test for paired data with post-hoc False discovery rate. Significant differences are marked in the graphs (A-D) correspond to p-values<0.05. Table **E** represents significant p-values when FDR indicated q-values<0.15.

6. Structural model of the antigen presentation of HIV-derived peptides through on HLA-E to NK cells

In order to further understand the interplay between HLA-E alleles (E*01:01 and E*01:03), NKG2X receptors and HIV-derived peptides that triggered NK responses, a structural model was constructed. The structural model of HLA-E-CD94-NKG2X (see Figure 30) illustrates that the presentation of HIV-derived PM9 and RL9 peptides differs in the binding mode compared to canonical VL9 peptides. In particular, the first residue (P1) in both, the PM9 and RL9 epitopes is exposed to NKG2A, providing evidence for a new structural interaction between the presented epitope and NKG2X position Arg215, which localizes close to position 197 in NKG2A and NKG2C. The position 197 in NKG2A and NKG2C is occupied by a Glu and Lys residue, respectively. Additionally, position P5 in the presented epitope points towards the CD94-NKG2A/C interface. Differences in NKG2X affinity for the HLA-E/epitope complex may be then determined by the ASILP motif in NKG2C / SIISP in NKG2A that change the CD94 interface similarly to what happens when canonical VL9 peptides are presented[377]. Interestingly, HLA-E*01:01 and *01:03 differ only in residue Arg/Gly 107, which is outside the epitope binding pocket. It is however located next to another charged residue (Arg108) which is responsible for the interaction with NK cells receptors NKG2A and NKG2C through Asp202 (Fig. 30). Hence, the NKG2A and NKG2C molecules can be expected to be very sensitive to minor changes in HLA-E allotypes affecting this position (Arg108) (Fig. 30).

Our structural model describes new interactions between non-canonical HIV-derived HLA-E presented peptides and NKG2X receptors in an allele-dependent manner, providing the potential explanation for differential NK-cell recognition of infected cells through the HLA-E/NKG2X axis. In addition, Position 5 in the presented epitope may further determine the affinity to the activator (NKG2C) or inhibitory (NKG2A) receptor.
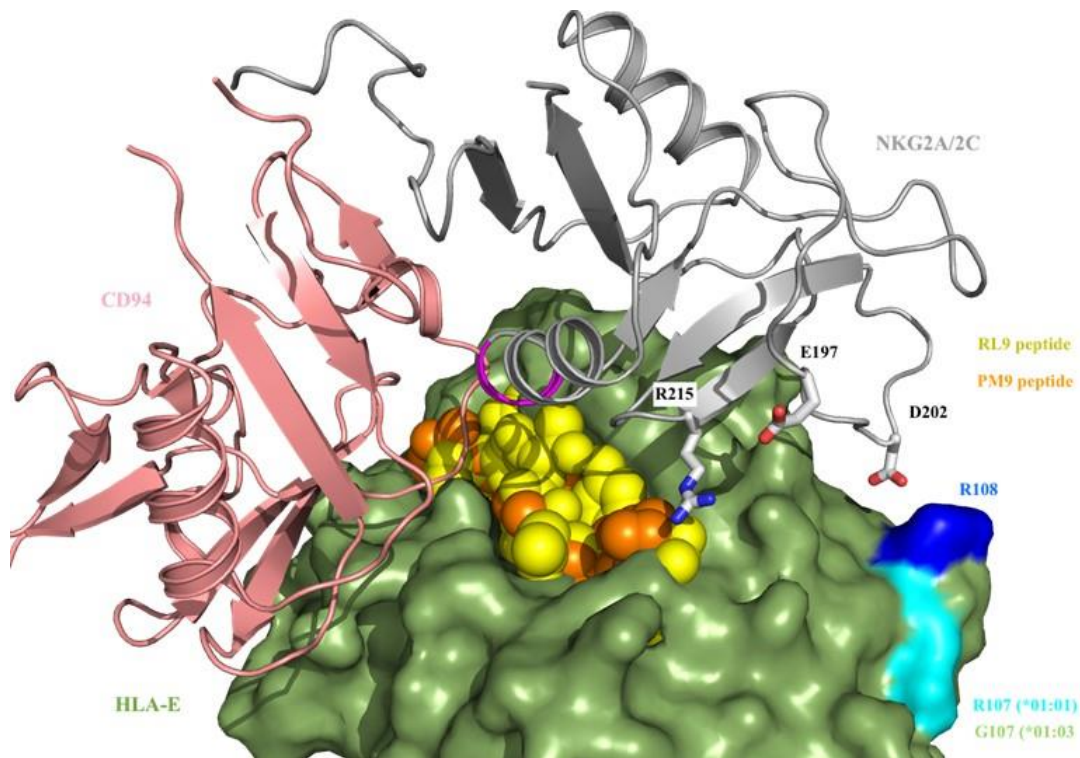
Figure 30. CD94-NKG2(A/C) interaction with HLA-E-VL9/PM9 peptide. VL9 (in yellow) and PM9 (in orange) peptides protrude from HLA-E (in green) allowing for an additional interaction with Arg215 from NKG2A/2C (in grey). Residue 197 (Glu residue in NKG2A and Lys residue in NKG2C, respectively) is close to Arg 215. The ASILP and SIISP sequence motifs (in magenta) presented by NKG2A and NKG2C, are respectively in close proximity to position P5 of VL9 and PM9/RL9 peptide. HLA-E (in green) differs in Arg/Gly 108 (in cyan), which interacts with NKG2A/2C Asp 201 through Arg 108 (in blue).

7. Limitations of the study

This study has some limitations. First, peripheral blood NK cell phenotype and functions might differ from those of tissue resident NK cells. The CD56[brght] and CD56^{dim} dichotomy is also observed in tissue distribution as they express a divergent variety of chemokine receptor repertoire and adhesion molecules, resulting into different migration routes[180]. CD56^{bright} only represents 8-15% of peripheral blood total NK in healthy conditions[187], but they are enriched in most human tissues, including secondary lymphoid organs such as lymph nodes and tonsils, where they represent the majority of the NK cell population[188,189]. Access to such samples is limited and thus complicates the study of CD56^{bright} NK cells response to HIV infection within the lymph node, which is considered one of the main sanctuaries of the latent HIV reservoir[378]. Secondly, longitudinal studies in the absence of cART might be required in order to understand how NK cells from HIV-infected individuals suffer a progressive and continuous functional

impairment. Our results are in line with the NKG2A/NKG2C ratio reversion that has been decribed for NK cells from HIV infected individuals with HCMV co-infection[379]. HCMV is a highly disseminated virus within the human population, with an estimated worldwide seroprevalence of 83% in 2019 (95%UI: 78-88)[59], and, although we could not determine the CMV status for all participants in the present study, its high prevalence suggests that the vast majority of these HIV-infected individuals were HCMV infected as well.
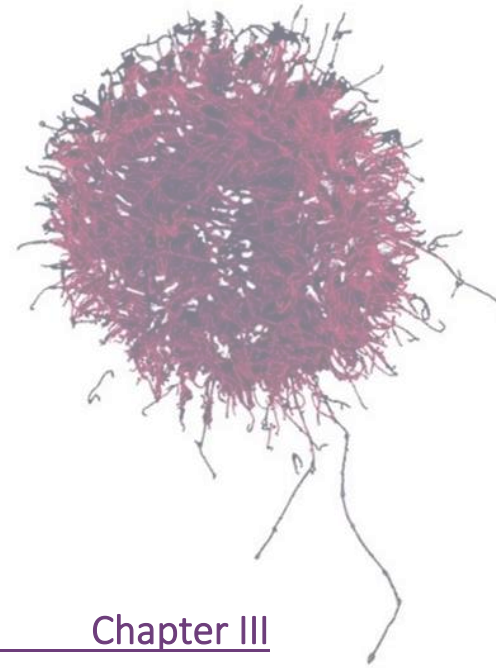
Alternative adaptive cellular responses to acute viral infection

Differences in T-cell immunity against SARS-CoV-2 nucleocapsid are related to COVID-19 outcome
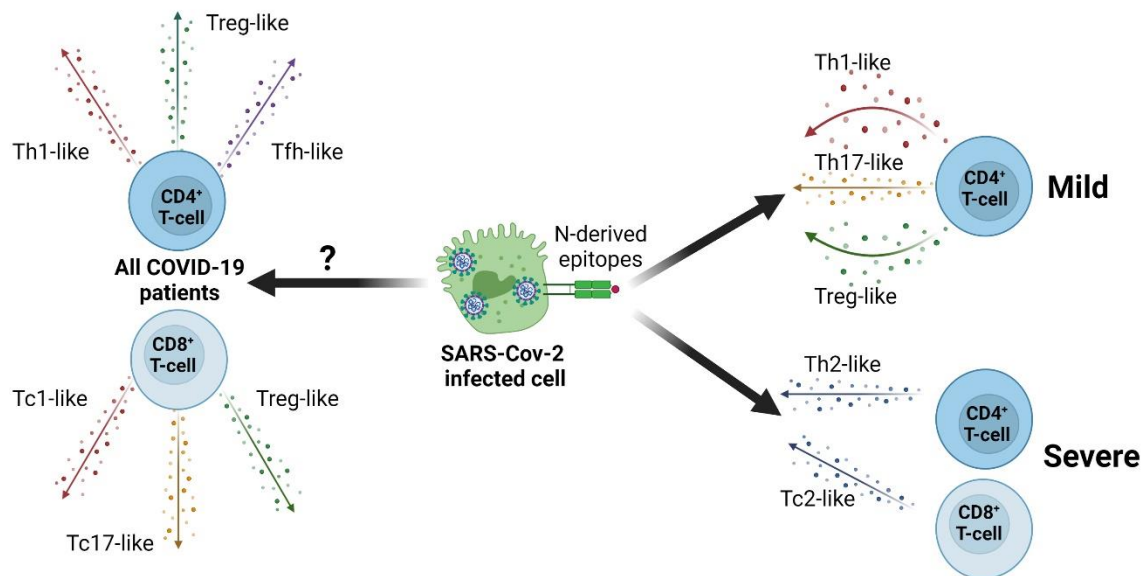
Abstract

Previous studies reported a relationship between T-cell phenotype, antigen-specific responses to SARS-CoV-2 epitopes and COVID-19 outcome. A disbalance between type 1 and type 2 T-cell responses was suggested as a risk factor of severity. We studied Th1/Tc1, Th2/Tc2, Th17/Tc17, Treg and Tfh/Tfc responses to SARS-CoV-2 S and N and determined memory phenotypes in groups of individuals with different disease course, including severe, mild and non-seroconvertors. We identified an increased basal production of Th1/Tc1, Treg, Tfh and Tc17 related cytokines associated with SARS-CoV-2 infection. Nucleocapsid-specific Th1/Tc1, Th17 and Treg responses were also increased in mild patients and discriminated patient groups. In particular, severe disease patients showed strong and fast type 2 responses to N that were absent in mild or non-seroconvertors. Memory populations were also altered among groups as we identified a loss of naïve T-cells in severe patients. In conclusion, our findings indicate that T cell responses are of greater magnitude in COVID-19 patients with mild disease. Interestingly, non-seroconvertors did not elicit particularly strong cellular responses either. Our data give support to the inclusion of N as an antigen to SARS-CoV-2 vaccines in order to obtain better T-cell responses that could help increase vaccine memory and protection from symptomatic disease.

1

1. SARS-CoV-2 infection is associated with increased CD4$^+$ and CD8$^+$ T-cells basal activation

In order to evaluate the impact of SARS-CoV-2 infection on polarized T-cell activation, we first compared basal activation of CD4$^+$ (Th1, Th2, Th17, Treg and Tfh) and CD8$^+$ (Tc1, Tc2, Tc17, Treg and Tfc) between COVID-19 patients (n=9) and uninfected individuals (n=5) after 24h inhibition of protein transport by *boosted flow* cytometry. Uninfected individuals corresponded to sample from healthy people obtained before March 2020 to ensure that we did not include any asymptomatic infection in the comparison.

COVID-19 patients had an overall increased T-cell activation levels compared to uninfected individuals. We observed stronger in signals in CD4$^+$ Th1-like (MW, p = 0.0031), Treg-like (MW, p = 0.0010) and Tfh-like (MW, p = 0.0055) (Fig. 31A) and Tc1-like (MW, p = 0.0010), Tc17-like (MW, p = 0.0040) and CD8$^+$ Treg-like (MW, p = 0.0070) (Fig. 31B). There were no significant differences between type 2 (Th2-like and Tc2-like) basal status.

We then tested whether this augmented signal was particularly associated with COVID-19 outcome and compared basal activation between severe (n=8), mild (n=8) and non-NSC (n=8) COVID-19 patients. Severe COVID-19 was associated with significantly increased % of Th2-like CD4$^+$ T-cell basal activation when compared to mild (MW, p = 0.0051) and NSC (MW, p = 0.0104) (Fig. 32C). Type 2 responses were also increased in CD8$^+$ T-cells when comparing Tc2-like signal with both mild (MW, p = 0.0062) and NSC (MW, p = 0.0190) (Figure 31D). Although statistically not significant, we observed a trend towards higher % of Tfh-like CD4$^+$ T-cells in severe patients (Fig. 31C) compared to patient with mild disease course. We did not observe any significant differences for Th17/Tc17-like or Treg in CD4$^+$ nor CD8$^+$ T-cells (Fig. S14).

Together, our results indicate that COVID-19 patients had increased type 1 (Th1/Tc1) and Treg basal activation than people that never passed SARS-CoV-2 infection although these differences were not associated with different COVID-19 outcome. Nevertheless, severe COVID-19 was associated with particularly increased type 2 (Th2/Tc2) basal activation.
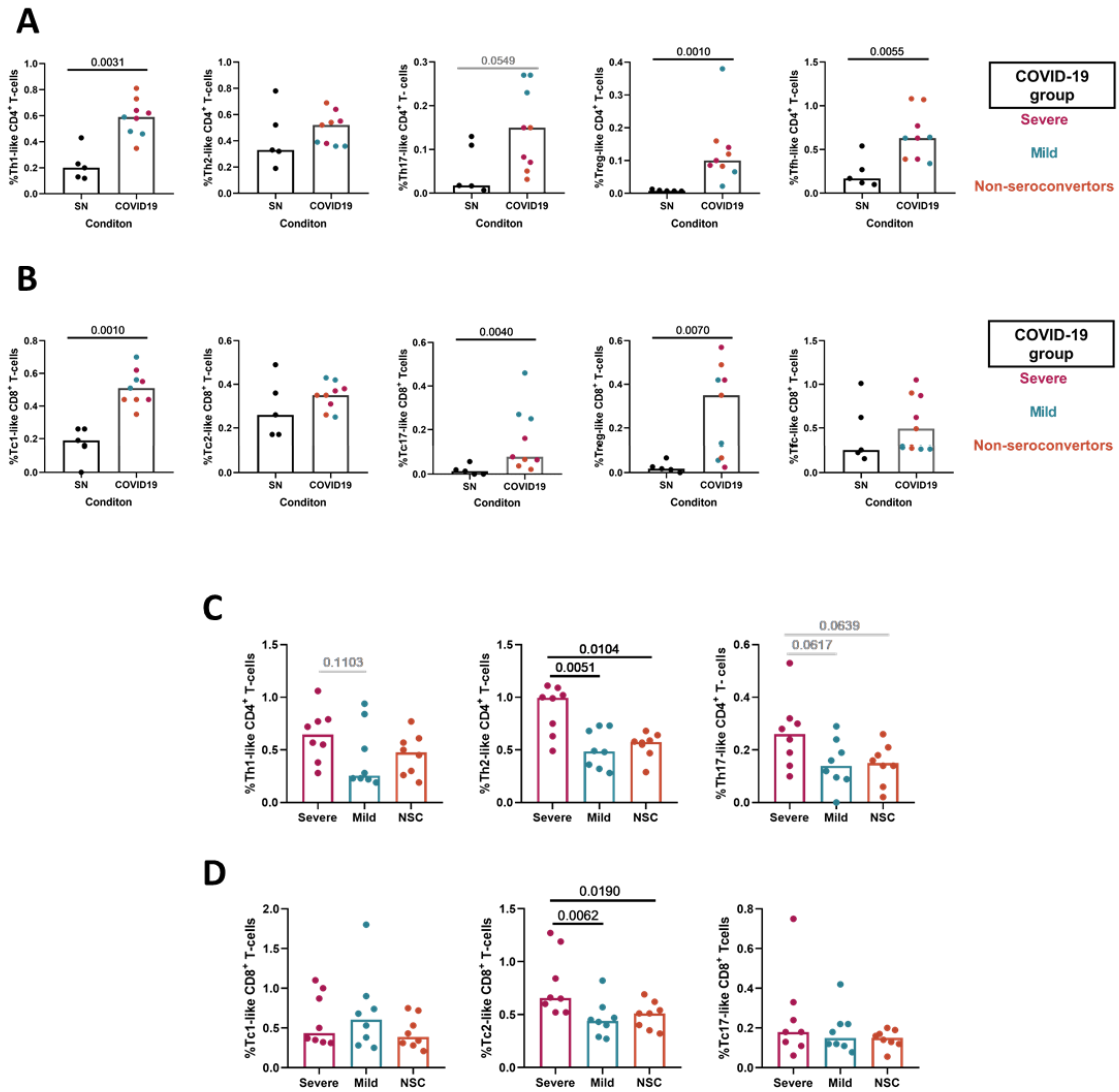
Figure 31. Basal activation of peripheral T-cells in is increased in COVID-19 patients. (A) Basal activation of polarized CD4+ T-cells , after 24h incubation with protein transport inhibitor monensin (Golgi Stop), in uninfected individuals (n=4) compared to COVID-19 patients (n=9) with diverse levels of disease severity (severe in magenta, n=3; mild in blue, n =3; non-seroconvertors in orange, n=3). Scatter plots represent % of Th1-like, Th2-like, Th17-like, Treg-like and Tfh-like CD4+ T cells, in order. **(B)** Basal activation of polarized CD8+ T-cells , after 24h incubation with protein transport inhibitor monensin (Golgi Stop), in uninfected individuals (n=4) and COVID-19 patients (n=9) with diverse levels of disease severity (severe, n=3, mild n =3, non-seroconvertors n=3). Scatter plots represent % of Tc1-like, Tc2-like, Tc17-like, Treg-like and Tfc-like CD8+ T-cells, in order. **(C)** Basal activation of CD4+ Th1-like (left), Th2-like (middle) and Th17-like (right) upon 12h culture with protein transport inhibitor monensin (Golgi Stop) was compared among severe (magenta, n=8), mild (blue, n=8) and non-seroconvertors (NSC, orange, n=8) COVID-19 patients. **(D)** Basal activation of CD8+ Tc1-like (left), Tc2-like (middle) and Tc17-like (right) upon 12h culture with protein transport inhibitor monensin (Golgi Stop) was compared among (magenta, n=8), mild (blue, n=8) and non-seroconvertors (NSC, orange, n=8) COVID-19 patients. Statistical significance was evaluated by non-parametric Mann-Whitney test, statistical significance was set at p<0.05, trends are shown in grey (p<0.15).

2. Dynamics in antigen-specific T-cell responses against SARS-CoV-2 nucleocapsid are associated with different COVID-19 disease course

We next evaluated whether SARS-CoV-2-specific T-cell responses could discriminate among COVID-19 outcome. For this purpose, we stimulated PBMCs from severe (n=8), mild (n=8) and NSC (n=8) COVID-19 patients with two full-length recombinant SARS-CoV-2 proteins (nucleocapsid, N; spike, S) and a pool of 16 OLPs covering conserved regions among all human coronaviruses (Hu-CoV pool)[362]. We evaluated in parallel: 1) fast responses by performing the stimulation for 12h prior to the addition of monensin for another 12 h and 2) slower responses by stimulating cells for 5 days with a final recall of stimulation for 24 in the presence monensin.

We first examined the percentage of individuals capable of eliciting antigen-specific T-cell responses with particular polarization (% of responders) and determined whether the frequency of responders within each T-cell profile was different among COVID-19 groups. Among mild COVID-19 patients, T-cell responders to N after 5 days of stimulation were more frequent than responders to S or the Hu-CoV pool. Indeed, CD4$^+$ Th1-like (χ^2, p = 0.0007), Th17-like (χ^2, p = 0.0412), Treg-like (χ^2, p = 0.0324) (Fig. 32A) and CD8$^+$ Tc1-like (χ^2, p = 0.0375) (Fig. 32B). Frequency of T-cell responders discriminated among the different groups of patients and were particularly increased in mild patients. We also observed a trend, towards higher frequencies of CD8$^+$ Tc17-like, Treg-like and Tfc-like responders to N in the mild group. No significant differences were observed in the frequency of either CD4$^+$ nor CD8$^+$ responders to S, with the exception of a trend showing more frequent CD4$^+$ Th1-like and Treg-like responders in severe and mild patients compared to NSC (Fig. 32A). Remarkably, only severe COVID-19 patients elicited delayed CD8$^+$ Tc1-like responses to the conserved epitopes at day 5 and this was significantly different among groups (χ^2, p = 0.0082) (Fig. 32B), while a trend showed more CD4$^+$ Th1-like and Tfh-like responders in mild patients (Fig. 32A). Of note, we did not observe any significant differences in the frequency of antigen-specific responders when stimulation were performed for 12 h (Fig. S15). However, CD4$^+$ T-cells from severe COVID-19 patients appeared to respond more frequently to N than mild patients and NSC, especially with a Th2-like profile. Whereas CD4$^+$ Th1-like and Tfh-like and CD8$^+$ Tc1-like to conserved epitopes among human coronaviruses seemed to be more frequent in mild patients, suggesting a faster capacity to recall pre-existing responses.

When comparing the magnitude of T-cell responses to N and S at day 5, we observed significantly more potent CD4$^+$ Th1-like responses to N in mild COVID-19 patients compared to severe (MW,

p = 0.0033) and NSC (MW, p = 0.0154). Similarly, mild patients showed increased CD4$^+$ Th17-like responses compared to severe (MW, p = 0.0294) (Fig. 33A).
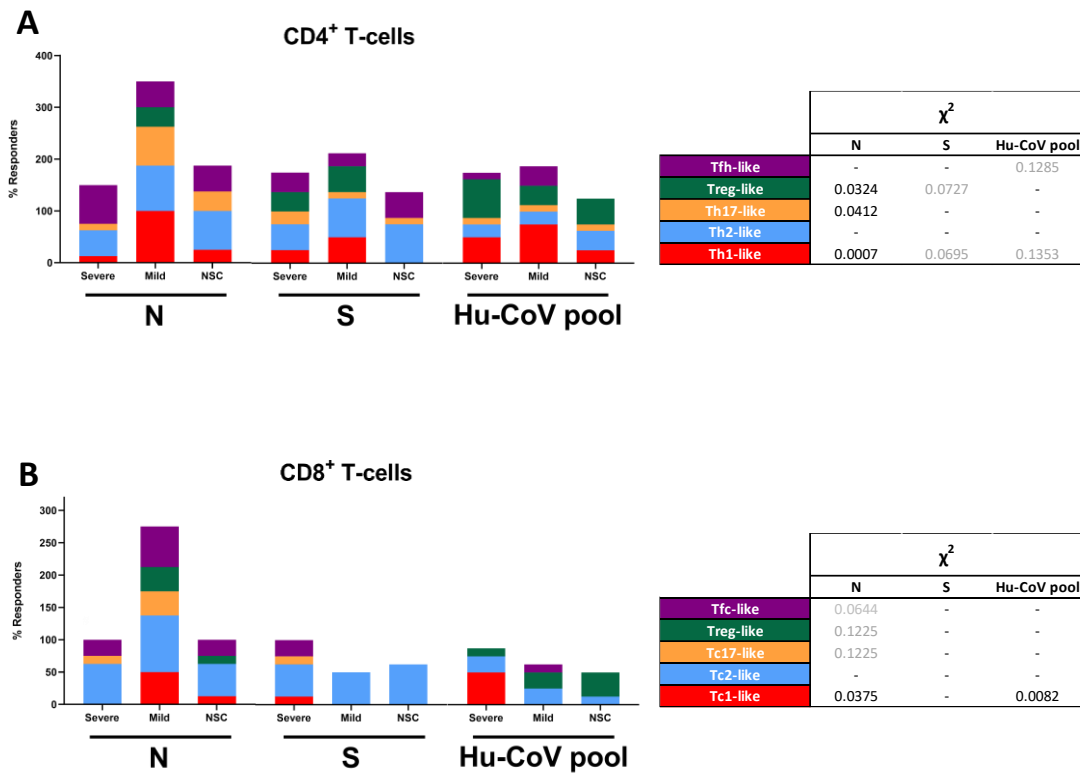
Figure 32. Percentage of responders per group to SARS-CoV-2 nucleocapsid (N), spike (S) and a pool of 16 conserved epitopes among human coronaviruses (Hu-CoV pool) after 5 days of stimulation. (A) Stacked histograms of individuals who elicited CD4$^+$ Th1-like (red), Th2-like (blue), Th17-like (yellow), Treg-like (green) and Tfh-like (purple) responses to N, S or Hu-CoV pool among severe (S, n=8), mild (M, n=8) and non-seroconvertors (NSC, n=8). **(B)** Stacked histograms of individuals who elicited CD8$^+$ Tc1-like (red), Tc2-like (blue), Tc17-like (yellow), Treg-like (green) and Tfc-like (purple) responses to N, S or Hu-CoV pool among severe (S, n=8), mild (M, n=8) and non-seroconvertors (NSC, n=8). Tables on the right represent p-values from χ^2 test applied to each profile in each stimulation in order to determine different T-cell profiles of responders among groups. Trends are represented in grey (p<0.15).

In terms of magnitude of the T-cell response after 12h of stimulation, severe patients had significantly stronger CD4$^+$ Th2-like responses to N compared to NSC (MW, p = 0.0406) while showing a trend when compared to mild (Fig. S16).

Figure 33. Magnitude of the T-cell response against SARS-CoV-2 nucleocapsid (N) and spike (S) after 5 days of stimulation. (A) Scatter plots represent CD4+ T-cell responses in this order: Th1-like, Th2-like, Th17-like, Treg-like and Tfh-like to N and S. Results are shown comparing severe (S, magenta, n=8), mild (M, blue, n=8) and non-seroconvertors (NSC, orange, n=8) COVID-19 patients. **(B)** Scatter plots represent CD8+ T-cell responses in this order: Tc1-like, Tc2-like, Tc17-like, Treg-like and Tfc-like to N and S in severe (S, magenta, n=8), mild (M, blue, n=8) and non-seroconvertors (NSC, orange, n=8) COVID-19 patients. Statistical significance was evaluated by non-parametric Mann-Whitney test, statistical significance was set at p<0.05, trends are shown in grey (p<0.15).

Our findings suggest that the nucleocapsid protein is highly immunogenic for T-cells, even more than the main vaccine immunogen S and especially after longer exposure to the recall antigen. Also, a mild COVID-19 course was associated with more frequent type 1 (Th1/Tc1), type 3 (Th17/Tc17) and Treg responses. Severe COVID-19 was also linked to faster and increased type 2 (Th2/Tc2) responses to N and a delayed CD8$^+$ Tc1-like response to epitopes that are highly conserved among human coronaviruses. Interestingly, the group of NSC patients did not elicit any particularly strong T-cell response to the antigen-specific stimulation.

3. Loss of naïve T-cells is associated with COVID-19 severity

To determine whether the outcome of SARS-CoV-2 infection and disease course were related to the distribution of memory T-cell populations, we determined CCR7 and CD45RA expression on total CD4$^+$ and CD8$^+$ T-cells from severe, mild and NSC COVID-19 patients. T-cells were then classified as T_{CM} (CD45RA$^-$ CCR7$^+$), T_{EM} (CD45RA$^-$ CCR7$^-$), T_{EMRA} (CD45RA$^+$ CCR7$^-$) and $T_{Naïve}$ (CD45RA$^+$ CCR7$^+$).

Severe COVID-19 patients had significantly lower levels of CD4$^+$ $T_{Naïve}$ compared to mild (ANOVA, p = 0.0067) and NSC (ANOVA, p < 0.0001) in their PBMC. In line with this, severe patients showed an augmented accumulation of T_{CM} compared to mild patients (ANOVA, p = 0.0271) (Fig. 34A). No significant differences among different groups of patients were observed for the levels of T_{EM} or T_{EMRA}.

Surprisingly, NSC had significantly higher levels of CD8$^+$ $T_{Naïve}$ compared to individuals with mild (ANOVA, p = 0.0067) and severe (ANOVA, p < 0.0001) disease course. A clear trend, yet not statistically significant, also suggested that individuals suffering from mild COVID-19 had higher levels of CD8$^+$ $T_{Naïve}$ than severe. No differences were found neither in CD8$^+$ T_{CM}, T_{EM} nor T_{EMRA} (Fig. 34).

In order control for the effect of age in the redistribution of memory T-cell populations[380], we performed a correlation analysis within our groups of patients but did not observe any significant correlation between age and specific memory T-cell subsets distribution (data not shown). Together, these observations suggest that the loss of both CD4$^+$ and CD8$^+$ $T_{Naïve}$ populations is associated with COVID-19 severity, independently of patient age.
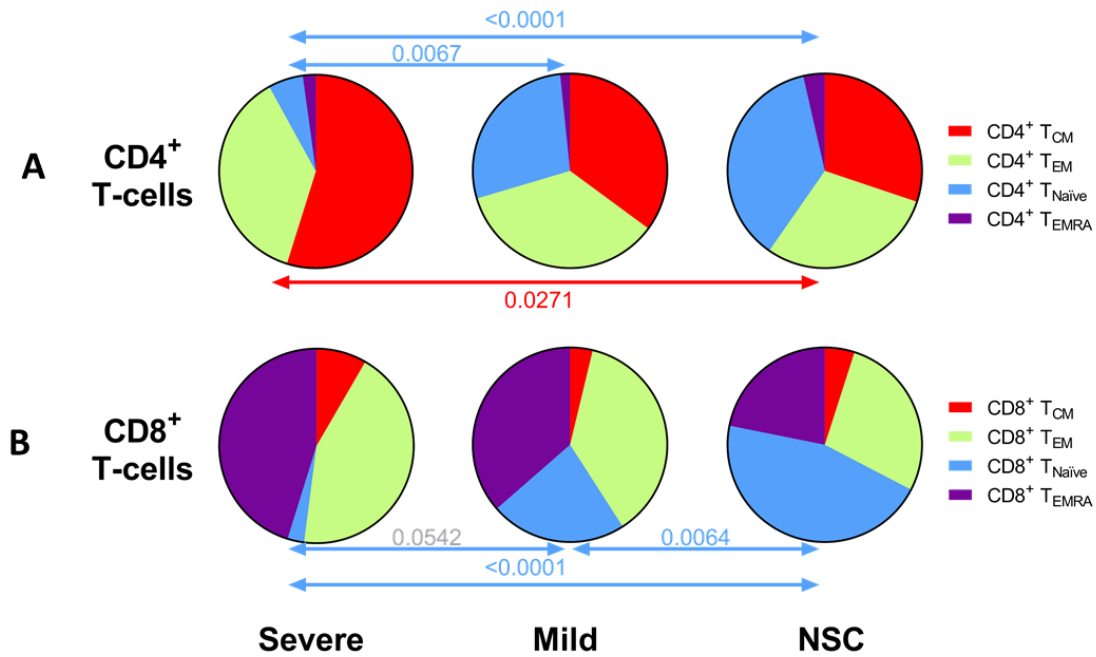
Figure 34. T-cell memory subsets in COVID-19 patients. T-cells were classified as T$_{CM}$ (CD45RA$^-$ CCR7$^+$), T$_{EM}$ (CD45RA$^-$ CCR7$^-$), T$_{EMRA}$ (CD45RA$^+$ CCR7$^-$) and T$_{Naïve}$ (CD45RA$^+$ CCR7$^+$). **(A)** Pie charts represent CD4+ T-cell memory subsets (T$_{Naïve}$, T$_{CM}$, T$_{EM}$ and T$_{EMRA}$) in severe (S, n=8), mild (M, n=8) and non-seroconvertors (NSC, n=8) COVID-19 patients. **(B)** Pie charts represent CD8$^+$ T-cell memory subsets (T$_{Naïve}$, T$_{CM}$, T$_{EM}$ and T$_{EMRA}$) in severe (S, n=8), mild (M, n=8) and non-seroconvertors (NSC, n=8) COVID-19 patients. Multiple comparisons were performed by ANOVA with false discovery rate (FDR) correction, statistical significance was set at p<0.05 and q<0.15, trends are shown in grey (p<0.15)

4. Follicular CD4$^+$ and CD8$^+$ T-cell responses to SARS-CoV-2 N are associated with increased neutralizing activity

We next asked whether any specifically polarized, SARS-CoV-2 specific T-cell response was related to the development of neutralizing antibodies. We evaluated the SARS-CoV-2 pseudovirus neutralizing capacity of individuals in the Severe, Mild and NSC groups plasma and correlated the maximum neutralizing capacity observed to N, S and Hu-CoV pool T-cell responses after 12h or 5 days of stimulation.

Remarkably, severe COVID-19 patients had the highest neutralizing titers compared to mild (MW, p = 0.0148) or NSC (MW, p = 0.0057). Mild patients also had higher neutralizing capacity compared to NSC (MW, p = 0.0002) (Fig. 35A). Interestingly, we observed a strong positive correlation between the magnitude of CD4$^+$ Tfh-like responses to N after 12h and the maximum neutralizing capacity in plasma (r = 0.5646, p = 0.0041) (Fig. 35B). A similar trend was observed for CD8$^+$ Tfc-like responses (Fig. 35C).

Overall, this finding links the development of follicular T-cell responses to the N viral antigen and the neutralizing capacity of the plasma, indicating that T-cell responses not elicited by currently approved SARS-CoV-2 vaccines could provide T-helper cell support to B cells and promote antibody maturation in the follicle.
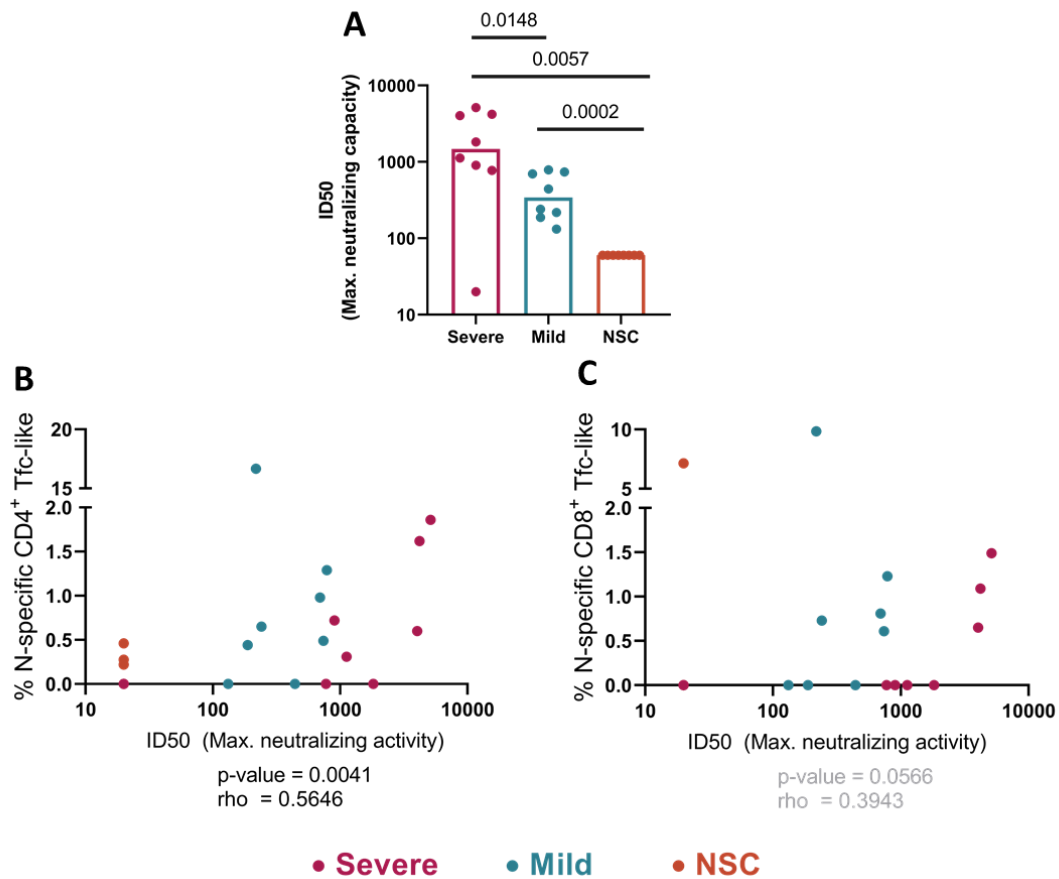
Figure 5. Correlations between maximum neutralizing capacity of sample plasma and T-cell responses to SARS-CoV-2. (A) Maximum neutralizing capacity of plasma between severe (n=8), mild (n=8) and non-seroconvertors (NSC, n=8) **(B**) Correlation between N-specific CD4+ Tfh-like responses and neutralization **(C)** Correlation between N-specific CD8+ Tfh-like responses and neutralization. Statistical significance was evaluated by non-parametric Mann-Whitney test, correlations were performed by Spearman's rank test, statistical significance was set at p<0.05, trends are shown in grey (p<0.15).

5. Limitations of the study

In this study we observed several aspects of the T-cell immunity against SARS-CoV-2 infection that are related to the severity of COVID-19 course. Still, there are a number of limitations. First, the relatively big size of SARS-CoV-2 genome (29 Kb) complicates the comprehensive screening for T-cell responses against the entire viral proteome. We thus focused on the main SARS-CoV-2 virion antigens: the spike and the nucleocapsid, which need to be produced in large amounts by infected cells and could thus potentially drive broad and strong T-cell responses. However, we cannot exclude that other viral antigens could provoke equally strong cellular immune responses[381].

Second, our results had a limited statistical power given the size of our groups. This could have reduced our chances to find correlation between memory T-cell populations and age, as previously demonstrated elsewhere[380]. In addition, although we included wide range of ages in all groups (table 5), especially in patients with severe COVID-19, the number of individuals in the high risk (>65 years) age groups was limited.
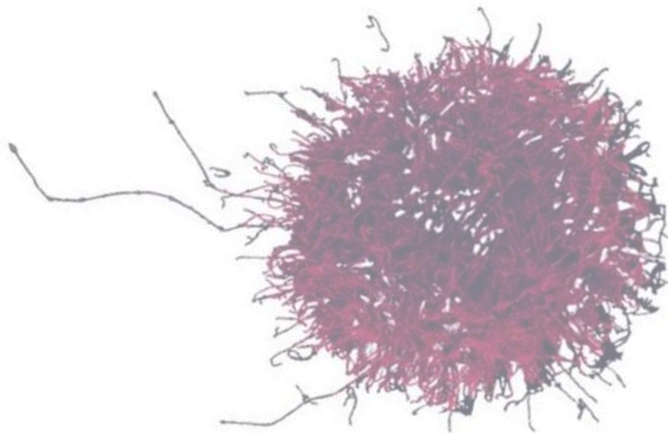
Alternative adaptive responses to chronic viral infection

T-follicular-like CD8+ T cell responses in chronic HIV infection are associated with virus control and antibody isotype switching to IgG
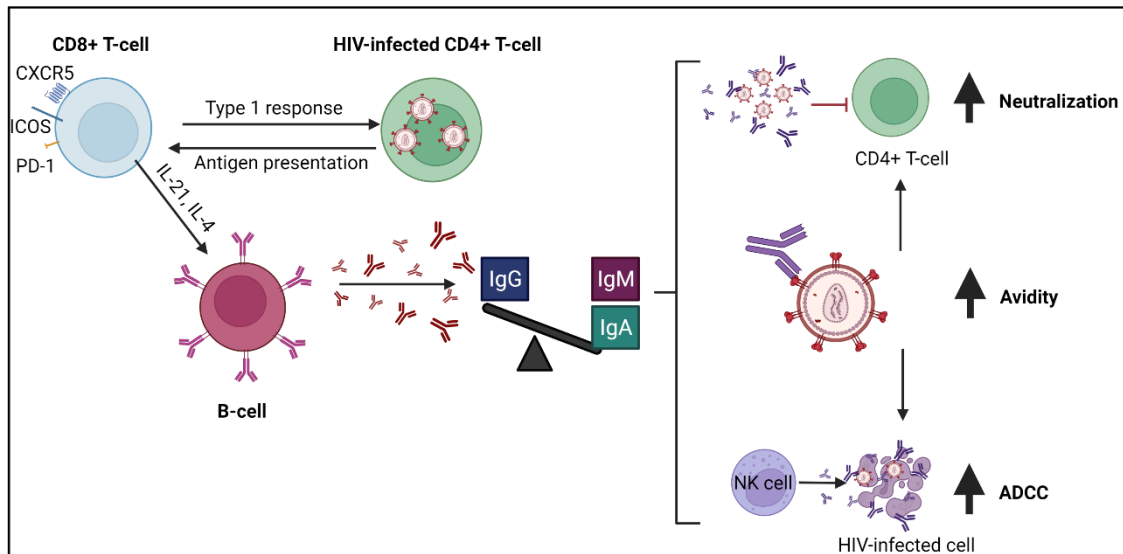
Abstract:

T cell responses are considered critical for the *in vivo* control of HIV, but the contribution of different T cell subsets to this control remains unclear. Using a boosted flow cytometric approach that is able to differentiate CD4$^+$ and CD8$^+$ T cell Th1/Tc1, Th2/Tc2, Th17/Tc17, Treg and Tfh/Tfc-like HIV-specific T cell populations, we identified CD8$^+$ Tfc responses that were related to HIV plasma viral loads and associated with rate of antibody isotype class switching to IgG. This favorable balance towards IgG responses positively correlated with increased virus neutralization, higher avidity of neutralizing antibodies and more potent antibody-dependent cell cytotoxicity (ADCC) in PBMCs from HIV controllers compared to non-controllers. Our results identify the CD8$^+$ Tfc-like T-cell response as a potentially critical component of effective virus control which could possibly be exploited therapeutically.

1. HIV-specific T-cell responses with Tc2 and CD8⁺ Tfc-like cytokine polarization profile are associated with viral control

To evaluate the presence of HIV-specific T-cells with alternative (non-IFN-γ dominated, i.e., Th1) cytokine polarization profiles, a comprehensive screening of HIV-specific cellular responses by *boosted flow* was performed. Total PBMCs from a cohort of 15 HIV⁺ controllers (C) and 14 HIV⁺ non-controllers (NC) were stimulated with a set of 17 peptide pools covering the entire HIV proteome. Observed signals in the flow cytometry data were expressed as the number of responders (% of individuals eliciting a specific polarized response), as well as breadth (number of reactive peptide pools) and magnitude (% of positive cells) of the response. While anti-HIV responses of type-1 CD4⁺ Th1-like cells and CD8⁺ Tc1-like cells were the most commonly detected responses, 86% (14 controllers and 11 non-controllers) of the tested29 individuals also showed non-type-1-like responses (Figure 36A). Of these, five individuals (two controllers and three non-controllers) elicited exclusively responses with alternative polarization and no type-1 CD4⁺ or CD8⁺ T-cell responses. The dominant non-type-1 responses were type-2 in CD4⁺ (percentage of responders: CD4⁺ Th2-like cells 50% and CD8⁺ Tc2-like cells 47%) and follicular-like cells in the CD8 T cell compartment (percentage of responders: CD4⁺ Tfh-like cells 44%, CD8⁺ Tfc-like cells 53.5%). Type-3 polarized responses (percentage of responders: CD4⁺ Th17-like cells 16%, CD8⁺ Tc17-like cells 13%) and cells with regulatory functions (percentage of responders:CD4⁺ Treg-like 24%, CD8⁺ Treg-like 20%) were also observed in both groups (Figure 36).

We found an elevated magnitude (p = 0.0268) and breadth (p = 0.0582) of HIV-specific CD4⁺ Tfh-like cells (Fig. 36B) in HIV⁺ controllers compared to non-controllers. CD8⁺ T-cell mediated responses with Tc2- and Tfc-like profiles were also more frequent (χ^2 p= 0.0402 and 0.0015, respectively) in HIV⁺ controllers (Fig. 36B), who also showed significantly greater magnitude and breadth of CD8⁺ Tfc-like responses (magnitude, p= 0.0005; breadth p= 0.0002) (Fig. 36B). The predominance of these CD8⁺ T-cell responses in HIV controllers was further evidenced by a negative correlation between the breadth and magnitude of HIV-specific CD8⁺ Tfc-like responses and the HIV plasma viral load (Fig. 36C).

Since the presence of CD8⁺ Tfc-like responses was remarkably increased in HIV controllers versus non-controllers, we tested whether the acquisition of an anti-HIV CD8⁺ Tfc-like phenotype was related to a higher capacity of PBMCs to secrete T-cell follicular-related cytokines (IL-4 and IL-21). Total PBMCs (8 HIV⁺ C and 14 HIV⁺ NC from the boosted flow study) were stimulated with

the peptide pools that were previously found to trigger Tfc-like responses in the initial *boosted flow* cytometry screening. The screening was assessed individually or in combination (IL-4 and IL-21) by single-cytokine or combined ELISpot. In line with the boosted flow cytometry, 60% of stimulations induced IL-21 SFC and 30% induced IL-4 producing SFC. However, the combined detection of IL-4 and IL-21 increased the sensitivity of the ELISpot assay and responses against 80% of the pools were detected (Fig. S17). Interestingly, individuals who showed the presence of HIV-specific CD8+ Tfc-like responses had a significantly higher innate capability to secrete IL-21, but not IL-4 in response to an unspecific stimulus (PHA, Fig. 36D).
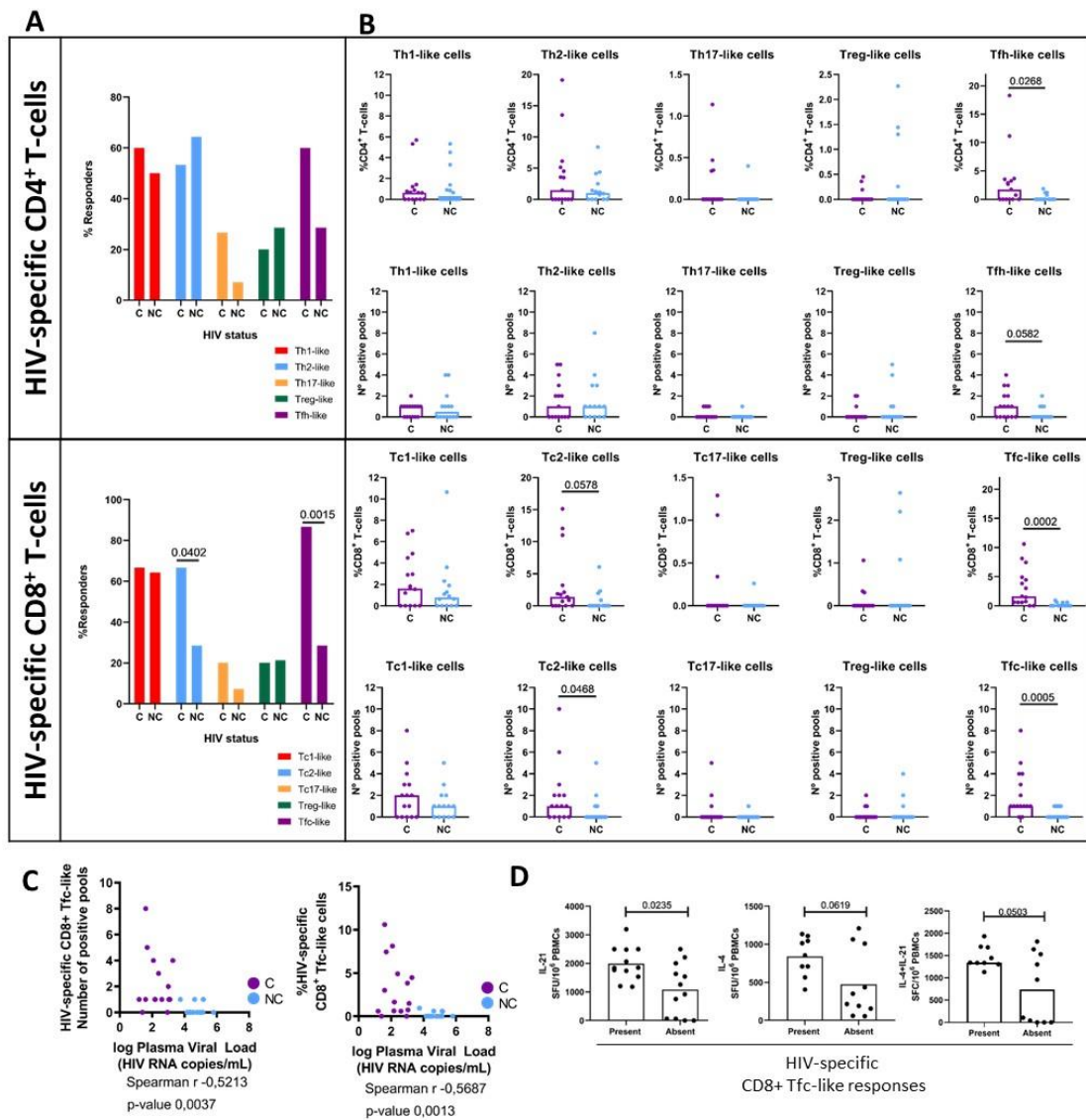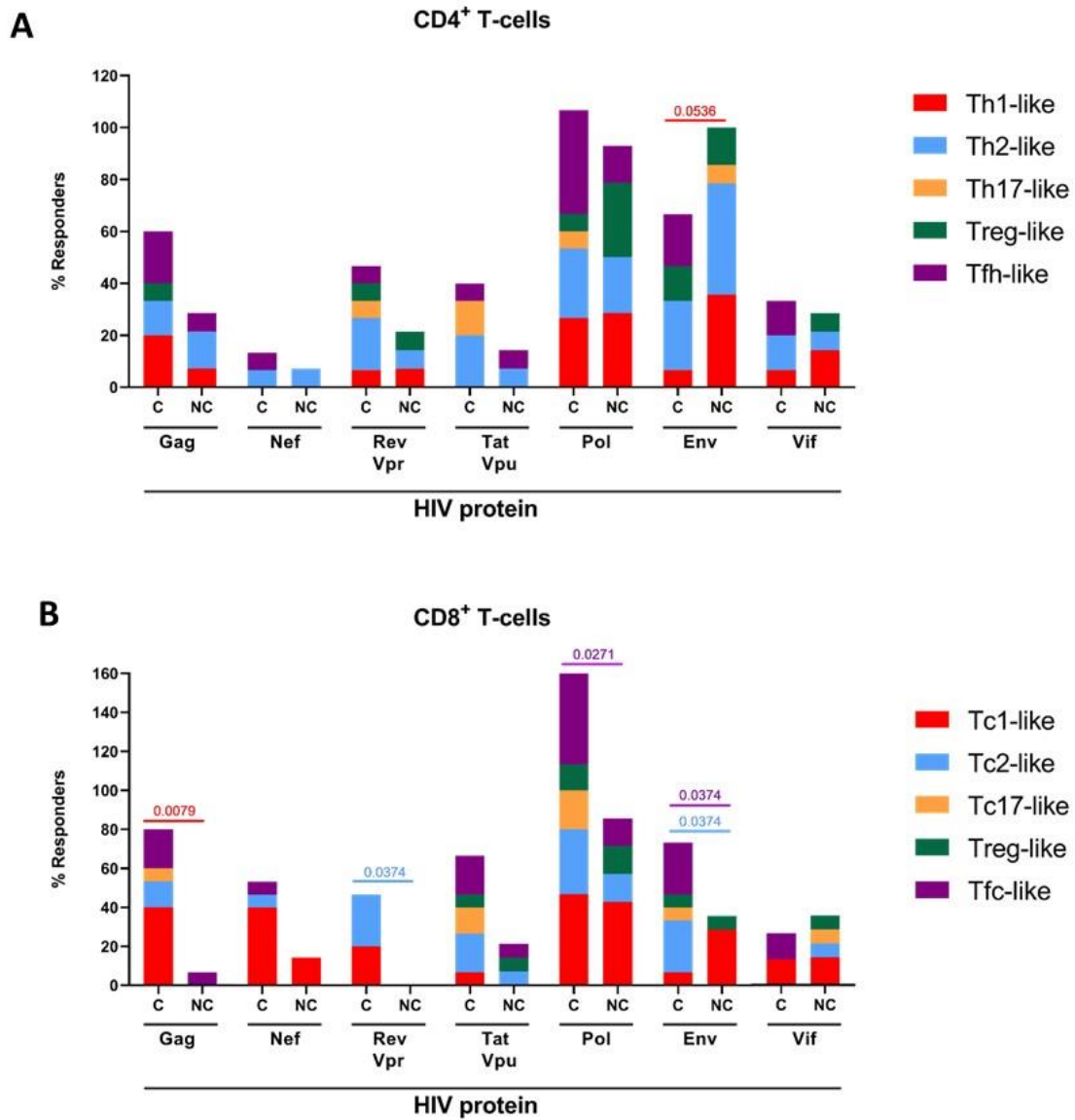
Figure 36. HIV-specific T-cell polarized responses. *Boosted Flow* screening of specific-T-cell responses against whole HIV proteome in a cohort of 15 HIV+ controllers (C, purple) and 14 HIV+ non-controllers (NC, light blue) revealed a highly-diverse set of polarized T-cell responses in terms of **(A)** number of responders **(B)** percentage of circulating HIV-specific T-cells (up) and number of reactive pools (down). **(C)** Negative correlation between plasma viral load and CD8+ Tfc-like responses to HIV measured in terms of breadth (left) and magnitude (right). **(D)** Inner capacity of total PBMCs to secrete T-follicular associated cytokines IL-21 (left scatter plot), IL-4 (middle scatter plot) and IL-21/IL-4 simultaneously (right scatter plot) upon non-specific PHA stimulation stratified by the presence (left bar) or the absence (right bar) of HIV-specific circulating Tfc-like responses. Statistical significance of differences in frequency of responders was evaluated by Chi-square test, between group medians by non-parametric Mann-Whitney test and correlation between Tfc-like responses and plasma viral load by Spearman correlation and its correspondent p-value. Statistical significance was set on p<0.05.

T-cell responses targeting different HIV proteins have been shown to exert different antiviral activity[382–385]. This difference may be related to antigen presentation, viral sequence variability, but also to alterations in maturation and effector profile polarization in response to different viral proteins[386]. Indeed, the analysis of T-cell responders stratified by HIV-derived protein revealed marked differences in the polarization profiles of responding T-cell populations (Figure 37) and these alterations were different in HIV controllers and non-controllers, linking viral protein specificity and effector function polarization to viral control. In particular and in line with previous studies, Th1-like CD4+ T-cell responses to Envelope (Env) were more frequent in HIV+ non-controllers compared than in controllers (χ^2 p= 0.0536)[382,383], while more CD4+ Tfh-like, Env-specific responders were preferentially, but not only, seen in HIV+ controllers (χ^2 p= 0.0772). HIV+ non-controllers also triggered more prominent Pol-specific Treg-like response (Fig. 37A). In the case of CD8+ T-cells, statistically significant differences were observed for the frequency of type-1 responses to Gag-reactive responses in HIV controllers (χ^2 p= 0.0079), also in line with previous studies using single cytokine-based (IFN-γ) ELISpot analyses[46]. Controllers also showed significantly higher number of Tc2-like responders upon Rev/Vpr or Env stimulation (χ^2 p= 0.0374) and Tfc-like upon Pol and Env stimulation (χ^2 p= 0.0271 and 0.0374, respectively, Fig. 37B). When comparing the magnitude of responses, CD8+ Tc1-like Gag-specific (MW p= 0.0169) and Tfc-like Pol-specific (MW p= 0.0245) were stronger in controllers compared to non-controllers. Remarkably, accessory proteins (Rev, Vpr, Tat and Vpu) elicited more alternative effector functions than type-1 responses (Fig. S18).

Polyfunctional analysis performed using the SPICE v6 software revealed mostly T-cell responses with single polarization profiles, indicating that responses might have matured into distinct polarization profiles, which are mutually exclusive, and supporting the specificity of the employed boosted flow analyses (Fig. S19). For instance, Tfh and Tfc responses showed very little overlap with Th1 and Tc1, respectively, indicating that those subsets specifically produced

IL-4/IL-21 but not IFN-γ/IL-2/TNF-α. These results suggest that alternative HIV-specific T-cell profiling beyond conventional antiviral type-1 responses might be associated with viral control in a protein-dependent manner. The data also suggest that CD8+ Tfc-like cells might play a particularly important role in anti-HIV immune response.

Figure 37. HIV protein-specific polarized T-cell responses. *Boosted Flow* cytometry screening of HIV protein-specific T-cell responses resulted in protein-dependent differently polarized profiles in both CD4+ T-cells and CD8+ T-cells. The percentage of responders to each of the HIV derived proteins is indicated in stacked bars for CD4+ (**A**) and CD8+ (**B**) T-cells. Statistically significant (p<0.05) differences in protein-specific frequency of response between HIV+ controllers (C) and HIV+ non-controllers (NC) are indicated. Statistical significance was evaluated by Chi-square.

2. Circulating type 2 and follicular-like T-cells show different memory profiles in HIV⁺ controllers and non-controllers

To determine whether the polarization of the virus-specific effector T-cell responses and the apparent *in vivo* viral control were associated with the induction of specific T-cell differentiation and maturation, we determined CCR7 and CD45RA expression on HIV-specific CD4⁺ and CD8⁺ type-1, type-2 and follicular-like T-cells. No statistically significant differences were observed between unstimulated total CD4⁺ and CD8⁺ memory phenotypes in HIV⁺ controllers, compared to non-controllers (median percentage of CD4⁺ populations: T_{CM} 18%, T_{EM} 34.5%, T_{EMRA} 7.5% and T_{Naive} 40%; CD8⁺ T-cells: T_{CM} 3%, T_{EM} 37.8%, T_{EMRA} 29.9% and T_{Naive} 29.3%, Fig.38). In contrast, HIV-specific T-cells showed marked differences for T_{Naive} and T-memory subsets in the CD4⁺ Th2-like and Tfh-like, but not Th1 polarized cells. Of note, the levels of CD4⁺ T_{EM} contributing with Th2-like polarization were significantly higher (χ^2 p= 0.007) in HIV⁺ controllers, while T_{Naive} were more frequent in non-controllers (χ^2 p= 0.0247). While differences in memory subset distribution were less evident for CD8⁺ T-cells, we observed a significant increase of T_{EM} Tc2 frequencies (χ^2= 0.0247) and a reduction of T_{Naive} Tc2 populations, HIV-specific CD8⁺ cells in controllers compared to non-controllers. Altogether, these data revealed differences in the memory phenotype of HIV-specific type 2 T-cells that differ between HIV controllers and non-controllers.
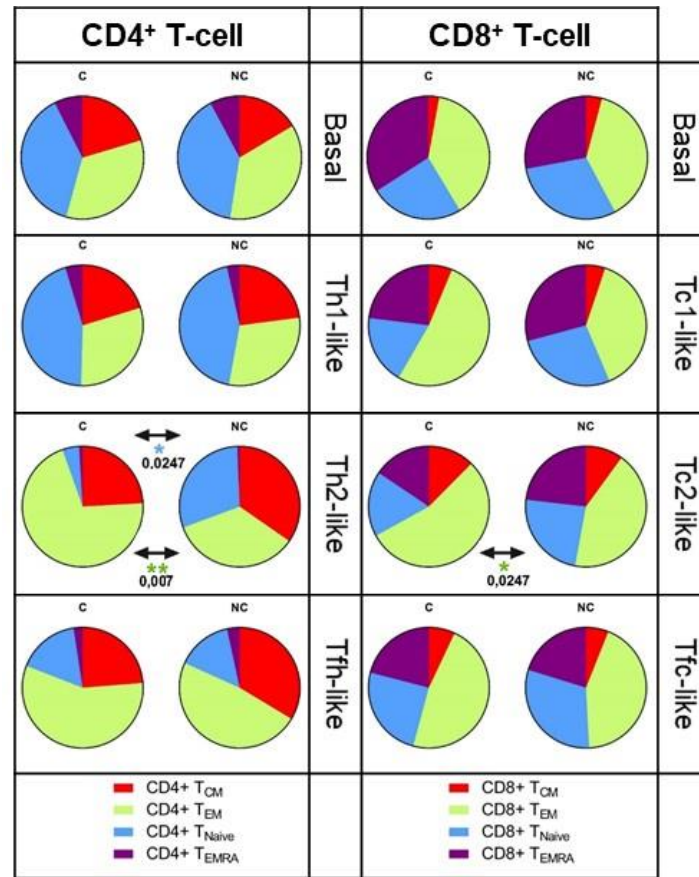
Figure 38. Memory phenotype of the HIV-specific polarized T-cell responses. The frequency of cells expressing memory markers CD45RA and CCR7 was evaluated in both HIV-specific polarized CD4$^+$ and CD8$^+$ T-cells. The percentage of basal, Th1/Tc1, Th2/Tc2 and Tfh/Tfc-like cells classified as T$_{CM}$ (CD45RA$^-$ CCR7$^+$), T$_{EM}$ (CD45RA$^-$ CCR7$^-$), T$_{EMRA}$ (CD45RA$^+$ CCR7$^-$) and T$_{Naive}$ (CD45RA$^+$ CCR7$^+$) are shown in pie charts. Statistical significance of the differences between HIV-specific memory phenotype in HIV$^+$ controllers (C, left) and HIV$^+$ non-controllers (NC, right) was evaluated by non-parametric Mann-Whitney test, statistical significance was set at p>0.05, only significant results are shown.

3. Expression of cell surface specific markers in individuals showing CD8$^+$ Tc2- and Tfc-like responses

To further validate that the CD4$^+$ and CD8$^+$ type 2-like and follicular-like, HIV-specific T-cells identified by our boosted flow cytometry approach expressed traditional markers of Th2/Tc2 or Tfh/Tfc, we determined expression of CRTH2[387,388] for Th2/Tc2 or CXCR5, PD-1 and ICOS for Tfh/Tfc (Fig. S4) by flow cytometry. An unsupervised analysis by X-Shift yielded a total of 45 clusters based on the expression of CD4, CD8, CCR7, CD45RA, CRTH2, CXCR5, PD-1 and ICOS. A heatmap was generated based on the level of expression (MFI) of each marker. We compared

the contribution of each cluster inside the CD3⁺ population between controllers and non-controllers. Clusters contributing with a 2-fold change to the CD3⁺ population (%) were included in the analysis. Three different clusters, one corresponding to CD8⁺ T-cells and two belonging to CD4⁺ were overrepresented in HIV⁺ non-controllers. Of those, one cluster was formed by CD4⁺ Tfh cells expressing ICOS, CXCR5 and PD-1, while the other two clusters (one CD4⁺ and one CD8⁺) expressed high levels of CXCR5 but lacked the expression of PD-1 and ICOS. We then explored by manual supervised gating the potential relationship between the presence of circulating CRTH2+ Th2/Tc2, circulating CXCR5⁺ Tfh/Tfc populations and HIV control (Figure 39B). These analyses did not reveal any differences in the levels of CD4⁺ Th2 cells expressing CRTH2, or CD4⁺ Tfh cells expressing CXCR5, PD-1 and ICOS. Similarly, no difference in CRTH2 expressing Th2 CD8⁺ T-cells was observed. However, CD8⁺ CXCR5⁺PD-1⁺ICOS⁺ T-cells were significantly elevated in HIV⁺ controllers (MW, p = 0.0479) and also in those individuals capable to elicit HIV-specific CD8⁺ Tfc-like cytokine responses, as seen within the *boosted flow* analysis. These results thus, provided evidence of the existence of peripheral Tfc-like cells with deficient expression of follicular markers in HIV non-controllers, which could impact their function and ability for B-cell interaction and antibody maturation.
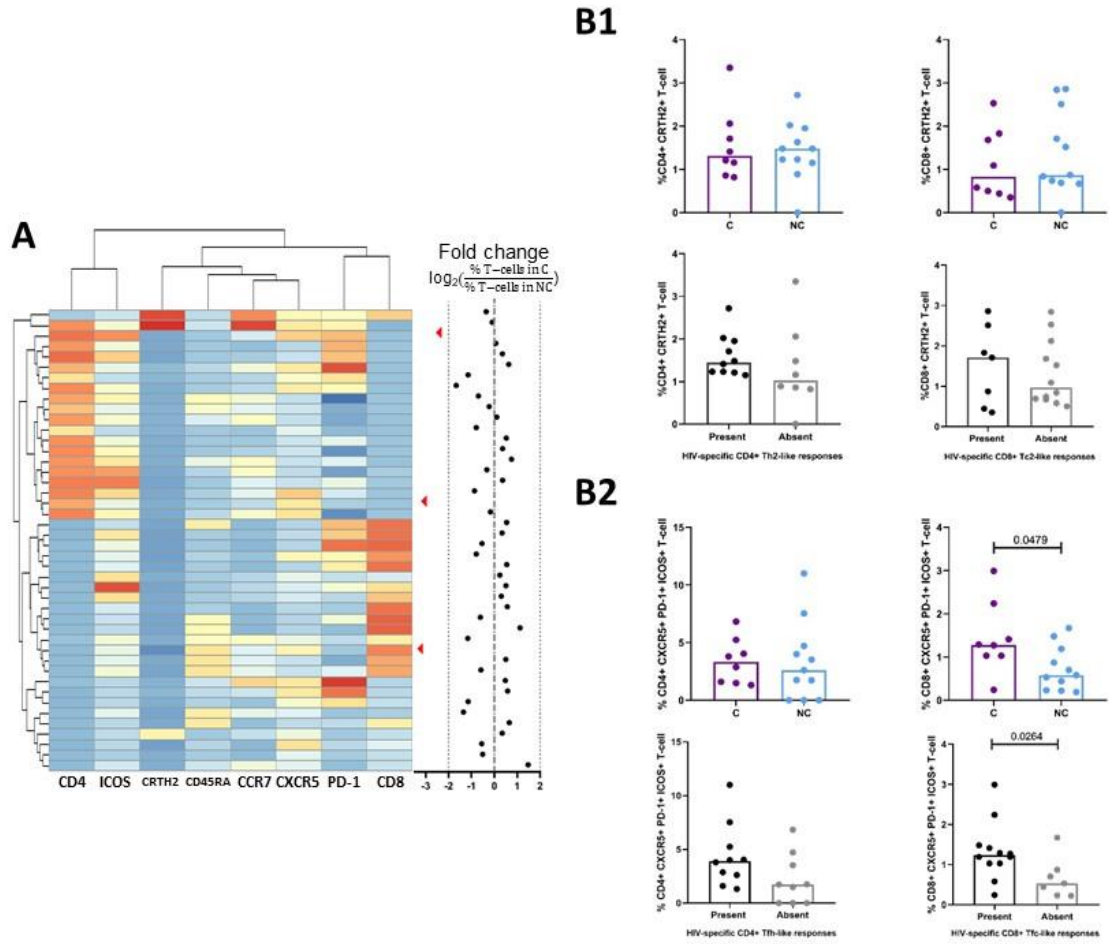
Figure 40. Comparison of CD4+ Th2 and Tfh and CD8+ Tc2 and Tfc subpopulations between controllers and non controllers. (A) Unsupervised clustering of CD4+ and CD8+ T-cell population based on the expression of Th2/Tc2 marker (CRTH2), Tfh/Tfc markers (CXCR5, PD-1, ICOS) and memory phenotype markers (CCR7, CD45RA) by FlowSOM. Results are expressed as a fold change between the presence of the clusters in HIV+ controllers (C, purple) compared to HIV+ non-controllers (NC, light blue). **(B1)** Comparison of the percentage of CRTH2+ CD4+ Th2-cells (left) and CD8+ Tc2 cells (right) stratifying by HIV control status (above) or the presence or absence of HIV-specific Th2/Tc2 responses (below). **(B2)** Comparison of the percentage of CXCR5+PD-1+ICOS+ CD4+ Tfh-cells (left) and CD8+ Tfc cells (right) stratifying by HIV control status (above) and the presence or absence of HIV-specific Tfh/Tfc-like cytokine responses by boosted flow responses (below).

4. Higher levels of CD8⁺ Tfc-like cells in HIV⁺ controllers are associated with maturation of the humoral immune response and antibody effector functions

CD4⁺ Tfh-like cells have been shown to be required for the induction of effective humoral immunity. Thus, we assessed whether HIV-specific CD4⁺ and especially also CD8⁺ Tfc-like cells due to their strong association with HIV control, were related with antibody isotype switching, neutralization capacity and ADCC effector function. To this end, we first determined plasma titers of $HIV_{BaL.01}$ and HIV_{NL4-3} Env-specific IgA, IgM and IgG in 24 HIV⁺C, 20 HIV⁺ NC and 8 HIV uninfected individuals (SN). Uncontrolled HIV infection was associated with increased median IgA (p= 0.0515) and IgM titers (p= 0.0009), while HIV⁺ controllers' plasma contained higher titers of IgG (p= 0.0182, Fig. 40A). IgG/IgM and IgG/IgA ratios, reflecting isotype class switching towards IgG, were elevated in HIV controllers (Fig. 40B). Furthermore, the avidity of the anti-$HIV_{BaL.01}$-gp120 specific IgG response was significantly higher in plasma from HIV⁺ controllers (MW, p= 0.0027) (Fig. 40C).
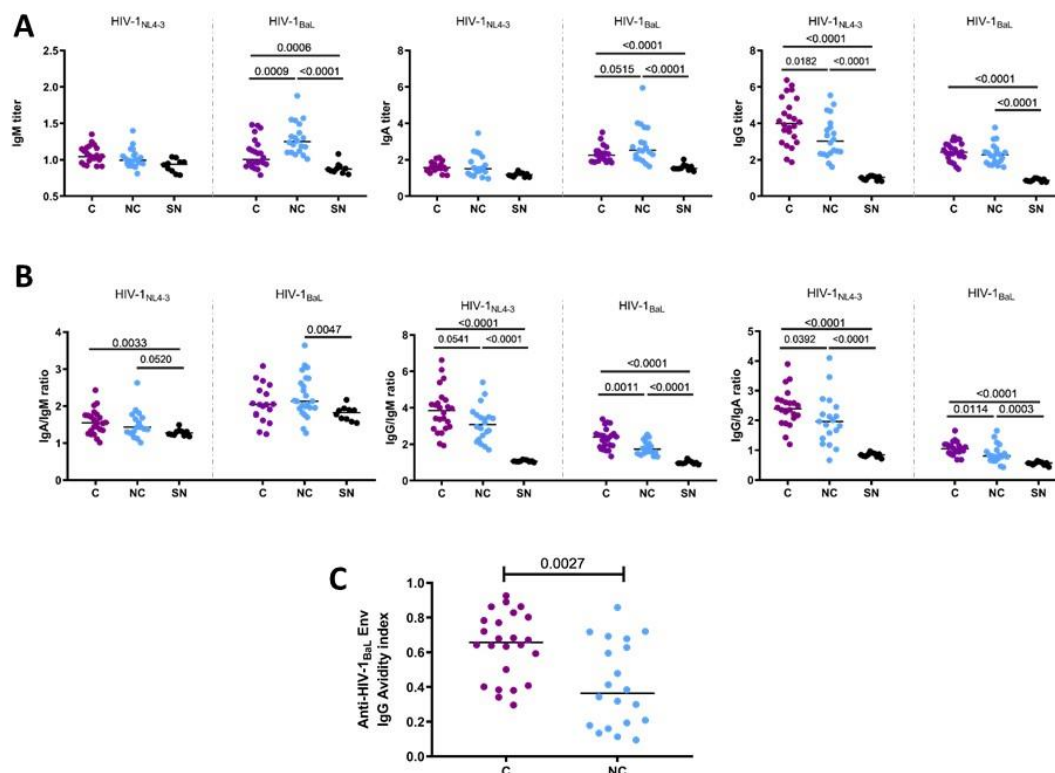
Figure 40. Titers of anti-HIV Env IgA, IgG and IgM. Titers and affinity were compared between controllers (N=24, C, purple dots) and non-controllers (N=20, NC, light blue dots) and HIV seronegatives (N= 8, SN, black dots). **(A)** Plasma dilution titers of anti-HIV Env IgA, IgG and IgM were determined with MOLT-4 cell lines expressing HIV_{NL4-3} and HIV_{BAL} Env in the surface. **(B)** Isotype class switching extend was estimated by the ratio of anti-HIV Env IgA/IgM, IgG/IgM and IgG/IgA in each individual. **(C)** Avidity index of HIV_{BaL} Env-specific IgG. Statistical significance (p< 0.05) was evaluated by applying non-parametric Mann-Whitney test.

Neutralization capacity and ADCC activity were determined as measures of antibody-mediated effector function. As shown in Figure 41A, neutralization capacity was assessed against a panel of five HIV pseudovirus, including strains from tiers 1A (NL4-3), 1B (BaL.01) and 2 (398F1, TRO11 and AC10). Among HIV controllers, a significantly higher proportion of individuals (76%) were able to neutralize HIV_{NL4-3} compared to NC (37%, χ^2 p= 0.0052). A similar trend was observed for neutralization of the $HIV_{BaL.01}$ isolate (68% C vs 42% NC, χ^2 p= 0.0664) (Fig. 41B). Neutralization breadth was also significantly increased in controllers compared to non-controllers (median: 40% and 20% respectively; χ^2, p= 0.0111). The neutralization capacity against HIV_{NL4-3} strain was also significantly elevated in controllers (MW, p= 0.0059) and a trend (MW, p= 0.0819) for neutralization of $HIV_{BaL.01}$ was observed as well (Fig. 41C).

Along with neutralization, more potent ADCC activity was observed in controllers' plasma compared to non-controllers. We also observed significant positive correlations between ADCC capacity ($1:10^{3.6}$ dilution) and neutralization IC50 for HIV_{NL4-3} (r = 0.4562, p= 0.0019) and $HIV_{BaL.01}$ (r = 0.3461, p= 0.0214, Fig 41J). These associations were driven by the titers of IgG and IgG avidity in the plasma samples, as we found Env-specific IgG (but not other isotypes) titers to be positively correlated with logIC50 for HIV_{NL4-3} (r = 0.5919, p<0.0001) and $HIV_{BaL.01}$ (r = 0.6423, p<0.0001) and avidity to be positively correlated with ADCC capacity (r = 0.5348, p= 0.0002) (Fig. 41H) and neutralization against HIV_{NL4-3} (r = 0.4053, p= 0.0063) and $HIV_{BaL.01}$ (r = 0.4461, p= 0.0023) (Fig. 41I). IgG/IgM ratios also correlated with neutralization of HIV_{NL4-3} (r = 0.5573, p<0.0001) and $HIV_{BaL.01}$ (r = 0.3028, p= 0.0458). A similar relation of the IgG/IgM ratio was seen with the ADCC capacity not only with the IgG/IgM ratio for the HIV_{NL4-3} Env (r = 0.2770, p = 0.0687), which is the same HIV strain expressed by the CEM.NKR-CCR5 ADCC target cells, but also with the IgG/IgM ratio for the $HIV_{BaL.01}$ Env (r = 0.3799, p = 0.0110, Fig. 41G).
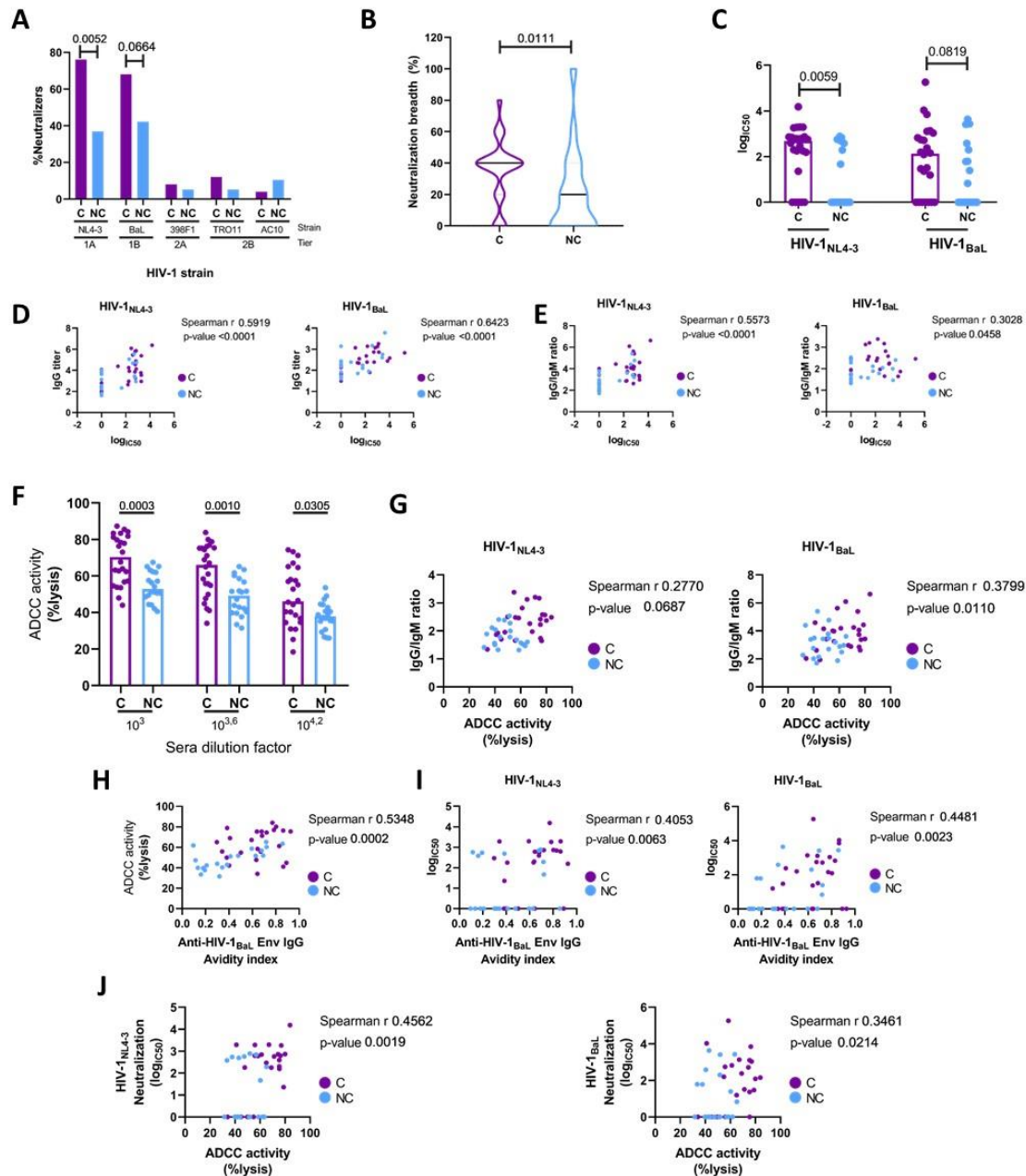
Figure 41. Antibody mediated anti-HIV functional responses. Humoral responses are compared between controllers (C, purple) and non-controllers (NC, light blue). **(A)** Percentage of individuals capable to neutralize a panel of 5 HIV pseudoviruses, including 5 strains from tier 1A (NL4-3), 1B (BaL), 2A (398F1) and 2B (TRO11 and AC10). **(B)** Neutralizing breadth (left) in HIV+ controllers (C) and non-controllers (NC) calculated as: number of pseudovirus neutralized/number of pseudovirus evaluated (5) *100. **(C)** IC_{50} neutralizing capacity of HIV+ controllers (C) and non-controllers (NC) against HIV_{NL4-3} (left) and HIV_{BaL} (right). **(D)** Spearman correlation of logIC50 neutralizing capacity with IgG titers. **(E)** Correlation of logIC50 neutralizing capacity with IgG/IgM ratio. **(F)** Antibody-dependent cellular cytotoxicity (ADCC) induced by the presence of serial sera dilutions from controllers (C) and non-controllers (NC). **(G)** Correlation between ADCC at 1:10^{4,2} serum dilution with IgG/IgM ratio. **(H)** Correlation between ADCC at 1:10^{4,2} serum dilution with avidity index. **(I)** Correlations between IC_{50} neutralizing capacity against HIV_{NL4-3} (left) and HIV_{BaL} (right) with avidity. **(J)** Correlation between ADCC at 1:10^{4,2} serum dilution with neutralization log(IC50). Statistical significance of the presence of neutralizing activity (A) in both groups was evaluated by Chi-square, while comparison of medians (B, C and F) was determined by non-parametric Mann-Whitney test. Correlations were performed by non-parametric Spearman r test, r and p-values are displayed in the correspondent plots.

To further explore a possible relationship between the humoral immune response with HIV control, antibody titers and functional responses were correlated with three clinical parameters (CD4 count, CD4/CD8 ratio and plasma viral load). Anti-HIV$_{BaL.01}$ IgM titers showed a negative correlation with CD4 count (r = -0.6352, p<0.0001), CD4/CD8 ratio (Spearman r r =-0.5628, p<0.0001) and a positive correlation with plasma viral load (Spearman r r = 0.4177, p= 0.0048) (Fig 42), in line with the elevated IgM levels seen in HIV non-controllers. Furthermore, plasma viral load was also negatively correlated with IgG/IgM ratio (r = -0.3094, p= 0.0410), plasma avidity (r =-0.4716, p= 0.0012), neutralizing capacity against HIV$_{NL4-3}$ (r =-0.3989, p= 0.0073) and ADCC activity (r = -0.4863, p= 0.0008; Fig. 42). Our results demonstrate a higher extent of anti-Env IgG with increased avidity and a decrease of IgM antibodies in individuals with natural control, which was related to a higher neutralizing capacity and elevated ADCC activity.
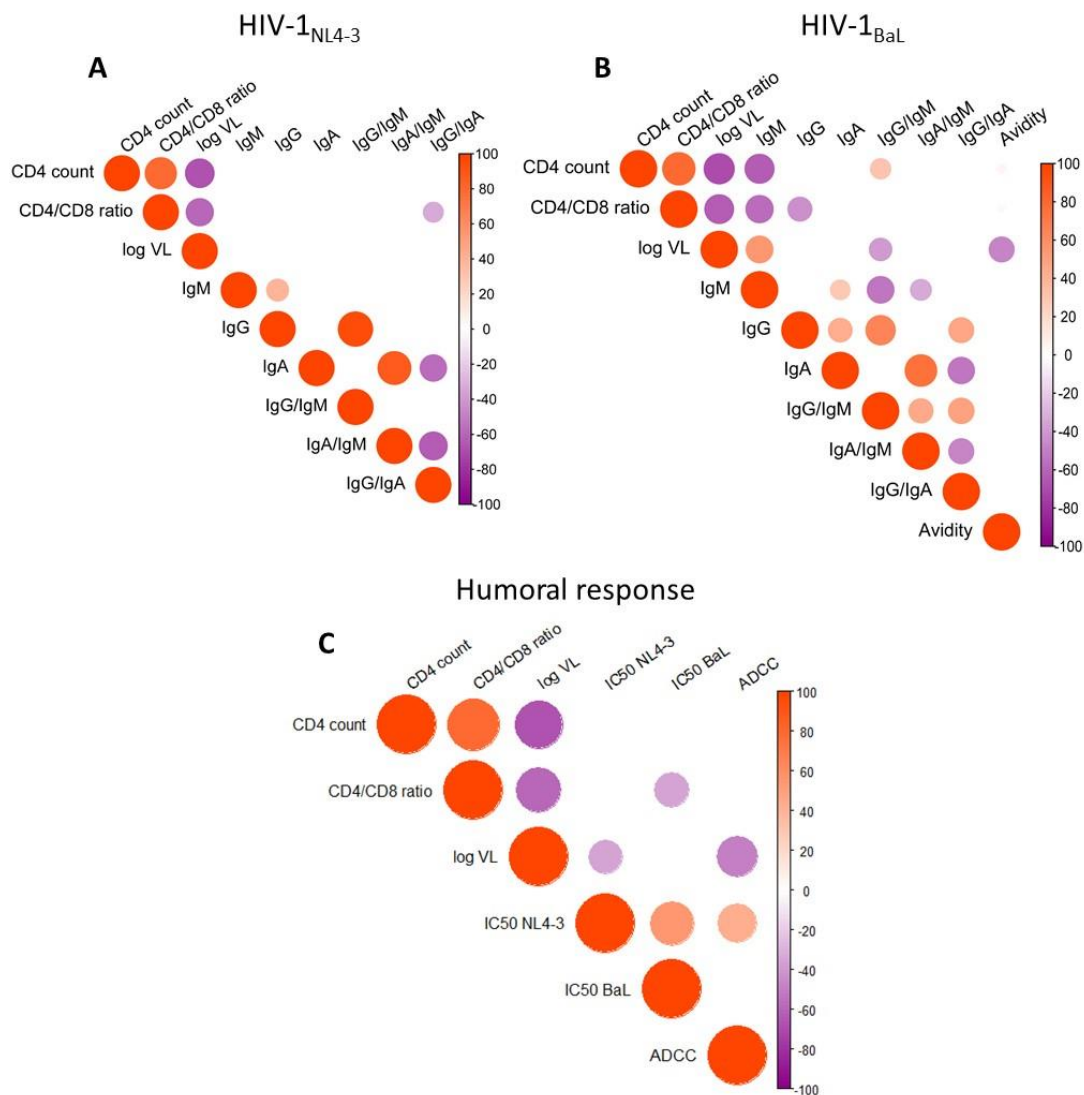
Figure 42. Humoral anti-HIV functional responses link with clinical parameter's. (**A**) Correlation between anti-HIV$_{NL4-3}$ antibody titers and CD4 count, CD4/CD8 ratio and plasma viral load. (**B**) Correlation between anti-HIV$_{BaL}$ antibody

titers and CD4 count, CD4/CD8 ratio and plasma viral load. (**C**) Correlation between humoral functional response (HIV$_{NL4-3}$ and HIV$_{BaL}$) neutralization activity, ADCC and CD4 count, with CD4/CD8 ratio and plasma viral load. Correlations were performed by non-parametric Spearman r test. Positive correlations are indicated in red while negative correlations in purple, color intensity in proportional to Spearman's r and circle size is related to the p-value when significant.

5. HIV-specific CD8$^+$ Tfc-like responses are linked to antibody isotype class switching and humoral function

Our data show HIV-specific CD8$^+$ Tfc-like responses to be elevated in HIV controllers, as well as to be linked to isotype ratios and IgG titers. Thus, we tested directly how the presence of CD8$^+$ Tfc-like cells was related to these beneficial markers of the humoral immune response. Plasma samples from individuals with detectable CD8$^+$ Tfc-like cells demonstrated increased titers of IgG to HIV$_{NL4-3}$ Env (p= 0.0037) and decreased titers of IgM HIV$_{BaL.01}$ Env (p= 0.0118) compared to samples were these responses were absent. This finding resulted in a significantly higher IgG/IgM ratio for both viral isolates (HIV$_{NL4-3}$ MW p= 0.0215, HIV$_{BaL.01}$ MW p= 0.0123) and reflected increased antibody isotype class switching when compared to individuals with no detectable CD8$^+$ Tfc-like responses. When measuring the balance of IgG with IgA levels, the results showed a clear dominance of IgG mediated antibody activity when CD8$^+$ Tfc-like responses were present (HIV$_{NL4-3}$ MW p= 0.0059, HIV$_{BaL.01}$ MW p= 0.0037). In addition, we observed that the magnitude and breadth of the CD8$^+$ Tfc-like response correlated negatively with anti-HIV$_{BaL.01}$ IgM (Magnitude: r = -0.5764, p= 0.0011; Breadth: r = -0.5561, p= -0.0017 - Fig. 43B) and positively with anti-HIV$_{NL4-3}$ IgG (Breadth: r = 0.4729, p = 0.0096 - Fig. 43C) and IgG/IgM ratio for both strains (HIV$_{NL4-3}$: r = 0.3849, p = 0.0393; HIV$_{BaL.01}$: r = 0.4252, p = 0.0215 – Fig. 43D). Interestingly, IgG/IgA ratio also positively correlated with Tfc-like magnitude and breadth, showing a preferential isotype switching towards IgG over IgA in those individuals who showed an expansion of HIV-specific CD8$^+$ Tfc-like cells (Fig. 43E).
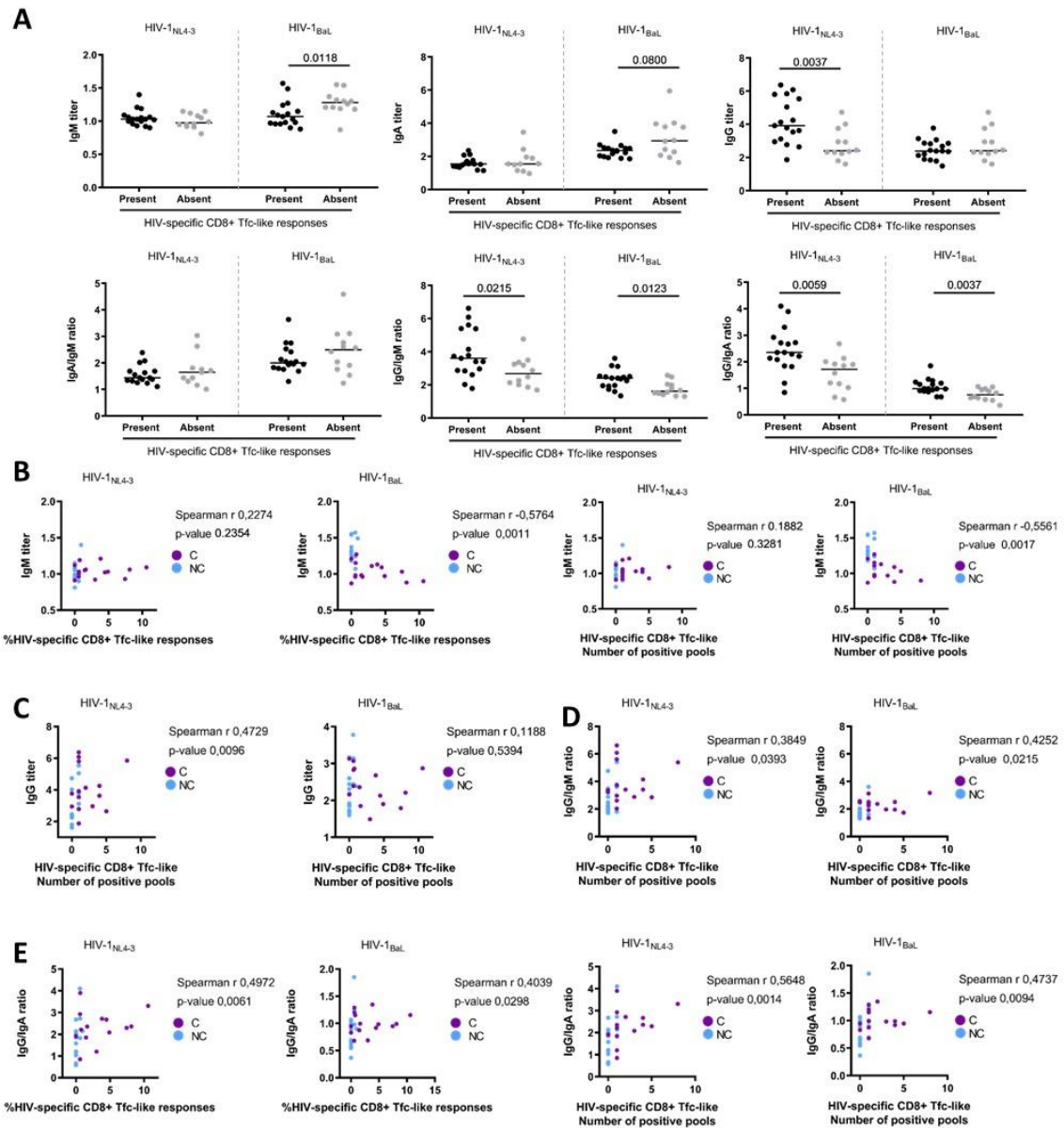
Figure 43. Link between HIV-specific CD8+ Tfc-like responses and humoral responses. (**A**) Individuals were stratified by the presence (n=17) or the absence (n=13) of HIV-specific CD8+ Tfc-like responses in the PBMC. The titers of IgA, IgG and IgM were compared, as well as the IgA/IgM, IgG/IgM and IgG/IgA ratios. (**B**) Correlation between anti-HIV$_{NL4-3}$ (left) and HIV$_{BaL}$ (right) IgM titers with CD8+ Tfc-like magnitude (left) and breadth (right). (**C**) Correlation between anti-HIV$_{NL4-3}$ (left) and HIV$_{BaL}$ (right) IgG titers with CD8+ Tfc-like breadth. (**D**) Correlation between anti-HIV$_{NL4-3}$ (left) and HIV$_{BaL}$ (right) IgG/IgM ratio with CD8+ Tfc-like breadth. (**E**) Correlation between anti-HIV$_{NL4-3}$ (left) and HIV$_{BaL}$ (right) IgG/IgA ratios with CD8+ Tfc-like magnitude (left) and breadth (right). Statistical significance of the comparison were performed by non-parametrical Mann-Whitney test while non-parametric Spearman r correlations were applied.

6. Limitations of the study

This study has a number of limitations regarding the study of humoral effector functions and isotype switching. First, BCR sequencing would be required to confirm that the higher IgG/IgM ratio is due to a larger extent of specific B-cell clones with isotype class switching. Second, T helper polarization might be relevant for the induction of specific IgG subtypes with different functional effects. Notwithstanding these limitations, humoral response was clearly related to CD8^{+} Tfc responses, but not Tfh or other T helper functions, pointing towards a central role of this subset in the orchestration of the anti-HIV immunity. Furthermore, peripheral blood Tfc-like responses might not properly reflect germinal center interaction and partially explain the lack of correlation between avidity and Tfc or Tfh-like responses against HIV[389]. TCR clonotyping in CD8 Tfc from different tissue could help overcome this caveat.
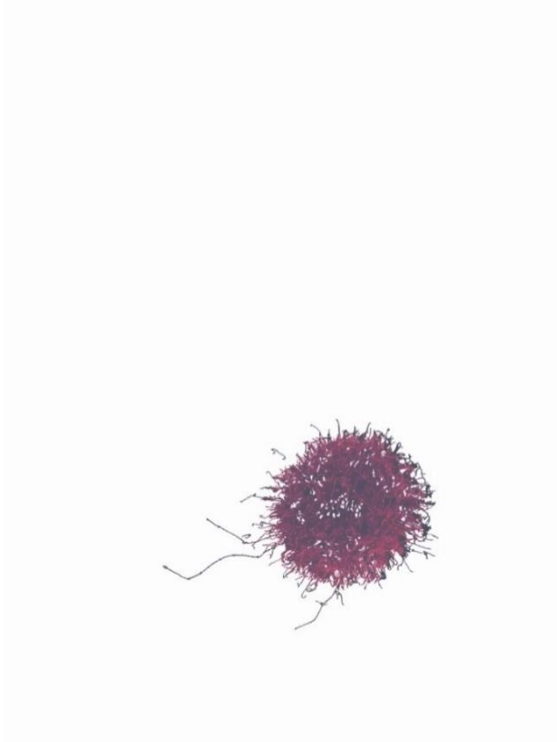
DISCUSSION AND FUTURE PERSPECTIVES
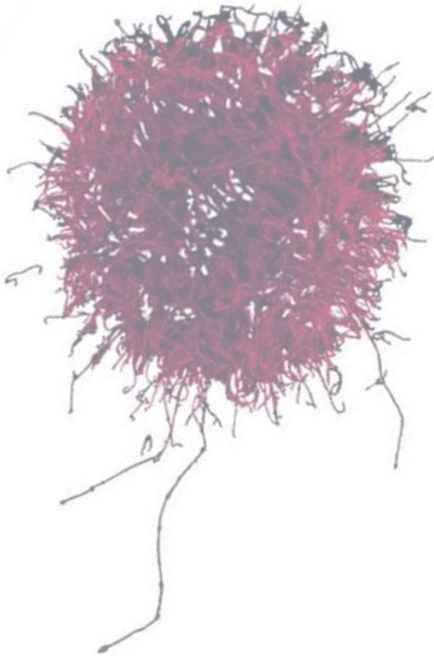
Since its first description less than 3 years ago, SARS-CoV-2 have caused more than 600 million infections and 6 million associated-death[2], while 79.3 million people have been infected with HIV since the beginning of the pandemic in the early 1980s, of which 36.3 million people have deceased of AIDS-related causes[98]. The evolution of these two pandemics shows that, despite the development of new antiviral drugs and vaccines, viral diseases have remained one of the biggest treats to global health in the XXI century. This may seem more relevant in the case of the HIV pandemic, for which we still miss a cure or an effective preventive vaccine after forty years of research. At the same time, the economic and social impact of the COVID-19 pandemic and the emergence of new SARS-CoV-2 variants, indicates that we need to better understand how viral infections can be controlled by the immune system, in order to apply such knowledge to develop new immune-based therapies and prevent new infections and deaths.

The study of cellular immunity against viral infections has been traditionally focused on CD8+ CTL responses while giving less importance to other components of the cellular immunity such as T-cells with alternative effector functions and NK cells. In some cases, a clear association between virus-specific CTL responses and infection clearance has been shown. This is the case for respiratory syncytial virus (RSV), human metapneumovirus (HMPV), influenza A virus (IAV) and dengue virus infection (DENV)[390,391]. However, in SARS-CoV-2 and HIV infections, although the CTL responses have been widely evaluated no reliable functional correlate of protection from disease progression has been described up to date. For SARS-CoV-2, aberrant activation of CTLs were linked to COVID-19 severity and increased levels of cytolytic molecules (granzymes and perforin) were found in severe patients when compared to milder forms of the disease[392]. Additional studies screened the SARS-CoV-2 proteome for T-cell epitopes restricted by common HLA CLASS I alleles[393]. In the case of HIV, the lack of reliable correlates of protection may in part be due to CTL responses being highly variable among infected individuals, including elite controllers, and explaining only 10-15% of the disease course variability, which is further determined by other immunological and viral factors[162–164].

These observations suggest that it is highly unlikely that immune control of SARS-CoV-2 and HIV-1 infections will rely uniquely on cytotoxic T-cell responses and that they need to be supported by additional cytotoxic and regulatory cellular responses, in addition to humoral responses, to have the chance to achieve viral control. For this reason, in the present study we focused on cellular immune responses that show alternative effector functions from those attributed to classical cytotoxic CTL responses and included cellular immune responses mediated by NK cells in the analysis. We evaluated the association between these responses and viral control while

trying to elucidate which effector and regulatory functions can explain viral control. We first focused on NK cells, since they represent a first barrier to viral infections. Their lower dependence on HLA class I and -II genotypes in comparison to T-cells allows them to directly detect and eliminate infected cells without the involvement of professional APCs. Hence, understanding the events that induce virus-mediated disruption of NK cell immunity might be crucial to develop new therapies against SARS-CoV-2 and HIV-1 infections. On the other hand, T-cells can polarize into a vast diversity of effector functions beyond the classical cytotoxic, Th1, IFN-γ mediated, responses to HLA class I or II presented pathogen-specific epitopes. Our analysis suggests that, beyond pathogen-specific elimination of infected cells, alternatively polarized T-cell subpopulations like Th2, Th17 or T follicular could play an essential role in the orchestration of the immune response by promoting the development of pathogen specific humoral responses. The rational for widening the current knowledge about T-cell polarization is supported by the relative plasticity of T-cell polarization, which might open up opportunities for new immunotherapies against viral infections.

1. Innate cellular responses against SARS-CoV-2 and HIV infection

NK cells play a crucial role in antiviral immunity, a fact evidenced by the increased susceptibility to viral infections of individuals in whom NK cells are impaired or depleted[220–222]. Aside from surface molecules such as Fc-receptors, NK cells exert a large portion of their activity by detecting changes in HLA surface expression or in the HLA epitope repertoire, caused by viral gene expression inside the infected cell. The importance of NK cell-mediated defense mechanisms is strongly supported by the observation that some virus causing chronic infections, such as CMV[236], EBV[394] or HIV[264] have developed mechanisms to avoid such NK mediated cell lysis, including the reduction of HLA expression on infected cells, expressing epitopes mimicking human HLA canonical epitopes or influencing NK subset differentiation and its receptor repertoire[191,395]. Of all NK receptors, the interaction of NKG2 receptor family with HLA-E on the surface of target cells is especially interesting given the conserved nature of the HLA-E locus compared to classical HLA class I loci (HLA-A, B, or –C). This could make NK cell-mediated recognition of virally infected cells through HLA-E an antiviral mechanism that extends across all the human population, not restricted to individuals expressing a specific classical HLA class I

genotype. For these reasons, in the present study, we aimed to determine the relevance of NK cell activation by the HLA-E/NKG2X axis in the control of viral infections.

We studied this regulation in an acute infection setting with SARS-CoV-2, which is generally cleared after a short period of time, and compared this to a chronic infection like HIV, which is characterized by a long latency phase and for which only two cases of viral clearance have been reported[396,397]. Despite the differences in these viral agents, their rout of transmission and disease progression, we observed a number of interesting parallels in the HLA-E restricted NK cell response to infection.

First, HLA-E expression was increased in patients suffering from severe COVID-19 as well as in HIV non-controllers, both patient populations with less effective virus control. In the context of COVID-19, we evaluated whether the increased HLA-E expression reported in immune (e.g. lung macrophages) and epithelial cells[242,398] was also observed in PBMCs. We found a very significant increase of peripheral HLA-E expression in COVID-19 patients compared to uninfected individuals, which was especially heightened in patients with more severe forms of the disease. In addition, we observed a trend to an increased presence of plasma HLA-E in those patients, suggesting that HLA.E could be a soluble factor suppressing NK cell function. In the case of HIV infection, HLA-E expression was also augmented in non-controllers and showed a strong positive correlation with ineffective viral control, measured as plasma viral loads or as proviral DNA. Several pro-inflammatory cytokines have been related to severe COVID-19 and uncontrolled HIV infection , for instance IL-6[32] and IL-27[399], and could be driving up this increased HLA-E expression[400,401]. In fact, it has been demonstrated that IL-27 is capable of upregulating surface expression of HLA-E[401] and it is significantly increased in individuals with high HIV plasma viremia[402].

The limited polymorphism reported in the HLA-E locus compared to classical HLA-I loci (HLA-A, B or C) is especially interesting in the context of exploring a conserved NK-mediated antiviral mechanism through the HLA-E/NKG2X axis. Still, given some functional differences in the two main HLA-E alleles, it is important to control for HLA-E allelic differences, which was included in our studies when assessing the relationship between COVID-19 and HIV disease progression and NK cell activation. This aspect has been largely neglected in the past, probably due to the fact that the two main alleles, HLA-E*01:01 and *01:03, only differ in one amino acid. However, it is well known that such small differences can cause important functional differences. For instance, different HLA-B*58 alleles can result in opposite effects on HIV disease progression[385]. Furthermore, HLA-E*01:01 allele was described as a risk factor for COVID-19 severity[241], a finding

that our analyses did not corroborate. Probably the sample size of our cohorts was too small and may have reduced the power of the study to find significant associations between HLA-E genotype and COVID-19 outcome. In contrast, in HIV-1 infection, HLA-E heterozygosity (HLA-E*01:01/01:03) was significantly more common in individuals with naturally controlled HIV infection and with undetectable viral loads. Such an advantage of heterozygous HLA genetics against HIV infection has been described in the past for classical HLA class I alleles and for rare allele variants[403], but not for the less polymorphic HLA-E locus. This observation also suggests that the functional differences between the two alleles may be pronounced enough to provide heterozygous individuals an advantage to control HIV more effectively than HLA-E homozygous individuals.

Viral infections have been reported to induce profound changes in NK cell phenotype repertoire and function[404]. We observed a redistribution of circulating NK cell subtypes that could be related with disease progression and virus control in both infections. In particular, unconventional CD56^{neg} NK with a relatively unresponsive profile were expanded in severe COVID-19 patients, similarly to what has been seen in the context of chronic HIV-1, HCV, EBV or HCMV[192,405]. Correspondingly, circulating CD56^{bright} NK cells were reduced in patients with uncontrolled HIV-1 infection as well as in individuals suffering from more severe forms of COVID-19, in line with data reported by Maccourant et al.[239]. These findings attribute these cells a critical role in immune control of viral infection, which is also supported by data showing CD56^{bright} cells function to correlate negatively with HCV viremia and being associated with spontaneous clearance of HCV in HIV co-infected individuals[406,407]. The receptor repertoire of CD56^{bright} NK cells, which includes CCR7 and CD62L, allows them to migrate to tissues and secondary lymphoid organs[48], shaping the adaptive immune response by the crosstalk with both antigen presenting cells and T-cells[401,409,410]. Hence, the reduction of this specific NK cell subset in SARS-CoV-2 and HIV-1 infections could be partially explained by the infiltration of NK cells in tissues, in particular the accumulation of CD56^{bright} NK cells in lungs observed in COVID-19 patients with respiratory issues[398]. We also observed a reduction in the CD56^{dim} population in severe COVID-19 patients but not in the context of HIV-1. CD56^{dim} cells, contrary to CD56^{bright}, preferentially migrate to sites of inflammation[411]. COVID-19 severity and uncontrolled HIV-1 infection were also characterized by the expansion of differentiated adaptive NK cells (defined as CD56^{dim}CD16^{+}CD57^{+}) which also occurs after HCMV infection[191,412]. This had been previously reported in severe COVID-19[239], but to the best of our knowledge, not for chronic HIV infection.

Since the expression of the main receptors for HLA-E on NK cells, namely NKG2A and NKG2C, occurs at different stages of maturation and from our data also in a mutually exclusive manner, we determined the NKG2A/NKG2C ratios as formerly reported in HIV and HCMV coinfection[379]. We found a reversion of the NKG2A/NKG2C ratio in the total NK cell population when comparing severe COVID-19 patients and uninfected individuals. Assessing the different NK subpopulations individually, severe COVID-19 patients showed an increased NKG2C and reduced NKG2A expression in all NK subsets except CD56^{bright} cells. Remarkably, a reversion of the NKG2A/NKG2C ratio in the total NK cell population and the adaptive NK cells effectively differentiated between mild and severe COVID-19 patients. On the other hand, HIV infected individuals, especially those with high viral loads, also showed a switch of the NKG2A/NKG2C ratio, in line with previous studies[379]. This switch emerged especially from the expression levels of those receptors in CD56^{bright} and adaptive NK cells. To validate these observations in HIV infection, we extended our analyses to HIV uninfected individuals and found common patterns in NK cells subsets between HIV seronegative and HIV-low that differed from those in HIV-high individuals. These included the maintenance of NKG2A expressing CD56^{bright} NK cells and the reduction of the terminally differentiated NKG2C$^+$ adaptive NK cells compared to individuals with elevated viremia. Notably, we also observed a cluster of CD56^{dim}CD57^{bright}NKG2C$^+$ NK cells which was increased in PLWH compared to uninfected subjects, suggestive of a progressive increase of NKG2C$^+$ adaptive NK cells in advanced HIV disease.

Interestingly, we also observed a more exhausted phenotype on different NK cell subsets in severe COVID-19 patients. Especially, there was a significant increase of PD-1$^+$ total, CD56^{neg} and CD56^{bright} NK cells and a reduction of LAG-3$^+$ total NK cells. Although there are still some concerns regarding the surface characterization of exhausted NK cells[267], PD-1 expression showed a negative correlation with degranulation and cytotoxicity, whereas LAG-3 expression correlated positively with these effector functions. Exhaustion of the total NK cell fraction in COVID-19 has been reported previously[238] and therapies involving inhibition of PD-1 checkpoint in NK cells have been suggested[413]. Previous studies also pointed out an expansion of NKG2A$^+$ NK cells and reduced cytokine secretion, even though there was not a direct correlation between NKG2A expression and reduced IFN-γ production[414]. Although we did not measure potential NK cell exhaustion markers in the HIV infected cohort, NK cells of HIV infected individuals were less functional and showed changes in NKG2A/NKG2C ratios equivalent to those seen in COVID-19 infected samples. This suggests that NK cells of HIV infected individuals could also be exhausted and that this could be a common phenomenon in different viral infections.

In agreement with these previous results, NK cells from SARS-CoV-2 and HIV infected individuals showed a loss of activation capacity through HLA-E "missing self" as they were less activated when exposed to target cells lacking HLA-E. We observed a remarkable basal IFN-γ and TNF-α production in CD56^{bright} and adaptive NK cells from patients with severe COVID-19, in line with previous studies[239]. Nevertheless, this arming was not reflected in an increased capacity to respond to HLA-E null target cells as all SARS-CoV-2 infected individuals showed diminished degranulation and cytokine production, more pronounced in severe patients, in total NK cell, but especially in CD56^{bright}. The same pattern was found in NK cells from HIV infected individuals, which showed a loss of activation through HLA-E "missing self". Of note, the previously mentioned plasma factors IL-6 and IL-27[240,415], which may promote HLA-E expression, have also been associated with NK cell inhibition. This NK cell impairment also translated into a reduced capacity to kill target cells, which might be detrimental *in vivo* for the elimination of both SARS-CoV-2 and HIV infected cells. Of note, this killing impairment might protect hyperactivated macrophages from lysis, which represent the principal agent of the cytokine storm induction in COVID-19[416].

In order to elucidate the mechanism causing the impairment of the NK cell response, we performed correlation analysis between HLA-E expression, surface markers and functional response profiles. Remarkably, when evaluating the total NK cell fraction in COVID-19, both HLA-E and PD-1 expression showed a negative correlation with cytotoxic capacity and a positive correlation with NKG2C expression. As expected, cytotoxicity correlated positively with degranulation capacity within all studied NK cell subsets. CD56^{bright} was the subset with the strongest correlations with both high HLA-E and PD-1 expression, which impacted negatively on CD56^{bright} abundance and function.

Regarding HIV-1 infection, HLA-E expression correlated negatively with NKG2A/NKG2C ratio and NK cell function including cytotoxic capacity, degranulation and cytokine secretion. These findings were in line with those of Merino et al[417], who suggested that chronic *in vitro* stimulation of NK cells through the HLA-E/NKG2X axis, using plate-bound agonistic antibodies, promoted the expansion of adaptive NK cells expressing NKG2C and CD57. Interestingly, these cells presented an epigenetic reprogramming that caused an exhausted phenotype and a profound NK cell dysfunction. In other infections like HCMV, an epigenetic imprint modulates NK cell function and drives the expansion of mature, memory-like, NKG2C^{+}CD57^{+} NK cells[190,191]. This mechanism also could be relevant in the context of HIV infection, given that HIV is also a chronic infection, where NK cells might be exposed to a constant activation by HIV derived peptides

presented on HLA-E and recognized by NKG2C. Furthermore, epigenetic profiles have been identified in total PBMC that also support epigenetically dysregulated NK cell function and which related to *in vivo* HIV viral control[418].

For HIV infection we were able to develop an ex-vivo model of NK mediated inhibition of viral replication. Using this assay, we were capable of evaluating whether the role of HLA-E/NKG2X axis changed while HIV infection progressed. We observed a positive correlation between NK-mediated antiviral activity and HLA-E expression within the first seven days of culture. After fourteen days of culture however, NK mediated viral control was significantly reduced and the correlation with HLA-E expression was lost. We observed a shift towards NKG2C expression in HIV$_{BaL}$ infected cultures concomitant with a reduced NK killing activity in longer-term cultures. These results are in line with previous *in vitro* HIV studies, were the continuous stimulation through the HLA-E/NKG2X axis reduced NK functionality[417]. Importantly, the in vitro data directly support the *in vitro* observations and a scenario where elevated HLA-E expression in response to chronic HIV infection will drive a shift in the NKG2A/NKG2C balance on NK cells which eventually will hamper their ability to exert effective antiviral activity.

As HLA-E expression levels as well as signaling via NGK2X receptors can be influenced by the epitope-repertoire presented by HLA-E, we tested whether HIV-derived epitopes presented by HLA-E could affect NK cells activation, potentially by displacing the canonical VL9 epitope and thus leading to NK-mediated cell killing by the "missing-self" mechanism. We used single HLA-E transfected K562 cells, pulsed with canonical and non-canonical HIV-derived peptides competing with an endogenously expressed VL9-B7 epitope as NK target cells. Although the impact of HIV epitopes on HLA-E stabilization was low, we observed profound differences in the activation of NK cells in response to peptide-pulsed target cells. Interestingly, different HIV derived HLA-E epitopes triggered different effector functions such as cytotoxicity, degranulation and cytokine (IFN-γ and/or TNF-α) secretion in NK cells derived from HIV seronegative donors. Unfortunately, these analyses could not be repeated in NK cells from HIV infected individuals due to the high cell demand of the assays. They could also not be performed with SARS-CoV-2 derived HLA-E restricted epitopes, because none has been described so far. However, it will be interesting to perform them in the future, considering that previous studies showed the SARS-CoV-2 Spike-1 protein to negatively regulate NK cell activation through NKG2A recognition[242].

Finally, we have used structural models to evaluate the impact of the different HLA-E epitopes on NKG2X recognition of HLA-E, considering NKG2A/NKG2C receptor and HLA-E allele polymorphisms. Our analyses indicate that the amino acid differences between NKG2A and

NKG2C may influence the interaction with HLA-E alleles and the bound epitopes in different ways: (1) through the ASILP/SIISP motif on NGK2X that interacts with position P5 of the bound epitope and which could directly determine the affinity to the activator (NKG2C) or inhibitory (NKG2A) receptor to the HLA-E/epitope complex; (2) through Glu/Gly 197 residues that locates close to the presented epitopes, and (3) through Asp202 that interacts with Arg 108, located in close proximity to Arg107 and representing the only change between HLA-E*01:01 and *01:03. This may support the observation of the benefits of HLA-E heterozygosity in HIV control as heterozygous individuals might have a broader ability to present a wider range of epitopes and in consequence trigger differential NK responses. The expanded structural insights gained from these analyses may also explain the reported 6-fold lower affinity for the HLA-E-peptide complex to NKG2C compared to NKG2A [377] which may be the driver behind the observed switch from NKG2A to NKG2C expression, with its downstream functional consequences on NK-mediated antiviral activity.

Overall, our data give support to the existence of an NK cell immunosuppressive effect that may share common features in SARS-CoV-2 and HIV-1 infections: i) viral infection increase HLA-E expression levels; ii) continuously stimulating NK cells through the NKG2X receptors by pathogen-derived presented epitopes and ii) driving a change in NK subpopulations from CD56^{bright} towards phenotypes with impaired function (Fig.45). These changes appear to go hand in hand with a profound disruption of the regulation of the "missing-self" NK activation pathway through the HLA-E/NKG2X axis, which can be further influenced by changes in the HLA-E presented epitope repertoire. This scenario could be worsening the course of the infection as i) the lack of activation through HLA-E could lead to higher survival of infected cells and ii) killing of autologous activated T-cells depends on NKG2A regulation. Hence, the loss of this inhibitory receptor observed in severe COVID-19 patients and PLWH with high viremia could be associated with an indiscriminate elimination of effector cells and the consequent loss of orchestration of the immune response. This could be particularly relevant in the HIV context as the NK killing of autologous activated CD4^{+} T-cells, target cells for new infections, has been shown to be regulated through HLA-E sensing[185]. Our results are further supported by previous studies showing that NK cells from COVID-19 and HIV patients are in an unresponsiveness state. For instance, NK cells from COVID-19 patients were found to be exhausted[47,238], while NK cells from HIV-patients express transcriptomic signatures related to exhaustion markers[243], loss of surface NK cytotoxicity receptors expression[419] and a consequent reduction in cytolytic capacity, despite showing elevated levels of activation markers[420]. This dysfunctionality might contribute to the loss of HIV control, even after starting antiretroviral therapy for viral suppression[421].

Given their central role in immunosurveillance, understanding NK cell dynamics during viral infections and their link to disease course is essential in order to advance NK cell-based therapies. However, there still remain many gaps in our knowledge. For instance, the cause of the shifted abundance of CD56^{bright} and CD56^{dim} cells in peripheral blood observed in severe COVID-19 cases or in HIV non-controllers is still unclear. This could be of special interest in HIV infection since CD56^{bright} NK cells are the most abundant subset in lymphoid tissues, including lymph nodes[182]. Previous studies reported an accumulation of CXCR5^{+} NK cells within the follicle, one of the sanctuaries for HIV latent reservoir and was related to SHIV control[422]. In our unsupervised clustering analyses, the CD56^{bright} were also the only subtype that differentiated between mild and severe forms of COVID-19. The NK cell redistribution observed in COVID-19 and HIV-1 patients suggests that designing strategies to restore a healthy distribution of NK cell subpopulations could be beneficial. The blockade of PD-1/PD-1L and HLA-E/NKG2A checkpoints has been proposed as novel therapies for COVID-19[423] as they are related to NK cell impairment. Although NKG2A blockade has shown very promising results in tumor immunosurveillance[424], the differences in the HLA-E restricted immunopeptidome in infected cells might result in a different outcome in the context of viral infections. The increase of NKG2A expression might result in functional exhaustion of NK cells when self-peptides are presented and NK cell receive continuously an inhibitory input, but might trigger NK cell mediated response when the exposure to foreign peptides avoids NKG2A/CD94 engagement by HLA-E and consequently silences the blocking signal[266]. Thus, COVID-19 therapies involving blocking HLA-E/NKG2A axis should be designed not to trigger CD56^{bright} specific lysis of activated autologous T-cells within the lymph nodes and the consequent alteration in the orchestration of immune response against infected cells. Some NK cell-based therapies, such as enhancing antibody dependent cell cytotoxicity (ADCC)[67], enhancement of NK activity using TLR ligands[68,69] or the infusion of engineered NK cells expressing CAR receptors[50] have been proposed to treat HIV infection. Indeed, there are some reports indicating that NK cells function can be rescued with the addition of IL-15[425], at least *in vitro*, and that the exhausted transcriptomic signature observed in uncontrolled HIV infection can at least partly be restored after vaccination[243]. Harper et al. also demonstrated that IL-21 and IFN-α therapy rescued terminally differentiated NKG2X^{+} CD16^{+} NK cells in a pathogenic model of SIV progression and reduced the viral reservoir size[426]. This NK cell subpopulation is the simian homologue for the adaptive NKG2C^{+} CD16^{+} NK cell in the present study, thus directly supporting our findings.
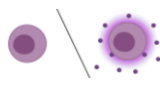
Although we did not have access to samples from clinical trials based on therapeutic vaccines against HIV, we demonstrated that COVID-19 vaccination also had a beneficial effect on the NK

cell mediated response. Vaccinated individuals that were never infected showed a redistribution of NK cell subsets with higher levels of active CD56^{dim} NK cells together with augmented levels of IFN-γ-producing CD56^{bright} cells, in line with previous post-vaccination studies[427]. Although Comirnaty (Pfizer/Biontech) and Spikevax (Moderna) were designed with chemical alterations in mRNA nucleotides to avoid detection of PAMPs[86], the lipid nanoparticle used for mRNA delivery has been reported to be proinflammatory[248] and NK cell activation might occur during CD4^{+} T-cell – NK cell crosstalk, as observed previously in protein subunit vaccines[246]. Remarkably, RNA persistence and expression after different routes of application through lipid nanoparticles appears to be below 10 days[428], supporting a more prolonged effect of vaccination on innate responses as our samples were taken approximately one month after the last injection. How long this effect could last is still an open question, but other authors reported some lasting effects six months after an heterologous viral-vectored vaccine regimen[244].

Additionally, vaccination might also be helpful to understand the role of exhaustion and HLA-E/NKG2X axis response in COVID-19. We showed that NK cell exhaustion and NKG2A diminution were associated with more severe forms of COVID-19. Vaccination led to lower levels PD-1 and higher levels of LAG-3 when compared to unvaccinated, uninfected, individuals. However, vaccination also reduced dramatically NKG2A expression as observed in severe patients. This dichotomy might suggest: i) NK cell exhaustion might be a risk for severe COVID-19, but might improve with vaccination, identifying a potential mechanism of prophylaxis against SARS-CoV-2 infection; and ii) the reduction of NKG2A expression observed in severe COVID-19 patients might be a consequence of the infection, since Spike-1-derived peptides, also expressed after vaccination, inhibit NK cell function allowing only NKG2A^{-} NK cells to proliferate[242]. Further studies are required in order to properly characterize the effect of COVID-19 vaccination on NK cell phenotype and function.

SARS-CoV-2 infection		HLA-E		HIV-1 infection
↑ expression in severe	qPCR		qPCR	↑ expression in non-controllers
↑ %sHLA-E⁺ in severe	Soluble		Soluble	n/d
=	Haplotype		Haplotype	↑ %heterozygosity in controllers with undetectable viral load
↑ % in severe	CD56ⁿᵉᵍ	NK cell populations	CD56ⁿᵉᵍ	=
↓ % in severe	CD56ᵇʳⁱᵍʰᵗ		CD56ᵇʳⁱᵍʰᵗ	↓ % in non-controllers
↓ % in severe	CD56ᵈⁱᵐ		CD56ᵈⁱᵐ	=
↑ % in severe	Adaptive		Adaptive	↑ % in non-controllers
↓ in severe		NKG2A/NKG2C ratio		↓ in non-controllers
Total NK cells, CD56ⁿᵉᵍ, CD56ᵈⁱᵐ, Adaptive				Total NK cells, CD56ᵇʳⁱᵍʰᵗ, Adaptive
↑ % in severe — Total NK cells, CD56ⁿᵉᵍ, CD56ᵇʳⁱᵍʰᵗ	PD-1	NK cell exhaustion/ativation	PD-1	n/d
↓ % in severe — Total NK cells	LAG-3		LAG-3	n/d
↓ % in severe — Total NK cells, CD56ⁿᵉᵍ, CD56ᵇʳⁱᵍʰᵗ, Adaptive	Degranulation	NK cell function	Degranulation	↓ % in non-controllers — CD56ᵇʳⁱᵍʰᵗ
↓ % in severe — Total NK cells, CD56ᵇʳⁱᵍʰᵗ	IFN-γ		IFN-γ	↓ % in non-controllers — Total NK cells, CD56ᵇʳⁱᵍʰᵗ, Adaptive
↓ % in severe — Total NK cells, CD56ⁿᵉᵍ, CD56ᵇʳⁱᵍʰᵗ, CD56ᵈⁱᵐ	TNF-α		TNF-α	↓ % in non-controllers — CD56ᵇʳⁱᵍʰᵗ, Adaptive
↓ % in severe	Cytotoxicity		Cytotoxicity	↓ % in non-controllers

Figure 45. Common features across the HLA-E/NKG2X regulation axis between uncontrolled SARS-CoV-2 and HIV infection.

157

2. Alternative effector functions against SARS-CoV-2 and HIV infection

Polarization of T-cell immunity has been suggested to play a role in virus control and relative abundance of specifically polarized T-cell populations have been used as a correlate of immunity. For instance, COVID-19 severity was linked to a disbalanced type 1/type 2 immune response and aberrant proportions of circulating Th2/Tc2 and Tc17 have been associated with poorer prognosis[324,325]. Aside from the original descriptions of Th1 and Th2 profiles in HIV infection[338,339], some previous studies found the Th17/Treg balance to influence HIV control as well [342,343]. However, little new insights have been gained on alternative polarization profiles and their impact on viral control and disease course[429]. Using a novel, *boosted* flow cytometry approach, we here analyzed alternative polarization profiles of virus-specific CD4$^+$ and CD8$^+$ T-cell subsets and determined their role in the response against viral infections. We identified differences in SARS-CoV-2 N-specific polarized CD4$^+$ T-cell responses that were associated with milder disease course. In parallel, we identified a HIV-specific CD8$^+$ Tfc-like cell subset in individuals with superior natural control of infection linked to the antibody isotype switching to IgG, higher plasma avidity and superior neutralization capacity and more potent ADCC activity. To the best of our knowledge, these data identify a novel link between a particular HIV-specific CD8$^+$ T-cell population and the humoral immunity to HIV, which may provide guidance for future vaccine development.

Our results also show that COVID-19 patients had high levels of basal T-cell activation in Th1 and Tc1 cells, reflecting a general inflamed state that was previously described by increased levels of type 1 cytokines, including IFN-γ[430]. Of note, this basal type 1 activation was not linked to COVID-19 severity and no differences were observed between mild and severe forms of the disease. We also identified other T-cell subsets that were activated in all COVID-19 patients in the absence of antigen recall, such as CD4$^+$ Tfh, CD8$^+$ Tc17 and Tregs (both CD4$^+$ and CD8$^+$ T-cells). These findings lend further support to previous studies indicating that increased levels of CD4$^+$ Tfh, Tregs and CD8$^+$ Tc17 are observed in COVID-19 patients[326,329,331] and that Th2 and Tc2 elevated basal activation can discriminate between severe and mild patients[324,325,431].

Boosted flow technology also allowed us to identify antigen-specific T-cell effector functions associated with improved immune control of SARS-CoV-2 and HIV. Type 1 CD4$^+$ and CD8$^+$ T-cell responses to SARS-CoV-2 and HIV have traditionally been the focus of cellular immune analyses, especially those mediated by cells producing IFN-γ[334,393]. However, IFN-γ production is only a part of the T-cell effector function profile and different cytokines are orchestrating various arms

of the host immunity. Yet, only few studies have analyzed CD4^{+} and CD8^{+} T-cell subsets beyond type 1 responses in relation to viral control[336]. To some degree, this may be due to the fact that these alternative subsets in some cases represent a small proportion of the virus-specific T-cell population in peripheral blood. In addition, these cells may not produce large amounts of individual, profile-defining cytokines, thus escaping detection by current standard intracellular staining flow cytometry-based assays. *Boosted flow* cytometry assay fills this critical gap by pooling multiple cytokine signals into the same detection channel, thus adding up individuals signals and raising the staining intensity above the limits of detection. This was original shown by our lab where *boosted flow* cytometry allowed for the detection of alternative effector functions in virus-specific T cells in HIV controllers and, importantly, in highly-exposed individuals that remained HIV negative[402,432].

Here, applying a *boosted flow* cytometry panel with improved coverage compared to the original design, allowed us to identify SARS-CoV-2 and HIV-specific T-cell responses beyond type 1 T-cells that would have been missed by single cytokine detection assays. We observed T-cell responses against N and S proteins and a pool of conserved epitopes among human coronaviruses in COVID-19 patients. Although both N and S protein-specific antibodies have been correlated with neutralizing activity against SARS-CoV-2, vaccine development has been focused on anti-S (and, more specifically, anti-RBD) IgG elicitation due to its stronger correlation with protection[433]. However, we observed more frequent and potent cellular responses to N protein that were more functionally diverse in mild COVID-19. In particular, mild COVID-19 patients were more frequently responsive to N protein by T-cells with a Th1, Th17 and Treg profiles than severe and NSC individuals. These responses were detected after 5 days of stimulations rather than in shorter time of incubations, indicating that they need more time to be recalled as expected, at least for Th17 responses. In addition, and in line with the observed higher basal signal, severe patients showed significantly increased N protein-specific Th2 and Tc2 responses compared to mild or NSC at 12h, reflecting the detrimental role of type 2 polarization in COVID-19 course[434]. Altogether our data suggest a benefit of including N-derived antigens in future generations of anti-SARS-CoV-2 vaccines in order to generate more protective responses. The use of N protein as antigen is also supported by more mechanistic reasons. The N protein is present at high copy numbers in the virion structure and needs to be produced by infected cells, increasing the chances that N protein derived epitopes are presented by them. Thus, vaccination with SARS-CoV-2 N protein should allow cytotoxic T-cells to detect and eliminate infected cells more rapidly. However, our data also indicate that N protein-specific cellular immune responses would have to be triggered with the right T-cell polarization. In that sense, the selection of the

most appropriate adjuvant to trigger anti-N protein type 1 and type 3 polarization, avoiding type 2 polarization could be very relevant.

Although previous studies reported a protective role of type 1 T-cell immunity against conserved human coronaviruses epitopes[435], we found that a sustained Tc1 response to these common epitopes after 5 days of stimulation was significantly associated with severe COVID-19. This could be driven by a reduction in CD8^{+} Treg responses to the Hu-CoV pool in severe patients. NSC, a group of patients composed of SARS-CoV-2 infected individuals with mild disease symptoms despite not producing IgM nor IgG against SARS-CoV-2, did not show any relevant T-cell response either. These results were quite surprising, because in the absence of neutralizing antibodies, T cells were expected to play an important role in controlling infection in these individuals. This suggests that other components of the immune response, beyond adaptive immunity, may play a crucial role in controlling SARS-CoV-2 infection in NSC. Our data on the NK response in mild and severe COVID-19 patients suggest NK cells could mediate such responses and be important players in the control of SARS-CoV-2 infection control. Nevertheless, the low T-cell responses we observed in NSC suggest that the lack of antibody responses in those individuals could be caused by a lack of T helper support, but still does not fully explain that these individuals showed a relatively mild disease course. It is also possible that these individuals were infected by virus mutants with lower replication capacity. This has not been observed in SARS-CoV-2 infection, but it has been reported for HIV[436].

We also identified alternative effector functions in the context of HIV that were related to natural control of the infection. Among them, CD4^{+} Tfh, CD8^{+} Tc2 and, especially, Tfc-like responses were more frequent and showed greater magnitude and breadth in individuals with natural control of HIV infection. Of these subsets, CD8^{+} Tfc-like responses showed particularly strong associations with parameters of virus control and correlated directly with markers of a more efficacious humoral immune responses to HIV. These responses were detected by boosted flow cytometry, but not when detecting IL-4 and IL-21 in separate channels by conventional ICS (data not shown). Similarly, few IL-4 or IL-21 secreting T-cells were identified by single cytokine ELISpot, unless the detection of both cytokines was combined in the assay. Of note, polyfunctional analysis showed that most of the pool-specific responses showed a single polarization profile, indicating that mixed T-cell polarization profiles may be infrequent[293]. CD8^{+} Tfc have just recently been identified and share characteristics with both CD4^{+} Tfc and CD8^{+} Tc1 cells. As CD4^{+} Tfh-like T-cells, they maintain a self-renewal phenotype and the ability to promote B-cell maturation and isotype class switching. This, in addition to their cytotoxic activity and ability to migrate to the follicles, support the potential importance of CD8^{+} Tfc in controlling HIV

replication and reducing viral reservoir[319], which may be of significant interest for HIV immunotherapeutic strategies.

Finally, the present data indicate that viral proteins trigger different polarization profiles and that these protein-specific T-cell subsets can be related to viral control, as it has been described for Tc1 and Th1 responses to HIV[382–384]. In line with these results, we observed an increase in CD4^{+} Th1-like responses to Env in HIV^{+} non-controllers, while controllers had stronger CD8^{+} Tc1-like responses to Gag. Additionally, CD8^{+} Tfc responses of higher magnitude to HIV Pol and Env were observed in controllers. A similar observation had already been reported for CD4^{+} Tfh responses, which showed a different protein specificity compared to the classical CD4^{+} Th1-like cells. As shown in previous studies, we observed that CD4^{+} Tfh-like cells are preferentially linked to responses against Gag over Env[349]. Here, we also show that accessory proteins were mainly targeted by Th2 polarized CD8^{+} T-cell subsets, which usually secrete lower cytokine levels and could be largely missed when using standard intracellular cytokine staining. Peptide HLA binding affinity, protein expression kinetics, protein levels and antigen processing preferences have been proposed as potential mechanisms for these different polarization profiles triggered by different HIV proteins[386].

Analysis of the surface expression of CCR7 and CD45RA memory markers revealed differences related to disease course. The loss of $T_{Naïve}$ cells associated with age has been proposed as one of the risk factors for developing severe COVID-19, due to the inability of the T-cell repertoire to fight against new infections in elder people[437]. We could not identify any correlation with age in our study cohort, possibly due to low statistical power. However, severe patients showed a profound loss of both CD4^{+} and CD8^{+} $T_{Naïve}$ cells. On the opposite, NSC showed well-preserved $T_{Naïve}$ cell populations, indicating that the lack of T-cell responses was not due to a depletion of these cells. In the context of HIV- infection, a more abundant HIV-specific T-cell populations allowed us to evaluate memory phenotypes in Th1/Tc1, Th2/Tc2 and Tfh/Tfc polarized T cells. In particular, Th2 and Tfh showed increased T_{EM} (CD45RA^{-} CCR7^{-}) subpopulations and decreased T_{Naive} (CD45RA^{+} CCR7^{+}) compared to Th1 polarized CD4^{+} T cells. Also, an increased percentage of CD4^{+} T_{Naive} cells with a Th2 profile in HIV^{+} non-controllers, along with a significant reduction of T_{EM} in CD4^{+} Th2 and CD8^{+} Tc2, was observed, indicating a higher capacity to express type 2 cytokines in HIV controllers. These results suggest that, although T_{EM} Th2 and Tc2 populations persist long term *in vivo* and have been associated with severe asthma[438,439], their role in chronic HIV infection might be beneficial as their presence is associated with viral control.

Interestingly, we could associate virus-specific follicular CD4^{+} and CD8^{+} T-cell responses with virus-specific antibody-mediated immunity. In the case of SARS-CoV-2, severe patients had the

highest neutralizing capacity against SARS-CoV-2 pseudoviruses and this was strongly correlated with N protein specific CD4^{+} Tfh-like responses and, to a lesser extent, CD8^{+} Tfc-like responses. This additionally indicates that the viral N protein could be a suitable vaccine antigen since, beyond triggering effector T cell responses, it would generate Tfh responses to develop and mature antibody responses.

However, the more striking associations between T follicular cells and antibody responses was observed in HIV infection. The strong association between CD8^{+} Tfc cells and HIV control prompted us to further characterize this populations and the define the role of their CD4+ Tfh counterparts in antibody maturation. CXCR5^{+} CD8^{+} T-cells have been described as a major source of IL-21 and have been shown to be related to lower HIV viral loads[440]. Here, we observed indeed higher numbers of HIV-specific CD8^{+} Tfc-like responses in controllers and an increased innate IL-21 and IL-4 secretion in total PBMCs, together with a higher proportion of circulating CD8^{+} Tfc (CXCR5^{+}PD-1^{+}ICOS^{+}) in individuals showing Tfc-like responses. Our unsupervised analysis of circulating Th2/Tc2 and Tfh/Tfc populations also revealed a higher proportion of peripheral CD4^{+} CXCR5^{+} PD-1^{+} ICOS^{+} cells in non-controllers, as suggested by previous studies[352]. We also observed more prominent CXCR5^{+} CD4^{+} and CD8^{+} T-cell populations in non-controllers that lacked the expression of ICOS or/and PD-1. Since these surface proteins are important for the interaction with B-cells, the reduced expression may explain the limited antibody isotype class switching and maturation in these individuals[318]. This fact might represent an innate predisposition to generate CD8^{+} Tfc responses upon HIV infection in some individuals, with potential consequences on antibody isotype switching and viral control. Indeed, HIV^{+} non-controllers showed differences in the anti-Env antibody response characterized by a reduction in IgG and an increase in IgM isotype use. This fact was in line with reduced antibody switching to IgG and diminished avidity in HIV[+] non-controllers compared to controllers, estimated as the IgG/IgM and IgG/IgA ratios and avidity index, respectively. Chronic HIV infection has been associated with the dysregulation of the germinal center reaction, compromising the generation of memory B-cells[441]. Thus, the presence of higher levels of reactive Tfc-like cells could reflect a better-preserved germinal center interaction in individuals with natural control of HIV infection[442,443]. However, peripheral blood Tfc-like responses may not properly reflect germinal center interaction and partially explain the lack of correlation between avidity and Tfc or Tfh-like responses against HIV[389].

The strong relationship between IgG/IgM and IgG/IgA ratios in plasma and CD8^{+} Tfc-like cells supports a role of this specific subset in the maturation of the antibody response. Furthermore,

humoral effector functions, determined as the neutralization capacity and ADCC activity, were more robust among HIV controllers and correlated with isotype class switching to IgG. Neutralization and ADCC capacity correlated with each other and with the IgG/IgM ratios and IgG avidity, in line with previous studies[444,445]. Interestingly, the neutralization capacity was also related to IgA/IgM titers. Mucosal IgA has been reported to neutralize HIV[155], but the role of this isotype in plasma has been less explored, although some studies reported a correlation between serum IgA titers and neutralization capacity[446].

Thanks to the extensive coverage of different effector functions, their detection by accumulating signals using the boosted flow cytometry was critical to identify effector T-cell responses associated with better prognosis after SARS-CoV-2 and HIV infection. As expected, the presence of CD4+ Tfh responses was associated with higher SARS-CoV-2 neutralization capacity. For HIV-1, the integration of alternative T-cells with antibody isotype class switching to IgG and the associated humoral responses analysis highlighted the link between Tfc responses and clinical course of HIV infection. The presence of these cells was associated with lower viral load and preferential antibody isotype class switching to IgG, which are associated with increased neutralizing and ADCC activity. IgM titers were observed to be detrimental and are related not only to higher plasma viremia, but also with the loss of CD4$^+$ T-cells. The identification of diverse virus-specific T-cell responses, especially also CD8$^+$ T-cell subsets that can orchestrate the humoral responses and can infiltrate tissues of viral reservoir is of potential interest for vaccine development. Leveraging the potential plasticity of polarized T-cell populations, may also open the door for future therapeutic interventions as has been suggested with strategies aiming to improve anti-cancer immunity[447].

Figure 46. Common features in alternative effector T-cell immunity in SARS-CoV-2 and HIV infection

CONCLUDING REMARKS
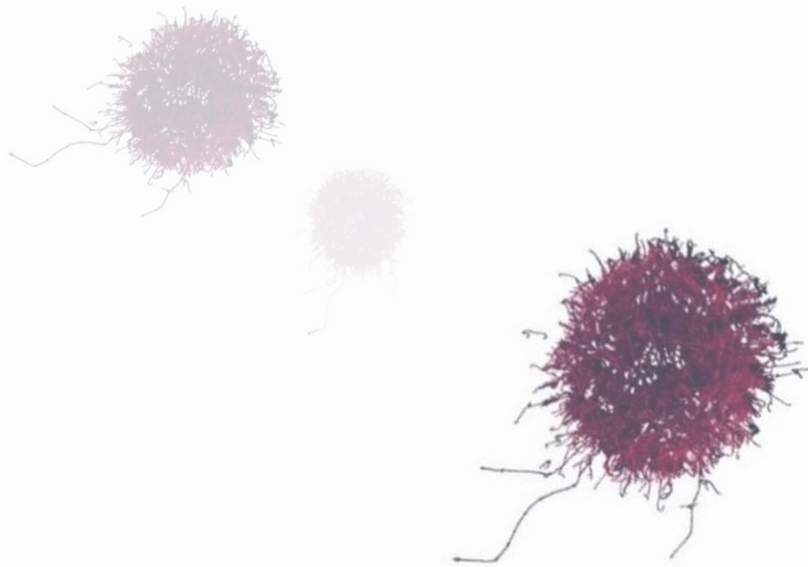
1. Increased HLA-E expression on PBMCs is associated with COVID-19 severity and higher HIV viremia, pointing towards a common mechanism of loss of NK-cell mediated immunosurveillance in viral infections. HLA-E expression correlated negatively with NK cell cytotoxic capacity, degranulation and cytokine production and is one of the mechanisms driving NK cell exhaustion,.

2. An inverted NKG2A/NKG2C ratio was observed in severe COVID-19 patients and individuals with higher HIV viremia. The lower affinity of NKG2C to HLA-E compared to NKG2A indicated a loss of NK cell regulation through HLA-E/NKG2X axis in uncontrolled viral infections.

3. SARS-CoV-2 and HIV infections were associated with profound changes within the NK cell subset distribution. COVID-19 severity and higher HIV viremia were both linked to a loss of CD56^{bright} and increased numbers of adaptive NK cells, suggesting a shared mechanism of altering NK immunosurveillance.

4. LAG-3 worked as a marker of NK cell activation in our hands, especially given its positive correlation with NK cell effector functions. NK cell exhaustion, reflected as increased PD-1 and decreased LAG-3 expression, was associated with COVID-19 severity and correlated negatively with NK effector functions.

5. The structural differences between HLA-E*01:01 and HLA-E*01:03 explained differences in epitope repertoire and the interaction with NKG2A and NKG2C receptors. HLA-E heterozygosis was associated with increased number of individuals with undetectable viral loads among the HIV controllers.

6. HIV derived peptides presented on HLA-E were detected by NK cells and alter NK cell effector functions when compared to the canonical self-antigen HLA-B7 VL9.

7. HLA-E expression correlated positively with short-term NK cell control of HIV viral growth in an in vitro model of acute infection, suggesting an initial role of NK in HIV control. However, this control was lost in long-term assays, suggesting a failure of NK control after a long exposure to infected cells.

8. The increased sensitivity of boosted flow technology allowed the detection of T-cells with alternative effector functions that would have been missed otherwise. Beyond the classical Th1/Tc1 antiviral phenotype, we identified Th2/Tc2, Th17/Tc17, Treg and Tfh/Tfc responses to HIV and SARS-CoV-2.

9. COVID-19 was associated with an increased basal activation of CD4^{+} Th1, Treg and Tfh and CD8^{+} Tc1, Tc17 and Treg cells. Severity of the disease was linked to higher levels of CD4^{+} Th2 and CD8^{+} signals basal activation at diagnosis.

10. T-cell responses to SARS-CoV-2 Nucleocapsid protein were more frequent and stronger than responses directed to the Spike protein. CD4^{+} Th1, Th17 and Treg responses to Nucleocapsid protein differentiate among mild, severe and non-seroconvertors COVID-19 patients. Severe COVID-19 patients showed potent and fast CD4^{+} Th2 and CD8^{+} Tc2 mediated recall *in vitro* to Nucleocapsid protein when compared to mild or non-seroconvertors.

11. Distribution of T-cell memory populations was different among COVID-19 groups of patients and a selective loss of $T_{Naïve}$ CD4^{+} and CD8^{+} T-cells was observed in severe patients.

12. The magnitude of SARS-CoV-2 Nucleopcapsid-specific CD4^{+} Tfh-like responses were correlated to a higher neutralizing capacity of the plasma.

13. The CD8+ Tfc-like T-cell response was a component of effective HIV control and was related to antibody isotype switching to IgG. This favorable balance towards IgG responses positively correlated with increased virus neutralization, higher avidity of neutralizing antibodies and more potent antibody-dependent cell cytotoxicity (ADCC) in PBMCs from HIV controllers compared to non-controllers.

REFERENCES
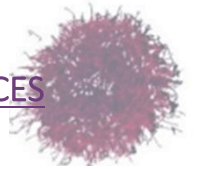
1. Holmes, E. C. *et al.* The origins of SARS-CoV-2: A critical review. *Cell* vol. 184 (2021).

2. WHO Coronavirus (COVID-19) Dashboard | WHO Coronavirus (COVID-19) Dashboard With Vaccination Data.

3. Gorbalenya, A. E. *et al.* The species Severe acute respiratory syndrome-related coronavirus: classifying 2019-nCoV and naming it SARS-CoV-2. *Nature Microbiology* vol. 5 (2020).

4. Coronaviridae - Positive Sense RNA Viruses - Positive Sense RNA Viruses (2011) - ICTV.

5. Callaway, E. The mutation that helps Delta spread like wildfire. *Nature* vol. 596 (2021).

6. Fei, Y., Tsoi, M. F. & Cheung, B. M. Y. Cardiovascular outcomes in trials of new antidiabetic drug classes: A network meta-analysis. *Cardiovasc. Diabetol.* **18**, (2019).

7. Johnson, B. A. *et al.* Furin Cleavage Site Is Key to SARS-CoV-2 Pathogenesis. *bioRxiv Prepr. Serv. Biol.* (2020) doi:10.1101/2020.08.26.268854.

8. Kim, D. *et al.* The Architecture of SARS-CoV-2 Transcriptome. *Cell* **181**, (2020).

9. Huang, C. *et al.* SARS coronavirus nsp1 protein induces template-dependent endonucleolytic cleavage of mRNAs: Viral mRNAs are resistant to nsp1-induced RNA cleavage. *PLoS Pathog.* **7**, (2011).

10. Hackbart, M., Deng, X. & Baker, S. C. Coronavirus endoribonuclease targets viral polyuridine sequences to evade activating host sensors. *Proc. Natl. Acad. Sci. U. S. A.* **117**, (2020).

11. Yoshimoto, F. K. The Proteins of Severe Acute Respiratory Syndrome Coronavirus-2 (SARS CoV-2 or n-COV19), the Cause of COVID-19. *Protein Journal* vol. 39 (2020).

12. Pancer, K. *et al.* The SARS-CoV-2 ORF10 is not essential in vitro or in vivo in humans. *PLoS Pathog.* **16**, (2020).

13. Gómez, S. A. *et al.* Binding of SARS-CoV-2 to Cell Receptors: A Tale of Molecular Evolution. *ChemBioChem* **22**, (2021).

14. Hardenbrook, N. J. & Zhang, P. A structural view of the SARS-CoV-2 virus and its

assembly. *Current Opinion in Virology* vol. 52 (2022).

15. Yao, H. *et al.* Molecular Architecture of the SARS-CoV-2 Virus. *Cell* **183**, (2020).

16. Poland, G. A., Ovsyannikova, I. G. & Kennedy, R. B. SARS-CoV-2 immunity: review and applications to phase 3 vaccine candidates. *The Lancet* vol. 396 (2020).

17. V'kovski, P., Kratzel, A., Steiner, S., Stalder, H. & Thiel, V. Coronavirus biology and replication: implications for SARS-CoV-2. *Nature Reviews Microbiology* vol. 19 (2021).

18. Hoffmann, M. *et al.* SARS-CoV-2 Cell Entry Depends on ACE2 and TMPRSS2 and Is Blocked by a Clinically Proven Protease Inhibitor. *Cell* **181**, (2020).

19. Zhang, Q. *et al.* Molecular mechanism of interaction between SARS-CoV-2 and host cells and interventional therapy. *Signal Transduction and Targeted Therapy* vol. 6 (2021).

20. Snijder, E. J., Decroly, E. & Ziebuhr, J. The Nonstructural Proteins Directing Coronavirus RNA Synthesis and Processing. *Advances in Virus Research* vol. 96 (2016).

21. Sawicki, S. G. & Sawicki, D. L. Coronaviruses use discontinuous extension for synthesis of subgenome-length negative strands. *Advances in experimental medicine and biology* vol. 380 (1995).

22. Ghosh, S. *et al.* β-Coronaviruses Use Lysosomes for Egress Instead of the Biosynthetic Secretory Pathway. *Cell* **183**, (2020).

23. Harrison, A. G., Lin, T. & Wang, P. Mechanisms of SARS-CoV-2 Transmission and Pathogenesis. *Trends in Immunology* vol. 41 (2020).

24. Salamanna, F., Maglio, M., Landini, M. P. & Fini, M. Body Localization of ACE-2: On the Trail of the Keyhole of SARS-CoV-2. *Frontiers in Medicine* vol. 7 (2020).

25. Hikmet, F. *et al.* The protein expression profile of ACE2 in human tissues. *Mol. Syst. Biol.* **16**, (2020).

26. Clinical Spectrum | COVID-19 Treatment Guidelines.

27. Yang, L. *et al.* The signal pathways and treatment of cytokine storm in COVID-19. *Signal Transduction and Targeted Therapy* vol. 6 (2021).

28. Wang, F. *et al.* Characteristics of peripheral lymphocyte subset alteration in covid-19 pneumonia. *J. Infect. Dis.* **221**, (2020).

29. Fan, B. E. *et al.* Hematologic parameters in patients with COVID-19 infection. *American Journal of Hematology* vol. 95 (2020).

30. Xu, Y. *et al.* Clinical Characteristics of SARS-CoV-2 Pneumonia Compared to Controls in Chinese Han Population. doi:10.1101/2020.03.08.20031658.

31. Varchetta, S. *et al.* Unique immunological profile in patients with COVID-19. *Cell. Mol. Immunol.* **18**, (2021).

32. Diao, B. *et al.* Reduction and Functional Exhaustion of T Cells in Patients With Coronavirus Disease 2019 (COVID-19). *Front. Immunol.* **11**, (2020).

33. Mazzoni, A. *et al.* Impaired immune cell cytotoxicity in severe COVID-19 is IL-6 dependent. *J. Clin. Invest.* **130**, (2020).

34. Romera-Liebana, L. *et al.* Down-regulated gene expression spectrum and immune responses changed during the disease progression in COVID-19 patients. *Clin. Infect. Dis.* (2020).

35. Middleton, E. A. *et al.* Neutrophil extracellular traps contribute to immunothrombosis in COVID-19 acute respiratory distress syndrome. *Blood* **136**, (2020).

36. Xia, H. *et al.* Evasion of Type I Interferon by SARS-CoV-2. *Cell Rep.* **33**, (2020).

37. Abul K, A. M., Andrew H. Lichtman MD, P. & Shiv Pillai MBBS, P. *ABBAS Celular and Molecular Immunology . Procedia Engineering* vol. 9 (2015).

38. Yang, D. *et al.* Attenuated interferon and proinflammatory response in SARS-CoV-2-infected human dendritic cells is associated with viral antagonism of STAT1 phosphorylation. *J. Infect. Dis.* **222**, (2020).

39. Spinetti, T. *et al.* Reduced Monocytic Human Leukocyte Antigen-DR Expression Indicates Immunosuppression in Critically Ill COVID-19 Patients. *Anesth. Analg.* (2020) doi:10.1213/ANE.0000000000005044.

References

40.   Falck-Jones, S. *et al.* Functional monocytic myeloid-derived suppressor cells increase in blood but not airways and predict COVID-19 severity. *J. Clin. Invest.* **131**, (2021).

41.   Khanmohammadi, S. & Rezaei, N. Role of Toll-like receptors in the pathogenesis of COVID-19. *Journal of Medical Virology* vol. 93 (2021).

42.   Onomoto, K., Onoguchi, K. & Yoneyama, M. Regulation of RIG-I-like receptor-mediated signaling: interaction between host and viral factors. *Cellular and Molecular Immunology* vol. 18 (2021).

43.   Sarohan, A. R. *et al.* A novel hypothesis for COVID-19 pathogenesis: Retinol depletion and retinoid signaling disorder. *Cell. Signal.* **87**, (2021).

44.   Chen, R. *et al.* Cytokine Storm: The Primary Determinant for the Pathophysiological Evolution of COVID-19 Deterioration. *Front. Immunol.* **12**, 1409 (2021).

45.   Ragab, D., Salah Eldin, H., Taeimah, M., Khattab, R. & Salem, R. The COVID-19 Cytokine Storm; What We Know So Far. *Front. Immunol.* **11**, 1446 (2020).

46.   Chen, J. *et al.* Cellular Immune Responses to Severe Acute Respiratory Syndrome Coronavirus (SARS-CoV) Infection in Senescent BALB/c Mice: CD4 + T Cells Are Important in Control of SARS-CoV Infection . *J. Virol.* **84**, (2010).

47.   Huang, C. *et al.* Clinical features of patients infected with 2019 novel coronavirus in Wuhan, China. *Lancet* **395**, (2020).

48.   Wölfel, R. *et al.* Virological assessment of hospitalized patients with COVID-2019. *Nature* **581**, (2020).

49.   Batah, S. S. & Fabro, A. T. Pulmonary pathology of ARDS in COVID-19: A pathological review for clinicians. *Respiratory Medicine* vol. 176 (2021).

50.   Ye, Q., Wang, B. & Mao, J. The pathogenesis and treatment of the `Cytokine Storm' in COVID-19. *J. Infect.* **80**, 607 (2020).

51.   Lopes-Pacheco, M. *et al.* Pathogenesis of Multiple Organ Injury in COVID-19 and Potential Therapeutic Strategies. *Frontiers in Physiology* vol. 12 (2021).

52. Gupta, A. *et al.* Extrapulmonary manifestations of COVID-19. *Nature Medicine* vol. 26 (2020).

53. Guo, T. *et al.* Cardiovascular Implications of Fatal Outcomes of Patients with Coronavirus Disease 2019 (COVID-19). *JAMA Cardiol.* **5**, (2020).

54. Mondello, C. *et al.* Pathological Findings in COVID-19 as a Tool to Define SARS-CoV-2 Pathogenesis. A Systematic Review. *Frontiers in Pharmacology* vol. 12 (2021).

55. Zhang, C., Shi, L. & Wang, F. S. Liver injury in COVID-19: management and challenges. *The Lancet Gastroenterology and Hepatology* vol. 5 (2020).

56. Wang, M., Xiong, H., Chen, H., Li, Q. & Ruan, X. Z. Renal Injury by SARS-CoV-2 Infection: A Systematic Review. *Kidney Dis.* (2020) doi:10.1159/000512683.

57. Gavriatopoulou, M. *et al.* Organ-specific manifestations of COVID-19 infection. *Clinical and Experimental Medicine* vol. 20 (2020).

58. Fernández-Castañeda, A. *et al.* Mild respiratory SARS-CoV-2 infection can cause multi-lineage cellular dysregulation and myelin loss in the brain. *bioRxiv* (2022) doi:10.1101/2022.01.07.475453.

59. Levi, M., Thachil, J., Iba, T. & Levy, J. H. Coagulation abnormalities and thrombosis in patients with COVID-19. *Lancet. Haematol.* **7**, e438 (2020).

60. Tang, N., Li, D., Wang, X. & Sun, Z. Abnormal coagulation parameters are associated with poor prognosis in patients with novel coronavirus pneumonia. *J. Thromb. Haemost.* **18**, 844–847 (2020).

61. Ramakrishnan, R. K., Kashour, T., Hamid, Q., Halwani, R. & Tleyjeh, I. M. Unraveling the Mystery Surrounding Post-Acute Sequelae of COVID-19. *Frontiers in Immunology* vol. 12 (2021).

62. Yong, S. J. Persistent Brainstem Dysfunction in Long-COVID: A Hypothesis. *ACS Chemical Neuroscience* vol. 12 (2021).

63. Huang, C. *et al.* 6-month consequences of COVID-19 in patients discharged from hospital: a cohort study. *Lancet* **397**, 220–232 (2021).

64. Malkova, A. *et al.* Post covid-19 syndrome in patients with asymptomatic/mild form. *Pathogens* vol. 10 (2021).

65. Kalkeri, R., Goebel, S. & Sharma, G. D. SARS-CoV-2 shedding from asymptomatic patients: Contribution of potential extrapulmonary tissue reservoirs. *American Journal of Tropical Medicine and Hygiene* vol. 103 (2020).

66. Wang, E. Y. *et al.* Diverse functional autoantibodies in patients with COVID-19. *Nature* **595**, (2021).

67. Singh, K. K., Chaubey, G., Chen, J. Y. & Suravajhala, P. Decoding sars-cov-2 hijacking of host mitochondria in covid-19 pathogenesis. *American Journal of Physiology - Cell Physiology* vol. 319 (2020).

68. Armstrong, C. W., McGregor, N. R., Butt, H. L. & Gooley, P. R. Metabolism in chronic fatigue syndrome. *Advances in Clinical Chemistry* vol. 66 (2014).

69. Diamond, M. S. & Kanneganti, T. D. Innate immunity: the first line of defense against SARS-CoV-2. *Nature Immunology* vol. 23 (2022).

70. BURKE, J. M., ST CLAIR, L. A., PERERA, R. & PARKER, R. SARS-CoV-2 infection triggers widespread host mRNA decay leading to an mRNA export block. *RNA* **27**, (2021).

71. Grifoni, A. *et al.* SARS-CoV-2 human T cell epitopes: Adaptive immune response against COVID-19. *Cell Host and Microbe* vol. 29 (2021).

72. Carsetti, R. *et al.* Different Innate and Adaptive Immune Responses to SARS-CoV-2 Infection of Asymptomatic, Mild, and Severe Cases. *Front. Immunol.* **11**, (2020).

73. Chvatal-Medina, M., Mendez-Cortina, Y., Patiño, P. J., Velilla, P. A. & Rugeles, M. T. Antibody Responses in COVID-19: A Review. *Frontiers in Immunology* vol. 12 (2021).

74. Trinité, B. *et al.* SARS-CoV-2 infection elicits a rapid neutralizing antibody response that correlates with disease severity. *Sci. Rep.* **11**, (2021).

75. Sekine, T. *et al.* Robust T Cell Immunity in Convalescent Individuals with Asymptomatic or Mild COVID-19. *Cell* **183**, (2020).

76.   Kilpeläinen, A. *et al.* Highly functional Cellular Immunity in SARS-CoV-2 Non-Seroconvertors is associated with immune protection. *bioRxiv* 2021.05.04.438781 (2021) doi:10.1101/2021.05.04.438781.

77.   Kudlay, D. & Svistunov, A. COVID-19 Vaccines: An Overview of Different Platforms. *Bioeng. (Basel, Switzerland)* **9**, (2022).

78.   Park, K. S., Sun, X., Aikins, M. E. & Moon, J. J. Non-viral COVID-19 vaccine delivery systems. *Adv. Drug Deliv. Rev.* **169**, 137–151 (2021).

79.   COVID-19 vaccine tracker and landscape.

80.   Darnell, M. E. R., Subbarao, K., Feinstone, S. M. & Taylor, D. R. Inactivation of the coronavirus that induces severe acute respiratory syndrome, SARS-CoV. *J. Virol. Methods* **121**, 85–91 (2004).

81.   Ura, T. *et al.* Designed recombinant adenovirus type 5 vector induced envelope-specific CD8+ cytotoxic T lymphocytes and cross-reactive neutralizing antibodies against human immunodeficiency virus type 1. *J. Gene Med.* **11**, (2009).

82.   Keech, C. *et al.* Phase 1–2 Trial of a SARS-CoV-2 Recombinant Spike Protein Nanoparticle Vaccine. *N. Engl. J. Med.* **383**, (2020).

83.   Fathizadeh, H. *et al.* SARS-CoV-2 (Covid-19) vaccines structure, mechanisms and effectiveness: A review. *International Journal of Biological Macromolecules* vol. 188 (2021).

84.   Tariq, H., Batool, S., Asif, S., Ali, M. & Abbasi, B. H. Virus-Like Particles: Revolutionary Platforms for Developing Vaccines Against Emerging Infectious Diseases. *Front. Microbiol.* **12**, 4137 (2022).

85.   Huang, Q., Zeng, J. & Yan, J. COVID-19 mRNA vaccines. *Journal of Genetics and Genomics* vol. 48 (2021).

86.   Heinz, F. X. & Stiasny, K. Distinguishing features of current COVID-19 vaccines: knowns and unknowns of antigen presentation and modes of action. *npj Vaccines* vol. 6 (2021).

87.   Yang Lee, L. Y., Izzard, L. & Hurt, A. C. A review of DNA vaccines against influenza. *Front.*

Immunol. **9**, 1568 (2018).

88.   Zhao, Y. *et al.* The global transmission of new coronavirus variants. *Environ. Res.* **206**,
        (2022).

89.   Soriano, B., Krupovic, M. & Llorens, C. ICTV virus taxonomy profile: Belpaoviridae 2021.
        J. Gen. Virol. **102**, (2021).

90.   Kaposi's Sarcoma and Pneumocystis Pneumonia Among Homosexual Men-New York
        City and California Source: Morbidity and Mortality Weekly Report.

91.   Barré-Sinoussi, F. *et al.* Isolation of a T-lymphotropic retrovirus from a patient at risk for
        acquired immune deficiency syndrome (AIDS). *Science (80-.).* **220**, (1983).

92.   Gallo, R. C. *et al.* Isolation of human T-cell leukemia virus in acquired immune deficiency
        syndrome (AIDS). *Science (80-.).* **220**, (1983).

93.   Sharp, P. M. *et al.* Origins and evolution of AIDS viruses: estimating the time-scale.
        Biochem. Soc. Trans. **28**, 275–282 (2000).

94.   Gao, F. *et al.* Origin of HIV-1 in the chimpanzee Pan troglodytes troglodytes. *Nat. 1999
        3976718* **397**, 436–441 (1999).

95.   Nyamweya, S. *et al.* Comparing HIV-1 and HIV-2 infection: Lessons for viral
        immunopathogenesis. *Reviews in Medical Virology* vol. 23 (2013).

96.   Whittle, H. *et al.* HIV-2-infected patients survive longer than HIV-1-infected patients.
        AIDS **8**, (1994).

97.   Eberle, J. & Gürtler, L. HIV types, groups, subtypes and recombinant forms: Errors in
        replication, selection pressure and quasispecies. *Intervirology* **55**, (2012).

98.   Global HIV & AIDS statistics — Fact sheet | UNAIDS.

99.   Ratner, L. *et al.* Complete nucleotide sequence of the AIDS virus, HTLV-III. *Nature* **313**,
        (1985).

100.   Frankel, A. D. & Young, J. A. T. HIV-1: Fifteen proteins and an RNA. *Annual Review of
        Biochemistry* vol. 67 (1998).

101. Sanchez-Pescador, R. *et al.* Nucleotide sequence and expression of an AIDS-associated retrovirus (ARV-2). *Science* **227**, 484–492 (1985).

102. Rabson, A. B. & Martin, M. A. Molecular organization of the AIDS retrovirus. *Cell* **40**, 477–480 (1985).

103. Fernandes, J. D. *et al.* Functional Segregation of Overlapping Genes in HIV. *Cell* **167**, (2016).

104. Mashiba, M. & Collins, K. L. Molecular mechanisms of HIV immune evasion of the innate immune response in myeloid cells. *Viruses* **5**, 1–14 (2012).

105. Cervera, L. *et al.* Production of HIV-1-based virus-like particles for vaccination: achievements and limits. *Applied Microbiology and Biotechnology* vol. 103 (2019).

106. Zhu, P. *et al.* Distribution and three-dimensional structure of AIDS virus envelope spikes. *Nature* **441**, (2006).

107. Chojnacki, J. *et al.* Maturation-dependent HIV-1 surface protein redistribution revealed by fluorescence nanoscopy. *Science (80-.).* **338**, (2012).

108. Sakuragi, J. I. Morphogenesis of the infectious HIV-1 virion. *Front. Microbiol.* **2**, (2011).

109. Wu, L. *et al.* CD4-induced interaction of primary HIV-1 gp120 glycoproteins with the chemokine receptor CCR-5. *Nature* **384**, (1996).

110. Oberlin, E. *et al.* The CXC chemokine SDF-1 is the ligand for LESTR/fusin and prevents infection by T-cell-line-adapted HIV-1. *Nature* **382**, (1996).

111. Simmons, G. *et al.* Primary, syncytium-inducing human immunodeficiency virus type 1 isolates are dual-tropic and most can use either Lestr or CCR5 as coreceptors for virus entry. *J. Virol.* **70**, (1996).

112. Arhel, N. Revisiting HIV-1 uncoating. *Retrovirology* vol. 7 (2010).

113. Hu, W. S. & Hughes, S. H. HIV-1 reverse transcription. *Cold Spring Harb. Perspect. Med.* **2**, (2012).

114. Cuevas, J. M., Geller, R., Garijo, R., López-Aldeguer, J. & Sanjuán, R. Extremely High

Mutation Rate of HIV-1 In Vivo. *PLoS Biol.* **13**, (2015).

115. Domingo, E. & Perales, C. Quasispecies and virus. *Eur. Biophys. J.* **47**, (2018).

116. Korber, B. *et al.* Evolutionary and immunological implications of contemporary HIV-1 variation. *British Medical Bulletin* vol. 58 (2001).

117. Suzuki, Y. & Craigie, R. The road to chromatin - Nuclear entry of retroviruses. *Nature Reviews Microbiology* vol. 5 (2007).

118. Schröder, A. R. W. *et al.* HIV-1 integration in the human genome favors active genes and local hotspots. *Cell* **110**, (2002).

119. Castro-Gonzalez, S., Colomer-Lluch, M. & Serra-Moreno, R. Barriers for HIV Cure: The Latent Reservoir. *AIDS Research and Human Retroviruses* vol. 34 (2018).

120. Laspia, M. F., Rice, A. P. & Mathews, M. B. HIV-1 Tat protein increases transcriptional initiation and stabilizes elongation. *Cell* **59**, (1989).

121. Malim, M. H., Hauber, J., Le, S. Y., Maizel, J. V. & Cullen, B. R. The HIV-1 rev trans-activator acts through a structured target sequence to activate nuclear export of unspliced viral mRNA. *Nature* **338**, (1989).

122. Chen, J. *et al.* Visualizing the translation and packaging of HIV-1 full-length RNA. *Proc. Natl. Acad. Sci. U. S. A.* **117**, (2020).

123. Sundquist, W. I. & Kräusslich, H. G. HIV-1 assembly, budding, and maturation. *Cold Spring Harbor Perspectives in Medicine* vol. 2 (2012).

124. Könnyu, B. *et al.* Gag-Pol Processing during HIV-1 Virion Maturation: A Systems Biology Approach. *PLoS Comput. Biol.* **9**, (2013).

125. Checkley, M. A., Luttge, B. G. & Freed, E. O. HIV-1 envelope glycoprotein biosynthesis, trafficking, and incorporation. *Journal of Molecular Biology* vol. 410 (2011).

126. Schneck, N. A., Ivleva, V. B., Cai, C. X., Cooper, J. W. & Lei, Q. P. Characterization of the furin cleavage motif for HIV-1 trimeric envelope glycoprotein by intact LC-MS analysis. *Analyst* **145**, (2020).

127. Klein, J. S. & Bjorkman, P. J. Few and far between: How HIV may be evading antibody avidity. *PLoS Pathog.* **6**, (2010).

128. Izquierdo-Useros, N., Puertas, M. C., Borràs, F. E., Blanco, J. & Martinez-Picado, J. Exosomes and retroviruses: The chicken or the egg? *Cellular Microbiology* vol. 13 (2011).

129. Hockett, R. D. *et al.* Constant mean viral copy number per infected cell in tissues regardless of high, low, or undetectable plasma HIV RNA. *J. Exp. Med.* **189**, (1999).

130. Perelson, A. S., Neumann, A. U., Markowitz, M., Leonard, J. M. & Ho, D. D. HIV-1 dynamics in vivo: Virion clearance rate, infected cell life-span, and viral generation time. *Science (80-.).* **271**, (1996).

131. Shcherbatova, O., Grebennikov, D., Sazonov, I., Meyerhans, A. & Bocharov, G. Modeling of the hiv-1 life cycle in productively infected cells to predict novel therapeutic targets. *Pathogens* **9**, (2020).

132. Shaw, G. M. & Hunter, E. HIV transmission. *Cold Spring Harb. Perspect. Med.* **2**, (2012).

133. Simon, V., Ho, D. D. & Abdool Karim, Q. HIV/AIDS epidemiology, pathogenesis, prevention, and treatment. *Lancet* vol. 368 (2006).

134. Shattock, R. J. & Moore, J. P. Inhibiting sexual transmission of HIV-1 infection. *Nat. Rev. Microbiol.* **1**, (2003).

135. Moir, S., Chun, T. W. & Fauci, A. S. Pathogenic mechanisms of HIV disease. *Annu. Rev. Pathol. Mech. Dis.* **6**, (2011).

136. Keele, B. F. *et al.* Identification and characterization of transmitted and early founder virus envelopes in primary HIV-1 infection. *Proc. Natl. Acad. Sci. U. S. A.* **105**, (2008).

137. Connor, R. I., Sheridan, K. E., Ceradini, D., Choe, S. & Landau, N. R. Change in coreceptor use correlates with disease progression in HIV-1- infected individuals. *J. Exp. Med.* **185**, (1997).

138. Okoye, A. A. & Picker, L. J. CD4+ T-Cell Depletion In Hiv Infection: Mechanisms Of Immunological Failure. *Immunol. Rev.* **254**, (2013).

139. Vijayan, K. V., Karthigeyan, K. P., Tripathi, S. P. & Hanna, L. E. Pathophysiology of CD4+ T-Cell depletion in HIV-1 and HIV-2 infections. *Frontiers in Immunology* vol. 8 (2017).

140. Guadalupe, M. *et al.* Severe CD4 + T-Cell Depletion in Gut Lymphoid Tissue during Primary Human Immunodeficiency Virus Type 1 Infection and Substantial Delay in Restoration following Highly Active Antiretroviral Therapy . *J. Virol.* **77**, (2003).

141. MacNeal, R. J. & Dinulos, J. G. H. Acute Retroviral Syndrome. *Dermatologic Clinics* vol. 24 (2006).

142. Fiebig, E. W. *et al.* Dynamics of HIV viremia and antibody seroconversion in plasma donors: Implications for diagnosis and staging of primary HIV infection. *AIDS* **17**, (2003).

143. Huang, X. *et al.* Precise determination of time to reach viral load set point after acute HIV-1 infection. *J. Acquir. Immune Defic. Syndr.* **61**, (2012).

144. Douek, D. C., Picker, L. J. & Koup, R. A. T cell dynamics in HIV-1 infection. *Annual Review of Immunology* vol. 21 (2003).

145. McCune, J. M. The dynamics of CD4+ T-cell depletion in HIV disease. *Nature* **410**, 974–979 (2001).

146. Khaitan, A. & Unutmaz, D. Revisiting immune exhaustion during HIV infection. *Current HIV/AIDS Reports* vol. 8 (2011).

147. Sun, B. & Zhang, Y. Overview of orchestration of CD4+ T cell subsets in immune responses. *Advances in Experimental Medicine and Biology* vol. 841 (2014).

148. Pitchumoni, C. S. & Brun, A. HIV Disease Current Practice. *Geriatr. Gastroenterol.* (2020).

149. Poorolajal, J., Hooshmand, E., Mahjub, H., Esmailnasab, N. & Jenabi, E. Survival rate of AIDS disease and mortality in HIV-infected patients: a meta-analysis. *Public Health* vol. 139 (2016).

150. Sabin, C. A. & Lundgren, J. D. The natural history of HIV infection. *Current Opinion in HIV and AIDS* vol. 8 (2013).

151. Gaardbo, J. C., Hartling, H. J., Gerstoft, J. & Nielsen, S. D. Thirty years with HIV infection - Nonprogression is still puzzling: Lessons to be learned from controllers and long-term nonprogressors. *AIDS Research and Treatment* vol. 2012 (2012).

152. Gonzalo-Gil, E., Ikediobi, U. & Sutton, R. E. Mechanisms of virologic control and clinical characteristics of HIV+ elite/viremic controllers. *Yale Journal of Biology and Medicine* vol. 90 (2017).

153. Jacobs, E. S. *et al.* Cytokines Elevated in HIV Elite Controllers Reduce HIV Replication In Vitro and Modulate HIV Restriction Factor Expression. *J. Virol.* **91**, (2017).

154. Thèze, J., Chakrabarti, L. A., Vingert, B., Porichis, F. & Kaufmann, D. E. HIV controllers: A multifactorial phenotype of spontaneous viral suppression. *Clinical Immunology* (2011) doi:10.1016/j.clim.2011.07.007.

155. Hur, E. M. *et al.* Inhibitory effect of HIV-specific neutralizing IgA on mucosal transmission of HIV in humanized mice. *Blood* (2012) doi:10.1182/blood-2012-04-422303.

156. Grant, R. M. *et al.* Preexposure Chemoprophylaxis for HIV Prevention in Men Who Have Sex with Men. *N. Engl. J. Med.* **363**, (2010).

157. Olvera, A. *et al.* The HLA-C∗04:01/KIR2DS4 gene combination and human leukocyte antigen alleles with high population frequency drive rate of HIV disease progression. *AIDS* **29**, (2015).

158. Martin-Gayo, E. *et al.* Potent Cell-Intrinsic Immune Responses in Dendritic Cells Facilitate HIV-1-Specific T Cell Immunity in HIV-1 Elite Controllers. *PLoS Pathog.* **11**, (2015).

159. Huang, J. *et al.* Leukocyte Immunoglobulin-Like Receptors Maintain Unique Antigen-Presenting Properties of Circulating Myeloid Dendritic Cells in HIV-1-Infected Elite Controllers. *J. Virol.* **84**, (2010).

160. Potter, S. J. *et al.* Preserved Central Memory and Activated Effector Memory CD4 + T-Cell Subsets in Human Immunodeficiency Virus Controllers: an ANRS EP36 Study . *J. Virol.* **81**, (2007).

References

161. Jones, R. B. & Walker, B. D. HIV-specific CD8+ T cells and HIV eradication. *Journal of Clinical Investigation* (2016) doi:10.1172/JCI80566.

162. Fellay, J. *et al.* A whole-genome association study of major determinants for host control of HIV-1. *Science (80-.).* **317**, 944–947 (2007).

163. Pereyra, F. *et al.* Genetic and immunologic heterogeneity among persons who control HIV infection in the absence of therapy. *J. Infect. Dis.* (2008) doi:10.1086/526786.

164. Sáez-Cirión, A. *et al.* Heterogeneity in HIV Suppression by CD8 T Cells from HIV Controllers: Association with Gag-Specific CD8 T Cell Responses. *J. Immunol.* (2009) doi:10.4049/jimmunol.0803928.

165. Mendoza, P. *et al.* Combination therapy with anti-HIV-1 antibodies maintains viral suppression. *Nature* **561**, (2018).

166. Chen, X. *et al.* The early antibody-dependent cell-mediated cytotoxicity response is associated with lower viral set point in individuals with primary HIV infection. *Front. Immunol.* (2018) doi:10.3389/fimmu.2018.02322.

167. Su, B. *et al.* Update on Fc-Mediated Antibody Functions Against HIV-1 Beyond Neutralization. *Frontiers in Immunology* (2019) doi:10.3389/fimmu.2019.02968.

168. Overbaugh, J. & Morris, L. The antibody response against HIV-1. *Cold Spring Harb. Perspect. Med.* (2012) doi:10.1101/cshperspect.a007039.

169. Cruz, N. V. G., Amorim, R., Oliveira, F. E., Speranza, F. A. C. & Costa, L. J. Mutations in the nef and vif genes associated with progression to AIDS in elite controller and slow-progressor Patients. *J. Med. Virol.* **85**, (2013).

170. Mann, J. K. *et al.* Ability of HIV-1 Nef to downregulate CD4 and HLA class I differs among viral subtypes. *Retrovirology* **10**, (2013).

171. Lobritz, M. A., Lassen, K. G. & Arts, E. J. HIV-1 replicative fitness in elite controllers. *Curr. Opin. HIV AIDS* (2011) doi:10.1097/COH.0b013e3283454cf5.

172. Rappaport, J. *et al.* 32 bp CCR-5 gene deletion and resistance to fast progression in HIV-1 infected heterozygotes [3]. *Lancet* **349**, (1997).

173. Piacentini, L., Biasin, M., Fenizia, C. & Clerici, M. Genetic correlates of protection against HIV infection: The ally within. in *Journal of Internal Medicine* vol. 265 (2009).

174. Colomer-Lluch, M., Ruiz, A., Moris, A. & Prado, J. G. Restriction Factors: From Intrinsic Viral Restriction to Shaping Cellular Immunity Against HIV-1. *Frontiers in Immunology* vol. 9 (2018).

175. Sáez-Cirión, A. *et al.* Restriction of HIV-1 replication in macrophages and CD4+ T cells from HIV controllers. *Blood* **118**, (2011).

176. Van Grevenynghe, J. *et al.* Transcription factor FOXO3a controls the persistence of memory CD4 + T cells during HIV infection. *Nat. Med.* **14**, (2008).

177. Abel, A. M., Yang, C., Thakar, M. S. & Malarkannan, S. Natural killer cells: Development, maturation, and clinical utilization. *Frontiers in Immunology* vol. 9 (2018).

178. Bi, J. & Wang, X. Molecular Regulation of NK Cell Maturation. *Frontiers in Immunology* vol. 11 (2020).

179. Di Vito, C., Mikulak, J. & Mavilio, D. On the way to become a natural killer cell. *Frontiers in Immunology* vol. 10 (2019).

180. Poli, A. *et al.* CD56bright natural killer (NK) cells: An important NK cell subset. *Immunology* vol. 126 (2009).

181. Fehniger, T. A. *et al.* Differential cytokine and chemokine gene expression by human NK cells following activation with IL-18 or IL-15 in combination with IL-12: implications for the innate immune response. *J. Immunol.* **162**, (1999).

182. Cooper, M. A. *et al.* Human natural killer cells: A unique innate immunoregulatory role for the CD56bright subset. *Blood* **97**, (2001).

183. Nagler, A., Lanier, L. L., Cwirla, S. & Phillips, J. H. Comparative studies of human FcRIII-positive and negative natural killer cells. *J. Immunol.* **143**, (1989).

184. Cichocki, F. *et al.* Diversification and functional specialization of human NK cell subsets. *Curr. Top. Microbiol. Immunol.* **395**, (2016).

References

185. Nielsen, N., Ødum, N., Ursø, B., Lanier, L. L. & Spee, P. Cytotoxicity of CD56 bright NK cells towards autologous activated CD4 + T cells is mediated through NKG2D, LFA-1 and TRAIL and dampened via CD94/NKG2A. *PLoS One* **7**, (2012).

186. Jiang, W., Chai, N. R., Maric, D. & Bielekova, B. Unexpected role for granzyme K in CD56bright NK cell-mediated immunoregulation of multiple sclerosis. *J. Immunol.* **187**, 781 (2011).

187. Angelo, L. S. *et al.* Practical NK cell phenotyping and variability in healthy adults. *Immunol. Res.* **62**, (2015).

188. Fehniger, T. A. *et al.* CD56bright natural killer cells are present in human lymph nodes and are activated by T cell-derived IL-2: A potential new link between adaptive and innate immunity. *Blood* **101**, (2003).

189. Lugthart, G. *et al.* Human Lymphoid Tissues Harbor a Distinct CD69 + CXCR6 + NK Cell Population . *J. Immunol.* **197**, (2016).

190. Schlums, H. *et al.* Cytomegalovirus Infection Drives Adaptive Epigenetic.pdf. *Immunometabolism* vol. 42 443–456 (2016).

191. Lopez-Vergès, S. *et al.* CD57 defines a functionally distinct population of mature NK cells in the human CD56dimCD16+ NK-cell subset. *Blood* **116**, 3865–3874 (2010).

192. Müller-Durovic, B., Grählert, J., Devine, O. P., Akbar, A. N. & Hess, C. CD56-negative NK cells with impaired effector function expand in CMV and EBV co-infected healthy donors with age. *Aging (Albany. NY).* **11**, (2019).

193. Cao, W. J. *et al.* Immune Dysfunctions of CD56neg NK Cells Are Associated With HIV-1 Disease Progression. *Front. Immunol.* **12**, 5708 (2022).

194. Vivier, E., Tomasello, E., Baratin, M., Walzer, T. & Ugolini, S. Functions of natural killer cells. *Nature Immunology* (2008) doi:10.1038/ni1582.

195. Chen, Y., Lu, D., Churov, A. & Fu, R. Research Progress on NK Cell Receptors and Their Signaling Pathways. *Mediators of Inflammation* vol. 2020 (2020).

196. Long, E. O. Negative signaling by inhibitory receptors: The NK cell paradigm.

Immunological Reviews vol. 224 (2008).

197.   Pende, D. *et al.* Killer Ig-like receptors (KIRs): Their role in NK cell modulation and developments leading to their clinical exploitation. *Frontiers in Immunology* (2019) doi:10.3389/fimmu.2019.01179.

198.   Borrego, F., Masilamani, M., Marusina, A. I., Tang, X. & Coligan, J. E. The CD94/NKG2 family of receptors: From molecules and cells to clinical relevance. *Immunologic Research* vol. 35 (2006).

199.   Bastidas-Legarda, L. Y. & Khakoo, S. I. Conserved and variable natural killer cell receptors: diverse approaches to viral infections. *Immunology* vol. 156 (2019).

200.   Manser, A. R., Weinhold, S. & Uhrberg, M. Human KIR repertoires: Shaped by genetic diversity and evolution. *Immunol. Rev.* **267**, (2015).

201.   van der Touw, W., Chen, H. M., Pan, P. Y. & Chen, S. H. LILRB receptor-mediated regulation of myeloid cell maturation and function. *Cancer Immunology, Immunotherapy* vol. 66 (2017).

202.   Bottino, C., Biassoni, R., Millo, R., Moretta, L. & Moretta, A. The human natural cytotoxicity receptors (NCR) that induce HLA class I- independent NK cell triggering. *Hum. Immunol.* **61**, (2000).

203.   Parodi, M. *et al.* NKp44-NKp44 ligand interactions in the regulation of natural killer cells and other innate lymphoid cells in humans. *Frontiers in Immunology* vol. 10 (2019).

204.   von Strandmann, E. P., Shatnyeva, O. & Hansen, H. P. NKp30 and its ligands: Emerging players in tumor immune evasion from natural killer cells. *Annals of Translational Medicine* vol. 3 (2015).

205.   Zamai, L. *et al.* Understanding the Synergy of NKp46 and Co-Activating Signals in Various NK Cell Subpopulations: Paving the Way for More Successful NK-Cell-Based Immunotherapy. *Cells* **9**, (2020).

206.   Valés-Gómez, M., Reyburn, H. T., Erskine, R. A., López-Botet, M. & Strominger, J. L. Kinetics and peptide dependency of the binding of the inhibitory NK receptor CD94/NIKG2-A and the activating receptor CD94/NKG2-C to HLA-E. *EMBO J.* (1999)

doi:10.1093/emboj/18.15.4250.

207. Dukovska, D., Fernández-Soto, D., Valés-Gómez, M. & Reyburn, H. T. NKG2H-expressing T cells negatively regulate immune responses. *Front. Immunol.* **9**, (2018).

208. Orbelyan, G. A. *et al.* Human NKG2E Is Expressed and Forms an Intracytoplasmic Complex with CD94 and DAP12. *J. Immunol.* **193**, (2014).

209. Lanier, L. L. NKG2D receptor and its ligands in host defense. *Cancer Immunol. Res.* **3**, (2015).

210. Cronk, J. M., Fafoutis, E. & Brown, M. G. Licensing natural killers for antiviral immunity. *Pathogens* vol. 10 (2021).

211. Kim, S. *et al.* HLA alleles determine differences in human natural killer cell responsiveness and potency. *Proc. Natl. Acad. Sci. U. S. A.* **105**, (2008).

212. Vieira, V. A. *et al.* An HLA-I signature favouring KIR-educated Natural Killer cells mediates immune control of HIV in children and contrasts with the HLA-B-restricted CD8+ T-cell-mediated immune control in adults. *PLOS Pathog.* **17**, e1010090 (2021).

213. Grant, E. J. *et al.* The unconventional role of HLA-E: The road less traveled. *Molecular Immunology* (2020) doi:10.1016/j.molimm.2020.02.011.

214. Grimsley, C. & Ober, C. Population genetic studies of HLA-E: Evidence for selection. *Hum. Immunol.* (1997) doi:10.1016/S0198-8859(96)00241-8.

215. Celik, A. A., Kraemer, T., Huyton, T., Blasczyk, R. & Bade-Döding, C. The diversity of the HLA-E-restricted peptide repertoire explains the immunological impact of the Arg107Gly mismatch. *Immunogenetics* (2016) doi:10.1007/s00251-015-0880-z.

216. Borrego, F., Ulbrecht, M., Weiss, E. H., Coligan, J. E. & Brooks, A. G. Recognition of human histocompatibility leukocyte antigen (HLA)-E complexed with HLA class I signal sequence-derived peptides by CD94/NKG2 confers protection from natural killer cell-mediated lysis. *J. Exp. Med.* (1998) doi:10.1084/jem.187.5.813.

217. Joosten, S. A., Sullivan, L. C. & Ottenhoff, T. H. M. Characteristics of HLA-E Restricted T-Cell Responses and Their Role in Infectious Diseases. *Journal of Immunology Research*

(2016) doi:10.1155/2016/2695396.

218. Prezzemolo, T. *et al.* Detailed characterization of human Mycobacterium tuberculosis specific HLA-E restricted CD8+ T cells. *Eur. J. Immunol.* (2018) doi:10.1002/eji.201747184.

219. Sharpe, H. R., Bowyer, G., Brackenridge, S. & Lambe, T. HLA-E: exploiting pathogen-host interactions for vaccine development. *Clinical and Experimental Immunology* (2019) doi:10.1111/cei.13292.

220. Lee, S. H., Miyagi, T. & Biron, C. A. Keeping NK cells in highly regulated antiviral warfare. *Trends Immunol.* (2007) doi:10.1016/j.it.2007.04.001.

221. Chijioke, O., Landtwing, V. & Münz, C. NK cell influence on the outcome of primary Epstein-Barr virus infection. *Frontiers in Immunology* (2016) doi:10.3389/fimmu.2016.00323.

222. Zimmer, C. L. *et al.* NK cells are activated and primed for skin-homing during acute dengue virus infection in humans. *Nat. Commun.* (2019) doi:10.1038/s41467-019-11878-3.

223. Yoon, J. C., Yang, C. M., Song, Y. & Lee, J. M. Natural killer cells in hepatitis C: Current progress. *World journal of gastroenterology* (2016) doi:10.3748/wjg.v22.i4.1449.

224. Long, E. O., Sik Kim, H., Liu, D., Peterson, M. E. & Rajagopalan, S. Controlling natural killer cell responses: Integration of signals for activation and inhibition. *Annual Review of Immunology* (2013) doi:10.1146/annurev-immunol-020711-075005.

225. Cooper, M. A., Fehniger, T. A. & Caligiuri, M. A. The biology of human natural killer-cell subsets. *Trends in Immunology* (2001) doi:10.1016/S1471-4906(01)02060-9.

226. Mirandola, P. *et al.* Activated human NK and CD8+ T cells express both TNF-related apoptosis-inducing ligand (TRAIL) and TRAIL receptors but are resistant to TRAIL-mediated cytotoxicity. *Blood* (2004) doi:10.1182/blood-2004-04-1294.

227. Sun, J. C. & Lanier, L. L. NK cell development, homeostasis and function: Parallels with CD8 + T cells. *Nat. Rev. Immunol.* **11**, 645–657 (2011).

References

228. Federici, C. *et al.* Natural-Killer-Derived Extracellular Vesicles: Immune Sensors and Interactors. *Front. Immunol.* (2020) doi:10.3389/fimmu.2020.00262.

229. Oliva, A. *et al.* Natural killer cells from human immunodeficiency virus (HIV)-infected individuals are an important source of CC-chemokines and suppress HIV-1 entry and replication in vitro. *J. Clin. Invest.* (1998) doi:10.1172/JCI2323.

230. Waggoner, S. N. *et al.* Roles of natural killer cells in antiviral immunity. *Current Opinion in Virology* (2016) doi:10.1016/j.coviro.2015.10.008.

231. Waggoner, S. N., Cornberg, M., Selin, L. K. & Welsh, R. M. Natural killer cells act as rheostats modulating antiviral T cells. *Nature* (2012) doi:10.1038/nature10624.

232. Cook, K. D., Waggoner, S. N. & Whitmire, J. K. NK cells and their ability to modulate T cells during virus infections. *Crit. Rev. Immunol.* **34**, 359–388 (2014).

233. Welsh, R. M. & Waggoner, S. N. NK cells controlling virus-specific T cells: Rheostats for acute vs. persistent infections. *Virology* (2013) doi:10.1016/j.virol.2012.10.005.

234. Orange, J. S., Fassett, M. S., Koopman, L. A., Boyson, J. E. & Strominger, J. L. Viral evasion of natural killer cells. *Nature Immunology* (2002) doi:10.1038/ni1102-1006.

235. Jonjić, S., Babić, M., Polić, B. & Krmpotić, A. Immune evasion of natural killer cells by viruses. *Current Opinion in Immunology* (2008) doi:10.1016/j.coi.2007.11.002.

236. Heatley, S. L. *et al.* Polymorphism in human cytomegalovirus UL40 impacts on recognition of human leukocyte antigen-E (HLA-E) by natural killer cells. *J. Biol. Chem.* (2013) doi:10.1074/jbc.M112.409672.

237. Fadda, L. *et al.* HLA-Cw*0102-restricted HIV-1 p24 epitope variants can modulate the binding of the inhibitory KIR2DL2 receptor and primary NK cell function. *PLoS Pathog.* (2012) doi:10.1371/journal.ppat.1002805.

238. Li, M. *et al.* Elevated Exhaustion Levels of NK and CD8+ T Cells as Indicators for Progression and Prognosis of COVID-19 Disease. *Front. Immunol.* **11**, (2020).

239. Maucourant, C. *et al.* Natural killer cell immunotypes related to COVID-19 disease severity. *Sci. Immunol.* (2020) doi:10.1126/SCIIMMUNOL.ABD6832.

240.   Cifaldi, L. *et al.* Inhibition of natural killer cell cytotoxicity by interleukin-6: Implications for the pathogenesis of macrophage activation syndrome. *Arthritis Rheumatol.* **67**, (2015).

241.   Vietzen, H. *et al.* Deletion of the NKG2C receptor encoding KLRC2 gene and HLA-E variants are risk factors for severe COVID-19. *Genet. Med.* **23**, (2021).

242.   Bortolotti, D., Gentili, V., Rizzo, S., Rotola, A. & Rizzo, R. SARS-CoV-2 Spike 1 Protein Controls Natural Killer Cell Activation via the HLA-E/NKG2A Pathway. *Cells* **9**, (2020).

243.   Costanzo, M. C. *et al.* Transcriptomic signatures of NK cells suggest impaired responsiveness in HIV-1 infection and increased activity post-vaccination. *Nat. Commun.* **9**, (2018).

244.   Wagstaffe, H. R. *et al.* Durable natural killer cell responses after heterologous two-dose Ebola vaccination. *npj Vaccines 2021 61* **6**, 1–10 (2021).

245.   Palgen, J. L. *et al.* NK cell immune responses differ after prime and boost vaccination. *J. Leukoc. Biol.* **105**, 1055–1073 (2019).

246.   Jost, S. *et al.* CD4+ T-Cell Help Enhances NK Cell Function following Therapeutic HIV-1 Vaccination. *J. Virol.* **88**, 8349 (2014).

247.   Cox, A. *et al.* Targeting natural killer cells to enhance vaccine responses. *Trends in Pharmacological Sciences* vol. 42 (2021).

248.   Ndeupen, S. *et al.* The mRNA-LNP platform's lipid nanoparticle component used in preclinical vaccine studies is highly inflammatory. *iScience* **24**, 103479 (2021).

249.   Flórez-Álvarez, L., Hernandez, J. C. & Zapata, W. NK cells in HIV-1 infection: From basic science to vaccine strategies. *Frontiers in Immunology* vol. 9 (2018).

250.   Scott-Algara, D. *et al.* Cutting Edge: Increased NK Cell Activity in HIV-1-Exposed but Uninfected Vietnamese Intravascular Drug Users. *J. Immunol.* **171**, (2003).

251.   Madhavi, V. *et al.* HIV-1 Env- and Vpu-Specific Antibody-Dependent Cellular Cytotoxicity Responses Associated with Elite Control of HIV. *J. Virol.* **91**, (2017).

252. Haynes, B. F. *et al.* Immune-Correlates Analysis of an HIV-1 Vaccine Efficacy Trial. *N. Engl. J. Med.* (2012) doi:10.1056/nejmoa1113425.

253. Holder, K. A., Burt, K. & Grant, M. D. TIGIT blockade enhances NK cell activity against autologous HIV-1-infected CD4+ T cells. *Clin. Transl. Immunol.* **10**, (2021).

254. Clayton, K. L. *et al.* HIV-infected macrophages resist efficient NK cell-mediated killing while preserving inflammatory cytokine responses. *Cell Host Microbe* **29**, (2021).

255. Quillay, H. *et al.* NK cells control HIV-1 infection of macrophages through soluble factors and cellular contacts in the human decidua. *Retrovirology* **13**, (2016).

256. Jiang, Y. *et al.* Higher NK cell IFN-γ production is associated with delayed HIV disease progression in LTNPs. *J. Clin. Immunol.* **33**, (2013).

257. Montoya, C. J., Velilla, P. A., Chougnet, C., Landay, A. L. & Rugeles, M. T. Increased IFN-γ production by NK and CD3+/CD56+ cells in sexually HIV-1-exposed but uninfected individuals. *Clin. Immunol.* **120**, (2006).

258. Gerosa, F. *et al.* Reciprocal activating interaction between natural killer cells and dendritic cells. *J. Exp. Med.* **195**, (2002).

259. Ferlazzo, G. & Moretta, L. Dendritic cell editing by natural killer cells. *Crit. Rev. Oncog.* **19**, (2014).

260. Quaranta, M. G. *et al.* HIV-1 Nef impairs the dynamic of DC/NK crosstalk: different outcome of CD56 dim and CD56 bright NK cell subsets . *FASEB J.* **21**, (2007).

261. Cook, K. D., Waggoner, S. N. & Whitmire, J. K. NK cells and their ability to modulate T cells during virus infections. *Crit. Rev. Immunol.* (2014) doi:10.1615/CritRevImmunol.2014010604.

262. Gyurova, I. E., Ali, A. & Waggoner, S. N. Natural Killer Cell Regulation of B Cell Responses in the Context of Viral Infection. *Viral Immunol.* **33**, (2020).

263. Hong, H. S. *et al.* Loss of CCR7 Expression on CD56bright NK Cells Is Associated with a CD56dimCD16+ NK Cell-Like Phenotype and Correlates with HIV Viral Load. *PLoS One* **7**, (2012).

264. van Stigt Thans, T. *et al.* Primary HIV-1 Strains Use Nef To Downmodulate HLA-E Surface Expression. *J. Virol.* (2019) doi:10.1128/jvi.00719-19.

265. Hannoun, Z. *et al.* Identification of novel HIV-1-derived HLA-E-binding peptides. *Immunol. Lett.* **202**, (2018).

266. Davis, Z. B. *et al.* A Conserved HIV-1-Derived Peptide Presented by HLA-E Renders Infected T-cells Highly Susceptible to Attack by NKG2A/CD94-Bearing Natural Killer Cells. *PLoS Pathog.* **12**, (2016).

267. Judge, S. J., Murphy, W. J. & Canter, R. J. Characterizing the Dysfunctional NK Cell: Assessing the Clinical Relevance of Exhaustion, Anergy, and Senescence. *Frontiers in Cellular and Infection Microbiology* vol. 10 (2020).

268. Beldi-Ferchiou, A. *et al.* PD-1 mediates functional exhaustion of activated NK cells in patients with Kaposi sarcoma. *Oncotarget* **7**, (2016).

269. Da Silva, I. P. *et al.* Reversal of NK-cell exhaustion in advanced melanoma by Tim-3 blockade. *Cancer Immunol. Res.* **2**, (2014).

270. Seo, H. *et al.* IL-21-mediated reversal of NK cell exhaustion facilitates anti-Tumour immunity in MHC class I-deficient tumours. *Nat. Commun.* **8**, (2017).

271. Sun, C. *et al.* High NKG2A expression contributes to NK cell exhaustion and predicts a poor prognosis of patients with liver cancer. *Oncoimmunology* **6**, (2017).

272. Benson, D. M. *et al.* The PD-1/PD-L1 axis modulates the natural killer cell versus multiple myeloma effect: A therapeutic target for CT-011, a novel monoclonal anti-PD-1 antibody. *Blood* **116**, (2010).

273. Zhang, Q. *et al.* Blockade of the checkpoint receptor TIGIT prevents NK cell exhaustion and elicits potent anti-tumor immunity. *Nat. Immunol.* **19**, (2018).

274. Judge, S. J. *et al.* Minimal PD-1 expression in mouse and human NK cells under diverse conditions. *J. Clin. Invest.* **130**, (2020).

275. Vidard, L. *et al.* CD137 (4-1BB) Engagement Fine-Tunes Synergistic IL-15– and IL-21– Driven NK Cell Proliferation. *J. Immunol.* **203**, (2019).

276. Lopez-Vergès, S. *et al.* CD57 defines a functionally distinct population of mature NK cells in the human CD56dimCD16+ NK-cell subset. *Blood* **116**, (2010).

277. Jamieson, B. D. & Ahmed, R. T cell memory. Long-term persistence of virus-specific cytotoxic T cells. *J. Exp. Med.* **169**, (1989).

278. Mueller, S. N., Gebhardt, T., Carbone, F. R. & Heath, W. R. Memory T cell subsets, migration patterns, and tissue residence. *Annual Review of Immunology* vol. 31 (2013).

279. Jameson, S. C. & Masopust, D. Understanding Subset Diversity in T Cell Memory. *Immunity* vol. 48 (2018).

280. Kondo, K., Ohigashi, I. & Takahama, Y. Thymus machinery for T-cell selection. *Int. Immunol.* **31**, (2019).

281. Blattman, J. N. *et al.* Estimating the precursor frequency of naive antigen-specific CD8 T cells. *J. Exp. Med.* **195**, (2002).

282. Brinkman, C. C., Rouhani, S. J., Srinivasan, N. & Engelhard, V. H. Peripheral tissue homing receptors enable T cell entry into lymph nodes and affect the anatomical distribution of memory cells. *J. Immunol.* **191**, 2412 (2013).

283. Sallusto, F., Lenig, D., Förster, R., Lipp, M. & Lanzavecchia, A. Two subsets of memory T lymphocytes with distinct homing potentials and effector functions. *Nature* **401**, (1999).

284. Kaech, S. M., Wherry, E. J. & Ahmed, R. Effector and memory T-cell differentiation: Implications for vaccine development. *Nature Reviews Immunology* vol. 2 (2002).

285. Sallusto, F., Geginat, J. & Lanzavecchia, A. Central memory and effector memory T cell subsets: Function, generation, and maintenance. *Annual Review of Immunology* vol. 22 (2004).

286. Hussain, T. & Quinn, K. M. Similar but different: virtual memory CD8 T cells as a memory-like cell population. *Immunology and Cell Biology* vol. 97 (2019).

287. Gattinoni, L. *et al.* A human memory T cell subset with stem cell-like properties. *Nat. Med.* **17**, (2011).

288. Geginat, J., Lanzavecchia, A. & Sallusto, F. Proliferation and differentiation potential of human CD8+ memory T-cell subsets in response to antigen or homeostatic cytokines. *Blood* **101**, (2003).

289. Clark, R. A. Resident memory T cells in human health and disease. *Science Translational Medicine* vol. 7 (2015).

290. Sathaliyawala, T. *et al.* Distribution and Compartmentalization of Human Circulating and Tissue-Resident Memory T Cell Subsets. *Immunity* **38**, (2013).

291. Sallusto, F. Heterogeneity of Human CD4+ T Cells Against Microbes. *Annual Review of Immunology* vol. 34 (2016).

292. Reiner, S. L., Sallusto, F. & Lanzavecchia, A. Division of Labor with a workforce of one: Challenges in specifying effector and memory T cell fate. *Science* vol. 317 (2007).

293. Sallusto, F. Heterogeneity of Human CD4+ T Cells Against Microbes. *Annu. Rev. Immunol.* **34**, 317–334 (2016).

294. Valentine, K. M. & Hoyer, K. K. CXCR5+ CD8 T cells: Protective or pathogenic? *Frontiers in Immunology* (2019) doi:10.3389/fimmu.2019.01322.

295. Annunziato, F., Romagnani, C. & Romagnani, S. The 3 major types of innate and adaptive cell-mediated effector immunity. *J. Allergy Clin. Immunol.* **135**, 626–635 (2015).

296. Joosten, S. A. & Ottenhoff, T. H. M. Human CD4 and CD8 regulatory T cells in infectious diseases and vaccination. *Hum. Immunol.* **69**, 760–770 (2008).

297. Murphy, E. *et al.* Reversibility of T helper 1 and 2 populations is lost after long-term stimulation. *J. Exp. Med.* **183**, (1996).

298. Crotty, S. Do Memory CD4 T Cells Keep Their Cell-Type Programming: Plasticity versus Fate Commitment? *Cold Spring Harb. Perspect. Biol.* **10**, (2018).

299. Morita, R. *et al.* Human Blood CXCR5+CD4+ T Cells Are Counterparts of T Follicular Cells and Contain Specific Subsets that Differentially Support Antibody Secretion. *Immunity* **34**, (2011).

300. Annunziato, F., Romagnani, C. & Romagnani, S. The 3 major types of innate and adaptive cell-mediated effector immunity. *Journal of Allergy and Clinical Immunology* vol. 135 (2015).

301. Tuzlak, S. *et al.* Repositioning TH cell polarization from single cytokines to complex help. *Nature Immunology* vol. 22 (2021).

302. Idriss, H. T. & Naismith, J. H. TNFα and the TNF receptor superfamily: Structure-function relationship(s). *Microsc. Res. Tech.* **50**, (2000).

303. Hildemann, S. K. *et al.* High Efficiency of Antiviral CD4+ Killer T Cells. *PLoS One* **8**, (2013).

304. Walker, J. A. & McKenzie, A. N. J. TH2 cell development and function. *Nature Reviews Immunology* vol. 18 (2018).

305. Yagi, R., Zhu, J. & Paul, W. E. An updated view on transcription factor GATA3-mediated regulation of Th1 and Th2 cell differentiation. *International Immunology* vol. 23 (2011).

306. Punnonen, J., Yssel, H. & De Vries, J. E. The relative contribution of IL-4 and IL-13 to human IgE synthesis induced by activated CD4+ or CD8+ T cells. *J. Allergy Clin. Immunol.* **100**, (1997).

307. Gelfand, E. W. *et al.* Eosinophils in Human Disease. *Eosinophils in Health and Disease* (2013) doi:10.1016/B978-0-12-394385-9.00013-4.

308. Harrington, L. E. *et al.* Interleukin 17-producing CD4+ effector T cells develop via a lineage distinct from the T helper type 1 and 2 lineages. *Nat. Immunol.* **6**, (2005).

309. Chen, H. W. *et al.* TGF-β and IL-21 cooperatively stimulate activated CD8+ T cells to differentiate into Tc17 cells. *Immunol. Lett.* **174**, (2016).

310. Furlan, S. N. *et al.* Systems analysis uncovers inflammatory Th/Tc17-driven modules during acute GVHD in monkey and human T cells. *Blood* **128**, (2016).

311. Wang, C., Kang, S. G., Lee, J., Sun, Z. & Kim, C. H. The roles of CCR6 in migration of Th17 cells and regulation of effector T-cell balance in the gut. *Mucosal Immunol.* **2**, (2009).

312. Flannigan, K. L. *et al.* IL-17A-mediated neutrophil recruitment limits expansion of

segmented filamentous bacteria. *Mucosal Immunol.* **10**, (2017).

313.   Archer, N. K. *et al.* Interleukin-17A (IL-17A) and IL-17F are critical for antimicrobial peptide production and clearance of Staphylococcus aureus nasal colonization. *Infect. Immun.* **84**, (2016).

314.   O'Connor, W. *et al.* A protective function for interleukin 17A in T cell-mediated intestinal inflammation. *Nat. Immunol.* **10**, (2009).

315.   Rutz, S., Eidenschenk, C. & Ouyang, W. IL-22, not simply a Th17 cytokine. *Immunol. Rev.* **252**, (2013).

316.   Song, W. & Craft, J. T follicular helper cell heterogeneity: Time, space, and function. *Immunol. Rev.* **288**, 85–96 (2019).

317.   Bentebibel, S. E. *et al.* ICOS + PD-1 + CXCR3 + T follicular helper cells contribute to the generation of high-avidity antibodies following influenza vaccination. *Sci. Rep.* **6**, (2016).

318.   Koutsakos, M., Nguyen, T. H. O. & Kedzierska, K. With a Little Help from T Follicular Helper Friends: Humoral Immunity to Influenza Vaccination. *J. Immunol.* **202**, 360–367 (2019).

319.   Yu, D. & Ye, L. A Portrait of CXCR5+ Follicular Cytotoxic CD8+ T cells. *Trends Immunol.* **39**, 965–979 (2018).

320.   Josefowicz, S. Z., Lu, L. F. & Rudensky, A. Y. Regulatory T cells: Mechanisms of differentiation and function. *Annual Review of Immunology* vol. 30 (2012).

321.   Yu, Y. *et al.* Recent advances in CD8+ regulatory t cell research (Review). *Oncology Letters* vol. 15 (2018).

322.   Saraiva, M., Vieira, P. & O'Garra, A. Biology and therapeutic potential of interleukin-10. *J. Exp. Med.* **217**, (2020).

323.   Batlle, E. & Massagué, J. Transforming Growth Factor-β Signaling in Immunity and Cancer. *Immunity* vol. 50 (2019).

324.   Pavel, A. B. *et al.* Th2/Th1 Cytokine Imbalance Is Associated With Higher COVID-19 Risk

Mortality. *Front. Genet.* **12**, (2021).

325. Gil-Etayo, F. J. *et al.* T-Helper Cell Subset Response Is a Determining Factor in COVID-19 Progression. *Front. Cell. Infect. Microbiol.* **11**, (2021).

326. Garcia-Gasalla, M. *et al.* Hyperinflammatory State and Low T1 Adaptive Immune Response in Severe and Critical Acute COVID-19 Patients. *Front. Med.* **0**, 462 (2022).

327. Hotez, P. J., Bottazzi, M. E. & Corry, D. B. The potential role of Th17 immune responses in coronavirus immunopathology and vaccine-induced immune enhancement. *Microbes and Infection* vol. 22 (2020).

328. Cagan, E. *et al.* The Age-Dependent Role of Th22, Tc22, and Tc17 Cells in the Severity of Pneumonia in COVID-19 Immunopathogenesis. doi:10.1089/vim.2021.0132.

329. Caldrer, S. *et al.* Regulatory T Cells as Predictors of Clinical Course in Hospitalised COVID-19 Patients. *Front. Immunol.* **12**, (2021).

330. Galván-Peña, S. *et al.* Profound Treg perturbations correlate with COVID-19 severity. *Proc. Natl. Acad. Sci. U. S. A.* **118**, (2021).

331. Zhang, J. *et al.* Spike-specific circulating T follicular helper cell and cross-neutralizing antibody responses in COVID-19-convalescent individuals. *Nat. Microbiol.* **6**, (2021).

332. Meckiff, B. J. *et al.* Imbalance of Regulatory and Cytotoxic SARS-CoV-2-Reactive CD4+ T Cells in COVID-19. *Cell* **183**, (2020).

333. Kaneko, N. *et al.* Loss of Bcl-6-Expressing T Follicular Helper Cells and Germinal Centers in COVID-19. *Cell* **183**, (2020).

334. Walker, B. & McMichael, A. The T-cell response to HIV. *Cold Spring Harb. Perspect. Med.* (2012) doi:10.1101/cshperspect.a007054.

335. Johnson, S. *et al.* Cooperativity of HIV-Specific Cytolytic CD4 T Cells and CD8 T Cells in Control of HIV Viremia. *J. Virol.* **89**, 7494–7505 (2015).

336. Sauce, D., Gorochov, G. & Larsen, M. HIV-specific Th2 and Th17 responses predict HIV vaccine protection efficacy. *Sci. Rep.* (2016) doi:10.1038/srep28129.

337. Crotty, S. Do Memory CD4 T Cells Keep Their Cell-Type Programming: Plasticity versus Fate Commitment? *Cold Spring Harb. Perspect. Biol.* **10**, a032102 (2018).

338. Clerici, M. & Shearer, G. M. A TH1→TH2 switch is a critical step in the etiology of HIV infection. *Immunology Today* vol. 14 (1993).

339. Graziosi, C. *et al.* Lack of evidence for the dichotomy of TH1 and TH2 predominance in HIV-infected individuals. *Science (80-.).* **265**, (1994).

340. Hasenkrug, K. J., Chougnet, C. A. & Dittmer, U. Regulatory T cells in retroviral infections. *PLoS Pathog.* **14**, 1–22 (2018).

341. Fenoglio, D. *et al.* CD8+CD28−CD127loCD39+ regulatory T-cell expansion: A new possible pathogenic mechanism for HIV infection? *J. Allergy Clin. Immunol.* **141**, 2220-2233.e4 (2018).

342. Li, D. *et al.* Loss of balance between T helper type 17 and regulatory T cells in chronic human immunodeficiency virus infection. *Clin. Exp. Immunol.* **165**, (2011).

343. Hartigan-O'Connor, D. J., Hirao, L. A., McCune, J. M. & Dandekar, S. Th17 cells and regulatory T cells in elite control over HIV and SIV. *Curr. Opin. HIV AIDS* **6**, (2011).

344. Hartigan-O'Connor, D. J., Abel, K., Van Rompay, K. K. A., Kanwar, B. & McCune, J. M. SIV replication in the infected rhesus macaque is limited by the size of the preexisting T H17 cell compartment. *Sci. Transl. Med.* **4**, (2012).

345. Gonzalez, S. M., Taborda, N. A. & Rugeles, M. T. Role of different subpopulations of CD8+ T cells during HIV exposure and infection. *Front. Immunol.* **8**, 1–9 (2017).

346. Perdomo-Celis, F., Feria, M. G., Taborda, N. A. & Rugeles, M. T. A Low Frequency of IL-17-Producing CD8+ T-Cells Is Associated With Persistent Immune Activation in People Living With HIV Despite HAART-Induced Viral Suppression. *Front. Immunol.* **9**, 2502 (2018).

347. Locci, M. *et al.* Human Circulating PD-1 + CXCR3 − CXCR5 + Memory Tfh Cells Are Highly Functional and Correlate with Broadly Neutralizing HIV Antibody Responses International AIDS Vaccine Initiative Protocol C Principal Investigators NIH Public Access. *Immunity* **39**, 758–769 (2013).

348. Martin-Gayo, E. *et al.* Circulating CXCR5+CXCR3+PD-1lo Tfh-like cells in HIV-1 controllers with neutralizing antibody breadth. *JCI Insight* **2**, 1–17 (2017).

349. Schultz, B. T. *et al.* Circulating HIV-Specific Interleukin-21+CD4+ T Cells Represent Peripheral Tfh Cells with Antigen-Dependent Helper Functions. *Immunity* **44**, 167–178 (2016).

350. Kohler, S. L. *et al.* Germinal Center T Follicular Helper Cells Are Highly Permissive to HIV-1 and Alter Their Phenotype during Virus Replication. *J. Immunol.* (2016) doi:10.4049/jimmunol.1502174.

351. Aid, M. *et al.* Follicular CD4 T helper cells as a major HIV reservoir compartment: A molecular perspective. *Front. Immunol.* (2018) doi:10.3389/fimmu.2018.00895.

352. Lu, J. *et al.* Expansion of circulating T follicular helper cells is associated with disease progression in HIV-infected individuals. *J. Infect. Public Health* **11**, 685–690 (2018).

353. Miles, B. & Connick, E. T FH in HIV Latency and as Sources of Replication-Competent Virus. *Trends in Microbiology* (2016) doi:10.1016/j.tim.2016.02.006.

354. Petrovas, C. *et al.* Follicular CD8 T cells accumulate in HIV infection and can kill infected cells in vitro via bispecific antibodies. *Sci. Transl. Med.* (2017) doi:10.1126/scitranslmed.aag2285.

355. He, R. *et al.* Follicular CXCR5-expressing CD8+ T cells curtail chronic viral infection. *Nature* (2016) doi:10.1038/nature19317.

356. Mylvaganam, G. H. *et al.* Dynamics of SIV-specific CXCR5+ CD8 T cells during chronic SIV infection. *Proc. Natl. Acad. Sci. U. S. A.* (2017) doi:10.1073/pnas.1621418114.

357. Fukazawa, Y. *et al.* B cell follicle sanctuary permits persistent productive simian immunodeficiency virus infection in elite controllers. *Nat. Med.* **21**, (2015).

358. Strong, R. K. *et al.* HLA-E allelic variants: Correlating differential expression, peptide affinities, crystal structures, and thermal stabilities. *J. Biol. Chem.* **278**, (2003).

359. Ulbrecht, M. *et al.* Cutting Edge: The Human Cytomegalovirus UL40 Gene Product Contains a Ligand for HLA-E and Prevents NK Cell-Mediated Lysis . *J. Immunol.* **164**,

(2000).

360. Gillissen, M. A. *et al.* The modified FACS calcein AM retention assay: A high throughput flow cytometer based method to measure cytotoxicity. *J. Immunol. Methods* **434**, (2016).

361. Bryant, J., Day, R., Whiteside, T. L. & Herberman, R. B. Calculation of lytic units for the expression of cell-mediated cytotoxicity. *J. Immunol. Methods* **146**, (1992).

362. Olvera, A. *et al.* Sars-cov-2 consensus-sequence and matching overlapping peptides design for covid19 immune studies and vaccine development. *Vaccines* **8**, (2020).

363. Ruiz-Riol, M. *et al.* Alternative effector-function profiling identifies broad HIV-specific T-cell responses in highly HIV-exposed individuals who remain uninfected. *J. Infect. Dis.* (2015) doi:10.1093/infdis/jiu534.

364. Roederer, M., Nozzi, J. L. & Nason, M. C. SPICE: Exploration and analysis of post-cytometric complex multivariate datasets. *Cytom. Part A* (2011) doi:10.1002/cyto.a.21015.

365. Blanco, J., Barretina, J., Clotet, B. & Esté, J. A. R5 HIV gp120-mediated cellular contacts induce the death of single CCR5-expressing CD4 T cells by a gp41-dependent mechanism. *J. Leukoc. Biol.* (2004) doi:10.1189/jlb.0204100.

366. Ou, X. *et al.* Characterization of spike glycoprotein of SARS-CoV-2 on virus entry and its immune cross-reactivity with SARS-CoV. *Nat. Commun.* **11**, (2020).

367. Connor, R. I., Chen, B. K., Choe, S. & Landau, N. R. Vpr is required for efficient replication of human immunodeficiency virus type-1 in mononuclear phagocytes. *Virology* **206**, 935–944 (1995).

368. Sánchez-Palomino, S. *et al.* A cell-to-cell HIV transfer assay identifies humoral responses with broad neutralization activity. *Vaccine* **29**, (2011).

369. Pradenas, E. *et al.* Clinical course impacts early kinetics,magnitude, and amplitude of SARS-CoV-2 neutralizing antibodies beyond 1 year after infection. *Cell Reports Med.* **3**, 100523 (2022).

370. Molinos-Albert, L. M. *et al.* Proteoliposomal formulations of an HIV-1 gp41-based miniprotein elicit a lipid-dependent immunodominant response overlapping the 2F5 binding motif. *Sci. Rep.* **7**, (2017).

371. Alpert, M. D. *et al.* A Novel Assay for Antibody-Dependent Cell-Mediated Cytotoxicity against HIV-1- or SIV-Infected Cells Reveals Incomplete Overlap with Antibodies Measured by Neutralization and Binding Assays. *J. Virol.* **86**, (2012).

372. Martínez-Bonet, M. *et al.* Establishment and Replenishment of the Viral Reservoir in Perinatally HIV-1-infected Children Initiating Very Early Antiretroviral Therapy. *Clin. Infect. Dis.* **61**, (2015).

373. Ulbrecht, M., Modrow, S., Srivastava, R., Peterson, P. A. & Weiss, E. H. Interaction of HLA-E with peptides and the peptide transporter in vitro: Implications for its function in antigen presentation. *J. Immunol.* **160**, (1998).

374. Hansen, S. G. *et al.* Broadly targeted CD8+ T cell responses restricted by major histocompatibility complex E. *Science (80-.).* (2016) doi:10.1126/science.aac9475.

375. Gumá, M. *et al.* Imprint of human cytomegalovirus infection on the NK cell receptor repertoire. *Blood* **104**, (2004).

376. Starke, K. R. *et al.* The isolated effect of age on the risk of COVID-19 severe outcomes: A systematic review with meta-analysis. *BMJ Glob. Heal.* (2021) doi:10.1101/2021.05.27.21257909.

377. Kaiser, B. K., Pizarro, J. C., Kerns, J. & Strong, R. K. Structural basis for NKG2A/CD94 recognition of HLA-E. *Proc. Natl. Acad. Sci. U. S. A.* (2008) doi:10.1073/pnas.0802736105.

378. McManus, W. R. *et al.* HIV-1 in lymph nodes is maintained by cellular proliferation during antiretroviral therapy. *J. Clin. Invest.* **129**, (2019).

379. Brunetta, E. *et al.* Chronic HIV-1 viremia reverses NKG2A/NKG2C ratio on natural killer cells in patients with human cytomegalovirus co-infection. *AIDS* (2010) doi:10.1097/QAD.0b013e3283328d1f.

380. Li, M. *et al.* Age related human T cell subset evolution and senescence. *Immun. Ageing*

16, (2019).

381. Saini, S. K. *et al.* SARS-CoV-2 genome-wide T cell epitope mapping reveals immunodominance and substantial CD8+ T cell activation in COVID-19 patients. *Sci. Immunol.* **6**, (2021).

382. Kiepiela, P. *et al.* CD8+ T-cell responses to different HIV proteins have discordant associations with viral load. *Nat. Med.* (2007) doi:10.1038/nm1520.

383. Kaufmann, D. E. *et al.* Comprehensive Analysis of Human Immunodeficiency Virus Type 1-Specific CD4 Responses Reveals Marked Immunodominance of gag and nef and the Presence of Broadly Recognized Peptides. *J. Virol.* (2004) doi:10.1128/jvi.78.9.4463-4477.2004.

384. Adland, E. *et al.* Nef-specific CD8+ T cell responses contribute to HIV-1 immune control. *PLoS One* (2013) doi:10.1371/journal.pone.0073117.

385. Ngumbela, K. C. *et al.* Targeting of a CD8 T cell env epitope presented by HLA-B*5802 is associated with markers of HIV disease progression and lack of selection pressure. *AIDS Res. Hum. Retroviruses* (2008) doi:10.1089/aid.2007.0124.

386. Shiner, E. K., Holbrook, B. C. & Alexander-Miller, M. A. CD4+ T cell subset differentiation and avidity setpoint are dictated by the interplay of cytokine and antigen mediated signals. *PLoS One* (2014) doi:10.1371/journal.pone.0100175.

387. Watanabe, S., Yamada, Y. & Murakami, H. Expression of Th1/Th2 cell–related chemokine receptors on CD4+ lymphocytes under physiological conditions. *Int. J. Lab. Hematol.* **42**, (2020).

388. Cosmi, L. *et al.* CRTH2 is the most reliable marker for the detection of circulating human type 2 Th and type 2 T cytotoxic cells in health and disease. *Eur. J. Immunol.* **30**, (2000).

389. Kumar, B. V., Connors, T. J. & Farber, D. L. Human T Cell Development, Localization, and Function throughout Life. *Immunity* vol. 48 (2018).

390. Schmidt, M. E. & Varga, S. M. The CD8 T cell response to respiratory virus infections. *Frontiers in Immunology* vol. 9 (2018).

391. Weiskopf, D. *et al.* Comprehensive analysis of dengue virus-specific responses supports an HLA-linked protective role for CD8+ T cells. *Proc. Natl. Acad. Sci. U. S. A.* **110**, (2013).

392. Song, J. W. *et al.* Immunological and inflammatory profiles in mild and severe cases of COVID-19. *Nat. Commun.* **11**, (2020).

393. Gangaev, A. *et al.* Identification and characterization of a SARS-CoV-2 specific CD8+ T cell response with immunodominant features. *Nat. Commun.* **12**, (2021).

394. Mbiribindi, B. *et al.* Epstein–Barr virus peptides derived from latent cycle proteins alter NKG2A + NK cell effector function. *Sci. Rep.* **10**, (2020).

395. Schlums, H. *et al.* Cytomegalovirus infection drives adaptive epigenetic diversification of NK cells with altered signaling and effector function. *Immunity* (2015) doi:10.1016/j.immuni.2015.02.008.

396. Turk, G. *et al.* A Possible Sterilizing Cure of HIV-1 Infection Without Stem Cell Transplantation. *Ann. Intern. Med.* **175**, (2022).

397. Jiang, C. *et al.* Distinct viral reservoirs in individuals with spontaneous control of HIV-1. *Nature* **585**, (2020).

398. Liao, M. *et al.* Single-cell landscape of bronchoalveolar immune cells in patients with COVID-19. *Nat. Med.* **26**, (2020).

399. Tamayo-Velasco, Á. *et al.* HGF, IL-1α, and IL-27 are robust biomarkers in early severity stratification of COVID-19 patients. *J. Clin. Med.* **10**, (2021).

400. Pereira, B. I. *et al.* Senescent cells evade immune clearance via HLA-E-mediated NK and CD8+ T cell inhibition. *Nat. Commun.* **10**, (2019).

401. Morandi, F., Airoldi, I. & Pistoia, V. IL-27 driven upregulation of surface HLA-e expression on monocytes inhibits IFN-γ release by autologous NK cells. *J. Immunol. Res.* **2014**, (2014).

402. Ruiz-Riol, M. *et al.* Identification of Interleukin-27 (IL-27)/IL-27 Receptor Subunit Alpha as a Critical Immune Axis for In Vivo HIV Control. *J. Virol.* **91**, (2017).

403. Trachtenberg, E. *et al.* Advantage of rare HLA supertype in HIV disease progression. *Nat. Med.* **9**, (2003).

404. Björkström, N. K., Strunz, B. & Ljunggren, H. G. Natural killer cells in antiviral immunity. *Nat. Rev. Immunol. 2021 222* **22**, 112–123 (2021).

405. Björkström, N. K., Ljunggren, H. G. & Sandberg, J. K. CD56 negative NK cells: Origin, function, and role in chronic viral disease. *Trends Immunol.* **31**, (2010).

406. Judge, C. J. *et al.* CD56 bright NK IL-7Rα expression negatively associates with HCV level, and IL-7-induced NK function is impaired during HCV and HIV infections . *J. Leukoc. Biol.* **102**, (2017).

407. Eisenhardt, M. *et al.* CD27(R)CD56Bright natural killer cells may be involved in spontaneous clearance of acute hepatitis C in HIV-positive patients. *AIDS* **28**, (2014).

408. Carrega, P. *et al.* CD56 bright Perforin low Noncytotoxic Human NK Cells Are Abundant in Both Healthy and Neoplastic Solid Tissues and Recirculate to Secondary Lymphoid Organs via Afferent Lymph . *J. Immunol.* **192**, (2014).

409. Mailliard, R. B. *et al.* Dendritic Cells Mediate NK Cell Help for Th1 and CTL Responses: Two-Signal Requirement for the Induction of NK Cell Helper Function. *J. Immunol.* **171**, (2003).

410. Pallmer, K. & Oxenius, A. Recognition and regulation of T cells by NK cells. *Frontiers in Immunology* vol. 7 (2016).

411. Castriconi, R. *et al.* Molecular mechanisms directing migration and retention of natural killer cells in human tissues. *Frontiers in Immunology* vol. 9 (2018).

412. Gumá, M. *et al.* Imprint of human cytomegalovirus infection on the NK cell receptor repertoire. *Blood* **104**, 3664–3671 (2004).

413. Demaria, O. *et al.* Identification of druggable inhibitory immune checkpoints on Natural Killer cells in COVID-19. *Cellular and Molecular Immunology* vol. 17 (2020).

414. Zheng, M. *et al.* Functional exhaustion of antiviral lymphocytes in COVID-19 patients. *Cellular and Molecular Immunology* vol. 17 (2020).

References

415. Nguyen, S. *et al.* HLA-E upregulation on IFN-γ-activated AML blasts impairs CD94/NKG2A-dependent NK cytolysis after haplo-mismatched hematopoietic SCT. *Bone Marrow Transplant.* **43**, (2009).

416. McGonagle, D., Sharif, K., O'Regan, A. & Bridgewood, C. The Role of Cytokines including Interleukin-6 in COVID-19 induced Pneumonia and Macrophage Activation Syndrome-Like Disease. *Autoimmunity Reviews* vol. 19 (2020).

417. Merino, A. *et al.* Chronic stimulation drives human NK cell dysfunction and epigenetic reprograming. *J. Clin. Invest.* (2019) doi:10.1172/JCI125916.

418. Oriol-Tordera, B. *et al.* Methylation regulation of Antiviral host factors, Interferon Stimulated Genes (ISGs) and T-cell responses associated with natural HIV control. *PLOS Pathog.* **16**, e1008678 (2020).

419. De Maria, A. *et al.* The impaired NK cell cytolytic function in viremic HIV-1 infection is associated with a reduced surface expression of natural cytotoxicity receptors (NKp46, NKp30 and NKp44). *Eur. J. Immunol.* **33**, (2003).

420. Fogli, M. *et al.* Significant NK cell activation associated with decreased cytolytic function in peripheral blood of HIV-1-infected patients. *Eur. J. Immunol.* **34**, (2004).

421. Luo, Z. *et al.* Increased natural killer cell activation in HIVInfected immunologic non-responders correlates with CD4+ T cell recovery after antiretroviral therapy and viral suppression. *PLoS One* **12**, (2017).

422. Rahman, S. A. *et al.* Lymph node CXCR5+ NK cells associate with control of chronic SHIV infection. *JCI Insight* **7**, (2022).

423. Yaqinuddin, A. & Kashir, J. Innate immunity in COVID-19 patients mediated by NKG2A receptors, and potential treatment using Monalizumab, Cholroquine, and antiviral agents. *Med. Hypotheses* **140**, (2020).

424. Van Hall, T. *et al.* Monalizumab: Inhibiting the novel immune checkpoint NKG2A. *Journal for ImmunoTherapy of Cancer* vol. 7 (2019).

425. Meier, U.-C. *et al.* Shared Alterations in NK Cell Frequency, Phenotype, and Function in Chronic Human Immunodeficiency Virus and Hepatitis C Virus Infections. *J. Virol.* **79**,

(2005).

426.   Harper, J. *et al.* IL-21 and IFNα therapy rescues terminally differentiated NK cells and limits SIV reservoir in ART-treated macaques. *Nat. Commun.* **12**, (2021).

427.   Long, B. R. *et al.* Elevated frequency of gamma interferon-producing NK cells in healthy adults vaccinated against influenza virus. *Clin. Vaccine Immunol.* **15**, (2008).

428.   Pardi, N. *et al.* Expression kinetics of nucleoside-modified mRNA delivered in lipid nanoparticles to mice by various routes. *J. Control. Release* **217**, (2015).

429.   Williams, L. D. *et al.* Immune Activation Is Associated with CD8 T Cell Interleukin-21 Production in HIV-1-Infected Individuals. *J. Virol.* **88**, (2014).

430.   De Biasi, S. *et al.* Marked T cell activation, senescence, exhaustion and skewing towards TH17 in patients with COVID-19 pneumonia. *Nat. Commun.* **11**, (2020).

431.   Roncati, L., Nasillo, V., Lusenti, B. & Riva, G. Signals of Th2 immune response from COVID-19 patients requiring intensive care. *Annals of Hematology* vol. 99 (2020).

432.   Guardo, A. C. *et al.* Detection of HIV-1-specific T-cell immune responses in highly HIV-exposed uninfected individuals by in-vitro dendritic cell co-culture. *AIDS* **29**, (2015).

433.   Brochot, E. *et al.* Anti-spike, Anti-nucleocapsid and Neutralizing Antibodies in SARS-CoV-2 Inpatients and Asymptomatic Individuals. *Front. Microbiol.* **11**, (2020).

434.   Baker, J. R. *et al.* Early Th2 inflammation in the upper respiratory mucosa as a predictor of severe COVID-19 and modulation by early treatment with inhaled corticosteroids: a mechanistic analysis. *Lancet Respir. Med.* **10**, 545–556 (2022).

435.   Mallajosyula, V. *et al.* CD8+T cells specific for conserved coronavirus epitopes correlate with milder disease in COVID-19 patients. *Sci. Immunol.* **6**, 5669 (2021).

436.   Woldemeskel, B. A., Kwaa, A. K. & Blankson, J. N. Viral reservoirs in elite controllers of HIV-1 infection: Implications for HIV cure strategies. *EBioMedicine* vol. 62 (2020).

437.   Bajaj, V. *et al.* Aging, Immunity, and COVID-19: How Age Influences the Host Immune Response to Coronavirus Infections? *Front. Physiol.* **11**, 1793 (2021).

438. Lee, N. *et al.* IL-6 receptor α defines effector memory CD81 T cells producing Th2 cytokines and expanding in asthma. *Am. J. Respir. Crit. Care Med.* **190**, (2014).

439. Hinks, T. S. C., Hoyle, R. D. & Gelfand, E. W. CD8+ Tc2 cells: Underappreciated contributors to severe asthma. *European Respiratory Review* vol. 28 (2019).

440. Williams, L. D. *et al.* Interleukin-21-Producing HIV-1-Specific CD8 T Cells Are Preferentially Seen in Elite Controllers. *J. Virol.* **85**, (2011).

441. Carrillo, J. *et al.* Memory B cell dysregulation in HIV-1-infected individuals. *AIDS* **32**, (2018).

442. Levesque, M. C. *et al.* Polyclonal B cell differentiation and loss of gastrointestinal tract germinal centers in the earliest stages of HIV-1 infection. *PLoS Med.* **6**, (2009).

443. Helmold Hait, S. *et al.* Early T Follicular Helper Cell Responses and Germinal Center Reactions Are Associated with Viremia Control in Immunized Rhesus Macaques. *J. Virol.* **93**, (2019).

444. de Taeye, S. W. *et al.* FcγR Binding and ADCC Activity of Human IgG Allotypes. *Front. Immunol.* (2020) doi:10.3389/fimmu.2020.00740.

445. Ren, Y. *et al.* Relationships between Neutralization, Binding, and ADCC of Broadly Neutralizing Antibodies against Reservoir HIV. *J. Virol.* (2020) doi:10.1128/jvi.01808-20.

446. Planque, S. *et al.* Neutralization of genetically diverse HIV-1 strains by IgA antibodies to the gp120-CD4-binding site from long-term survivors of HIV infection. *AIDS* (2010) doi:10.1097/QAD.0b013e3283376e88.

447. Renaude, E. *et al.* Epigenetic Reprogramming of CD4+ Helper T Cells as a Strategy to Improve Anticancer Immunotherapy. *Frontiers in Immunology* vol. 12 (2021).
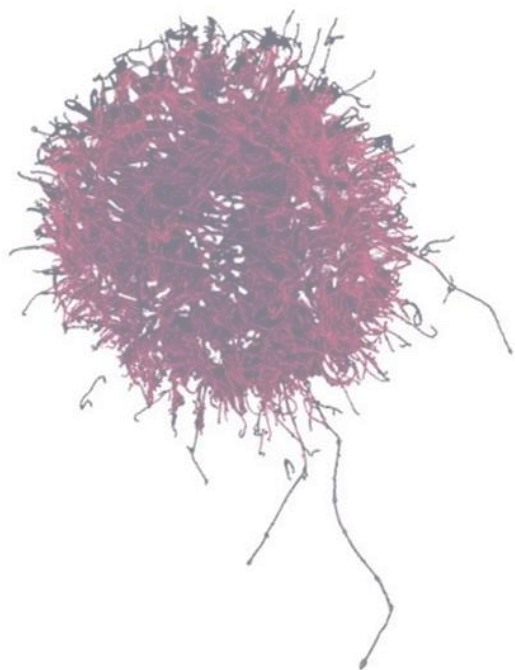
ANNEXES

Research subjects

Chapter I. Innate cellular response to acute viral infections. COVID-19 severity is related to exhausted NK cells with impaired HLA-E mediated response

Group	Age	Sex (M/F)	Days post inf/vacc	Risk factors	Oxygen required	Vaccination
Severe - 1	62	M	20		Low flow	
Severe - 2	50	M	18		Low flow	
Severe - 3	55	F	12	Dyslipidemia	High Flow	
Severe - 4	37	M	18	Dyslipidemia	Low flow	
Severe - 5	51	F	27	Hepatopathy	High Flow	
Severe - 6	61	F	28	Dyslipidemia, allergy,	Low flow	
Severe - 7	57	M	5	Allergy, dyslipidemia, active neoplasm	Low flow	
Severe - 8	58	M	13	HIV[+], dyslipidemia	Low flow	
Severe - 9	49	M	17	Obesity, dyslipidemia, OSAS	High Flow	
Severe - 10	43	F	10	Obesity	Low flow	
Severe - 11	63	M	26	Diabetes, dyslipidemia	High Flow	
Severe - 12	53	F	22	Allergy, obesity	Low flow	
Mild -1	41	F	15			
Mild -2	52	F	8			
Mild -3	61	M	9			
Mild -4	66	F	9	Dyslipidemia		
Mild -5	35	M	5			
Mild -6	26	M	12	Autoimmunity		
Mild -7	32	F	16			
Mild -8	55	F	16			
Mild -9	51	F	15	Allergy, dyslipidemia, hepatopathy		
Mild -10	30	F	18	Obesity		
Mild -11	64	M	19	Allergy, hepatopathy		
Mild -12	49	F	26	Asthma		
Uninfected - 1	61	F	-			
Uninfected - 2	49	F	-			
Uninfected - 3	36	M	-			
Uninfected - 4	61	M	-			
Uninfected - 5	48	M	-			
Uninfected - 6	54	F	-			
Uninfected - 7	59	M	-			
Uninfected - 8	58	M	-			
Uninfected - 9	51	M	-			
Uninfected - 10	43	F	-			
Uninfected - 11	65	M	-			
Uninfected - 12	51	F	-			
Vaccinated - 1	49	M	33			Moderna (2/2)
Vaccinated - 2	50	M	33			Moderna (2/2)
Vaccinated - 3	48	F	28			Moderna (2/2)
Vaccinated - 4	50	F	32			Pfizer (2/2)
Vaccinated - 5	42	M	31			Pfizer (2/2)
Vaccinated - 6	46	F	29			Pfizer (2/2)

Supplementary Table 1. Severe and Mild COVID-19, Uninfected and vaccinated individuals included in this study. Abbreviatures: M: Male, F: Female, N/D: not determined.

Chapter II. Innate cellular response to chronic viral infections. Disruption of the HLA-E/NKG2X axis is associated with uncontrolled chronic HIV infections

Sample	Age (years)	Gender (M/F)	Plasma viral load (HIV-1 RNA copies/mL)	Proviral (HIV-1 DNA copies/10^6 PBMCs)	CD4 count (cells/mm^3)
HIV-low 1	34	M	950	163.5	608
HIV-low 2	56	F	<50	16	873
HIV-low 3	35	M	9999	317.7	438
HIV-low 4	46	M	1100	76.7	485
HIV-low 5	46	F	<50	6.7	1083
HIV-low 6	48	F	8900	412.5	913
HIV-low 7	37	M	1800	180.8	511
HIV-low 8	50	F	<50	9.1	487
HIV-low 9	40	F	340	294.3	832
HIV-low 10	37	F	<50	25.7	665
HIV-low 11	33	M	530	25.8	948
HIV-low 12	29	M	<50	0	892
HIV-low 13	45	F	2900	278.5	582
HIV-low 14	46	F	2800	32.5	434
HIV-low 15	38	M	<50	90.4	583
HIV-low 16	26	M	2300	49.1	642
HIV-low 17	44	M	50	6.2	872
HIV-low 18	41	F	<50	20.9	672
HIV-low 19	50	F	50	0	1228
HIV-low 20	46	M	66	28.6	755
HIV-low 21	51	M	<50	41.5	450
HIV-low 22	48	F	230	15.9	516
HIV-low 23	43	M	330	31.3	1237
HIV-low 24	48	M	50	18.4	601
HIV-low 25	35	F	<50	11.5	930
HIV-low 26	36	F	880	12.1	1343
HIV-low 27	29	M	5624	1662.4	823
HIV-low 28	41	M	6127	50.2	531
HIV-low 29	34	M	400	220.1	1035
HIV-low 30	33	F	7923	366.5	524
HIV-low 31	30	M	4482	0	1151
HIV-high 1	37	F	140000	231.9	11
HIV-high 2	40	F	64000	922.6	282
HIV-high 3	24	F	610000	1722.4	128
HIV-high 4	33	F	1200000	80.1	75
HIV-high 5	50	F	54000	363.6	67
HIV-high 6	23	M	50925	1176.5	505
HIV-high 7	23	M	240039	1144.6	388
HIV-high 8	24	M	93928	3246.6	256
HIV-high 9	24	M	365977	1204.6	726
HIV-high 10	28	M	327087	2127.2	544
HIV-high 11	30	M	61078	558.4	380
HIV-high 12	31	M	194091	1962.5	271
HIV-high 13	32	M	170000	507	17
HIV-high 14	35	M	95365	3149.2	240
HIV-high 15	35	M	102936	1346.3	283
HIV-high 16	35	M	63381	1128.7	384
HIV-high 17	34	M	60841	N/D	348
HIV-high 18	42	M	85661	N/D	608
HIV-high 19	39	M	74285	N/D	156
HIV-high 20	26	M	640803	N/D	314

Supplementary Table 2. HIV-high and HIV-low samples included in this study. Abbreviatures: M: Male, F: Female, N/D: not determined.

Sample	Age (years)	Gender (M/F)	Plasma viral load (HIV-1 RNA copies/mL)	Proviral (HIV-1 DNA copies/10^6 PBMCs)	CD4 count (cells/mm^3)
Acute-1			327023	520	891
Acute-2			312060	2840	332
Acute-3			400	521	590
Acute-4			51638	570	673
Acute-5			25782	652	463
Acute-6			904569	3070	317
Acute-7			26348	414	646
Acute-8			64083	569.8	558
Chronics-1			13893	518	529
Chronics-2			11000	596	914
Chronics-3			12000	161	495
Chronics-4			27342	390	847
Chronics-5			44000	100	437
Chronics-6	46	M	4900	176	462
Chronics-7	32	M	7200	282	328
Chronics-8	28	F	15000	550	456
Chronics-9	44	M	50000	222	629
Chronics-10	34	F	8900	9	572
Chronics-11	29	M	13284	317.5	661
Treated-1	47	M	50	52	532
Treated-2	41	M	50	388	426
Treated-3	30	F	25	191	786
Treated-4	45	M	50	43	558
Treated-5	47	M	40	116	1053
Treated-6	40	M	40	89.3	659
LTNP-1	31	F	25	0	922
LTNP-2	40	F	40	9	752
LTNP-3	46	F	25	6	1557
LTNP-4	43	F	25	4	372
LTNP-5	59	M	25	11	411
LTNP-6	40	F	25	180	245
LTNP-7	40	F	56	4	898
LTNP-8	50	M	25	0	450
LTNP-9	46	M	25	3	940
LTNP-10	52	M	25	0	667
LTNP-11	53	M	25	21	959
LTNP-12	55	F	50	23.8	838
LTNP-13	45	F	790	467	588
LTNP-14	40	M	55	27	1014
LTNP-15	48	M	1978	9	1840
LTNP-16	36	F	374	75	594
LTNP-17		M	972	38	405
LTNP-18	44	F	1300	64	510
LTNP-19	47	M	1200	75	594
LTNP-20	47	M	1500	38	405
LTNP-21	41	M	200	64	510
LTNP-22	54	M	480	480	76
LTNP-23	52	F	1600	1600	201.8

Supplementary Table 3. Unrelated cohort samples included in this study. Abbreviatures: M: Male, F: Female.

Chapter III. Adaptive cellular response to acute viral infections. Differences in T-cell immunity against SARS-CoV-2 nucleocapsid are related to COVID-19 outcome

Group	Age	Sex (M/F)	Risk factors	Oxygen require	Basal activation	Specific stimulation
Severe - 1	29	M		High Flow		x
Severe - 2	69	M	Obesity, asthma, COPD,	Low flow		x
Severe - 3	64	F	Hypertension, obesity , cancer	Low flow		x
Severe - 4	73	F	Hypertension, diabetes, asthma	No Oxygen		x
Severe - 5	46	M		Low flow		x
Severe - 6	34	M		High Flow		x
Severe - 7	26	F		No Oxygen		x
Severe - 8	56	M	Hypertension, obesity, diabetes, COPD	Low flow	x	x
Severe - 9	76	F	Diabetes		x	
Severe - 10	70	M	Hypertension, CRI, Transplant		x	
Mild -1	24	F				x
Mild -2	29	F				x
Mild -3	61	M				x
Mild -4	43	F				x
Mild -5	45	F				x
Mild -6	45	M				x
Mild -7	44	F				x
Mild -8	42	F			x	x
Mild -9	63	F			x	
Mild -10	53	F			x	
Non-seroconvertor - 1	45	F				x
Non-seroconvertor - 2	43	M	Allergy			x
Non-seroconvertor - 3	38	F				x
Non-seroconvertor - 4	64	F	Hypertension			x
Non-seroconvertor - 5	40	F				x
Non-seroconvertor - 6	52	F				x
Non-seroconvertor - 7	44	F			x	x
Non-seroconvertor - 8	41	M			x	x
Non-seroconvertor - 9	50	F			x	

Supplementary Table 5. Severe, Mild and non-seroconvertors COVID-19 included in this study. Abbreviatures: M: Male, F: Female, N/D: not determined.

Chapter IV. Alternative adaptive responses to chronic viral infection. T-follicular-like CD8+ T cell responses in chronic HIV infection are associated with virus control and antibody isotype switching to IgG.

Sample	Age (years)	Gender (M/F)	Plasma viral load (HIV-1 RNA copies/mL)	CD4 count (cells/mm^3)	CD4/CD8 ratio
HIV-controller 1	34	F	159	1190	2,11
HIV-controller 2	56	M	40	945	1,22
HIV-controller 3	35	F	50	1134	1,36
HIV-controller 4	46	F	<25	1513	1,85
HIV-controller 5	46	M	41	871	0,66
HIV-controller 6	48	F	29	509	0,49
HIV-controller 7	37	F	<40	1344	2,86
HIV-controller 8	50	F	<40	855	1,80
HIV-controller 9	40	M	<25	770	0,64
HIV-controller 10	37	F	299	682	1,22
HIV-controller 11	33	F	250	638	0,47
HIV-controller 12	29	M	120	1638	1,24
HIV-controller 13	45	F	749	642	0,67
HIV-controller 14	46	M	250	934	0,93
HIV-controller 15	38	M	890	684	0,55
HIV-controller 16	26	M	149	997	0,75
HIV-controller 17	44	F	1102	660	0,36
HIV-controller 18	41	M	830	500	0,33
HIV-controller 19	50	M	1900	528	0,56
HIV-controller 20	46	M	290	1328	0,64
HIV-controller 21	51	M	1300	692	0,43
HIV-controller 22	48	F	410	802	1,00
HIV-controller 23	43	F	170	504	0,37
HIV-controller 24	48	M	1000	364	0,24
HIV-non-controller 1	37	M	64029	468	0,48
HIV-non-controller 2	40	M	74285	156	0,06
HIV-non-controller 3	24	M	59606	192	0,26
HIV-non-controller 4	33	M	640803	314	0,34
HIV-non-controller 5	50	F	275761	6	0,01
HIV-non-controller 6	23	M	148867	144	0,13
HIV-non-controller 7	23	M	23536	605	0,40
HIV-non-controller 8	24	M	42551	275	0,57
HIV-non-controller 9	24	M	24493	382	1,15
HIV-non-controller 10	28	M	14389	319	0,31
HIV-non-controller 11	30	M	144531	362	0,29
HIV-non-controller 12	31	M	19298	578	1,00
HIV-non-controller 13	32	M	139342	814	0,63
HIV-non-controller 14	35	M	41172	986	0,67
HIV-non-controller 15	35	M	100577	683	0,43
HIV-non-controller 16	35	M	35400	554	0,54
HIV-non-controller 17	34	M	635700	430	0,43
HIV-non-controller 18	42	M	60841	348	0,49
HIV-non-controller 19	39	M	5576	515	0,64
HIV-non-controller 20	26	M	85661	608	0,61

Supplementary Table 5. HIV-Controllers and Non-controllers included in this study.

**Abbreviatures: M: Male, F: Female.**

Supplementary Figures
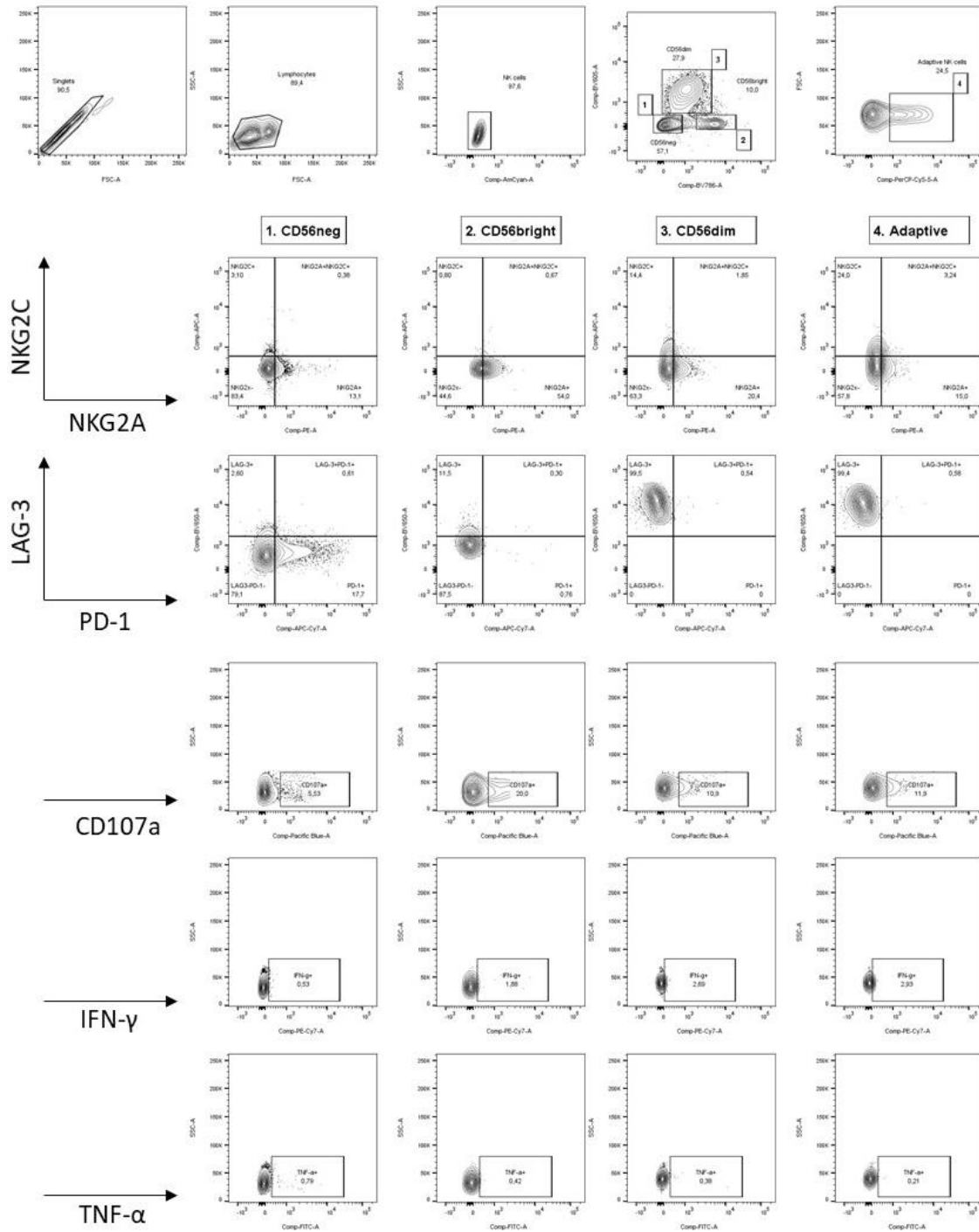
Supplementary Figure 1. Gating strategy for NK cell populations based on the expression of CD45, CD16, CD57, NKG2A and NKG2C. NK cells subpopulations were classified as CD56^{neg} (CD3$^-$CD56$^-$CD16$^-$CD57$^-$), CD56^{dim} (CD3$^-$CD56^{dim}CD16$^+$CD57$^-$), adaptive NK cells (CD3$^-$CD56^{dim}CD16$^+$CD57$^+$) and CD56^{bright} (CD3$^-$CD56^{bright}CD16$^-$CD57$^-$). HLA-E NK receptors NKG2A and NKG2C surface expression and exhaustion/activation markers PD-1 and LAG-3 were evaluated in all NK subpopulations. Degranulation was measured as CD107a+ and IFN-γ and TNF-α cytokine production as well.
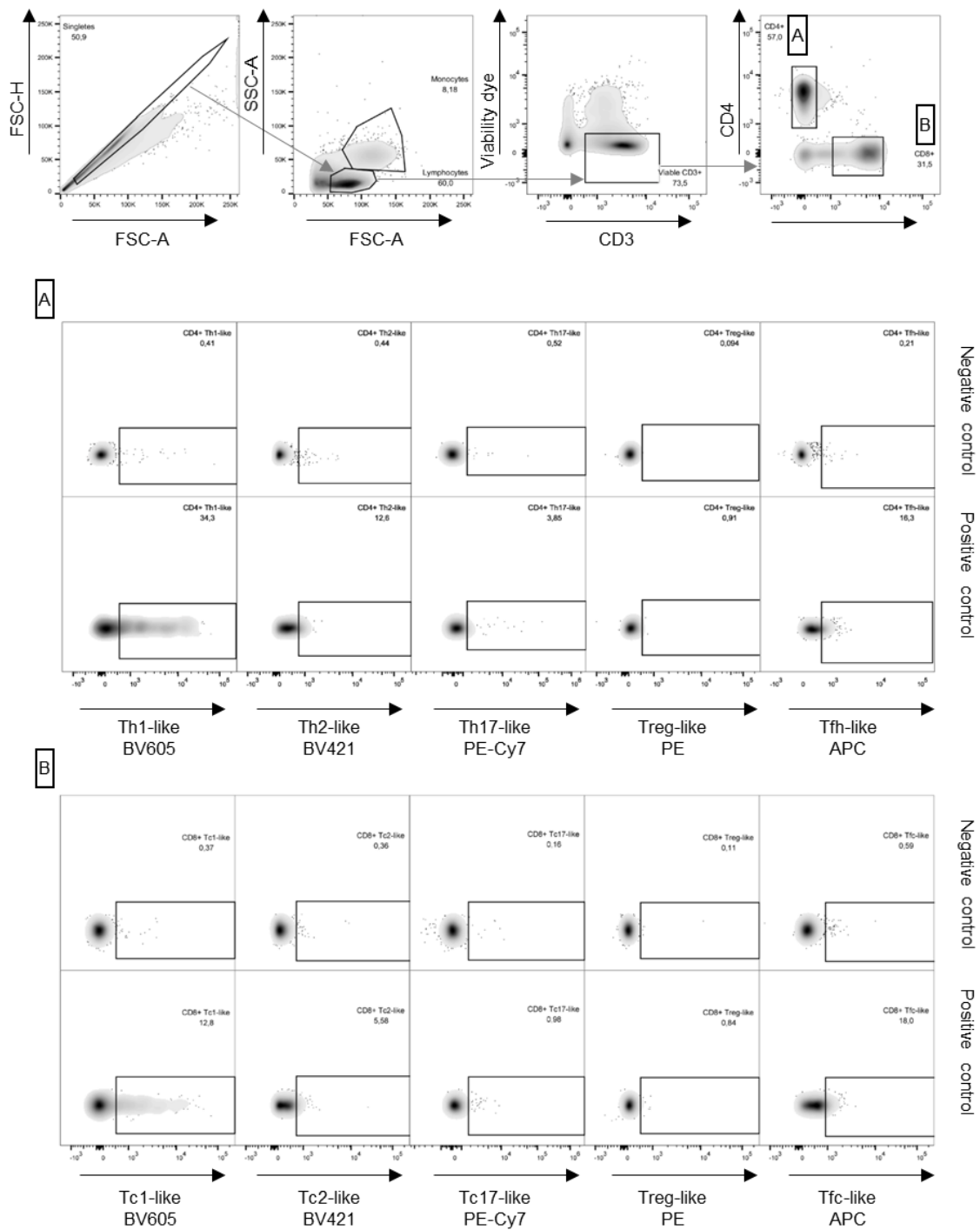
Supplementary Figure 2. Gating strategy for *Boosted flow* screening
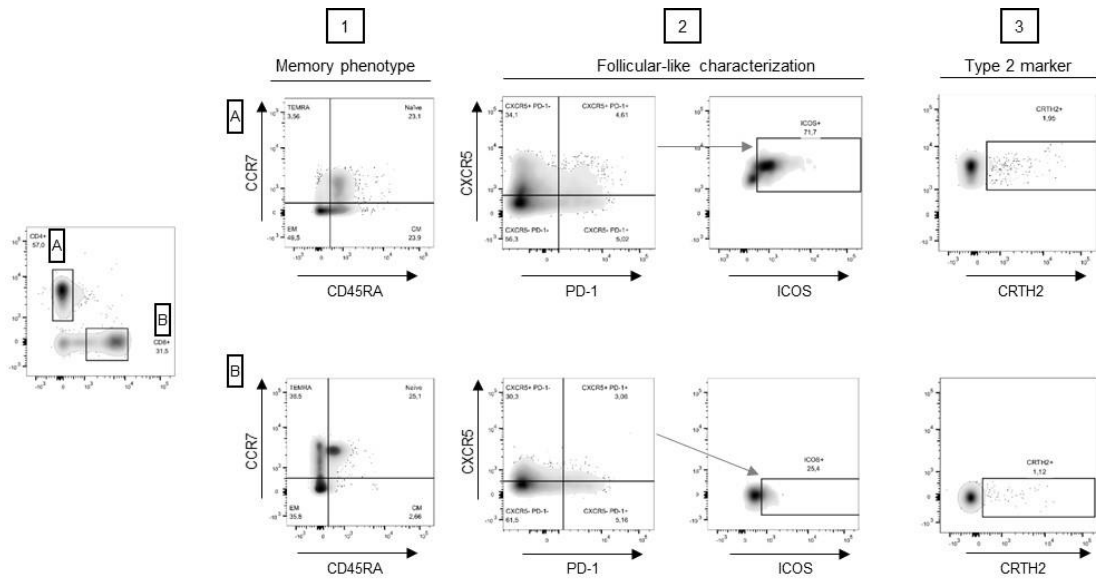
Supplementary Figure 3. Gating strategy for CD4+ (A) and CD8+ (B) T-cell memory phenotyping (1), Tfh/Tfc characterization (2) and Th2/Tc2 marker CRTH2 (3).
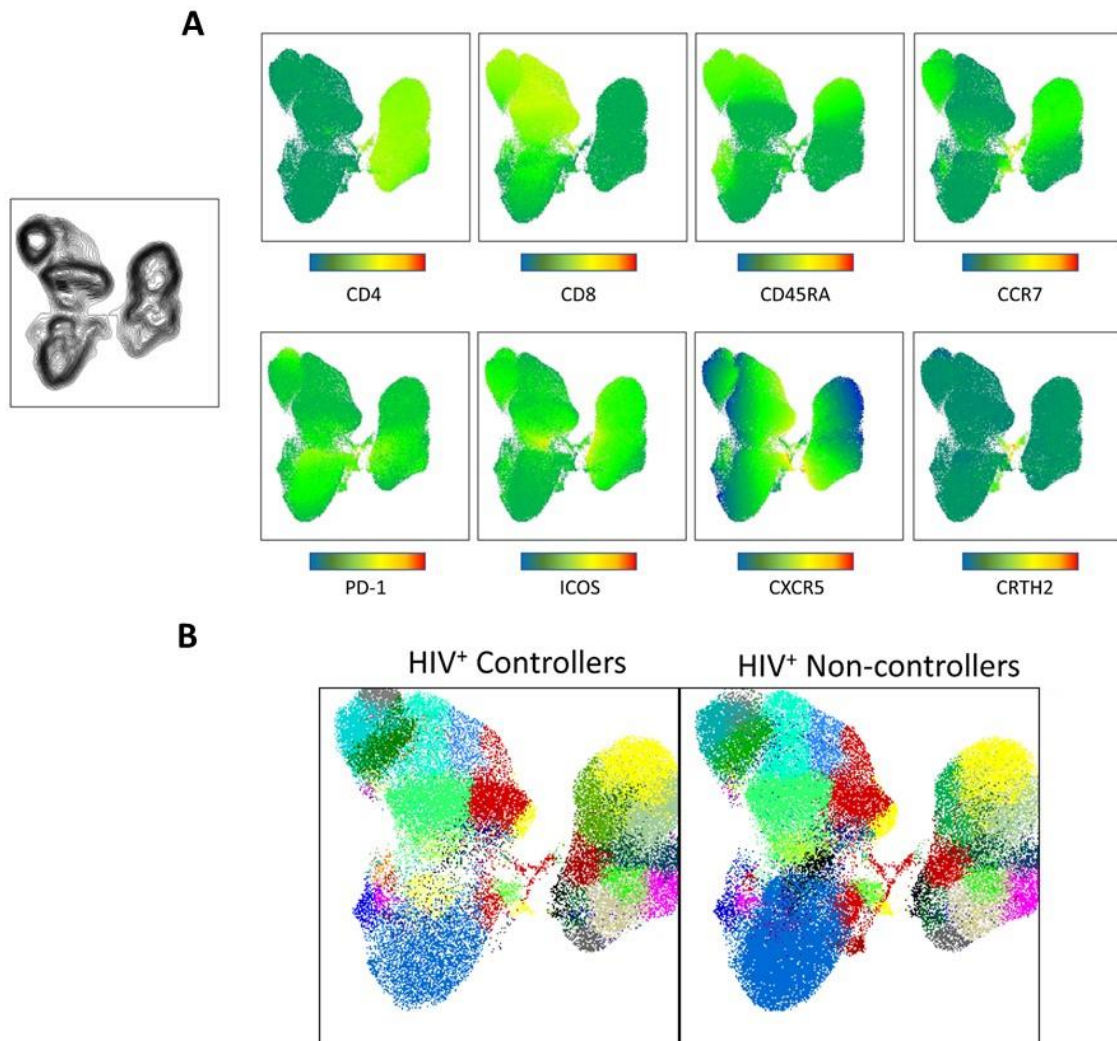
Supplementary Figure 3. UMAP visualization. (A) Dimensional reduction was applied based on the expression of T-cell lineage (CD4, CD8, CD45RA and CCR7), Tfh/Tfc (PD-1, ICOS and CXCR5) and Th2/Tc2 (CRTH2) markers. (**B**) Visualization of the FlowSOM clustering between HIV controllers and non-controllers. Increased representation of clusters in non-controllers (black).
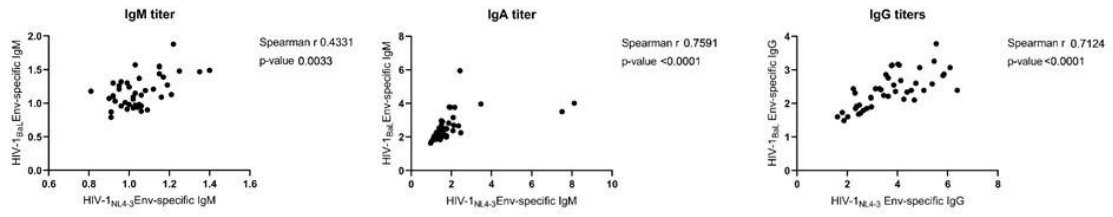
**Supplementary Figure 5. Direct correlation between HIV_{NL4-3} and HIV_{BaL} Env-specific IgM, IgA and IgG titers.**
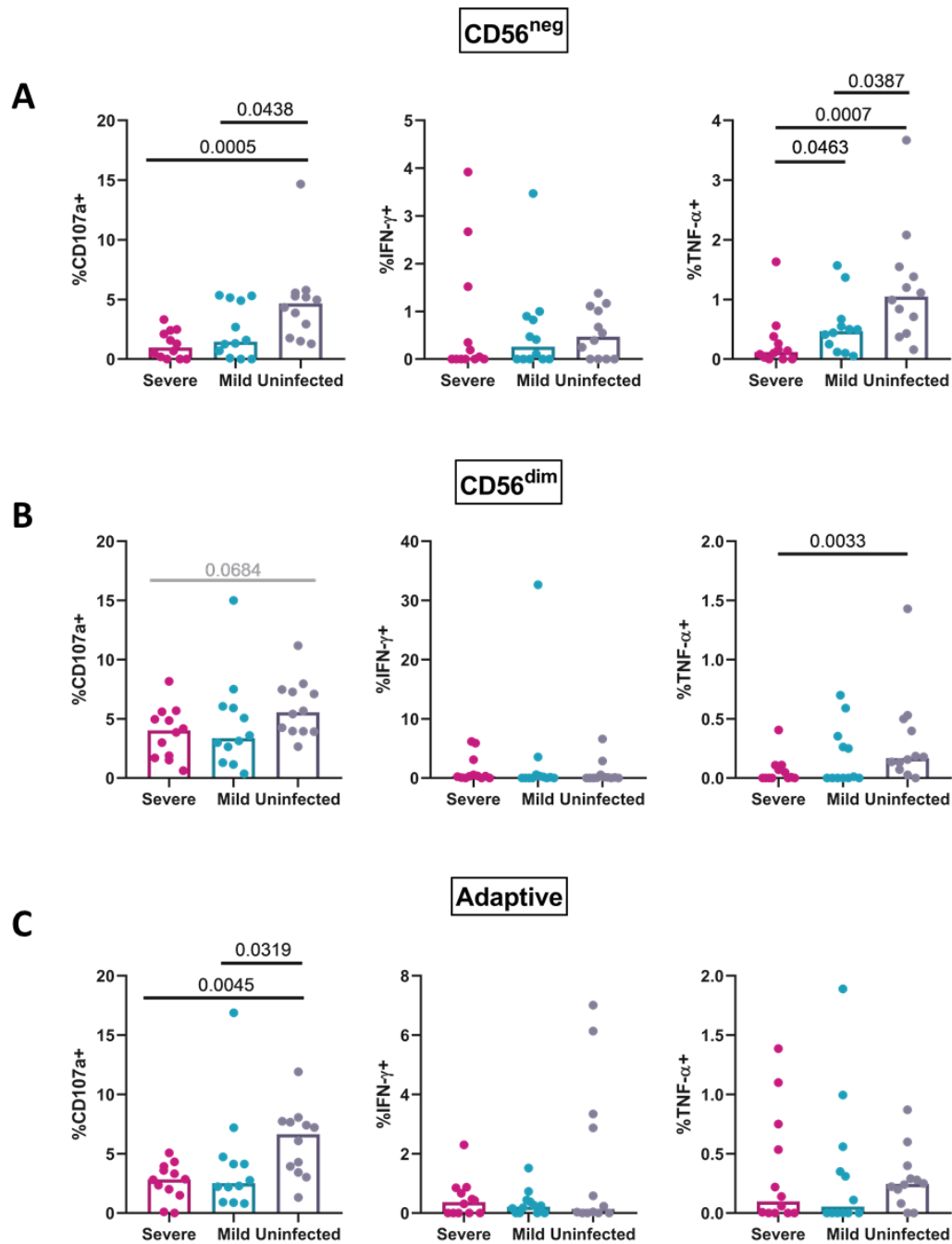
Supplementary Figure 6. NK cell susbets response to HLA-E null K562 cells. Gating of CD107a^{+}, IFN-γ^{+} and TNF-α^{+} NK cells from Severe COVID-19 (n=12, magenta), mild COVID- 19 (n=12, blue) and uninfected individuals (n=12, grey). **(A)** %CD107a^{+}, % IFN-γ^{+} and % TNF- α [+] of CD56^{neg} NK Cells in response to HLA-E null K562 cells. **(B)** %CD107a^{+}, % IFN-γ^{+} and % TNF- α [+] of CD56^{dim} NK Cells in response to HLA-E null K562 cells. **(C)** %CD107a^{+}, % IFN-γ^{+} and % TNF- α [+] of adaptive NK Cells in response to HLA-E null K562 cells Mann-Whitney test was performed to compared differences between groups and results were considered significant when p-value<0.05. Trends are marked in grey.

Supplementary Figure 7. NKG2X expression in Adaptive NK cells. NKG2A (A) and NKG2C (B) expression was determined in CD56^{dim} CD16$^+$ CD57$^+$ adaptive NK cells.
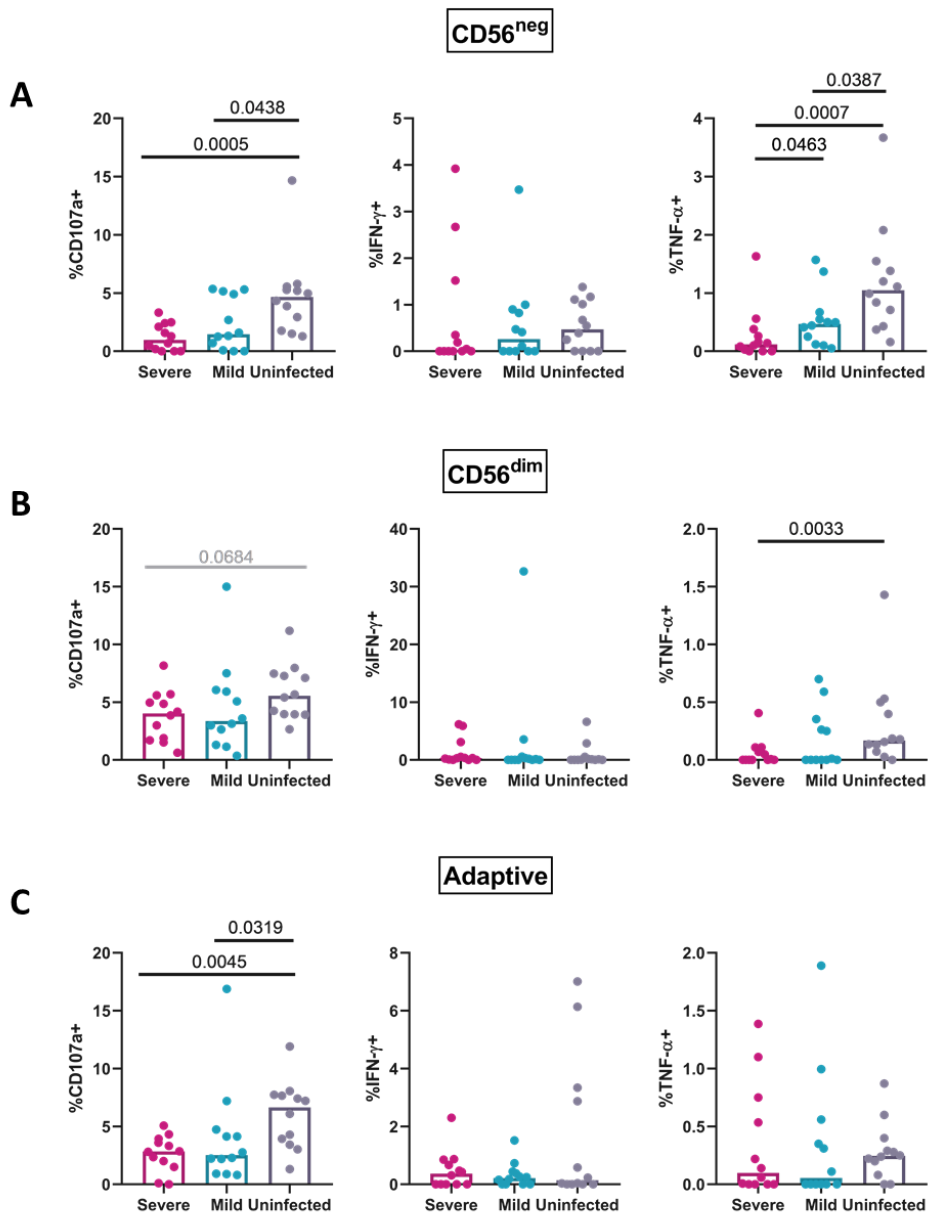
Supplementary Figure 8. NK cell susbets response to HLA-E null K562 cells. Gating of CD107a⁺, IFN-γ⁺ and TNF-α⁺ NK cells from Severe COVID-19 (n=12, magenta), mild COVID- 19 (n=12, blue) and uninfected individuals (n=12, grey). **(A)** %CD107a⁺, % IFN-γ⁺ and % TNF- α ⁺ of CD56^{neg} NK Cells in response to HLA-E null K562 cells. **(B)** %CD107a⁺, % IFN-γ⁺ and % TNF- α ⁺ of CD56^{dim} NK Cells in response to HLA-E null K562 cells. **(C)** %CD107a⁺, % IFN-γ⁺ and % TNF- α ⁺ of adaptive NK Cells in response to HLA-E null K562 cells Mann-Whitney test was performed to compared differences between groups and results were considered significant when p-value<0.05. Trends are marked in grey.

Supplementary Figure 9. Correlograms representing positive and negative correlation between NK cell phenotype, NK cell function and HLA-E expression. Spearman's rank correlation matrix was applied on samples from 36 individuals including Severe COVID-19 (n=12), mild COVID- 19 (n=12) and uninfected individuals (n=12) and significant correlations with p>0.05 and r > 0.35 (orange link) or r < -0.35 (violet link) were plotted using R 4.1.2 and ggcorrplot package. This analysis was performed on data based on the CD56^{neg} **(A)**, CD56^{dim} **(B)** and adaptive NK cells **(C)**. Only significant correlations (p<0.05) are shown and Spearman rank test is indicated in the circle.
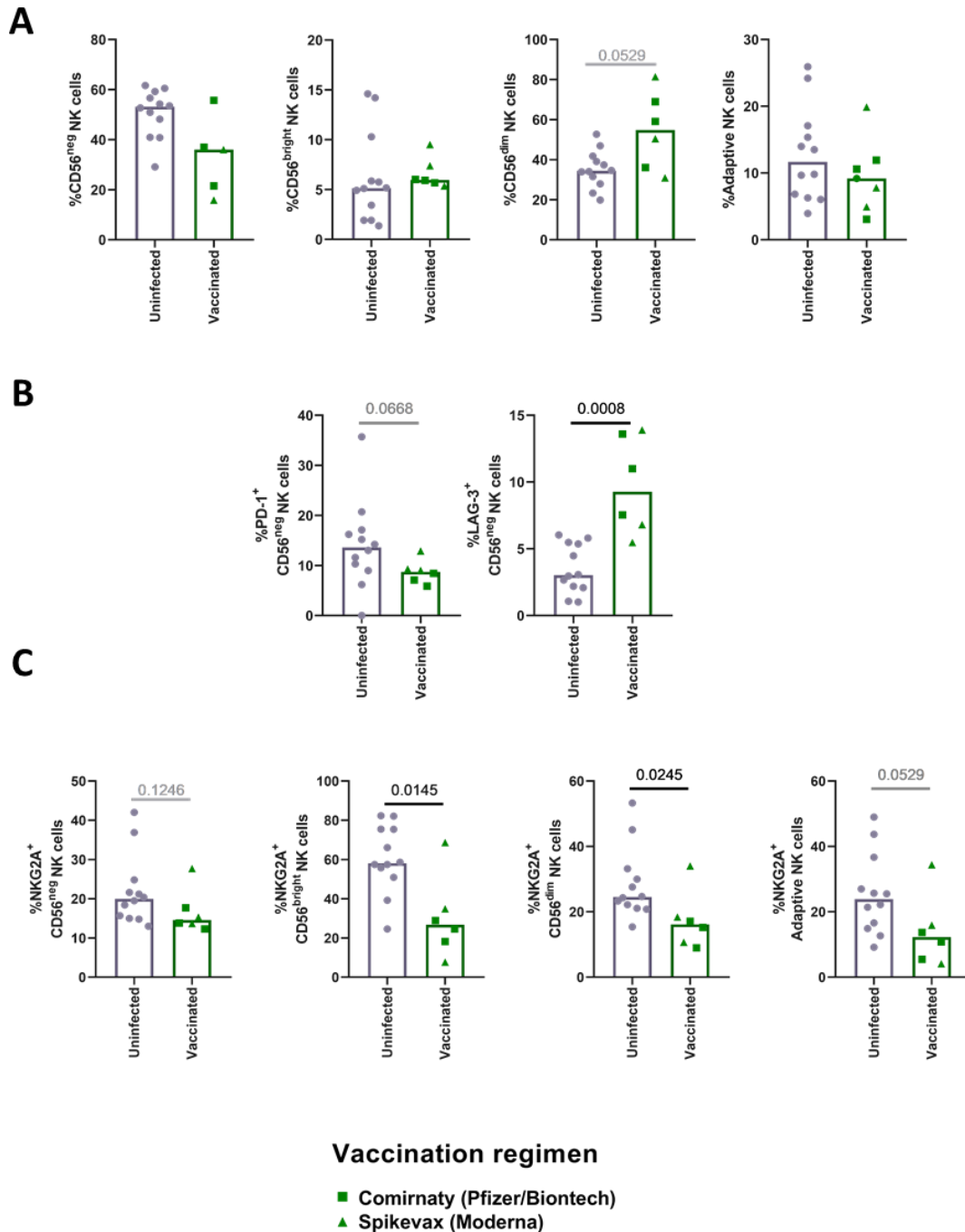
Supplementary Figure 10. Impact of SARS-Cov2 Spike-1 vaccination on NK cell function against HLA-E null target cell. (A) Scatter plot comparing abundance of CD56neg, CD56bright , CD56dim and adaptive NK cells in uninfected and vaccinated individuals. **(B)** % of PD-1+ and LAG-3+ cells within the CD56neg NK cell fraction. **(C)** % of NKG2A+ cells within CD56neg, CD56bright , CD56dim and adaptive NK cells. Mann-Whitney test was performed to compared differences between groups and results were considered significant when p-value<0.05. Trends are marked in grey. Mann-Whitney test was performed to compared differences between groups and results were considered significant when p-value<0.05.
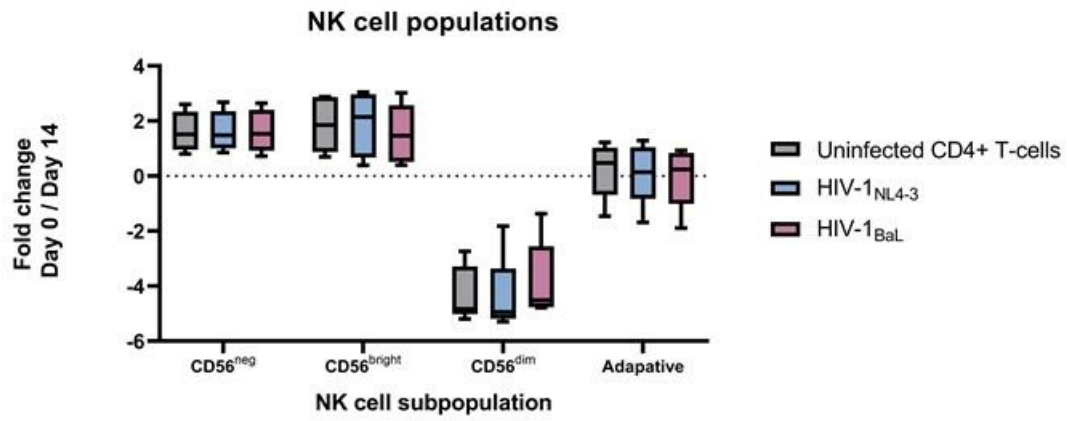
Supplementary Figure 11. NK populations changes observed in the two weeks culture with infected or uninfected autologous CD4+ T cells.
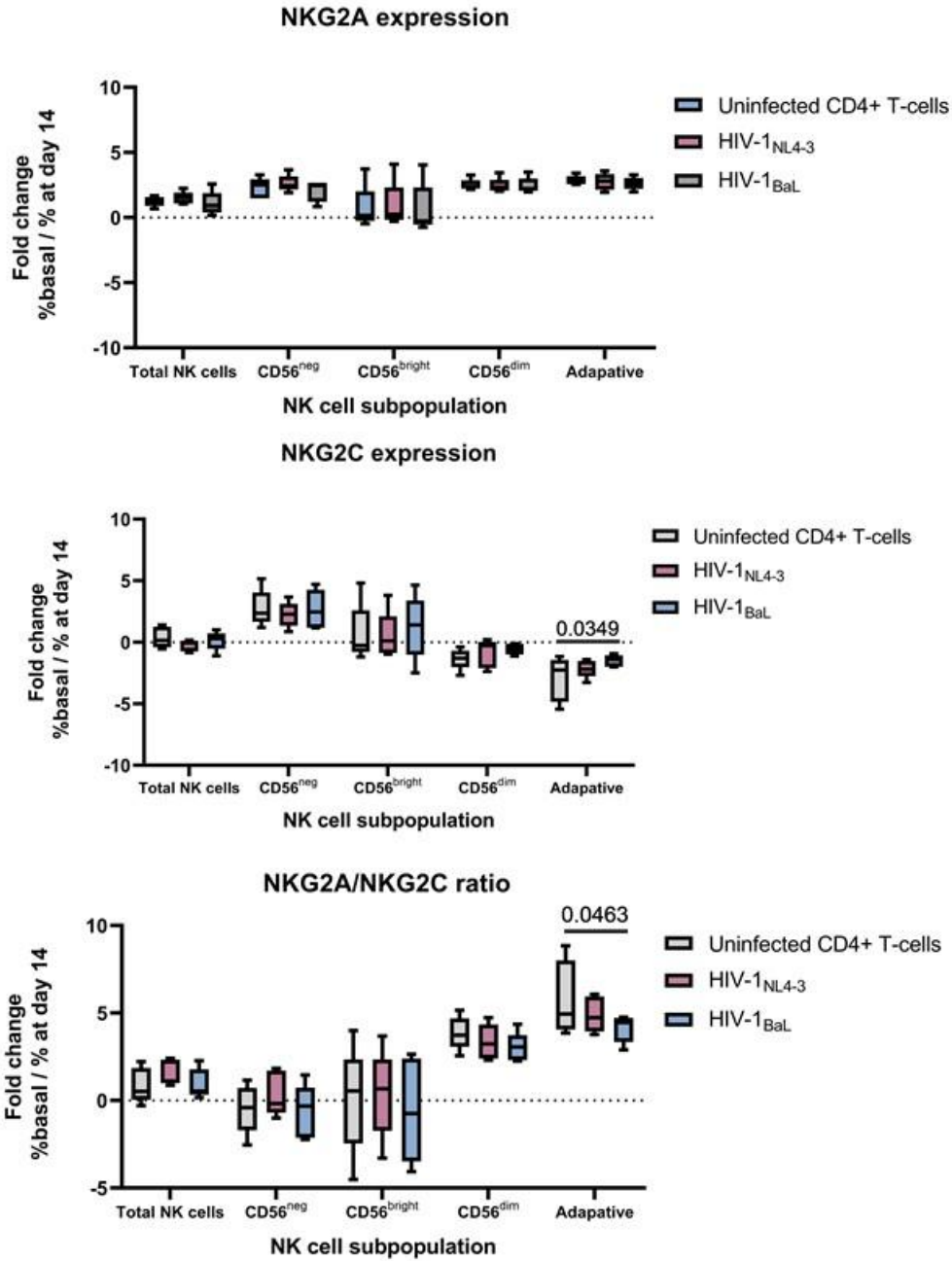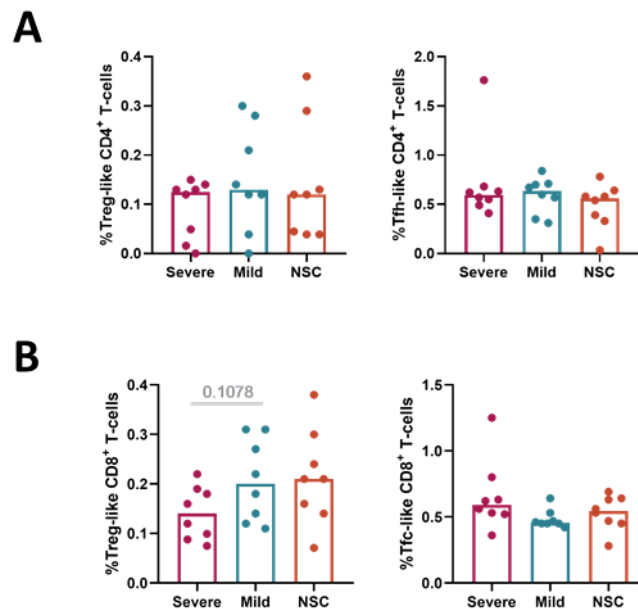
Supplementary Figure 12. NK populations changes observed in the two weeks culture with infected or uninfected autologous CD4+ T cells.
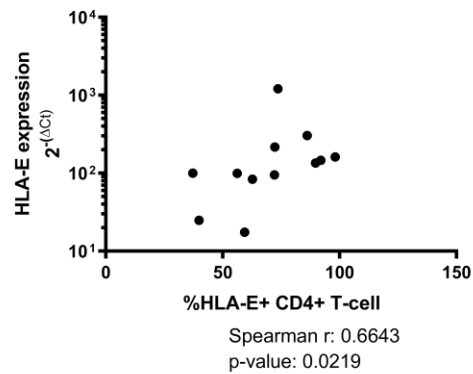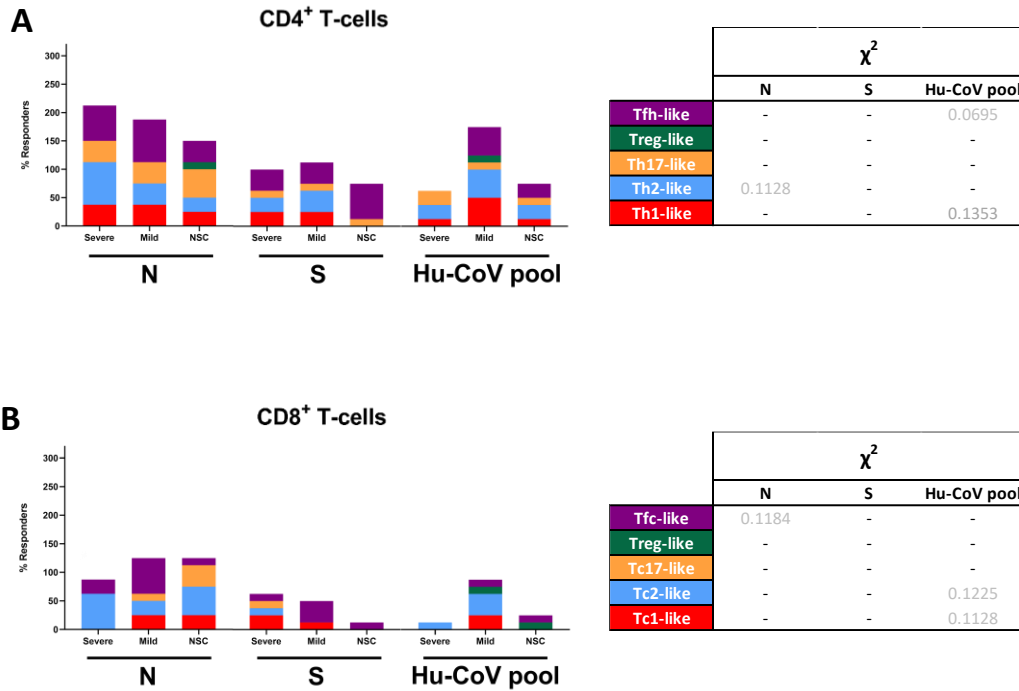
Supplementary Figure 13. Correlation between HLA-E Surface expression measured by Flow cytometry (X axis) and basal mRNA level measured by qPCR (Y axis).


Suppplementary Figure 14. Basal activation of peripheral T-cells in COVID-19 patients (A) CD4^{+} Treg-like (left) and Tfh-like (right) basal activation was compared among severe (magenta, n=8), mild (blue, n=8) and non-seroconvertors (NSC, orange, n=8) COVID-19 patients. **(B)** CD8^{+} Treg-like (left) and Tfc-like (right) basal activation was compared among (S, magenta, n=8), mild (M, blue, n=8) and non-seroconvertors (NSC, orange, n=8) COVID-19 patients. Statistical significance was evaluated by non-parametric Mann-Whitney test, statistical significance was set at p<0.05, trends are shown in grey (p<0.15)

A

CD4+ T-cells

	χ²		
	N	**S**	**Hu-CoV pool**
Tfh-like	-	-	0.0695
Treg-like	-	-	-
Th17-like	-	-	-
Th2-like	0.1128	-	-
Th1-like	-	-	0.1353

B

CD8+ T-cells

	χ²		
	N	**S**	**Hu-CoV pool**
Tfc-like	0.1184	-	-
Treg-like	-	-	-
Tc17-like	-	-	-
Tc2-like	-	-	0.1225
Tc1-like	-	-	0.1128

Supplementary Figure 15. Percentage of responders per group to SARS-CoV-2 nucleocapsid (N), spike (S) and a pool of 16 conserved epitopes among human coronaviruses (Hu-CoV pool) after 12 hours of stimulation. (A) Stacked histograms repof individuals who elicited CD4+ Th1-like (red), Th2-like (blue), Th17-like (yellow), Treg-like (green) and Tfh-like (purple) responses to N, S or Hu-CoV pool among severe (S, n=8), mild (M, n=8) and non-seroconvertors (NSC, n=8). **(B)** Stacked histograms repof individuals who elicited CD8+ Tc1-like (red), Tc2-like (blue), Tc17-like (yellow), Treg-like (green) and Tfc-like (purple) responses to N, S or Hu-CoV pool among severe (S, n=8), mild (M, n=8) and non-seroconvertors (NSC, n=8). Tables on the right represent p-values from χ² test applied to each profile in each stimulation in order to determine T-cell profiles that differentiate among groups. Trends are represented in grey (p<0.15).
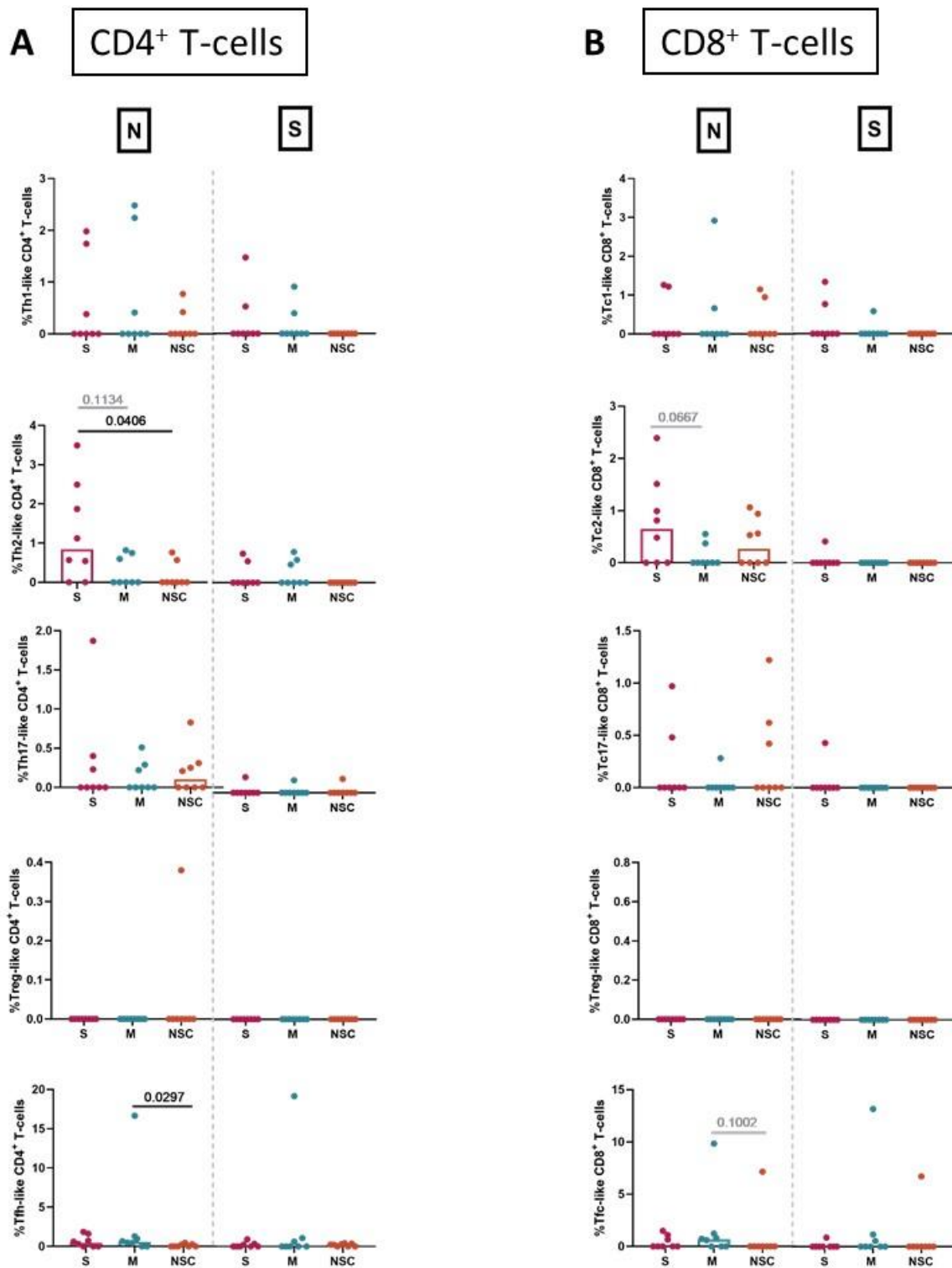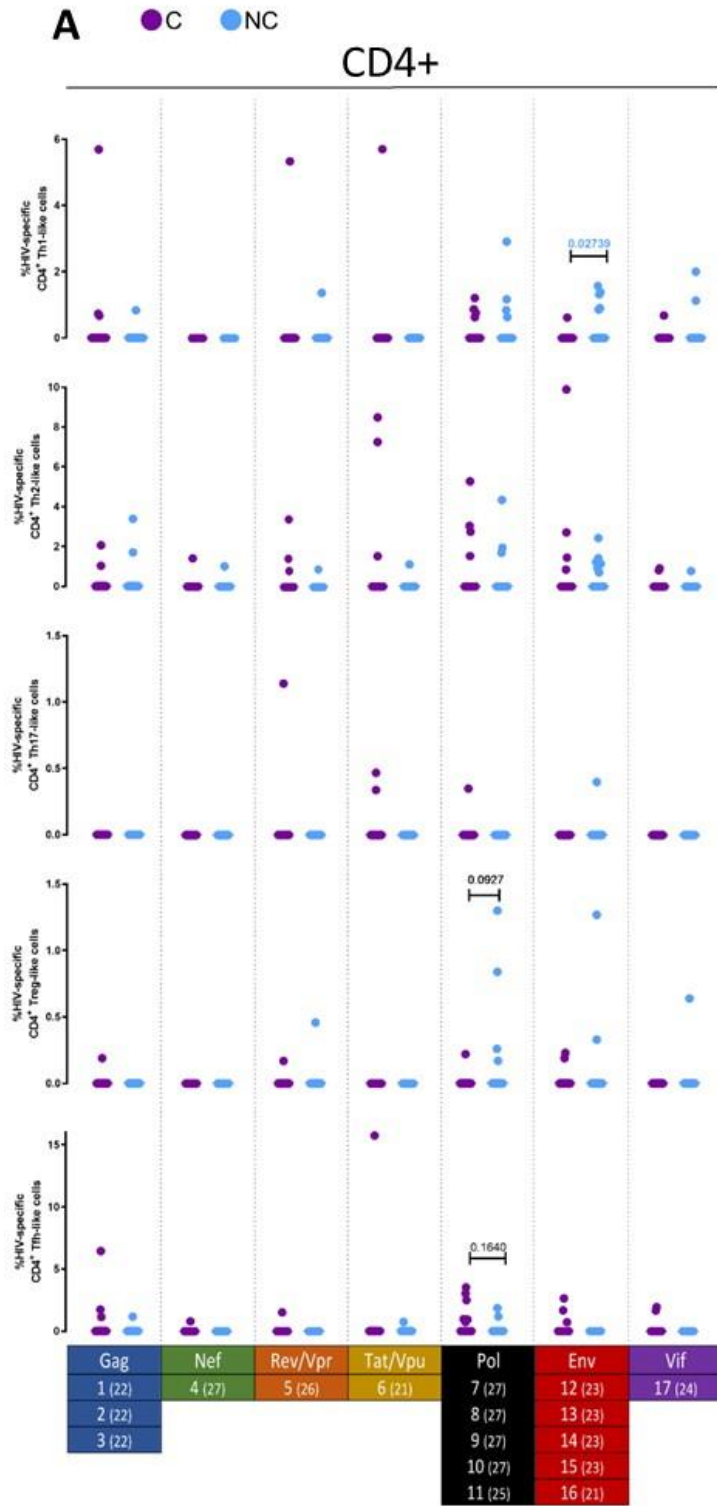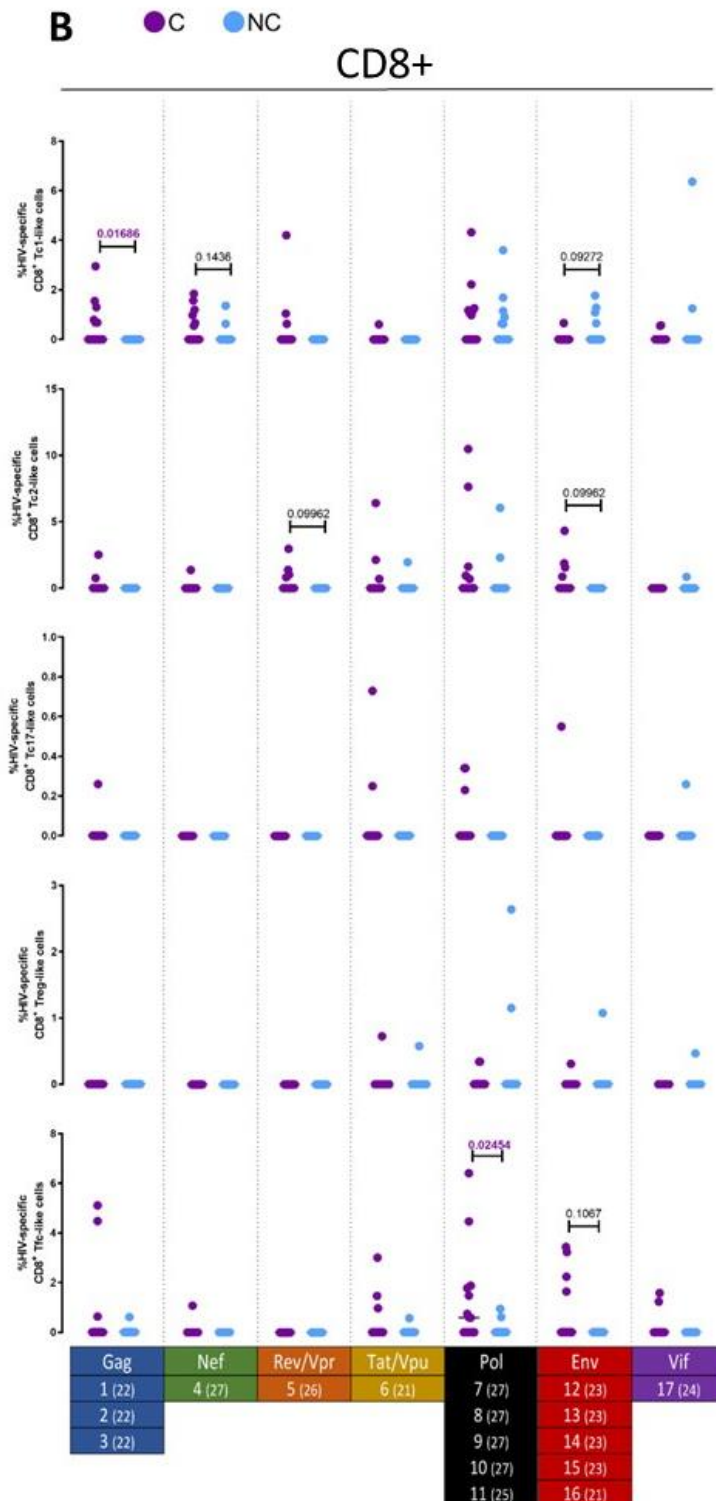
Supplementary Figure 16. Magnitude of the T-cell response against SARS-CoV-2 nucleocapsid (N) and spike (S) after 5 days of stimulation. (A) Scatter plot represent CD4+ T-cell responses (in this order: Th1-like, Th2-like, Th17-like, Treg-like, Tfh-like) to N and S in severe (S, magenta, n=8), mild (M, blue, n=8) and non-seroconvertors (NSC, orange, n=8) COVID-19 patients. **(B)** Scatter plot represent CD8+ T-cell responses (in this order: Tc1-like, Tc2-like, Tc17-like, Treg-like, Tch-like) to N and S in severe (S, magenta, n=8), mild (M, blue, n=8) and non-seroconvertors (NSC, orange, n=8) COVID-19 patients. Statistical significance was evaluated by non-parametric Mann-Whitney test, statistical significance was set at $p<0.05$, trends are shown in grey ($p<0.15$)
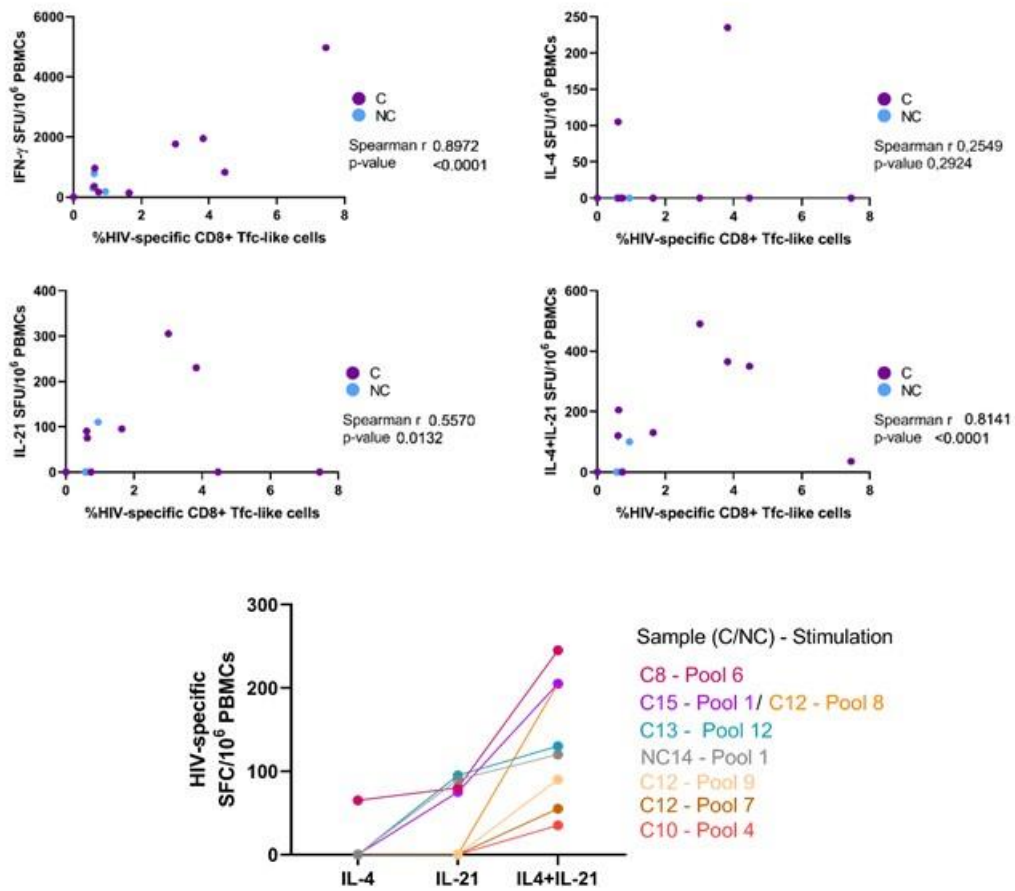
Supplementary Figure 17. Correlation between IL-4/IL-21 responses measured by *Boosted Flow* and ELISPOT on total PBMCs upon HIV-peptide pool specific stimulation. Correlation analysis was performed by non-parametric Spearman r test.
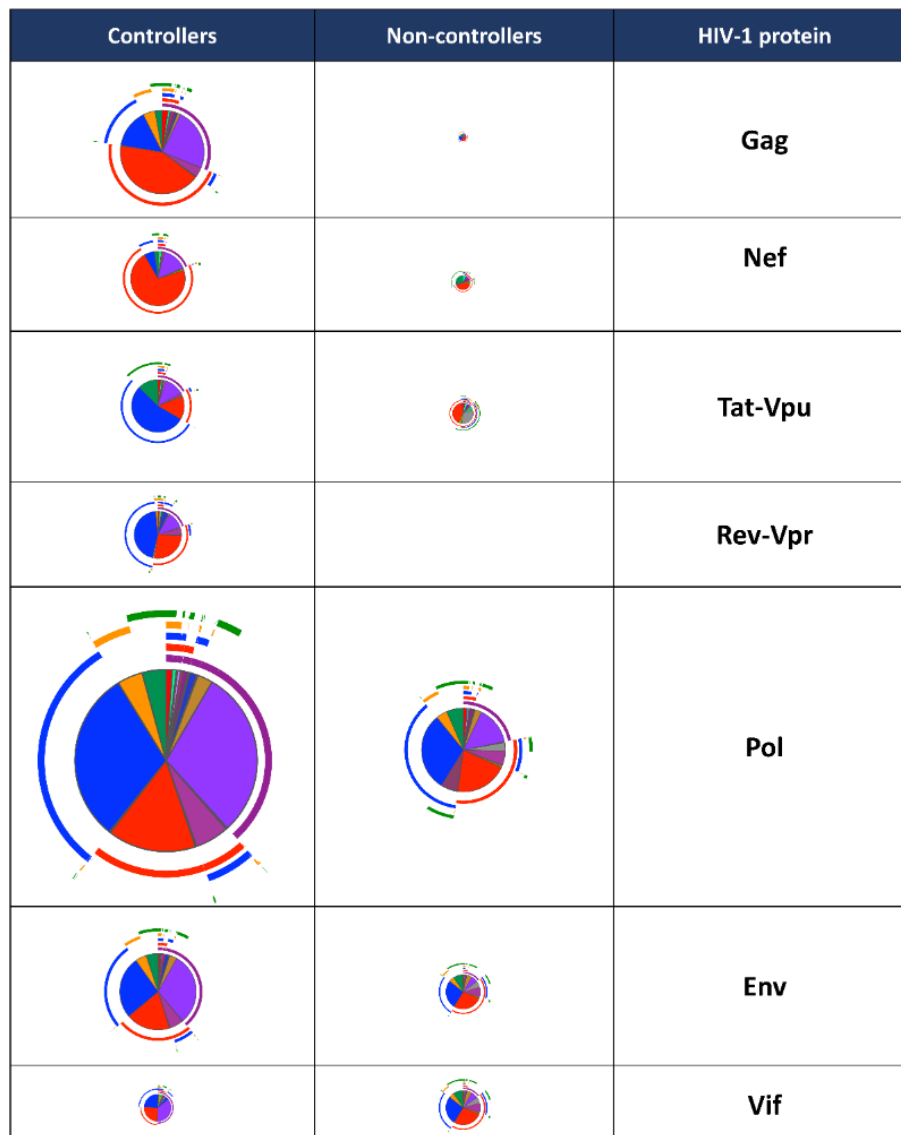
Supplementary Figure 18. HIV protein-specific polarized T-cell responses. Magnitude of the polarized responses in CD4+ T-cells (**A**) and CD8+ T-cells (**B**). Controllers are indicated by purple dots, and non-controllers by light blue dots. Significate p-values are highlighted in color, purple if responses were higher in controllers and light blue if responses were higher in non-controllers. The table below represent the number of pools contained in each protein-screening with the number of peptides in each pool in Brackets. Statistical significance was evaluated by non-parametric Mann-Whitney test (B).
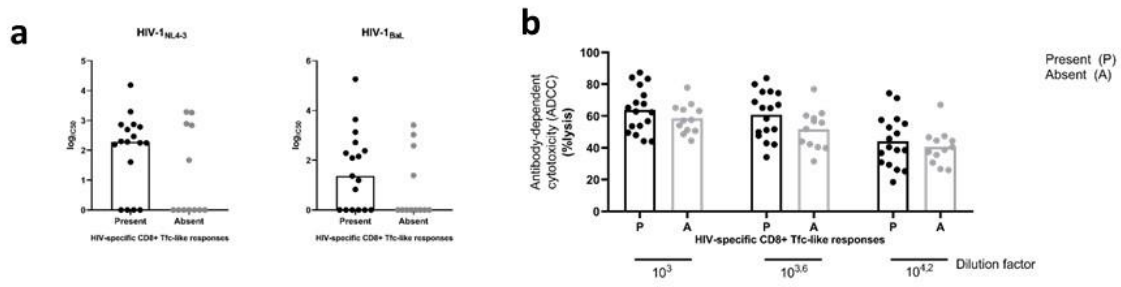
CD4⁺ T-cell

CD8+ T-cell

Supplementary Figure 19. SPICE polyfunctional analysis of HIV-specific CD4+ (left) and CD8+ (right) T-cell responses. Pie chart size are an estimation of the number of responders to each protein. Coloured arcs represent magnitude of each polarized response in that protein-specific response.

Supplementary Figure 20. Lack of significant correlation between HIV-specific CD8+ Tfc-like responses and humoral responses for (a) neutralization and (b) ADCC.

Publications

Publications related to this study

1. <u>Romero-Martin L</u>, Tarrés-Freixas F, Pedreno-Lopez N, Rodríguez de la Concepción ML, Cunyat F, Hartigan O'Connor D, et al. *T-follicular-like CD8+ T cells responses in chronic HIV infection are associated with virus control and antibody isotype switching to IgG*. Front Immunol [In press].

2. <u>Romero-Martin L</u>, Duran-Castells C, Olivella M, Rosás-Umbert M, Ruiz-Riol M, Sanchez, J Hartigan-O'Connor D, Mothe B, Olvera A, Brander C. *Disruption of the HLA-E/NKG2X axis is associated with uncontrolled HIV infections*. PLOS Pathogens [Under revision]

3. <u>Romero-Martin L</u>, Mateu L, Toledo R, Font M, Paredes R, Brander C, Massanella M, Olvera A. *COVID-19 severity is related to the presence of exhausted NK cells unresponsive to HLA-E mediated signaling*. [In preparation]

Other publications

1. Olvera A, Noguera-Julian M, Kilpelainen A, <u>Romero-Martín L</u>, Prado J. G., Brander C. (2020). *SARS-COV-2 consensus-sequence and matching overlapping peptides design for covid19 immune studies and vaccine development*. Vaccines, 8(3), 444. https://doi.org/10.3390/vaccines8030444

2. Borgognone A, Elizalde-Torrent A, Casadellà M, <u>Romero-Martín L</u>, Escribà T, Parera M, Català-Moll F, Noguera-Julian M, Brander C, Olvera A, Paredes R. *Vaccination with HIV T cell immunogen induces alterations in the mouse gut microbiota.* [In preparation]

3. Elizalde-Torrent A, Borgognone A, Casadellà M, <u>Romero-Martín L</u>, Escribà T, , Català-Moll F, Noguera-Julian M, Brander C, Paredes R, Olvera A. *Changes in the T cell response to vaccination with an HTI DNA prime followed by an HTI ChAdOx1-MVA boost in gut microbiota depleted mouse.* [In preparation]

4. Benet S, Blanch-Lombarte O, Ainsua-Enrich E, Pedreño-López N, Muñoz-Basagoiti J, Perez-Zsolt D, Peña R, Jiménez E, Rodríguez de la Concepción ML, Ávila c, Cedeño S, Escribà T, <u>Romero-Martín L</u>, Alarcón-Soto Y, Rodríguez-Lozano GF, Miranda C, González S, Bailón L, Blanco J, Massanella M, Brander C, Clotet B, Paredes R, Esteve M, Izquierdo-Useros N, Carrillo J, G. Prado J, Moltó J, Mothe B. *Limited humoral and specific T-cell responses after SARS-CoV-2 vaccination in PLWH with poor immune reconstitution.* Journal of Infectious Diseases [Under revision].